Department of Physics and Astronomy

University of Heidelberg

Diploma thesis

in Physics

submitted by

Nina Memenga

born in Nordenham

2012

A neutrinophilic two Higgs doublet model with an A_4 flavour symmetry for Dirac neutrinos

This diploma thesis has been carried out by
Nina Memenga
at the
Max Planck Institute for Nuclear Physics
under the supervision of
Dr. Werner Rodejohann

A neutrinophilic two Higgs doublet model with an A_4 flavour symmetry for Dirac neutrinos

We introduce three right-handed sterile neutrinos which acquire mass by coupling to a second Higgs doublet with a tiny vacuum expectation value, giving rise to naturally small neutrino masses. Majorana mass terms are forbidden by an additional global $U(1)$ symmetry. We discuss the phenomenology of this model, placing a special emphasis on processes involving leptons. In addition, an A_4 flavour symmetry is introduced in the lepton sector in order to explain the structure of the leptonic mixing matrix and the neutrino masses. We discuss how a tribimaximal leptonic mixing matrix can be achieved in this context and analyse numerically deviations from the exact tribimaximal form, which are required in order to be compatible with the recent experimental findings indicating a rather large θ_{13}. In particular, implications of the presence of this flavour symmetry on the phenomenology of the two Higgs doublet model are studied.

Ein neutrinophiles zwei-Higgs-Doublet-Modell mit einer A_4 Flavour-Symmetrie für Dirac Neutrinos

In dieser Arbeit wird ein zwei-Higgs-Doublet-Modell für Dirac Neutrinos untersucht, wobei die Neutrinos ausschliesslich an ein Higgsfeld mit einem sehr kleinen Vakuumerwartungswert koppeln und somit auf natürliche Weise eine sehr kleine Masse erlangen. Majoranamassenterme der Neutrinos werden durch eine zusätzliche $U(1)$-Symmetrie verboten. Änderungen der Higgsphänomenologie im Vergleich zum Standardmodell werden aufgezeigt, wobei wir den Schwerpunkt auf die Betrachtung von Prozessen mit Beteiligung von Leptonen legen. Im Folgenden wird das betrachtete Modell um eine A_4-Flavour-Symmetrie im Leptonsektor erweitert. Diese zusätzliche Symmetrie wird eingeführt, um die Struktur der leptonischen Mischungsmatrix sowie die Neutrinomassen zu erklären. Wir untersuchen zunächst, unter welchen Vorraussetzungen die resultierende Mischungsmatrix die tribimaximale Form aufweist. Danach bestimmen wir in einer numerischen Analyse die Auswirkungen von verschiedenen möglichen Störungen, welche zu einer Abweichung von der tribimaximalen Form führen. Solche Abweichungen sind notwendig, um die Kompatibilität des Modells mit den neuesten experimentellen Resultaten zu gewährleisten, welche das Nichtverschwinden des Mischunswinkels θ_{13} bestätigen. Zuletzt untersuchen wir die Auswirkungen, die sich für die Phänomenologie des zwei-Higgs-Doublet-Modells ergeben, wenn die leptonische Mischungsmatrix und die Neutrinomassen durch die betrachtete A_4-Symmetrie unter Berücksichtigung von geeigneten Störungen vorhergesagt werden.

Contents

1 Introduction **1**

2 Neutrino masses and neutrino oscillations **5**

2.1 The Standard Model 5

2.2 Neutrino oscillations 8

2.3 Neutrino mass models 13

2.3.1 Dirac neutrino mass term 14

2.3.2 Pure Majorana mass term 15

2.3.3 Majorana and Dirac mass term 16

2.3.4 Seesaw mechanism 17

2.4 Neutrinoless double beta decay 18

2.5 Absolute scale of neutrino masses 19

2.6 Flavour symmetries 20

3 The neutrinophilic two Higgs doublet model **27**

3.1 The scalar potential 29

3.2 Masses of the physical Higgs states 34

3.3 The kinetic term of the Higgs fields 37

3.4 The Yukawa sector 38

3.5 Phenomenology of the ν2HDM 41

3.5.1 Higgs decay rates and collider phenomenology 41

3.5.2 Unitarity constraints 49

3.5.3 Charged lepton flavour violation via $H^{\pm}$ loops 50

3.5.4 The anomalous magnetic moment of the muon 56

3.5.5 Tree-level muon and tauon decay - lepton universality . . . 60

4 Leptonic mixing from an A_4 flavour symmetry **65**
4.1 The A_4 group . . . 66
4.2 TBM mixing as a consequence of the A_4 symmetry . . . 70
4.3 Applying A_4 to the lepton sector . . . 72
4.4 The vev alignment problem . . . 80
4.5 Explaining the vev alignment in the 2S2T model via extra dimensions 84
4.5.1 Next-to-leading order effects in the 2S2T model with an extra dimension . . . 88
4.6 Possible dynamical origin of A_4 . . . 94
4.7 What about the quark sector? . . . 96

5 Phenomenology of the combined 2S2T and ν2HDM model **99**
5.1 Three ways to break $G_S \times A_{23}$ . . . 100
5.2 Combining deviations: Relaxing $a' = 0$, $c = d$ and the triplet vev alignment . . . 104
5.3 Higgs phenomenology in an A_4 − symmetric ν2HDM . . . 106
5.3.1 Leptonic decays of the charged Higgs . . . 107
5.3.2 Charged lepton flavour violation . . . 109
5.3.3 The anomalous magnetic moment of the muon . . . 111
5.3.4 Lepton universality . . . 112

6 Summary and conclusion **115**

A The Higgs sector in the Standard Model **119**

B Diagonalisation of a general fermion mass matrix **121**

C Dirac, Weyl and Majorana fermions **123**

D The Higgs interaction terms in the 2HDM **125**

E Tree-level decay modes of the SM Higgs **131**

F Deviations from TBM form in the real case - analytic derivation **133**

G Details of the numerical analysis of the 2S2T model **137**

Chapter 1

Introduction

The Standard Model of particle physics is the culmination of a concerted effort over several decades of the past century to provide a unified theoretical framework in which all observed matter particles and forces can be understood. The foundations were laid by the theory of the electroweak interactions known as the Glashow-Weinberg-Salam theory [1–3], which was soon extended to include also the theory of the strong force [4–9]. Over the years, many predictions of the Standard Model, like e.g. the existence of the top quark, have been famously experimentally verified, and today the Standard Model can be considered as one of the most precisely experimentally tested theories ever formulated. Nevertheless, there are several important open questions that remain unanswered, implying that the Standard Model in its current form cannot be regarded as the full theory of elementary particles and forces. For example, apart from the major theoretical problem that the Standard Model does not admit for a straightforward way of incorporating gravity, it also does not include any description of dark matter, which is estimated to account for about 84% of the total matter density of the universe. However, the most direct experimental evidence for the necessity of extending the Standard Model comes from the observation of neutrino oscillations, which require a non-vanishing neutrino mass. While a deficit of electron neutrinos in the solar neutrino flux with respect to the theoretical predictions was observed as early as the 1960s, the confirmation that this deficit was due to a neutrino flavour change effect was only provided in 2001 by the results of the SNO experiment [10].

While neutrinos are massless in the context of the Standard Model, mass terms of the required magnitude can actually be included into the existing framework rather easily in an ad hoc manner. From observations of the cosmic microwave background and from precise measurements of Tritium beta decay we know that neutrino masses must be smaller than 1 eV [11–13]. The main theoretical problem thus actually lies not in writing down the explicit mass terms, but rather in finding a natural explanation for their relative smallness in comparison with the masses of the other Standard Model particles. While large mass hierarchies between particles of different generations are present also in the Standard Model, the lepton

sector is the only case where such a large mass difference appears between particles of the same generation, which seems quite unnatural. Many approaches have been considered in the search for a theoretical explanation for the smallness of the neutrino masses. In particular, the different variants of the well-known seesaw mechanism have been discussed extensively in the literature. In chapter 2 we will give a brief overview of the most important topics in neutrino physics as well as the main features of the Standard Model.

Despite the aesthetically pleasing nature of the seesaw mechanism, we will focus on a second possibility in this work. Namely, we will introduce a second copy of the ordinary Higgs field and require that the vacuum expectation value of this additional Higgs field is small compared to that of the ordinary Higgs, for example of order 1 eV. This approach has the advantage that, after introducing a set of right-handed neutrino fields and combining them into Dirac spinors together with the left-handed fields already present in the Standard Model, the neutrinos can be treated in a completely analogous manner to all the other Standard Model fermions. The only difference is that the neutrinos should couple to a different Higgs field than the other fermions, which can for example be achieved in a very natural way by imposing an additional symmetry. In this thesis, we will implement a $U(1)$ symmetry in such a way that this separation is achieved and, at the same time, Majorana mass terms for the neutrinos are forbidden. At first glance, the existence of a large hierarchy between the two different Higgs vacuum expectation values might seem no more natural than the original hierarchy between the charged lepton and neutrino masses. However, we will confirm in a specific analysis of the Higgs potential that the required large splitting can indeed be achieved in a natural way. This so-called neutrinophilic two Higgs doublet model, whose main features we have just summarised, will be discussed in detail in chapter 3. In our analysis we will review and extend the results of [14], placing special emphasis on the Higgs phenomenology and in particular on those processes that are sensitive to the precise values of the neutrino masses and the magnitude of mixing in flavour space.

The strength of flavour mixing is encoded in the leptonic mixing matrix, which is known as the Pontecorvo-Maki-Nakagawa-Sakata matrix and is the leptonic analogue of the Cabibbo-Kobayashi-Maskawa (CKM) matrix that occurs in the quark sector. In the standard parametrisation, this leptonic mixing matrix is defined by three mixing angles, one Dirac phase and two additional Majorana phases that can be non-vanishing only if neutrinos are Majorana particles. Many experiments have been devised with the aim of investigating neutrino oscillations and determining the entries of the leptonic mixing matrix. These measurements show that the leptonic mixing matrix is very close to the so-called tribimaximal mixing matrix, which we will introduce in chapter 2. Note that the recent results of the Double Chooz [15], Daya Bay [16] and RENO [17] experiments have confirmed that the mixing angle θ_{13} is not as close to zero as formerly expected. Nevertheless, the tribimaximal form of the mixing matrix, in which $\theta_{13} = 0$, still provides a good first approximation to the leptonic mixing matrix. In particular, the leptonic

mixing matrix is found to be quite different from the CKM matrix, which is close to the unity matrix. The main objective of flavour physics lies in finding a natural explanation for the observed form of the mixing matrices and to explain the differences between the quark and lepton sectors. Put differently, the aim is to reduce the number of independent parameters that have to be put in by hand into the Standard Model. A brief overview of the main ideas of flavour physics is given in chapter 2.

Our main focus will lie on finding a possible explanation for the structure of the leptonic mixing matrix. A popular approach to this problem is to consider the introduction of discrete flavour symmetry groups. A very famous group in this context is the rotation group of the tetrahedron, the A_4 group. Implementing the corresponding symmetry into the Standard Model in an appropriate manner yields a leptonic mixing matrix of the tribimaximal form. Models based on the A_4 group have already been extensively studied over the last years. However, the existing models are based on the assumption that neutrinos are Majorana particles. In this work we will therefore consider an A_4 model for Dirac neutrinos. In combination with a neutrinophilic two Higgs doublet model, this leads to a framework in which both the relative smallness of the neutrino masses and the form of the mixing matrix can be explained. The general structure of the model will be discussed in detail in chapter 4. In particular, we will analyse how a deviation from the tribimaximal form can be achieved, which is needed in order to be compatible with the experimentally confirmed non-vanishing of θ_{13}. We analyse the effects of various possible deviations in a specific A_4 model using a numerical analysis in chapter 5. By plugging in the predictions for the leptonic mixing angles obtained from the numerical analysis, we explicitly discuss the implications on the Higgs phenomenology that arise from the presence of the additional A_4 flavour symmetry at the end of chapter 5.

Chapter 2

Neutrino masses and neutrino oscillations

To set the stage for the discussion of explicit neutrino mass models in the later chapters, we begin by briefly reviewing the salient features of the Standard Model as well as a selection of important ideas in neutrino physics. Rather than aiming for completeness we focus on the aspects that will be used in the following chapters.

2.1 The Standard Model

The Standard Model of particle physics (SM) is one of the most celebrated achievements of theoretical physics in the last decades. It provides a unified theoretical description of the electroweak (EW) and strong interactions of the known elementary matter particles listed in table 2.1 and has been tested experimentally to extremely high precision.

The SM is a combination of the Glashow-Salam-Weinberg theory of the weak left-handed isospin and hypercharge Y, described by the gauge group $SU(2)_{\mathrm{L}} \times U(1)_{\mathrm{Y}}$ [1–3], with the theory of quantum chromodynamics (QCD), described by the colour group $SU(3)_{\mathrm{C}}$ [4–9].

The left-handed leptons and quarks of a given generation are combined into

Generation	Quarks		Leptons	
1	u	d	ν_e	e
2	c	s	ν_μ	μ
3	t	b	ν_τ	τ

Table 2.1: Spin-1/2-fermions in the SM.

Field	$SU(3)_{\mathrm{C}}$	$SU(2)_{\mathrm{L}}$	$U(1)_{\mathrm{Y}}$
$\mathrm{Q_L}$	3	2	1/3
u_{R}	3	1	4/3
d_{R}	3	1	-2/3
$\mathrm{L_L}$	1	2	-1
ℓ_{R}	1	1	-2
Φ	1	2	1

Table 2.2: Transformation properties of the SM matter fields and Higgs field under $SU(3)_{\mathrm{C}} \times SU(2)_{\mathrm{L}} \times U(1)_{\mathrm{Y}}$. The hypercharge is normalised to obey $Q = Y/2 + T_3$, where Q is the electric charge and T_3 is the third component of the weak isospin of the particle.

$SU(2)_{\mathrm{L}}$ doublets

$$\mathrm{L}_{\mathrm{L},i} = \begin{pmatrix} \nu_{\mathrm{L},i} \\ \ell_{\mathrm{L},i} \end{pmatrix}, \quad \mathrm{Q}_{\mathrm{L},i} = \begin{pmatrix} u_{\mathrm{L},i} \\ d_{\mathrm{L},i} \end{pmatrix}, \tag{2.1}$$

whereas the right-handed particles $\ell_{\mathrm{R},i}$, $u_{\mathrm{R},i}$ and $d_{\mathrm{R},i}$ are $SU(2)_{\mathrm{L}}$ singlets. Here $i = 1, 2, 3$ labels the different generations. There are no right-handed neutrinos in the SM. In addition to the fermionic matter fields introduced above, each generator of the combined gauge group $SU(3)_{\mathrm{C}} \times SU(2)_{\mathrm{L}} \times U(1)_{\mathrm{Y}}$ yields a spin one gauge boson which mediates the corresponding interaction. In this way one obtains eight gluons G^a_μ corresponding to $SU(3)_C$, three vector fields W^i_μ arising from $SU(2)_{\mathrm{L}}$ and the hypercharge gauge boson B_μ of $U(1)_Y$. Finally, in order to give masses to the SM particles an $SU(2)_{\mathrm{L}}$ doublet scalar field Φ known as the Higgs field is introduced, and the mechanism of spontaneous symmetry breaking is invoked [18–21]. The Higgs doublet carries hypercharge +1 and transforms as a singlet under $SU(3)_{\mathrm{C}}$.

The Lagrangian of the Standard Model can be written in the form

$$\mathcal{L} = \mathcal{L}_{\text{gauge}} + \mathcal{L}_{\text{fermions}} + \mathcal{L}_{\text{scalar}} + \mathcal{L}_{\text{Yukawa}}. \tag{2.2}$$

Here $\mathcal{L}_{\text{gauge}}$ and $\mathcal{L}_{\text{fermions}}$ respectively contain the gauge kinetic terms and the kinetic terms of the fermions, while the kinetic and potential terms of the Higgs field are included in $\mathcal{L}_{\text{scalar}}$. Finally, the Yukawa interactions between the Higgs and fermion fields are encoded in $\mathcal{L}_{\text{Yukawa}}$. We will not discuss the full Lagrangian here and will provide only the expressions that are needed for the considerations of the following chapters (see for example [22, 23] for a more detailed discussion of the SM).

The spontaneous symmetry breaking of the EW $SU(2)_{\mathrm{L}} \times U(1)_{\mathrm{Y}}$ symmetry to $U(1)_{\text{em}}$ (the symmetry of electromagnetism) is achieved by letting the Higgs field acquire a non-vanishing vacuum expectation value (vev). Ensuring that only the neutral component of Φ acquires a vev, the term[1] $(\mathrm{D}_\mu\Phi)^\dagger \mathrm{D}^\mu\Phi$ in $\mathcal{L}_{\text{scalar}}$ leads

[1] The gauge covariant derivative D_μ acting on a given field is defined by $\mathrm{D}_\mu = \partial_\mu - iq_1 g_1 B_\mu/2 -$

to three massive gauge bosons $W^{\pm}$ and Z and a massless photon A. Since the Higgs does not transform under $SU(3)_C$ the colour group remains unbroken and the corresponding gauge bosons, the eight gluons, stay massless. See appendix A for the full expansion of $\mathcal{L}_{\text{scalar}}$ after electroweak symmetry breaking.

A Standard Model fermion Ψ acquires a mass through the Yukawa interactions, which schematically take the form $-Y\bar{\Psi}\Phi\Psi$ with Y a constant. After expanding Φ around its vev this yields a mass term for the field Ψ. As long as gauge invariance is guaranteed we can also allow for cross-couplings between different fermions in $\mathcal{L}_{\text{Yukawa}}$. For the lepton and quark sectors the general form of the interactions is then

$$\mathcal{L}_{\text{Yukawa}} = -\sum_{i,j=1}^{3} \left(Y^{\ell}_{ij} \overline{\mathrm{L}_{\mathrm{L},i}} \Phi \ell_{\mathrm{R},j} + Y^{u}_{ij} \overline{\mathrm{Q}_{\mathrm{L},i}} \widetilde{\Phi} u_{\mathrm{R},i} + Y^{d}_{ij} \overline{\mathrm{Q}_{\mathrm{L},i}} \Phi d_{\mathrm{R},i} + \text{h.c.} \right), \tag{2.3}$$

where the charge conjugate Higgs doublet is defined by $\widetilde{\Phi} = i\sigma_2\Phi^*$ with the Pauli matrix σ_2. Since right-handed neutrinos do not exist in the SM, the neutrinos remain massless in this framework.

The kinetic terms of the fermions are given by

$$\mathcal{L}_{\text{fermions}} = \overline{\mathrm{L_L}} i\not{\mathrm{D}} \mathrm{L_L} + \overline{e_{\mathrm{R}}} i\not{\mathrm{D}} e_{\mathrm{R}} + \overline{\mathrm{Q_L}} i\not{\mathrm{D}} \mathrm{Q_L} + \overline{d_{\mathrm{R}}} i\not{\mathrm{D}} d_{\mathrm{R}} + \overline{u_{\mathrm{R}}} i\not{\mathrm{D}} u_{\mathrm{R}}, \tag{2.4}$$

where $\not{\mathrm{D}} = \gamma^{\mu}\mathrm{D}_{\mu}$. This term yields the interactions between the fermions and the gauge bosons, which can be easily derived by expanding the covariant derivatives D_{μ}. In this way one obtains

$$\begin{aligned} \mathcal{L}_{\text{fermions}} \;=\; & -\frac{g_2}{\sqrt{2}} W^{-}_{\mu} \sum \left(\overline{\ell_{\mathrm{L},i}} \gamma^{\mu} \nu_{\mathrm{L},i} + \overline{d_{\mathrm{L},i}} \gamma^{\mu} u_{\mathrm{L},i} \right) + \text{h.c.} && (2.5) \\ & + eA_{\mu} \sum \left(\bar{\ell}_i \gamma^{\mu} \ell_i - \frac{2}{3} \bar{u}_i \gamma^{\mu} u_i + \frac{1}{3} \bar{d}_i \gamma^{\mu} d_i \right) \\ & + (\text{fermion couplings to } Z_{\mu}), && (2.6) \end{aligned}$$

where e is the electric charge and $f = (f_{\mathrm{L}},\ f_{\mathrm{R}})^{\mathrm{T}}$ (for $f = \ell,\ u,\ d$). Note that the sum runs over the fermion generations. The expressions for the couplings to the Z-boson are omitted for brevity as they are not needed in the following; they can be found for example in [23].

Equation (2.5) is given in the fermion flavour basis, where the W-interaction is diagonal. In general the flavour basis will not be equal to the mass eigenbasis of the fermions. This implies that particles which are produced in weak interactions will have contributions from different mass eigenstates, which describe the states of the propagating particles. The size of the different contributions is quantified by the so called mixing matrix, which describes the basis change between flavour and mass basis. The mass matrices $M^{u,d,\ell}$ that originate from the Yukawa term (2.3)

$iq_2 g_2 W_{\mu}/2 - iq_{\mathrm{C}} g_{\mathrm{C}} G_{\mu}$. q_1, q_2 and q_{C} are the charges of the field with respect to the different gauge groups, while g_1, g_2 and g_{C} are the respective coupling constants.

are in general complex 3×3 matrices. Each matrix can be diagonalized via a bi-unitary transformation which yields real and non-negative diagonal entries, so that these 'eigenvalues' can be interpreted as the physical masses of the corresponding particles (see appendix B for further details). As the form of the leptonic mixing matrix will be a crucial ingredient of our work, let us be a bit more precise here. The non-diagonal mass matrices $M^{u,d,\ell}$ can be diagonalized by

$$M^u_{\text{diag.}} = V_{\text{L}}^{u\,\dagger} M^u V_{\text{R}}^u, \qquad M^d_{\text{diag.}} = V_{\text{L}}^{d\,\dagger} M^d V_{\text{R}}^d, \qquad M^\ell_{\text{diag.}} = V_{\text{L}}^{\ell\,\dagger} M^\ell V_{\text{R}}^\ell. \quad (2.7)$$

The mass eigenstates are therefore given by

$$u^0_{\text{L,R}} = V^{u\,\dagger}_{\text{L,R}} u_{\text{L,R}}, \qquad d^0_{\text{L,R}} = V^{d\,\dagger}_{\text{L,R}} d_{\text{L,R}}, \qquad \ell^0_{\text{L,R}} = V^{\ell\,\dagger}_{\text{L,R}} \ell_{\text{L,R}}, \quad (2.8)$$

where $u_{\text{L,R}}$, $d_{\text{L,R}}$ and $\ell_{\text{L,R}}$ are the fields in the flavour basis introduced above. The W-boson interaction (2.5) in terms of the mass eigenstates then reads

$$\mathcal{L}_{\text{fermions}} \supset -\frac{g_2}{\sqrt{2}} W^-_\mu \left(\overline{\ell^0_{\text{L}}} V_{\text{L}}^{\ell\,\dagger} \gamma^\mu \nu_{\text{L}} + \overline{d^0_{\text{L}}} V_{\text{L}}^{d\,\dagger} \gamma^\mu V_{\text{L}}^u u^0_{\text{L}i} \right) + \text{h.c.} \quad (2.9)$$

Note that the summation over the different generations is implicit due to the matrix notation. We see that the basis change above leads to the appearance of the unitary CKM (Cabibbo-Kobayashi-Maskawa) mixing matrix, defined by $U_{\text{CKM}} = V_{\text{L}}^d V_{\text{L}}^{u\,\dagger}$, in the weak interactions of the quark sector [24, 25]. Non-trivial quark mixing is indeed observed in weak interactions, implying that the CKM matrix is different from the unity matrix. As long as the neutrinos are massless we have the freedom to redefine them according to $\nu^0_{\text{L}} = V_{\text{L}}^{\ell\,\dagger} \nu_{\text{L}}$. Therefore no mixing in the lepton sector occurs in the framework of the Standard Model. However, the discovery of neutrino oscillations showed that this cannot be the full picture and that neutrinos have to have a mass; this will be the subject of the next section. Let us stress that this is the first experimentally confirmed evidence for physics beyond the SM.

2.2 Neutrino oscillations

Following the discussion above let us now assume that the neutrinos have a mass, although we postpone the question of its origin to the following section 2.3. In particular we assume that flavour and mass eigenbasis in the lepton sector do not coincide, similar to the case of the quark sector. Then a mixing matrix analogous to the CKM matrix will occur in the lepton sector, which is known as the PMNS (Pontecorvo-Maki-Nakagawa-Sakata) matrix [26–28]. Assuming that the neutrino mass matrix is diagonalized by[2]

$$M^\nu_{\text{diag.}} = V_{\text{L}}^{\nu\,\dagger} M^\nu V_{\text{R}}^\nu \quad (2.10)$$

[2] Recall that any complex matrix can be brought to a diagonal form with real and non-negative entries by a bi-unitary transformation, see also appendix B.

and defining the mixing matrix and neutrino mass eigenstates

$$U^{\mathrm{PMNS}} = V_{\mathrm{L}}^{\ell\,\dagger} V_{\mathrm{L}}^{\nu}, \qquad \nu_{\mathrm{L,R}}^{0} = V_{\mathrm{L,R}}^{\nu\,\dagger} \nu_{\mathrm{L,R}}, \tag{2.11}$$

the weak interaction term of the lepton sector takes the form

$$\mathcal{L}_{\mathrm{fermions}} \supset -\frac{g_2}{\sqrt{2}} W_{\mu}^{-} \overline{\ell_{\mathrm{L}}^{0}} \gamma^{\mu} U^{\mathrm{PMNS}} \nu_{\mathrm{L}}^{0} + \mathrm{h.c.} \tag{2.12}$$

To illustrate the phenomenon of neutrino oscillations we consider a thought experiment whereby a W-boson decays into a lepton of generation i and an associated neutrino. From (2.12) we conclude that the produced neutrino is a mixture of the three neutrino mass eigenstates. To be more precise, the produced neutrino state is given by[3]

$$\nu_{\mathrm{L},i} = \sum_j U_{ij}^{*} \nu_{\mathrm{L},j}^{0}. \tag{2.13}$$

This neutrino state is now taken to propagate for a certain time before eventual detection via another weak interaction.

The simplest ansatz to describe the propagation of the neutrinos through space is via a simple plain wave approximation. Of course, this cannot be the correct quantum mechanical description as the neutrino wave function would not be localised in space. A more appropriate treatment can be given by using wave packets to describe the neutrinos, see for example [29, 30]. Another possible description is based on a quantum field theoretical approach where the propagating neutrinos are treated as virtual lines in a Feynman diagram connecting the production and detection processes (external wave packet models, see for example [31–34]). We will stick here to the simplest possible description, which suffices to illustrate the essential ideas.

In the plain wave approximation one assumes that one can consider a neutrino mass eigenstate with a well-defined energy E_j. The evolution in time of such a state is given by

$$\left|\nu_j^0(t)\right\rangle = e^{-iE_j t} \left|\nu_j^0\right\rangle, \tag{2.14}$$

where $\left|\nu_j^0\right\rangle = \left|\nu_j^0(t=0)\right\rangle$. As stated above, a mixture of the three neutrino mass eigenstates will be produced in weak interactions. Therefore the produced state will evolve in time according to

$$\left|\nu_i(t)\right\rangle = \sum_j U_{ij}^{*} e^{-iE_j t} \left|\nu_j^0\right\rangle. \tag{2.15}$$

After propagating for a certain amount of time, the neutrino is detected by observing a charged lepton which is produced in another weak interaction. Using

[3] Note that here and in the following the superscript 'PMNS' will be suppressed to keep the notation simple; furthermore we will skip the index L and switch to the Dirac notation when useful.

equation (2.12) one finds that the probability of detecting a charged lepton of flavour f in this manner is given by

$$P(\nu_i \to \nu_f) = |\langle \nu_f |\, \nu_i(t)\rangle|^2 = \left| \sum_j U_{ij}^* e^{-iE_j t} U_{fj} \right|^2 . \tag{2.16}$$

Taking into account that the neutrinos are extremely light and can be treated as ultrarelativistic particles we can approximate

$$E_j \approx p + \frac{m_j^2}{2p} \approx E + \frac{m_j^2}{2E}, \tag{2.17}$$

where $p \approx E$ is the momentum and $m_j = (M^\nu_{\text{diag.}})_{jj}$ the mass of the neutrino. Substituting this into equation (2.16) we find

$$P(\nu_i \to \nu_f) = \sum_{j,k} U_{ij}^* U_{fj} U_{ik} U_{fk}^* e^{-\frac{i\Delta m_{jk}^2 t}{2E}}, \tag{2.18}$$

where $\Delta m_{jk}^2 = m_j^2 - m_k^2$. Note that in addition we can use $L \approx t$ for relativistic neutrinos, where L is the distance travelled by the neutrino in the time t.

In order to easily compare experimental results concerning neutrino mixing with theoretical predictions, it is useful to parametrise U in the same way as the CKM matrix. In this so-called standard parametrisation the matrix is given in terms of three mixing angles θ_{12}, θ_{13} and θ_{23} in combination with one CP violating phase δ [35]. While this is the full story for Dirac neutrinos, two additional physical Majorana phases λ_2 and λ_3 occur for Majorana neutrinos[4]. As we do not know yet whether neutrinos are Dirac or Majorana particles, we will give here the most general expression, which reads [35]

$$U = \begin{pmatrix} c_{12}c_{13} & s_{12}c_{13} & s_{13}e^{-i\delta} \\ -s_{12}c_{23} - c_{12}s_{23}s_{13}e^{i\delta} & c_{12}c_{23} - s_{12}s_{23}s_{13}e^{i\delta} & s_{23}c_{13} \\ s_{12}s_{23} - c_{12}c_{23}s_{13}e^{i\delta} & -c_{12}s_{23} - s_{12}c_{23}s_{13}e^{i\delta} & c_{23}c_{13} \end{pmatrix} \begin{pmatrix} 1 & 0 & 0 \\ 0 & e^{i\lambda_2} & 0 \\ 0 & 0 & e^{i\lambda_3} \end{pmatrix}, \tag{2.19}$$

where we used the definitions $c_{ij} := \cos\theta_{ij}$ and $s_{ij} := \sin\theta_{ij}$. In the above parametrisation the angles take on values in the ranges $\theta_{ij} \in [0, \pi/2]$ and $\delta, \lambda_i \in [0, 2\pi]$. In order to obtain a quantitative measure for the magnitude of CP violation that is independent of the chosen parametrisation it is useful to define the rephasing-invariant Jarlskog variable [36–40]

$$J_{CP} = \Im\left(U_{\mu 3} U_{e2} U_{\mu 2}^* U_{e3}^*\right). \tag{2.20}$$

Using the standard parametrization of the mixing matrix this can be rewritten as

$$J_{CP} = \frac{1}{8} \sin 2\theta_{12} \sin 2\theta_{23} \sin 2\theta_{13} \cos\theta_{13} \sin\delta. \tag{2.21}$$

[4] The fact that neutrinos are electrically uncharged opens up the possibility that they could be their own antiparticles, and therefore be described mathematically by Majorana spinors, see appendix C.

From (2.21) we can easily derive that the value of J_{CP} corresponding to maximal CP violation is $|J_{CP}| = \frac{1}{6\sqrt{3}}$.

Note that the magnitude of CP violation can be experimentally investigated in neutrino oscillation experiments. On the other hand, using equation (2.18) one can show that oscillation experiments are not sensitive to the Majorana phases. Therefore these experiments are not able to answer the question whether neutrinos are of Dirac or Majorana type. Better suited to answer this question are experiments searching for neutrinoless double beta ($0\nu\beta\beta$), which occurs only if neutrinos are Majorana particles[5]. In particular, the neutrinoless double beta decay rate is sensitive to the Majorana phases, see section (2.4) for further details. Furthermore let us emphasise that only mass differences appear in the transition probability (2.18), so that oscillation experiments do not provide any information about the absolute mass scale of the neutrinos.

Note that in deriving the formulae above we have implicitly assumed that the neutrinos are propagating through vacuum. Matter effects have a strong impact on the observed mixing and can enhance the oscillation probability significantly compared to the vacuum probability. This has to be taken into account when analysing the experimental oscillation data. See for example [29, 30, 41, 42] and references therein for further details.

Neutrino sources which can be used to investigate neutrino oscillations include nuclear reactors, particle accelerators, the atmosphere and the sun. The corresponding experiments differ not only in the type of neutrinos which is initially produced, but also in the magnitude of L/E (recall that L is the distance the neutrinos travel before detection and E is the neutrino energy). Let us simplify equation (2.18) for two different limits of L/E, where in addition we assume[6] $|\Delta m^2_{21}| \ll |\Delta m^2_{31}| \simeq |\Delta m^2_{32}|$. For $L/E \ll 2/|\Delta m^2_{21}|$ we find the approximate expressions [42]

$$P(\nu_e \to \nu_\mu) \simeq s^2_{23} \sin^2 2\theta_{13} \sin^2\left(\frac{\Delta m^2_{31} L}{4E}\right), \tag{2.22}$$

$$P(\nu_e \to \nu_\tau) \simeq c^2_{23} \sin^2 2\theta_{13} \sin^2\left(\frac{\Delta m^2_{31} L}{4E}\right), \tag{2.23}$$

$$P(\nu_\mu \to \nu_\tau) \simeq c^4_{13} \sin^2 2\theta_{23} \sin^2\left(\frac{\Delta m^2_{31} L}{4E}\right), \tag{2.24}$$

[5] Note that effective higher dimensional operators can induce $0\nu\beta\beta$ decay even if neutrinos are Dirac particles to leading order. However such operators are suppressed by some higher energy scale like the Planck scale and lead to contributions that are negligible in comparison with the current experimental sensitivities; compare subsection 2.3.2. In this situation one usually refers to pseudo-Dirac particles, however we will refrain from explicitly mentioning this distinction in the following.

[6] This assumption can be justified by solar and atmospheric neutrino oscillation experiments, where one small mass squared difference $\Delta m^2_\odot \simeq 8\times10^{-5}\text{eV}^2$ and one larger difference $\Delta m^2_{\text{atm.}} \simeq 2\times10^{-3}\text{eV}^2$ is observed.

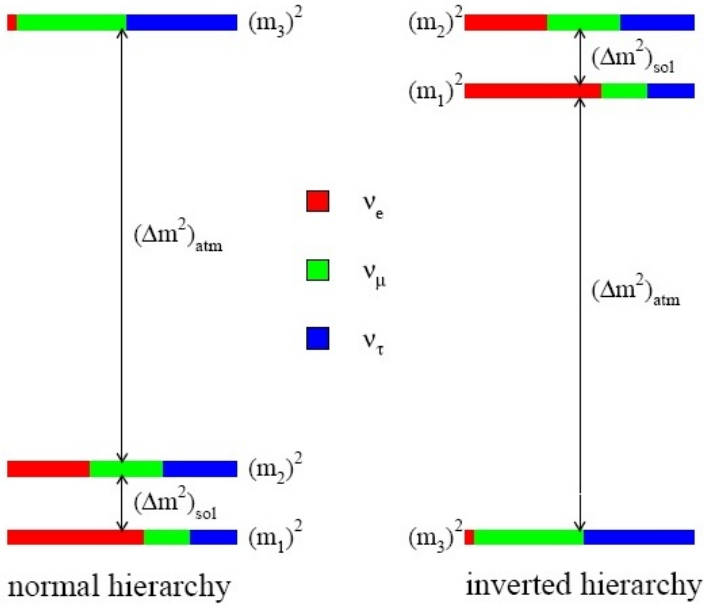

Figure 2.1: The two different neutrino mass orderings which are compatible with the oscillation data, taken from [43]. The colours denote the flavour decomposition of the mass eigenstates ν_1, ν_2 and ν_3.

$$P(\nu_e \to \nu_e) \simeq 1 - \sin^2 2\theta_{13} \sin^2 \left(\frac{\Delta m^2_{31} L}{4E} \right). \tag{2.25}$$

On the other hand, in the limit $L/E \gg 2/|\Delta m^2_{31}|$ we find [42]

$$P(\nu_e \to \nu_e) \simeq c^4_{13} \left(1 - \sin^2 2\theta_{12} \sin^2 \left(\frac{\Delta m^2_{21} L}{4E} \right) \right) + s^4_{13}. \tag{2.26}$$

The former limit is relevant for atmospheric (e.g. MACRO, IMB, Kamiokande, Super-Kamiokande), reactor (e.g. Double Chooz, RENO, Daya Bay) and accelerator (e.g. MiniBooNE, OPERA, T2K) neutrino experiments, whereas the latter is relevant for solar neutrino (e.g. Homestake, SNO, Borexino) and very long baseline reactor (e.g. KamLAND) experiments. Note that in the above expressions we have not taken matter effects into account. However, we can already see that the different types of experiments are sensitive to different mixing angles and mass differences. We refer the reader to the literature for a more detailed analysis (see e.g. [42] and references therein). Combining the results of the different experiments one can perform a global analysis of the data to extract the values of the mixing angles and mass differences. The results of such an analysis are summarised in table 2.3. Note that more recent results from Double Chooz, RENO and Daya Bay suggest a stronger bound on $\sin^2 \theta_{13}$. We will therefore sometimes also take into account the results of the newest, as yet unpublished, analysis of [44], which yields

$$\sin^2 \theta_{13} = 0.022^{+0.0033}_{-0.0030}. \tag{2.27}$$

Parameter	Best fit $\pm 1\sigma$	2σ range	3σ range
Δm^2_{21} $[10^{-5}\text{eV}^2]$	$7.59^{+0.20}_{-0.18}$	$7.24 - 7.99$	$7.09 - 9.19$
Δm^2_{31} $[10^{-3}\text{eV}^2]$	$2.50^{+0.09}_{-0.16}$ $-2.40^{+0.08}_{-0.09}$	$2.25 - 2.68$ $-(2.23 - 2.58)$	$2.14 - 2.76$ $-(2.13 - 2.67)$
$\sin^2\theta_{12}$	$0.312^{+0.017}_{-0.015}$	$0.28 - 0.35$	$0.27 - 0.36$
$\sin^2\theta_{23}$	$0.52^{+0.06}_{-0.07}$ 0.62 ± 0.06	$0.41 - 0.61$ $0.42 - 0.61$	$0.39 - 0.64$
$\sin^2\theta_{13}$	$0.013^{+0.007}_{-0.005}$ $0.016^{+0.008}_{-0.006}$	$0.004 - 0.028$ $0.005 - 0.031$	$7.29 \times 10^{-4} - 0.0529$
δ	$-0.61^{+0.75}_{-0.65}\pi$ $-0.41^{+0.65}_{-0.70}\pi$	$0 - 2\pi$	$0 - 2\pi$

Table 2.3: Neutrino oscillation parameters from a global analysis [15, 45]. The upper values belong to normal, the lower to inverted neutrino mass ordering.

The oscillation experiments do not yet provide any information about the sign of the mass difference Δm^2_{31}. Correspondingly, one distinguishes two different scenarios; $\Delta m^2_{31} > 0$ is referred to as normal mass ordering or normal hierarchy, whereas the possibility $\Delta m^2_{31} < 0$ is referred to as inverted mass ordering or inverted hierarchy. The two different possible cases are illustrated in figure 2.1, where in addition the decomposition of a mass eigenstate in terms of the flavour eigenstates are shown.

As already mentioned above, neutrino oscillation experiments also provide no information about the absolute mass scale of the neutrinos. Restricting the absolute neutrino mass scale is possible via experiments that investigate beta decay or from cosmological observations. Another possibility is given by experiments which search for neutrinoless double beta decay ($0\nu\beta\beta$). Since the latter is only possible if neutrinos have Majorana rather than Dirac character (keep in mind the comments in footnote [5]), we will first discuss the differences between Majorana and Dirac mass terms and postpone the discussion of the absolute mass scale to section 2.5.

2.3 Neutrino mass models

As discussed in the previous section, the observation of neutrino oscillations implies that at least two neutrinos must have a non-zero mass. Let us point out that

even without this experimental confirmation, massive neutrinos would be favoured also from a theoretical point of view. This is because left-handed neutrinos are the only fermions in the SM which do not appear in combination with a corresponding right-handed $SU(2)_{\mathrm{L}}$ singlet, which seems quite unnatural. In the SM one does not consider such right-handed neutrinos in order to prevent the neutrinos from obtaining a mass, but there exists no fundamental symmetry principle explaining why right-handed neutrinos should be absent.

If one considers introducing right-handed partners for the neutrinos, the neutrinos would obtain masses via the 'normal' Higgs-fermion Yukawa interaction discussed in section 2.1, just like the other SM fermions. However, when giving mass to the neutrinos in this standard manner one is confronted with the question why neutrino masses are so much smaller than the masses of the other SM fermions (from e.g. beta decay measurements the neutrino masses are expected to be at least five orders of magnitude smaller then the electron mass). One might be tempted to point out that a large hierarchy between the masses of the top quark and the electron (about five orders of magnitude) is already present in the SM as well. Nevertheless, in the SM fermions which correspond to the same $SU(2)$ doublet always have a comparable mass. This observation is no longer true when considering the masses of the charged leptons and neutrinos. Finding an explanation for this mass hierarchy is an open problem which theorists have tried to address for several decades. A directly correlated question is whether neutrinos are Dirac or Majorana particles. If neutrinos indeed turn out to be Majorana particles, then new mass terms that violate lepton number conservation by two units are possible. This opens up the possibility of implementing the well-known seesaw mechanism to explain the smallness of neutrino masses, see subsection 2.3.4[7].

In the following subsections we will discuss the differences between Dirac and Majorana neutrinos as well as considering in more detail different mass models which aim to explain the smallness of neutrino masses. Nevertheless one important model in this context, the so-called neutrinophilic two Higgs doublet model, will not be analysed here as this model will be extensively discussed in chapter 3.

2.3.1 Dirac neutrino mass term

Let us introduce three right-handed neutrinos ν_{R}, which are singlets of the SM gauge group, in addition to the SM particles. Note that the number of right-handed neutrinos is not restricted by the requirement of anomaly cancellation since the right-handed neutrinos are sterile (i.e. gauge singlets)[8]. Furthermore, we

[7] In addition the seesaw mechanism with its heavy right-handed neutrinos yields a framework to possibly explain the baryon asymmetry of the universe (baryogenesis from leptogenesis). See for example [41] and references therein for further details on this aspect.

[8] Note that adding new light degrees of freedom that are in equilibrium with the rest of the universe during the aera of big bang nucleosynthesis (BBN) will affect the predicted abundance of light elements. However, as long as no other particles are added to the SM, the sterile neutrinos considered here have sufficiently small couplings so as to decouple from the thermal bath early

assume for the moment that neutrinos are of Dirac type (see appendix C). In this case the neutrinos will obtain masses via the Higgs-fermion Yukawa interaction in the same way as the other SM fermions. The Yukawa term of the neutrinos is given in full analogy to the SM case by

$$-\mathcal{L} = \sum_{i,j=1}^{3} Y^{\nu}_{ij} \overline{\mathrm{L_{L,i}}} \widetilde{\Phi} \nu_{\mathrm{R,j}} + \mathrm{h.c.} \tag{2.28}$$

Recall that we had introduced the notation $\widetilde{\Phi} = i\sigma_2\Phi^*$. After EW symmetry breaking this yields the mass term

$$-\mathcal{L} = \overline{\nu_{\mathrm{L}}} M^{\nu} \nu_{\mathrm{R}} + \mathrm{h.c.}, \tag{2.29}$$

where $M^{\nu} = Y^{\nu} v/\sqrt{2}$ is the neutrino mass matrix (which, as discussed in section 2.2, is not necessarily diagonal in the flavour basis).

By comparing this to the analogous expressions for the charged lepton masses, it is clear that neutrino masses below the current upper limit of about 0.2 eV (see section 2.5) require that the Yukawa couplings of the neutrinos must be at least five orders of magnitude smaller than the Yukawa couplings of the corresponding charged leptons. From a theoretical point of view such a hierarchy between dimensionless couplings is disfavoured by naturalness arguments. One important model which can generate small neutrino masses without such a Yukawa hierarchy and without requiring Majorana mass terms is the neutrinophilic two Higgs doublet model, which will be the focus of chapter 3. However, let us first give a brief review on mass models involving Majorana neutrinos.

2.3.2 Pure Majorana mass term

Let us now assume that the neutrinos are Majorana particles, which are described by a Majorana spinor $\nu = \nu_{\mathrm{L}} + (\nu_{\mathrm{L}})^c$ (compare appendix C). Naively one could then try to introduce a Majorana mass term of the form $-1/2\overline{(\nu_{\mathrm{L}})^c} M \nu_{\mathrm{L}} + \mathrm{h.c.}$ However, this mass term is forbidden by gauge invariance since the left-handed neutrinos belong to an $SU(2)$ doublet and have non-vanishing hypercharge. In order to construct a gauge invariant mass term without introducing additional particles one has to consider the term [29]

$$\mathcal{L}_{\mathrm{eff.}} = \frac{f_{ij}}{M} (\mathrm{L}^T_{\mathrm{L},i} \sigma_2 \Phi) C^{\dagger} (\Phi^{\mathrm{T}} \sigma_2 L_{\mathrm{L},j}) + \mathrm{h.c.} \tag{2.30}$$

This term is of mass dimension five and therefore not renormalisable. Nevertheless it can be thought of as an effective operator, originating from integrating out new heavy particles in some underlying full theory. Then M lies at the energy scale of the high-energy theory (for example the Planck scale). After EW symmetry

enough. Therefore their introduction does not lead to a discrepancy with the observed element abundances. We will return to this point when introducing a second Higgs doublet in chapter 3.

breaking the effective operator (2.30) yields the neutrino mass $m_{ij} = f_{ij}v^2/M$. Hence neutrino masses arising in this manner are suppressed by the energy scale of the renormalisable theory.

A second possibility is to introduce an additional isotriplet Higgs field Δ with hypercharge Y=2 and mass m_Δ. This gives rise to a renormalisable Majorana mass term of the form [42]

$$-\mathcal{L} = \sum_{i,j=1}^{3} f_{ij}^{\Delta} \mathrm{L}_{\mathrm{L},i}^{\mathrm{T}} C i\sigma_2 \mathbf{\Delta} \mathrm{L}_{\mathrm{L},j} + \mathrm{h.c.}, \tag{2.31}$$

where $\mathbf{\Delta}$ is given in terms of the components of the isotriplet Δ by

$$\mathbf{\Delta} = \begin{pmatrix} \Delta^+ & \sqrt{2}\Delta^{++} \\ \sqrt{2}\Delta^0 & -\Delta^+ \end{pmatrix}. \tag{2.32}$$

This term yields neutrino masses which are proportional to $1/m_\Delta$. Hence by ensuring that the additional Higgs triplet is heavy enough, one can generate small neutrino masses while keeping the neutrino Yukawa couplings of the order of the charged lepton Yukawa couplings. This mechanism is referred to as type-II seesaw. See for example [42] and references therein for a discussion of the phenomenology of Higgs triplet models. We will not pursue this direction further as the main focus of this work will lie on Dirac neutrinos.

2.3.3 Majorana and Dirac mass term

In a more general context let us now consider simultaneously introducing mass terms of both Dirac and Majorana type in the neutrino sector[9]. Recall that in order to allow for a Dirac mass term we have to introduce right-handed neutrinos. As stated above, the number of such neutrinos is in principle arbitrary (assuming that bounds from cosmology can be satisfied, see footnote **??**), but in analogy to the SM fermion content we will introduce three right-handed neutrinos. Then the most general mass term is given by [42]

$$\mathcal{L}_{\mathrm{D+M}} = \overline{\nu_{\mathrm{L}}} m_{\mathrm{D}}^* \nu_{\mathrm{R}} + \frac{1}{2}\overline{(\nu_{\mathrm{L}})^c} m_L \nu_{\mathrm{L}} + \frac{1}{2}\overline{(\nu_{\mathrm{R}})^c} m_R^* \nu_{\mathrm{R}} + \mathrm{h.c.}, \tag{2.33}$$

where m_{D} and $m_{\mathrm{L,R}}$ are complex 3×3 matrices with the Majorana type mass matrices $m_{\mathrm{L,R}}$ symmetric (see appendix B). The Majorana mass term for the left-handed neutrinos has to either be an effective mass term or requires the introduction of a new Higgs field, as discussed in subsection 2.3.2. In contrast, the corresponding term for the right-handed neutrinos can be introduced directly without violating gauge invariance, as these neutrinos are sterile. Let us combine left- and right-handed neutrinos into the vector

$$n_{\mathrm{L}} := \begin{pmatrix} \nu_{\mathrm{L}} \\ (\nu_{\mathrm{R}})^c \end{pmatrix} \tag{2.34}$$

[9] As we will see below the neutrinos will in this context be described by Majorana spinors despite the presence of a so-called Dirac mass term.

and define the corresponding 6×6 mass matrix

$$M^\nu = \begin{pmatrix} m_\mathrm{L} & m_\mathrm{D} \\ m_\mathrm{D}^T & m_\mathrm{R} \end{pmatrix}. \tag{2.35}$$

The Lagrangian (2.33) then simply becomes

$$\mathcal{L}_\mathrm{D+M} = \frac{1}{2}\overline{(n_\mathrm{L})^c} M^\nu n_\mathrm{L} + \mathrm{h.c.} \tag{2.36}$$

Since M^ν is symmetric we can bring it into a diagonal form by

$$M^\nu_\mathrm{diag.} = U^\mathrm{T} M^\nu U, \tag{2.37}$$

where U is a suitable unitary 6×6 matrix (compare also appendix B). The resulting neutrino mass entries in $M^\mathrm{diag.}$ are real and non-negative. The mass term then takes the form

$$\mathcal{L}_\mathrm{D+M} = \frac{1}{2}\overline{(n^0_\mathrm{L})^c} M^\nu_\mathrm{diag.} n^0_\mathrm{L} + \mathrm{h.c.} \tag{2.38}$$

in terms of the mass eigenstates $n^0_\mathrm{L} = {U^\nu_\mathrm{L}}^\dagger n_\mathrm{L}$. Rewritten in this way it is clear that the resulting mass term is a Majorana mass term for the six Majorana fields $n^0_i = n^0_{\mathrm{L},i} + (n^0_{\mathrm{L},i})^c$, which by definition clearly obey the Majorana condition. This observation clarifies our statement above that the occurrence of a Dirac mass term does not imply that the neutrinos can be described by a Dirac spinor. The resulting neutrinos can thus be of Dirac type only if the diagonal elements in M vanish will.

2.3.4 Seesaw mechanism

As already stated above we aim to explain the large difference between the masses of the neutrinos and the corresponding charged leptons of the same generation, as this hierarchy does not occur in the quark sector. A very elegant way to explain this relative lightness of the neutrinos is the seesaw mechanism [46–50]. We start from the Lagrangian given by (2.33), allowing for three right-handed neutrinos. Let us assume $m_\mathrm{L} \simeq 0$, which can be justified by the arguments given in subsection 2.3.2. Furthermore we consider the case where $m_\mathrm{D} \ll m_\mathrm{R}$ (i.e. the right-handed neutrinos are assumed to be very heavy). Note that unlike the case of the left-handed neutrinos, the Majorana masses of the right-handed sterile neutrinos are not protected by the electroweak symmetry.

We can now consider the unitary 6×6 matrix

$$U = \begin{pmatrix} 1 & (m_\mathrm{D} m_\mathrm{R}^{-1})^* \\ -(m_\mathrm{D} m_\mathrm{R}^{-1})^\mathrm{T} & 1 \end{pmatrix}. \tag{2.39}$$

It is easy to check that to linear order in $m_\mathrm{D}/m_\mathrm{R}$ there holds

$$M^\nu_\mathrm{block} = U^\mathrm{T} M^\nu U \simeq \begin{pmatrix} -m_\mathrm{D} m_\mathrm{R}^{-1} m_\mathrm{D}^T & 0 \\ 0 & m_\mathrm{R} \end{pmatrix}. \tag{2.40}$$

Hence the matrix M^{ν}_{block} is block-diagonal to leading order of $m_{\text{D}}/m_{\text{R}}$. The upper block belongs to three light Majorana neutrinos, which are predominantly composed of the active left-handed neutrinos. On the other hand the lower block describes three heavy Majorana neutrinos, composed mostly of the sterile right-handed neutrinos. If we assume that m_{R} is of the order of the GUT scale, i.e. $m_{\text{R}} \simeq \mathcal{O}(10^{15}\text{ GeV})$ and m_{D} of the order of the EW scale, i.e. $m_{\text{D}} \simeq \mathcal{O}(200\text{ GeV})$ we find $m_{\text{D}} m_{\text{R}}^{-1} m_{\text{D}}^{T} \simeq \mathcal{O}(10^{-2}\text{ eV})$. Hence this so-called seesaw mechanism generates small neutrino masses without requiring that the Yukawa couplings are much smaller than the Yukawa couplings of the charged leptons of the same generation. The mechanism described here is sometimes also referred to as type-I seesaw.

The type-II seesaw mechanism was already introduced in (2.3.2). Another variation on the same theme can be constructed by assuming that the three additional right-handed neutrinos belong to an $SU(2)$ triplet Σ with hypercharge 0. The Yukawa term then yields neutrino masses which are suppressed by the triplet mass. This mechanism is referred to as type-III seesaw. See for example [51] and references therein for further details.

2.4 Neutrinoless double beta decay

As has been repeatedly mentioned above, an important question that has yet to be answered experimentally is whether neutrinos are Majorana or Dirac particles. The possible Majorana nature of neutrinos can be experimentally probed by searching for neutrinoless double beta decays ($0\nu\beta\beta$ decay), in which a nucleus $A(Z,N)$ decays while emitting two electrons but no neutrinos. To be more precise the transition of the nucleus is described by

$$A(Z,N) \to A(Z \pm 2, N \mp 2) + 2e^{\mp}. \tag{2.41}$$

By the Schechter-Valle theorem [52], this process is possible only if the neutrinos are Majorana particles. Note that lepton number is violated by two units in this decay, which is not possible in the SM context. However, note that no fundamental principle is known yet that enforces lepton number conservation and that this conservation law in the SM only results from an accidental symmetry of the SM Lagrangian. Figure 2.2 shows the Feynman diagram for the process. The corresponding amplitude of the process depends on the Majorana masses m_i^{ν} of the active neutrinos through the combination

$$A(0\nu\beta\beta) \propto \sum_{i=1}^{3} \left(U_{ei}^{\text{PMNS}}\right)^2 m_i^{\nu} =: \langle m_{\nu_e} \rangle \,. \tag{2.42}$$

The parameter $\langle m_{\nu_e} \rangle$ defined in this manner is frequently called the effective neutrino mass.

The decay rate depends not only on the transition amplitude (2.42), but also on the phase space factor and the nuclear matrix element. The calculation of the

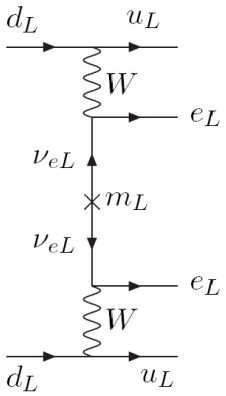

Figure 2.2: Feynman diagram of the $0\nu\beta\beta$ decay, taken from [42].

latter is often problematic and can give rise to large theoretical errors, which can limit the comparability of theory and experiment.

So far, neutrinoless double beta decay has not been detected experimentally. The best experimental upper limit for the effective Majorana mass is given by the Heidelberg-Moscow experiment [53, 54]

$$\langle m_{\nu_e} \rangle \lesssim 0.2 - 0.6 \text{ eV}, \tag{2.43}$$

where the different values arise from different calculations of the nuclear matrix element. The above limit on the effective mass corresponds to a limit on the half life of $T_{1/2}^{0\nu\beta\beta} \gtrsim 1.9 \times 10^{25}$ years [55]. There are a number of experiments either currently in planning or already running, which will improve the experimental sensitivity by at least one order of magnitude.

As a final side comment let us note that the $0\nu\beta\beta$ decay rate depends not only on the lightest neutrino mass, but also on the mass ordering of the neutrinos (at least for a wide range of values for the mass of the lightest neutrino). This implies that the detection of $0\nu\beta\beta$ decay could give rise to the possibility of distinguishing between the cases of normal and inverted hierarchy [55].

In this work we will focus on a detailed analysis of a particular model for Dirac neutrinos. This means that $0\nu\beta\beta$ decay will be forbidden at the renormalisable level in our model. Therefore we refrain from giving a more detailed analysis of the neutrinoless double beta decay here and refer the interested reader to the recent review [55] and the references given therein for further information.

2.5 Absolute scale of neutrino masses

Past experimental efforts of probing the absolute scale of neutrino masses have focused mainly on two different approaches. The first approach relies on precisely measuring the energy spectrum of charged leptons emitted in β decay, which yields

information on the quantity

$$m_\beta := \sqrt{\sum_i |U_{ei}|^2 m_i^2}. \tag{2.44}$$

However, at the time of writing the most precise investigations of Tritium β decay in the Mainz [11] and Troitsk [56] experiments have succeeded only in establishing an upper bound on this parameter. The more stringent bound has been obtained by the Mainz neutrino mass experiment and is given by [11]

$$m_\beta < 2.3 \text{ eV at } 95\% \text{ confidence level.} \tag{2.45}$$

The currently running KATRIN experiment aims to improve the sensitivity for this parameter by an order of magnitude [57]. It remains to be seen whether this added sensitivity is sufficient to obtain a measured value for m_β, or whether it will only improve the upper bound. Finally, let us also recall that besides classical beta decay experiments, searches for $0\nu\beta\beta$ decay can also yield bounds on the absolute neutrino mass, as the effective mass $\langle m_{\nu_e} \rangle$ defined in (2.42) is a function of the lightest neutrino mass.

The second main avenue of investigation concerning the absolute neutrino mass scale comes from cosmological measurements. The present contribution of neutrinos to the energy density of the universe can be evaluated either from data on the large scale structure of the universe [58] or from measurements of the temperature fluctuations of the cosmic microwave background (CMB). This gives rise to an upper limit on the summed neutrino masses. Currently the most stringent bound comes from the WMAP data on the CMB, which yields [12, 13]

$$\sum m_\nu := \sum_{i=1}^{3} |m_{\nu,i}| \lesssim 0.67 \text{ eV} \quad \text{at } 95\% \text{ confidence level.} \tag{2.46}$$

Taking the observed mass squared differences into account this can be easily translated into an upper limit on each neutrino mass

$$m_{\nu,i} \lesssim 0.2 \text{ eV}, \qquad i = 1, 2, 3. \tag{2.47}$$

See for example [41] for further details on this topic.

2.6 Flavour symmetries

An important theoretical problem lies in finding an explanation for the many free parameters that are present in the flavour sector of the Standard Model. Adding neutrino masses to the theory further exacerbates this problem as it leads to an increase of the total number of free parameters in the Lagrangian. In this way there arise three additional leptonic mixing angles, three neutrino masses and one

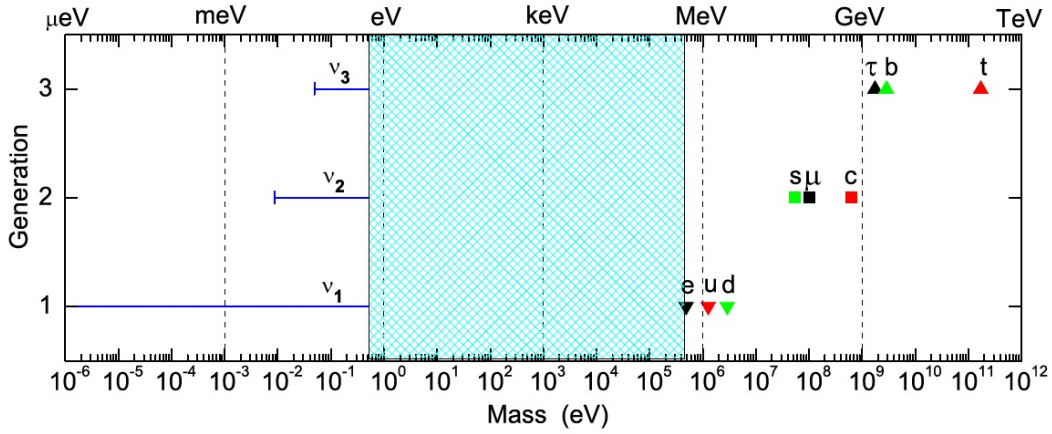

Figure 2.3: Hierarchy between the masses of the SM particles, taken from [59]. Normal mass ordering is assumed for the neutrino masses.

CP violating phase, as well as two additional Majorana phases if the neutrinos are Majorana particles (compare also (2.19)).

A closely correlated theoretical question concerns finding a fundamental principle that explains not only the number but also the observed relationships between the flavour parameters. The main idea in tackling this problem is to extend the symmetry group of the theory G_{gauge} by some additional family or flavour symmetry G_{flavour}, so that the full Lagrangian is invariant under $G_{\text{gauge}} \times G_{\text{flavour}}$. These flavour symmetries are sometimes also referred to as horizontal symmetries, because they describe symmetries between different particle generations. While in many applications G_{flavour} is taken to be a global symmetry, this is not a necessary condition and the extended group can also be gauged. Note that the introduction of the additional symmetry usually necessitates also the introduction of new scalar fields (and, in the gauged case, new gauge bosons). In order to have a predictive theory, this spectrum of new particles should not be too large, which is one of the major problems that arise in models attempting to explain the flavour structure in this manner.

Let us first have a look at the measured mass pattern of the SM particles, which is illustrated in figure 2.3. The figure shows a significant hierarchy between the different fermion generations. In particular, one approximately finds [51]

$$\begin{aligned} \frac{m_e}{m_\mu} \sim \frac{m_u}{m_c} \sim \frac{m_c}{m_t} \sim \lambda^4, \\ \frac{m_\mu}{m_\tau} \sim \frac{m_d}{m_s} \sim \frac{m_s}{m_b} \sim \lambda^2, \end{aligned} \tag{2.48}$$

where λ is defined in terms of the Cabibbo angle θ_C [24] by $\lambda = \sin\theta_C \approx 0.22$.

A popular mechanism that is often implemented to explain this hierarchy is the Froggatt-Nielsen mechanism [60]. The underlying idea is to introduce a global $U(1)_{\text{FN}}$ flavour symmetry which is spontaneously broken by the vev of a new

Field	$e_{\rm R}$	$\mu_{\rm R}$	$\tau_{\rm R}$	Φ_{FN}
FN charge	3	1	0	-1

Table 2.4: Assignment of Froggatt-Nielsen charges.

scalar field Φ_{FN}. This field is a singlet of the SM gauge group but carries charge under $U(1)_{\rm FN}$, the so-called Froggatt-Nielsen (FN) charge. Such an additional scalar field charged under the flavour group is known as a flavon. Giving FN charges to the SM fermions as well will lead to a certain structure of the mass matrix, the precise form of which depends of the special choice of FN charges. In particular, when implementing an appropriate choice of charges one can obtain precisely the observed mass hierarchy of (2.48). Note that the theory has to be understood as an effective theory, where the heavy Froggatt-Nielsen fields of the full theory have been integrated out. Therefore effective operators proportional to $\epsilon := \langle\Phi_{FN}\rangle / M$ will appear in the effective theory, where M is the mass of the Froggatt-Nielson fields associated with the energy scale of the full theory and $\langle\Phi_{FN}\rangle$ denotes the vev of the FN field.

Let us illustrate the Froggatt-Nielsen principle in a very simple example, by introducing the global $U(1)_{FN}$ symmetry and assigning the FN charges given in table 2.4 to the right-handed charged leptons and to the FN flavon. Furthermore we assume that the other SM particles are kept uncharged. Hence only the Yukawa terms of the charged leptons in the SM Lagrangian will be modified by this additional symmetry. Without loss of generality we can assume that the lepton mass matrix is already diagonal, since $U_{\rm L}^{\ell\,\dagger}$ can be absorbed into a redefinition of the neutrino flavour eigenstates. After the EW and $U(1)_{FN}$ symmetries have been broken the Yukawa term of the charged leptons is given by

$$\begin{aligned} -\mathcal{L}_{\rm Yukawa} \supset\ & \frac{1}{\sqrt{2}} Y^e v \left(\frac{\langle\Phi_{FN}\rangle}{M}\right)^3 \bar{e}_{\rm L} e_{\rm R} + \frac{1}{\sqrt{2}} Y^\mu v \frac{\langle\Phi_{FN}\rangle}{M} \bar{\mu}_{\rm L}\mu_{\rm R} \\ & + \frac{1}{\sqrt{2}} Y^\tau v \bar{\tau}_{\rm L}\tau_{\rm R} + \text{h.c.}, \end{aligned} \tag{2.49}$$

where $v/\sqrt{2}$ is the vev of the SM Higgs field. Hence one finds

$$\begin{aligned} m_e &= \frac{1}{\sqrt{2}} Y^e v \epsilon^3, \\ m_\mu &= \frac{1}{\sqrt{2}} Y^\mu v \epsilon\,, \\ m_\tau &= \frac{1}{\sqrt{2}} Y^\tau v\,, \end{aligned} \tag{2.50}$$

and therefore $m_e/m_\mu \sim \epsilon^2$ and $m_\mu/m_\tau \sim \epsilon$, if the Yukawa couplings are taken to be of the same order. Choosing $\langle\Phi_{FN}\rangle$ and M in such a way that $\epsilon = \lambda^2$, we find that the hierarchy for the charged leptons in (2.48) is reproduced.

This simple model can be enlarged to a model that simultaneously describes both the hierarchy of the charged leptons and of the neutrinos. Note that off-diagonal elements in at least one of the mass matrices have to occur in this case, which leads to a prediction of the form of the leptonic mixing matrix. Models of this type have been considered extensively in the literature in an attempt to predict mass patterns and mixing matrices which are compatible with the experimental data for both the quark and lepton sectors. However, we will not pursue this direction further in this work. Additional details on FN models can be found in [30,61] and in the references given therein.

A different possible approach is to look for an underlying structure in the mixing matrices. The CKM matrix is reasonably close to the unity matrix [35], whereas the best fit values of the mixing angles and the Dirac phase for the leptons listed in table 2.3 show that a good first approximation to the observed mixing matrix is given by

$$|U_{13}^{\mathrm{PMNS}}| \approx 0, \quad |U_{23}^{\mathrm{PMNS}}| \approx \frac{1}{\sqrt{2}}, \quad |U_{12}^{\mathrm{PMNS}}| \approx \frac{1}{\sqrt{3}}. \tag{2.51}$$

Let us focus on the leptonic mixing matrix in the following. Adopting the approximate values of (2.51) results in the mixing matrix

$$U_{\mathrm{TBM}} = \begin{pmatrix} \sqrt{\frac{2}{3}} & \frac{1}{\sqrt{3}} & 0 \\ -\frac{1}{\sqrt{6}} & \frac{1}{\sqrt{3}} & -\frac{1}{\sqrt{2}} \\ -\frac{1}{\sqrt{6}} & \frac{1}{\sqrt{3}} & \frac{1}{\sqrt{2}} \end{pmatrix}, \tag{2.52}$$

which was first considered in [62]. This specific form of the leptonic mixing matrix is known as tribimaximal (TBM), where the name originates from the following two observations. If the neutrino mass matrix can be brought into a diagonal form via U_{TBM}, then the mass eigenstate ν_3 consists of a mixture of only two of the flavour eigenstates, namely ν_μ and ν_τ, which contribute equally. The mass eigenstate ν_2 on the other hand is composed of an equal mixture of all three flavour eigenstates[10].

Let us analyse in more detail what a mixing matrix in TBM form would imply for the structure of the mass matrices. If we assume that the charged lepton mass matrix is already diagonal, which can always be achieved by a suitable redefinition of the neutrino flavour eigenstates, the neutrino mass matrix has to fulfill (see appendix B)

$$(M_{\mathrm{diag.}}^{\nu})^2 = U_{\mathrm{TBM}}^{\mathrm{T}} M^{\nu} M^{\nu\,\dagger} U_{\mathrm{TBM}}. \tag{2.53}$$

[10] Note however that the TBM form of the mixing matrix is only a good first approximation to the measured values. In particular the non-vanishing of θ_{13} (see table 2.3), which was confirmed experimentally in the last year, makes models leading to tribimaximal mixing less attractive. Nevertheless, one can consider models which lead to the TBM form at first order and which admit suitable deviations, arising for example from next-to-leading order effects, yielding a mixing matrix that is compatible with the recent data. Let us postpone a more detailed discussion of this to chapters 4 and 5, where a model based on the group A_4 is presented.

This implies that the squared mass matrix has to take the form

$$M^\nu M^{\nu\,\dagger} = A_{\rm TBM} := \begin{pmatrix} x & y & y \\ y & x+v & y-v \\ y & y-v & x+v \end{pmatrix}, \tag{2.54}$$

where $x,\ y$ and v are real parameters. They can be related to the squared neutrino masses $(m_i^\nu)^2 = (M^\nu_{\rm diag})^2_{ii}$ by

$$x = \frac{2}{3}(m_1^\nu)^2 + \frac{1}{3}(m_2^\nu)^2, \quad y = -\frac{1}{3}(m_1^\nu)^2 + \frac{1}{3}(m_2^\nu)^2,$$
$$v = -\frac{1}{2}(m_1^\nu)^2 + \frac{1}{2}(m_3^\nu)^2. \tag{2.55}$$

Recall that if the neutrinos are Majorana particles the mass matrix has to be symmetric, see appendix B. In this case the above relation simplifies to

$$M^\nu_{\rm diag.} = U^T_{\rm TBM} M^\nu U_{\rm TBM}. \tag{2.56}$$

Then the neutrino mass matrix itself has to take the form given in relation (2.54), i.e. $M^\nu = A_{\rm TBM}$. Of course one must then also substitute m_i^ν instead of $(m_i^\nu)^2$ into (2.54) for Majorana neutrinos. Note that if $M^\nu = A_{\rm TBM}$, then $M^\nu M^{\nu\,\dagger}$ will automatically have the specific TBM form $A_{\rm TBM}$ as well.

From the discussion above we conclude that the specific form of the mixing matrix gives rise to a certain texture of the neutrino mass matrix. One expects that such a specific structure of the mass matrix could occur due to an underlying symmetry. We immediately see that the mass matrix given above is symmetric under $\mu \leftrightarrow \tau$ exchange. However, this underlying symmetry only partially explains the structure of the mass matrix, and an additional symmetry has to be found to explain the complete texture. To identify this additional symmetry let us start with a general 3×3 matrix

$$A = \begin{pmatrix} a & b & c \\ d & e & f \\ g & h & j \end{pmatrix} \tag{2.57}$$

and consider the matrices

$$S := \frac{1}{3}\begin{pmatrix} -1 & 2 & 2 \\ 2 & -1 & 2 \\ 2 & 2 & -1 \end{pmatrix} \qquad \text{and} \qquad A_{23} := \begin{pmatrix} 1 & 0 & 0 \\ 0 & 0 & 1 \\ 0 & 1 & 0 \end{pmatrix}. \tag{2.58}$$

Note that $S^2 = A_{23}^2 = \mathbb{1}$, so that both matrices can be viewed as generating the cyclic group $\mathbb{Z}_2$. If we require that the candidate mass matrix A is invariant under the action of S, i.e. $A = SAS$, A has to have the form

$$A = \begin{pmatrix} a & b & -a+c+d \\ -a+d+e & c & a+b-e \\ b+c-e & d & e \end{pmatrix}. \tag{2.59}$$

The action of the matrix A_{23} obviously describes the exchange of the second and third components of a vector, so that a mass matrix which is invariant under the action of A_{23} will be $\mu\tau$-symmetric. Therefore requiring that A is also invariant under the action of A_{23}, i.e. $A = A_{23}AA_{23} = SAS$, yields the form

$$A = \begin{pmatrix} a & b & b \\ b & a+c & b-c \\ b & b-c & a+c \end{pmatrix}. \tag{2.60}$$

This is exactly the form of (2.54) that is necessary for the matrix to be diagonalised by U_{TBM}. The above seems to suggest that requiring invariance of the neutrino mass matrix under S and A_{23} leads directly to TBM mixing. Recall however that the mixing matrix appearing in the weak interaction Lagrangian is composed of the matrices diagonalising the neutrino and the charged lepton mass matrices. This means that if we want to achieve TBM mixing while assuming that the neutrino mass matrix (respectively $M^{\nu\dagger}M^{\nu}$) is brought to the diagonal form via U_{TBM} as above, we must ensure that the lepton mass matrix is already diagonal. This requirement can also be cast in the form of a symmetry principle using the fact that [63]

$$M^{\ell}M^{\ell\,\dagger} \text{ diagonal} \Longleftrightarrow M^{\ell}M^{\ell\,\dagger}{=}T^{\dagger}M^{\ell}M^{\ell\,\dagger}T \text{ for any diagonal phase matrix } T.$$

For example one can consider specifically the matrix

$$T = \begin{pmatrix} 1 & 0 & 0 \\ 0 & \omega & 0 \\ 0 & 0 & \omega^2 \end{pmatrix} \tag{2.61}$$

with $\omega^3 = 1$. Since $T^3 = \mathbb{1}$, T generates the cyclic group $\mathbb{Z}_3$. Now requiring invariance of the neutrino mass matrix under S and A_{23} together with invariance of the lepton mass matrix under T guarantees tribimaximal mixing.

The considerations presented above form the starting point when trying to find an extension of the SM symmetry group which will lead to a mixing matrix in tribimaximal form. In particular we search for a finite group G_{flavour} which contains two subgroups G_S and G_T, generated by S and T respectively. Note that the choice of T taken above was not unique, and we could also have chosen a different diagonal phase matrix. For simplicity we restrict ourselves to matrices obeying $T^n = \mathbb{1}$, such that T generates the cyclic group $\mathbb{Z}_n$. If we now break the full flavour group G_{flavor} down to G_S in the neutrino sector and to G_T in the charged lepton sector, we obtain a TBM mixing matrix as long as we guarantee that the neutrino sector is in addition invariant under A_{23}. This latter requirement can be fulfilled either by taking $A_{23} \subset G_{\text{flavour}}$ or by a suitable choice of symmetry breaking mechanism (see chapter 4 for further details).

As mentioned above, imposing an additional flavour symmetry on the Lagrangian can lead to a proliferation of new particles belonging to the different representations of the group. To avoid negating the idea of predictivity underlying the

Group	Order	Irreducible representations	Presentation
$D_3 \sim S_3$	6	$1,\ 1',\ 2$	$A^3 = B^2 = (AB)^2 = \mathbb{1}$
D_4	8	$1_1,\ 1_2,\ 1_3,\ 1_4,\ 2$	$A^4 = B^2 = (AB)^2 = \mathbb{1}$
D_7	14	$1,\ 1',\ 2,\ 2',\ 2''$	$A^7 = B^2 = (AB)^2 = \mathbb{1}$
A_4	12	$1,\ 1',\ 1'',\ 3$	$A^3 = B^2 = (AB)^3 = \mathbb{1}$
$A_5 \sim PSL_2(5)$	60	$1,\ 3,\ 3',\ 4,\ 5$	$A^3 = B^2 = (BA)^5 = \mathbb{1}$
T'	24	$1,\ 1',\ 1'',\ 2,\ 2',\ 2'',\ 3$	$A^3 = (AB)^3 = R^2 = \mathbb{1}$ and $B^2 = R$
S_4	24	$1,\ 1',\ 2,\ 3,\ 3'$	$A^3 = B^4 = (BA^2)^2 = \mathbb{1}$
$\Delta(27) \sim \mathbb{Z}_3 \rtimes \mathbb{Z}_3$	27	$1_1, ...1_9,\ 3,\ \bar{3}$	
$PSL_2(7)$	168	$1,\ 3,\ \bar{3},\ 6,\ 7,\ 8$	$A^3 = B^2 = ((BA)^7 = \mathbb{1}$ and $(B^{-1}A^{-1}BA)^4 = \mathbb{1}$
$T_7 \sim \mathbb{Z}_7 \rtimes \mathbb{Z}_3$	21	$1,\ 1',\ \bar{1}',\ 3, \bar{3}$	$A^7 = B^3 = \mathbb{1}$ and $AB = BA^4$

Table 2.5: Discrete groups often used in flavour models [63].

introduction of flavour symmetries in the first place, one of course tries to keep the flavour group as simple as possible. Table 2.5 shows a list of the simplest discrete groups that have been considered in this context in the literature (see e.g. [63] for a list of references on the subject). For further details on the mathematical properties of the groups listed see for example [64]. A very popular choice is the A_4 group, since the relative simplicity of the group representations and the field content is quite attractive. In chapters 4 and 5 we will consider a model based on the A_4 symmetry for the case of Dirac neutrinos, which has not yet been analysed in the existing literature. However, in the next chapter we will first discuss neutrinophilic two Higgs doublet models, which yield a natural framework for explaining the smallness of neutrino masses.

Chapter 3

The neutrinophilic two Higgs doublet model

When looking to extend the Standard Model, for example while aiming to explain the observed mass hierarchies and textures mentioned in the previous chapter, one of the simplest possibilities is to extend the Higgs sector. Starting with the seminal work of Lee [65], an idea that has been extensively studied in the subsequent literature relies on the introduction of a copy of the usual Higgs field. Such so-called two Higgs doublet models (2HDMs) therefore include two complex scalar fields in the representation $(1, 2, 1)$ of the SM gauge group $SU(3)_{\mathrm{C}} \times SU(2)_{\mathrm{L}} \times U_Y(1)$.

There are a wide variety of different aspects underlying the popularity of these 2HDMs. For example, the presence of an additional Higgs doublet is a necessary condition for the theory to admit an embedding into a supersymmetric (SUSY) theory. Another point is that the extended scalar spectrum in 2HDMs may give rise to additional sources of CP violation, which can play an important role in explaining the observed baryon-antibaryon asymmetry of the universe. In this work we will not go into much more detail on these issues, referring to the reviews [66,67] and references therein for a detailed overview of the different aspects relating to two Higgs doublet models. Instead, we will focus our attention on the effects which arise in the lepton sector when introducing a second Higgs.

An important point to consider when introducing a second Higgs is that one has to clarify the Yukawa coupling structure, as new possibilities for these couplings arise. In particular, we have to specify which matter fields couple to which Higgs field, which can have wide-ranging phenomenological consequences. One important constraint on the possible choices comes from the strong experimental bounds on flavour changing neutral currents (FCNCs)[1]. The buzzword in this context is the Paschos-Glashow-Weinberg theorem, which states that in order to avoid

[1]Suppression of FCNCs constitutes a big problem in all 2HDMs and additional symmetries often need to be imposed in order to be compatible with the experimental bounds. See section 3.1 for further details.

Type	Yukawa coupling structure
I	all fermions are coupled to only one of the Higgs fields
II	up-type quarks are coupled to Φ_2 down-type quarks and leptons are coupled to Φ_1
X (lepton-specific)	quarks are coupled to Φ_2 leptons are coupled to Φ_1
Y (flipped)	up-type quarks and leptons are coupled to Φ_2 down-type quarks are coupled to Φ_1
ν2HDM (neutrinophilic)	all quarks and charged leptons are coupled to Φ_2 neutrinos are coupled to Φ_1

Table 3.1: Couplings of the fermions to the two Higgs fields Φ_1 and Φ_2 in different types of 2HDMs.

FCNCs at tree-level one has to ensure that each fermion couples only to exactly one of the Higgs fields [68, 69]. Such a separation of the couplings of the two Higgs fields to distinct fermion sectors can be achieved by imposing an additional symmetry, such as a $\mathbb{Z}_2$ or global $U(1)$ symmetry, and assigning charges to the Higgs fields and fermions in an appropriate way. Restricting to models meeting the requirements of the Paschos-Glashow-Weinberg theorem leads to a finite list of distinct 2HDMs, which are listed in table 3.1[2]. All these models have been studied in great detail (see [67] for a list of references).

One very interesting model in the context of neutrino physics is the neutrinophilic two Higgs doublet model (ν2HDM). In this type of model one can achieve small neutrino masses by engineering a hierarchy between the vevs of the two Higgs fields, negating the need for a large hierarchy between the different Yukawa coupling constants or for variants of the seesaw mechanism discussed in subsection 2.3.4. Note that, as we will see, a hierarchy between the Higgs vevs can arise more naturally than a similar hierarchy between dimensionless Yukawa couplings, which would have to be imposed by hand. The ν2HDM was first considered by Ma in [70] and has been studied in great detail over the last years (ν2HDMs for Majorana neutrinos have been considered in [71–77], whereas in [14, 78–80] only Dirac mass terms were allowed). As we are interested in aspects pertaining to neutrino physics in this work, we focus on the ν2HDM in the following.

In order to generate a coupling of the neutrinos to a Higgs field we introduce three

[2] See [67] for an overview including also models with tree-level FCNCs.

Fields	Q_L	u_R	d_R	L_L	ℓ_R	ν_R	Φ_1	Φ_2	gauge bosons
$U(1)$ charge	0	0	0	0	0	1	1	0	0

Table 3.2: Assignment of $U(1)$ charges.

right-handed neutrinos in the singlet representation of the SM gauge group [3]. In this work we will consider the case of Dirac neutrinos, which, as discussed in section 2.3.3, requires Majorana mass terms to be absent. Introducing a global $U(1)$ symmetry and assigning charges to the particles as listed in table 3.2 yields the Yukawa structure of the ν2HDM (see table 3.1).

Note that this charge assignment automatically forbids Majorana mass terms for the right-handed neutrinos. This would not have been achieved if we had introduced a $\mathbb{Z}_2$ symmetry instead of the $U(1)$ symmetry (assigning the $\mathbb{Z}_2$ charges in a similar way)[4]. This implies that lepton number survives as an accidental symmetry of the considered model, even if the $U(1)$ symmetry is spontaneously broken or softly broken in the scalar potential [14]. Therefore in the considered model neutrinoless double beta decay is absent at the renormalisable level. Note that of course higher dimensional effective operators can still induce lepton number violation just as in the SM. Assuming however that such higher dimensional operators are suppressed by the Planck scale, this leads to $0\nu\beta\beta$ decay rates well below the sensitivity of currently running and planned experiments.

The 2HDM defined by the charge assignments above was first considered by Davidson and Logan in [14]. We will now proceed to analyse this model in full detail, reviewing and extending the results of Davidson and Logan. In particular we will take into account updated bounds on the neutrino oscillation parameters and neutrino masses when analysing the phenomenology of the model. Furthermore we will analyse the consequences for the Higgs phenomenology that arise when neutrino mass textures and leptonic mixing matrix are generated by a specific A_4 flavour symmetry model in chapter 5.

3.1 The scalar potential

Let us now analyse the scalar potential involving the two Higgs fields. The fields will be denoted as

$$\Phi_1 = \begin{pmatrix} \Phi_1^+ \\ \Phi_1^0 \end{pmatrix}, \qquad \Phi_2 = \begin{pmatrix} \Phi_2^+ \\ \Phi_2^0 \end{pmatrix}, \tag{3.1}$$

[3] See subsection 3.1 for a brief discussion of cosmological bounds on additional light neutrinos which arise in the context of a 2HDM.

[4] See also the next section for a discussion of further differences between models with $U(1)$ and $\mathbb{Z}_2$ symmetry.

where we have used a suggestive notation to distinguish the components that are respectively charged and neutral under the electromagnetic $U(1)_{\rm em}$ symmetry. In the following we consider the scalar potential for the two Higgs fields given by

$$\begin{aligned} V &= m_{11}^2 \Phi_1^\dagger \Phi_1 + m_{22}^2 \Phi_2^\dagger \Phi_2 - (m_{12}^2 \Phi_1^\dagger \Phi_2 + \text{h.c.}) + \frac{1}{2}\lambda_1 (\Phi_1^\dagger \Phi_1)^2 \\ &\quad + \frac{1}{2}\lambda_2 (\Phi_2^\dagger \Phi_2)^2 + \lambda_3 (\Phi_1^\dagger \Phi_1)(\Phi_2^\dagger \Phi_2) + \lambda_4 (\Phi_1^\dagger \Phi_2)(\Phi_2^\dagger \Phi_1). \end{aligned} \tag{3.2}$$

A few comments are in order regarding this choice of potential. In addition to all renormalisable couplings compatible with our global $U(1)$ symmetry we have also allowed for an explicit soft breaking term $m_{12}\Phi_1^\dagger \Phi_2 + \text{h.c.}$ This term was included in order to prevent the occurrence of an unwanted Goldstone boson, which would have appeared if the $U(1)$ symmetry was broken only spontaneously. Note that allowing for the explicit breaking term in the scalar potential does not lead to FCNCs at tree-level [67].

Let us also briefly consider what would change if we had decided to impose a $\mathbb{Z}_2$ symmetry instead of the $U(1)$ symmetry, giving charges to the Higgs fields and fermions in a similar way as before. In this case an additional term of the form $+\frac{1}{2}(\lambda_5 (\Phi_1^\dagger \Phi_2)^2 + \text{h.c.})$ would arise in the scalar potential, which is invariant under $\mathbb{Z}_2$ but not under $U(1)$. This term is sufficient to lift the flat direction in the potential and eliminate the would-be Goldstone boson without requiring the introduction of an explicit breaking term. Note however that in the absence of the explicit breaking term involving m_{12}^2 in the neutrinophilic $\mathbb{Z}_2$ model, one still obtains a very light Higgs scalar with mass $m^2 \sim \lambda_1 v_1^2$ (see [78, 79])[5].

The presence of this very light scalar leads to severe cosmological bounds on the neutrino Yukawa couplings. By analysing measurements of supernova neutrino fluxes, of the energy loss of supernovae and of the precise form of the CMB spectrum one obtains the bounds $Y_i^\nu \lesssim 3.5 \times 10^{-5}$ for the Yukawa coupling of $\nu_i,\ i = e, \mu, \tau$ [81]. Furthermore note that the standard theory of big bang nucleosynthesis (BBN) constrains the effective number of additional relativistic degrees of freedom and therefore the number of additional light neutrinos during BBN to $\delta N_\nu < 1.44$ [82]. When introducing three right-handed neutrinos one must therefore ensure that they decouple from the thermal bath at sufficiently high temperature; for example consistency with observations is achieved if this decoupling temperature is of the order of the quark-hadron transition temperature at ca. 200-400 MeV. In the $\mathbb{Z}_2$ model without explicit breaking, the couplings of the neutrinos to the light scalar are not sufficiently suppressed to fulfill these requirements. The authors of [78] argue that the BBN constraint can be circumvented in models of non-standard cosmology, however even then the other restrictions on the Yukawas mentioned above remain in force. As we will see, introducing the explicit breaking term involving m_{12}^2 increases the mass of the would-be light scalar

[5] Here v_1 is the vev of the additional Higgs. In order to allow for naturally small neutrino masses in the model, one of the Higgs vevs, here v_1, has to be of order eV.

sufficiently to significantly relax the abovementioned constraints on the Yukawa couplings.

These observations lead to the conclusion that explicit breaking must be considered in both the $\mathbb{Z}_2$ and $U(1)$ models. As already mentioned above, using the $U(1)$ symmetry has the added advantage of automatically forbidding Majorana mass terms. Therefore we will stick to the $U(1)$ symmetry and the potential (3.2) in the following. However, our results can be easily adapted to the case of the $\mathbb{Z}_2$ symmetry.

Note that in our model we must nevertheless ensure that the right-handed neutrinos decouple from the thermal bath at the quark hadron-transition temperature, which gives a bound on the Yukawa couplings. In the absence of the light neutral Higgs scalar mentioned above, the dominant interaction channel between the neutrinos and the thermal bath involves exchange of the charged Higgs. The exact bound on the Yukawa couplings therefore depends on the charged scalar mass given in (3.21) and on the values of the leptonic mixing angles. However, this bound is much less severe than the bounds that arise from the presence of a light neutral Higgs, and Yukawa couplings of order one can be obtained for reasonable values of the charged Higgs mass. A slightly more detailed discussion of these estimates can be found in [14].

After these preliminary remarks, we return to the analysis of the potential given in (3.2). First of all we immediately note that the parameters m_{11}^2, m_{22}^2 and $\lambda_{1,2,3,4}$ must be real to guarantee invariance of V under Hermitian conjugation. Without loss of generality we can also assume $m_{12}^2 \in \mathbb{R}^+$, as we can absorb any phase into a suitable redefinition of Φ_1 and Φ_2. Furthermore the scalar potential is of course required to be bounded from below. This amounts to imposing the following conditions on the parameters

$$\lambda_1 > 0, \quad \lambda_2 > 0, \quad \lambda_3 > -\sqrt{\lambda_1 \lambda_2}, \quad \lambda_3 + \lambda_4 > -\sqrt{\lambda_1 \lambda_2}. \tag{3.3}$$

In order to derive these conditions it is sufficient to consider the quartic terms of the potential. In order to analyse the effect of the λ_4 term it is helpful to rewrite

$$\left|\Phi_1^\dagger \Phi_2\right|^2 = \left|\left|\Phi_1^+\right| \left|\Phi_2^+\right| e^{i(\delta_2^+ - \delta_1^+)} + \left|\Phi_1^0\right| \left|\Phi_2^0\right| e^{i(\delta_2^0 - \delta_1^0)}\right|^2 \tag{3.4}$$

where $\delta_i^+,\ \delta_i^0 \in [0, 2\pi],\ i = 1, 2$ denote the phases of the corresponding fields in the decomposition (3.1). In addition we can write

$$\left|\Phi_i^+\right| = \sin\alpha_i \left|\Phi_i\right|, \qquad \left|\Phi_i^0\right| = \cos\alpha_i \left|\Phi_i\right| \tag{3.5}$$

for $i = 1, 2$ and $\alpha_i \in [0, \pi/2]$. Substituting (3.5) into (3.4) yields

$$\begin{aligned} \left|\Phi_1^\dagger \Phi_2\right|^2 \;=\; & |\Phi_1|^2 |\Phi_2|^2 \Big(\sin^2\alpha_1 \sin^2\alpha_2 + \cos^2\alpha_1 \cos^2\alpha_2 \\ & + 2\cos\widetilde{\delta} \cos\alpha_1 \cos\alpha_2 \sin\alpha_1 \sin\alpha_2\Big), \end{aligned} \tag{3.6}$$

where we have abbreviated $\widetilde{\delta} = \delta_2^+ - \delta_1^+ + \delta_1^0 - \delta_2^0$. We can use this to rewrite the quartic terms in the scalar potential (which dominate for large field values) in matrix form

$$V_{\text{quartic}} = (|\Phi_1|^2, |\Phi_2|^2) \begin{pmatrix} \lambda_1/2 & \lambda_3/2 + c\lambda_4/2 \\ \lambda_3/2 + c\lambda_4/2 & \lambda_2/2 \end{pmatrix} \begin{pmatrix} |\Phi_1|^2 \\ |\Phi_2|^2 \end{pmatrix}, \tag{3.7}$$

where we have further defined

$$c := \sin^2\alpha_1 \sin^2\alpha_2 + \cos^2\alpha_1 \cos^2\alpha_2 + 2\cos\widetilde{\delta} \cos\alpha_1 \cos\alpha_2 \sin\alpha_1 \sin\alpha_2.$$

Note that $c \in [0, 1]$. If we can ensure that the matrix in (3.7) is positive definite then this implies $V \to +\infty$ for large field values in any direction in field space, i.e. the potential is then guaranteed to be bounded from below. Making use of the Sylvester criterion[6] we immediately obtain the first condition in (3.3), namely $\lambda_1 > 0$, as well as

$$\lambda_1\lambda_2 > (\lambda_3 + c\lambda_4)^2. \tag{3.8}$$

Combining (3.8) with $\lambda_1 > 0$ yields the second condition $\lambda_2 > 0$. Taking the square root of (3.8) and noting that the weakest necessary conditions for λ_3 and λ_4 are obtained for the extremal values of $c \in [0, 1]$ finally leads to the other two conditions in (3.3).

We now turn to the search for the minima of the potential, which from the discussion above are guaranteed to exist provided we fulfill the conditions for boundedness from below. We will only consider vacua obeying two further restrictions. Namely, the vacua of the theory should conserve CP in addition to keeping the electromagnetic symmetry unbroken to guarantee a massless photon. This means that the minima of V_H must take the form

$$\Phi_1 = \frac{1}{\sqrt{2}} \begin{pmatrix} 0 \\ v_1 \end{pmatrix}, \qquad \Phi_2 = \frac{1}{\sqrt{2}} \begin{pmatrix} 0 \\ v_2 \end{pmatrix}, \tag{3.9}$$

with $v_{1,2} \in \mathbb{R}^+$. We refer to minima of this type as normal minima. Note that normal minima cannot coexist in the same potential with CP-breaking or charge-breaking minima [67]. In other words, if the parameters of the potential are such that a normal minimum exists, then any other minimum of V_H must also be a normal minimum. To look for a normal minimum, we set to zero the first derivatives of the potential (3.2) after plugging in the form (3.9), yielding

$$0 = 2m_{11}^2 v_1 - 2m_{12}^2 v_2 + (\lambda_3 + \lambda_4) v_1 v_2^2 + \lambda_1 v_1^3, \tag{3.10}$$

$$0 = 2m_{22}^2 v_2 - 2m_{12}^2 v_1 + (\lambda_3 + \lambda_4) v_2 v_1^2 + \lambda_2 v_2^3. \tag{3.11}$$

Of course, being able to find a simultaneous solution $(v_1,\ v_2)$ of these equations is only a necessary condition for the existence of a normal minimum. After finding

[6] The Sylvester criterion states that a Hermitian matrix is positive definite if and only if all principal minors are positive.

such a solution we still have confirm explicitly that it is indeed a global minimum of the potential.

To simplify solving the necessary conditions we recall that our aim is to give mass to the leptons and quarks via v_2 and to the neutrinos via v_1. Hence we require $v_1 \neq 0$ and $v_2 \neq 0$. In order to generate tiny neutrino masses without needing tiny Yukawa couplings we would furthermore like to find a solution with $v_1 \ll v_2$. In this limit the necessary minimum conditions yield

$$v_1 \simeq \frac{2m_{12}^2 v_2}{2m_{11}^2 + \lambda_{34} v_2^2}, \tag{3.12}$$

$$v_2 \simeq \sqrt{\frac{-2m_{22}^2}{\lambda_2}}. \tag{3.13}$$

Here and in the following we abbreviate $\lambda_{34} = \lambda_3 + \lambda_4$. Since we took $v_2 \in \mathbb{R}^+$, the existence of such a solution requires $m_{22}^2 < 0$. Now if we take the parameters to fulfill $\lambda_i \simeq \mathcal{O}(1)$, $|m_{11}| \simeq |m_{22}| \simeq 120$ GeV as well as a soft breaking term of the order $m_{12} \simeq \mathcal{O}(\text{MeV})$ we can in particular achieve the phenomenologically desirable values $v_2 \simeq 250$ GeV and $v_1 \simeq \mathcal{O}(10^{-1}\text{ eV})$[7].

It is still left to check whether the solution of the necessary minimum conditions found above is indeed a minimum of the potential. In fact, we will ask for a stronger condition and require that it represents the *global* minimum in order to avoid any issues pertaining to vacuum stability[8]. To confirm this, we will look for all other solutions of the necessary conditions (3.10) and (3.11) and then compare the value of the potential at these locations in field space.

First of all let us note that for the potential minimum above with $v_1 \ll v_2$ we have $V(v_1 \ll v_2) < 0$. This immediately implies that the trivial solution $v_1 = v_2 = 0$ of the necessary conditions is at a higher value, as $V(0,0) = 0$. Also, the presence of the m_{12}^2 term implies that there are no solutions of (3.10) and (3.11) in which one vev vanishes but the other does not. We are left with three possibilities with both vevs non-vanishing: (i) $v_1 \ll v_2$, (ii) $v_1 \gg v_2$ or (iii) $v_1 \sim v_2$. Case (i) was already considered above, and case (ii) can be treated in a similar manner. Namely, we can again neglect sub-leading terms in the necessary minimum conditions, which allows us to find approximate analytical expressions for v_1 and v_2. These can then be substituted back into the potential to estimate the magnitude of $V(v_1 \gg v_2)$. To similarly find approximate analytical expressions for v_1 and v_2 in case (iii) we must take into account that we expect $|m_{ii}^2| \gg m_{12}^2$ as the $U(1)$ symmetry is only softly broken. This again allows us to simplify the minimum conditions in the case $v_1 \sim v_2$, so that the equations can be solved analytically and we obtain an estimate for $V(v_1 \sim v_2)$. Having obtained these expressions we now require $V(v_1 \ll v_2) < V(v_1 \gg v_2)$ and $V(v_1 \ll v_2) < V(v_1 \sim v_2)$. In fact, to keep

[7] Note that this hierarchy between the vevs is stable against radiative corrections, because the $U(1)$ symmetry guarantees that the radiative corrections to m_{12} are proportional to m_{12} itself [77].

[8] See [77] for a discussion of vacuum stability in neutrinophilic 2HDMs.

the form of the resulting conditions simple we will actually ask for the stronger condition $V(v_1 \sim v_2) > 0$, which suffices to guarantee that our second requirement is fulfilled. The resulting conditions which we take to guarantee that the solution with $v_1 \ll v_2$ is a global minimum are then given by

$$\frac{m_{22}^4}{\lambda_2} > \frac{m_{11}^4}{\lambda_1} \qquad \text{and} \qquad \lambda_{34} > 0. \tag{3.14}$$

The upshot of the discussion above is that it is possible to find a minimum where the vev of the Higgs field Φ_2, which couples to the charged leptons and quarks, is close to the standard model value $v_2 \sim 250$ GeV; while $v_1 \sim 1$ eV, so that sub-eV neutrino masses are possible with Yukawa couplings of order one. Furthermore it is possible to achieve this in a natural manner, i.e. while keeping the dimensionless coefficients $\lambda_1, \ldots, \lambda_4$ of order one and with $|m_{ii}^2| \gg m_{12}^2$ which is consistent with the fact that m_{12}^2 is the soft breaking term of an otherwise conserved global symmetry. Finally, choosing the parameters to obey (3.14) we can ensure that this vacuum is the global minimum of the potential and is therefore absolutely stable.

3.2 Masses of the physical Higgs states

We are now in a position to implement the Higgs mechanism by expanding the Higgs fields around the vevs found above and substituting the resulting expression into the Lagrangian. This will break $SU(2) \times U(1)$ down to $U(1)_{\text{em}}$ just as in the case of only one Higgs. Our conventions for the expansions of the fields are given by

$$\Phi_i = \frac{1}{\sqrt{2}} \begin{pmatrix} \varphi_i^+ \\ v_i + \varphi_i^0 \end{pmatrix}. \tag{3.15}$$

Let us first derive the Higgs mass eigenstates and therefore substitute the expansions 3.15 into the scalar potential 3.2. This yields

$$\begin{aligned} V = \; & \frac{1}{4}\left|\varphi_1^+\right|^2 \left[2m_{11}^2 + \lambda_1 v_1^2 + \lambda_3 v_2^2\right] + \frac{1}{4}\left|\varphi_2^+\right|^2 \left[2m_{22}^2 + \lambda_2 v_2^2 + \lambda_3 v_1^2\right] \\ & + \frac{1}{4}\left|\varphi_1^0\right|^2 \left[2m_{11}^2 + \lambda_1 v_1^2 + \lambda_{34} v_2^2\right] + \frac{1}{4}\left|\varphi_2^0\right|^2 \left[2m_{22}^2 + \lambda_2 v_2^2 + \lambda_{34} v_1^2\right] \\ & + \frac{1}{2}\Re\left(\varphi_1^- \varphi_2^+\right)\left[\lambda_4 v_1 v_2 - 2m_{12}^2\right] + \frac{1}{2}\Re\left(\left(\varphi_1^0\right)^* \varphi_2^0\right)\left[\lambda_4 v_1 v_2 - 2m_{12}^2\right] \\ & + \frac{1}{2}\left(\Re\left(\varphi_1^0\right)\right)^2 \lambda_1 v_1^2 + \frac{1}{2}\left(\Re\left(\varphi_2^0\right)\right)^2 \lambda_2 v_2^2 \\ & + \frac{1}{2}\Re\left(\varphi_1^0 \varphi_2^0\right)\lambda_4 v_1 v_2 + \Re\left(\varphi_1^0\right)\Re\left(\varphi_2^0\right)\lambda_3 v_1 v_2 \\ & + \{\text{interaction terms}\}. \end{aligned} \tag{3.16}$$

The self-interaction terms of the Higgs fields are given in appendix D. To find the mass eigenstates we define $\tan\beta = v_2/v_1$ and make use of the minimum

conditions (3.10) and (3.11). It is simple to check that the combinations

$$H^{\pm} = \frac{1}{\sqrt{2}}\left(-\sin(\beta)\varphi_1^{\pm} + \cos(\beta)\varphi_2^{\pm}\right) \tag{3.17}$$

$$A^0 = -\sin(\beta)\Im(\varphi_1^0) + \cos(\beta)\Im(\varphi_2^0) \tag{3.18}$$

are Higgs mass eigenstates. As the notation suggests $H^{\pm}$ carry electromagnetic charge while A^0 is a neutral CP-odd pseudoscalar (in fact, A^0 is the only one of the physical Higgs states that is CP-odd). The corresponding masses are

$$m_{H^{\pm}}^2 = m_{12}^2\left(\frac{v_2}{v_1} + \frac{v_1}{v_2}\right) - \frac{1}{2}\lambda_4(v_1^2 + v_2^2), \tag{3.19}$$

$$m_{A^0}^2 = m_{12}^2\left(\frac{v_2}{v_1} + \frac{v_1}{v_2}\right). \tag{3.20}$$

Making use of the minimum conditions (3.10) and (3.11) we can rewrite $m_{H^{\pm}}^2$ and $m_{A^0}^2$ in the limit $v_1 \ll v_2$ as

$$m_{H^{\pm}}^2 \simeq m_{11}^2 + \frac{1}{2}\lambda_3 v_2^2, \tag{3.21}$$

$$m_{A^0}^2 \simeq m_{11}^2 + \frac{1}{2}\lambda_{34} v_2^2. \tag{3.22}$$

Requiring that these masses are positive yields necessary conditions for $(v_1,\ v_2)$ to define a local minimum, but of course we have already shown that our vevs can be chosen to define a global minimum of the potential.

Moving on, we find that the combination

$$G^0 = \cos(\beta)\Im(\varphi_1^0) + \sin(\beta)\Im(\varphi_2^0), \tag{3.23}$$

which is orthogonal to A^0, and the combinations

$$G^{\pm} = \frac{1}{\sqrt{2}}(\cos(\beta)\varphi_1^{\pm} + \sin(\beta)\varphi_2^{\pm}), \tag{3.24}$$

which are orthogonal to $H^{\pm}$, remain massless. This means that the corresponding directions of the scalar potential are flat. Note that the chosen form (3.9) of the vevs breaks three combinations of the four generators of $SU(2)_{\mathrm{L}} \times U(1)_Y$ under which the Φ_i are charged. Hence we expect three massless Goldstone bosons to appear in the expansion of the scalar potential, and it is natural to expect that G^0 and $G^{\pm}$ are these Goldstone bosons. One can indeed convince oneself that there exists an $SU(2)_{\mathrm{L}} \times U(1)_Y$ gauge transformation that can be used to set $G^0,\ G^{\pm} = 0$ while keeping a residual U_{em} unbroken. This gauge choice, in which the Goldstone bosons are eaten up by the gauge bosons $W^{\pm}$ and Z and are removed from the theory, is known as unitary gauge. Rather than going through with the explicit construction of the gauge transformation that is needed to go to unitary gauge, we will follow an easier approach. Namely, we note that the Goldstone bosons can

also be identified more easily by considering the gauge covariant kinetic terms of the Higgs, as they couple to the gauge bosons in a very specific manner. This will be discussed in the next section, where it will be confirmed that indeed G^0 and $G^\pm$ are precisely the unphysical Goldstone bosons. However, before proceeding with the analysis of the kinetic term we must still consider the sector of field space spanned by the real parts of the uncharged Higgs components.

In order to identify the remaining mass eigenstates we have to diagonalise the mass matrix in the subspace spanned by $\Re(\varphi_i^0),\ i = 1, 2$. Since the mass matrix is symmetric it can be brought into diagonal form through a rotation by an angle α. Performing this diagonalisation yields the solution

$$\cos 2\alpha = -\frac{\lambda_1 v_1^2 - \lambda_2 v_2^2 + m_{12}^2\left(\frac{v_2}{v_1} - \frac{v_1}{v_2}\right)}{\sqrt{4\left(v_1 v_2 \lambda_{34} + m_{12}^2\right)^2 + \left(\lambda_1 v_1^2 - \lambda_2 v_2^2 + m_{12}^2\left(\frac{v_2}{v_1} - \frac{v_1}{v_2}\right)\right)^2}}\,, \tag{3.25}$$

$$\sin 2\alpha = -\frac{2(v_1 v_2 \lambda_{34} + m_{12}^2)}{\sqrt{4\left(v_1 v_2 \lambda_{34} + m_{12}^2\right)^2 + \left(\lambda_1 v_1^2 - \lambda_2 v_2^2 + m_{12}^2\left(\frac{v_2}{v_1} - \frac{v_1}{v_2}\right)\right)^2}}\,. \tag{3.26}$$

The corresponding CP-even mass eigenstates are given by

$$H^0 = \cos\alpha\,\Re(\varphi_1^0) + \sin\alpha\,\Re(\varphi_2^0)\,, \tag{3.27}$$

with mass

$$\begin{aligned} m_{H^0}^2 = \frac{1}{2}\Bigg(&\lambda_1 v_1^2 + \lambda_2 v_2^2 + m_{12}^2\left(\frac{v_2}{v_1} + \frac{v_1}{v_2}\right) \\ &-\sqrt{\left(\lambda_1 v_1^2 - \lambda_2 v_2^2 + m_{12}^2\left(\frac{v_2}{v_1} + \frac{v_1}{v_2}\right)\right)^2 + 4\left(v_1 v_2 \lambda_{34} + m_{12}^2\right)^2}\Bigg)\,, \end{aligned} \tag{3.28}$$

and

$$h^0 = -\sin\alpha\,\Re(\varphi_1^0) + \cos\alpha\,\Re(\varphi_2^0)\,, \tag{3.29}$$

with mass

$$\begin{aligned} m_{h^0}^2 = \frac{1}{2}\Bigg(&\lambda_1 v_1^2 + \lambda_2 v_2^2 + m_{12}^2\left(\frac{v_2}{v_1} + \frac{v_1}{v_2}\right) \\ &+\sqrt{\left(\lambda_1 v_1^2 - \lambda_2 v_2^2 + m_{12}^2\left(\frac{v_2}{v_1} + \frac{v_1}{v_2}\right)\right)^2 + 4\left(v_1 v_2 \lambda_{34} + m_{12}^2\right)^2}\Bigg)\,. \end{aligned} \tag{3.30}$$

In the above we have again used the abbreviation $\lambda_{34} = \lambda_3 + \lambda_4$.

Recalling that we have chosen the vevs to obey $v_1 \ll v_2$ in order to generate small neutrino masses naturally, we can expand the expressions above into a Taylor series in v_1/v_2. In leading order we find

$$\begin{aligned} &\sin 2\alpha \simeq -\frac{v_1}{2v_2}, && \cos 2\alpha \simeq 1, \\ &m_{H^0}^2 \simeq \lambda_1 v_1^2 + m_{12}^2\frac{v_2}{v_1}, && m_{h^0}^2 \simeq \lambda_2 v_2^2. \end{aligned} \tag{3.31}$$

In particular using the expressions (3.21), (3.22) and (3.31) as well as the minimum conditions we see that

$$m^2_{H^0} = m^2_{A^0} = m^2_{H^\pm} + \lambda_4 v_2^2/2. \tag{3.32}$$

Due to the fact that $\alpha \ll 1$ the fields themselves are dominated by the contributions from one of the original fields Φ_1 and Φ_2, and very little mixing occurs. Specifically, to lowest order in v_1/v_2 we have

$$H^0 \simeq \Re(\varphi_1^0) \qquad\qquad h^0 \simeq \Re(\varphi_2^0). \tag{3.33}$$

From this we conclude that the field h^0 behaves similarly to the SM Higgs field (we will confirm in the following that this holds in particular for the interactions of h^0 with the gauge bosons and fermions).

Of course we can also have a look at the other fields defined above in the limit of $\tan^{-1}\beta = v_1/v_2 \ll 1$. We immediately see that the fields A^0 and $H^\pm$ are dominated by the contributions from $\Im(\varphi_1^0)$ and from $\varphi_1^\pm$, respectively. These observations will lead to interesting phenomenological implications which will be discussed in more detail in section 3.5. However before analysing the phenomenology let us first briefly consider the kinetic terms of the Higgs fields.

3.3 The kinetic term of the Higgs fields

The canonical gauge covariant kinetic term of the two Higgs scalars is given by

$$\mathcal{L}_{\Phi,\text{kin.}} = (D_\mu\Phi_1)^\dagger(D^\mu\Phi_1) + (D_\mu\Phi_2)^\dagger(D^\mu\Phi_2), \tag{3.34}$$

with the gauge covariant derivatives $D_\mu = \partial_\mu - \frac{ig_2}{2}\sigma_a W_\mu^a - \frac{ig_1}{2}B_\mu$ (as usual σ_a denotes the Pauli matrices). With the expressions for the physical gauge boson fields given in appendix A we find

$$\begin{aligned} |D_\mu\Phi_i|^2 &= \left|(\partial_\mu - \frac{i}{2}\sqrt{g_1^2+g_2^2}A_\mu)\Phi_i^+ - \frac{ig_2}{\sqrt{2}}W_\mu^+\Phi_i^0\right|^2 &(3.35)\\ &\quad + \left|-\frac{ig_2}{\sqrt{2}}W_\mu^-\Phi_i^+ + (\frac{i}{2}\sqrt{g_1^2+g_2^2}Z_\mu + \partial_\mu)\Phi_i^0\right|^2. &(3.36)\end{aligned}$$

Substituting in the expansion (3.15) of the Higgs fields one finds

$$\begin{aligned} \mathcal{L}_{\Phi,\text{kin.}} = \quad & \{\text{kinetic terms of the scalar fields}\}\\ & + \{\text{mass terms of the gauge bosons}\}\\ & + \{\text{interaction terms between scalar and gauge fields}\}\\ & + \frac{ig_2}{2^{\frac{2}{3}}}W_\mu^-\left[v_1\partial^\mu\varphi_1^+ + v_2\partial^\mu\varphi_2^+\right] + \text{h.c.}\\ & - \frac{i}{4}\sqrt{g_1^2+g_2^2}Z^\mu\left[v_1\partial_\mu\varphi_1^0 + v_2\partial_\mu\varphi_2^0\right] + \text{h.c.} \end{aligned} \tag{3.37}$$

Before turning to the kinetic and interaction terms let us point out that the last two lines above can be used to identify the unphysical Goldstone bosons. Namely, the presence of a direct coupling between a scalar ϕ and a gauge boson V^μ of the form $V^\mu \partial_\mu \phi$ implies that ϕ can be absorbed into a gauge transformation of V^μ. Now, recalling $\tan\beta = v_2/v_1$ and pulling out a factor of $v_1/\cos\beta$ in the last two lines above, we immediately see that G^0 and $G^\pm$ as defined in (3.23) and (3.24) are indeed the combinations corresponding to unphysical Goldstone bosons. As there is no coupling of this form to the photon A^μ this also confirms our assertion that one can go to unitary gauge and remove the Goldstone bosons using gauge transformations of $W^\pm$ and Z^μ only, so that the electromagnetic symmetry remains unbroken.

After fixing the gauge in the manner described above, the kinetic term can be written in terms of the physical Higgs fields to give

$$\begin{aligned}\mathcal{L}_{\Phi,\text{kin.}} \;=\;& \partial_\mu H^+ \partial^\mu H^- + \frac{1}{2}\partial_\mu A^0 \partial^\mu A^0 + \frac{1}{2}\partial_\mu H^0 \partial^\mu H^0 + \frac{1}{2}\partial_\mu h^0 \partial^\mu h^0 \\ & + \frac{g_2^2}{4}(v_1^2+v_2^2) W_\mu^- W^{+\mu} + \frac{g_2^2+g_1^2}{8}(v_1^2+v_2^2) Z_\mu Z^\mu \\ & + \{\text{interaction terms between the scalar and gauge fields}\}\,.\end{aligned} \tag{3.38}$$

The interaction terms between the Higgs scalars and the gauge fields in unitary gauge are given in appendix D. From the second line of (3.38) we read off the masses of the gauge bosons

$$m_{W^\pm}^2 = \frac{g_2^2}{4}(v_1^2+v_2^2), \qquad\qquad m_Z^2 = \frac{g_2^2+g_1^2}{8}(v_1^2+v_2^2), \tag{3.39}$$

while as expected the photon stays massless as a result of the chosen vev structure.

3.4 The Yukawa sector

Given the $U(1)$ charge assignments of table (3.2) we can immediately write down the most general Yukawa term compatible with this $U(1)$ symmetry,

$$\begin{aligned}-\mathcal{L}_{\text{Yukawa}} \;=\;& Y^d_{ij}\overline{\mathrm{Q}_{\mathrm{L},i}}\Phi_2 d_{\mathrm{R},j} + Y^u_{ij}\overline{\mathrm{Q}_{\mathrm{L},i}}\widetilde{\Phi}_2 u_{\mathrm{R},j} + Y^\ell_{ij}\overline{\mathrm{L}_{\mathrm{L},i}}\Phi_2 \ell_{\mathrm{R},j} \\ & + Y^\nu_{ij}\overline{\mathrm{L}_{\mathrm{L},i}}\widetilde{\Phi}_1 \nu_{\mathrm{R},j} + \text{h.c.},\end{aligned} \tag{3.40}$$

where again

$$\widetilde{\Phi}_{1,2} = i\sigma_2 \Phi^*_{1,2}\,. \tag{3.41}$$

Here and in the following the sum over the flavour indices i and j is implicit. After inserting the expansion (3.15) around the Higgs vevs this yields both the fermion mass terms and the Higgs-fermion interactions. In unitary gauge and after rewriting in terms of the Higgs mass eigenstates found in section 3.2 we

obtain

$$
\begin{aligned}
-\mathcal{L}_{\text{Yukawa}} \;=\;& \frac{v_2}{\sqrt{2}} Y^d_{ij} \overline{d_{\text{L},i}} d_{\text{R},i} + \frac{v_2}{\sqrt{2}} Y^u_{ij} \overline{u_{\text{L},i}} u_{\text{R},i} \\
&+ \frac{v_2}{\sqrt{2}} Y^\ell_{ij} \overline{\ell_{\text{L},i}} \ell_{\text{R},i} + \frac{v_1}{\sqrt{2}} Y^\nu_{ij} \overline{\nu_{\text{L},i}} \nu_{\text{R},i} \\
&+ \frac{1}{\sqrt{2}} H^0 \sin\alpha \left[Y^d_{ij} \overline{d_{\text{L},i}} d_{\text{R},j} + Y^u_{ij} \overline{u_{\text{L},i}} u_{\text{R},j} + Y^\ell_{ij} \overline{\ell_{\text{L},i}} \ell_{\text{R},j} \right. \\
&\qquad \left. + \frac{1}{\tan\alpha} Y^\nu_{ij} \overline{\nu_{\text{L},i}} \nu_{\text{R},j} \right] \\
&+ \frac{1}{\sqrt{2}} h^0 \cos\alpha \left[Y^d_{ij} \overline{d_{\text{L},i}} d_{\text{R},j} + Y^u_{ij} \overline{u_{\text{L},i}} u_{\text{R},j} + Y^\ell_{ij} \overline{\ell_{\text{L},i}} \ell_{\text{R},j} \right. \\
&\qquad \left. - \tan(\alpha) Y^\nu_{ij} \bar{\nu}_{L,i} \nu_{R,j} \right] \\
&+ \frac{i}{\sqrt{2}} A^0 \cos\beta \left[Y^d_{ij} \overline{d_{\text{L},i}} d_{\text{R},j} - Y^u_{ij} \overline{u_{\text{L},i}} u_{\text{R},j} + Y^\ell_{ij} \overline{\ell_{\text{L},i}} \ell_{\text{R},j} \right. \\
&\qquad \left. + \tan\beta Y^\nu_{ij} \overline{\nu_{\text{L},i}} \nu_{\text{R},j} \right] \\
&+ H^+ \cos(\beta) \left[Y^d_{ij} \overline{u_{\text{L},i}} d_{\text{R},j} - \left(Y^u_{ij}\right)^\dagger \overline{u_{\text{R},i}} d_{\text{L},j} + Y^\ell_{ij} \overline{\nu_{\text{L},i}} \ell_{\text{R},j} \right. \\
&\qquad \left. + \tan\beta \left(Y^\nu_{ij}\right)^\dagger \overline{\nu_{\text{R},i}} e_{\text{L},j} \right] \\
&+ \text{h.c.}
\end{aligned}
\tag{3.42}
$$

Note that the above equation is given in terms of the fermion flavour eigenstates. To facilitate the discussion of the phenomenology of this model in the next section it will be helpful to also rewrite $\mathcal{L}_{\text{Yukawa}}$ in terms of the mass eigenstates, to which task we now turn.

As discussed in appendix B the matrices $Y^{d,u,\ell,\nu}_{ij}$ can be brought to diagonal form using a biunitary transformation, yielding real and non-negative masses for the matter fields. In other words there exist unitary matrices $V^{u,d,\ell,\nu}_{\text{L}}$ and $V^{u,d,\ell,\nu}_{\text{R}}$ such that the matrices defined by

$$
\begin{aligned}
M^u_{\text{diag.}} &= \frac{v_2}{\sqrt{2}} V^{u\,\dagger}_{\text{L}} Y^u V^u_{\text{R}} \,, & M^d_{\text{diag.}} &= \frac{v_2}{\sqrt{2}} V^{d\,\dagger}_{\text{L}} Y^d V^d_{\text{R}} \,, \\
M^\ell_{\text{diag.}} &= \frac{v_2}{\sqrt{2}} V^{\ell\,\dagger}_{\text{L}} Y^\ell V^\ell_{\text{R}} \,, & M^\nu_{\text{diag.}} &= \frac{v_1}{\sqrt{2}} V^{\nu\,\dagger}_{\text{L}} Y^\nu V^\nu_{\text{R}} \,,
\end{aligned}
\tag{3.43}
$$

are diagonal and contain the masses of the matter fields. Recall that Majorana mass terms for the neutrinos are forbidden due to the $U(1)$ charge of the right-handed neutrinos, so that the neutrinos in our model are of Dirac type. The fermionic mass eigenstates are related to the fields in the flavour basis by

$$
\begin{aligned}
u^0_{\text{L,R}} &= V^{u\,\dagger}_{\text{L,R}} u_{\text{L,R}} \,, & d^0_{\text{L,R}} &= V^{d\,\dagger}_{\text{L,R}} d_{\text{L,R}} \,, \\
\ell^0_{\text{L,R}} &= V^{\ell\,\dagger}_{\text{L,R}} \ell_{\text{L,R}} \,, & \nu^0_{\text{L,R}} &= V^{\nu\,\dagger}_{\text{L,R}} \nu_{\text{L,R}} \,.
\end{aligned}
\tag{3.44}
$$

Recall that the quark and leptonic mixing matrix are given in terms of the diagonalisation matrices by

$$U_{\text{CKM}} = V_{\text{L}}^{u\,\dagger} V_{\text{L}}^{d} \qquad \text{and} \qquad U_{\text{PMNS}} = V_{\text{L}}^{\ell\,\dagger} V_{\text{L}}^{\nu}\,, \tag{3.45}$$

respectively. After performing the basis change, we therefore find for the Yukawa interactions in the mass basis

$$\begin{aligned}
-\mathcal{L}_{\text{Yukawa}} \;=\;& \overline{d_{\text{L}}^0} m_d d_{\text{R}}^0 + \overline{u_{\text{L}}^0} m_u u_R^0 + \overline{\ell_{\text{L}}^0} m_\ell \ell_{\text{R}}^0 + \overline{\nu_{\text{L}}^0} m_\nu \nu_{\text{R}}^0 \\
&+ \frac{1}{v} H^0 \left[\frac{\sin\alpha}{\sin\beta} \left(\overline{d_{\text{L}}^0} m_d d_{\text{R}}^0 + \overline{u_{\text{L}}^0} m_u u_{\text{R}}^0 + \overline{\ell_{\text{L}}^0} m_\ell \ell_{\text{R}}^0 \right) \right. \\
&\qquad \left. + \frac{\cos\alpha}{\cos\beta} \overline{\nu_{\text{L}}} m_\nu \nu_{\text{R}} \right] \\
&+ \frac{1}{v} h^0 \left[\frac{\cos\alpha}{\sin\beta} \left(\overline{d_{\text{L}}^0} m_d d_{\text{R}}^0 + \overline{u_{\text{L}}^0} m_u u_{\text{R}}^0 + \overline{\ell_{\text{L}}^0} m_\ell \ell_{\text{R}}^0 \right) \right. \\
&\qquad \left. + \frac{\sin\alpha}{\cos\beta} \overline{\nu_{\text{L}}^0} m_\nu \nu_{\text{R}}^0 \right] \\
&- \frac{i}{v} A^0 \left[\cot\beta \left(\overline{d_{\text{L}}^0} m_d d_{\text{R}}^0 - \overline{u_{\text{L}}^0} m_u u_{\text{R}}^0 + \overline{\ell_{\text{L}}^0} m_\ell \ell_{\text{R}}^0 \right) \right. \\
&\qquad \left. + \tan\beta \overline{\nu_{\text{L}}^0} m_\nu \nu_{\text{R}}^0 \right] \\
&+ \frac{\sqrt{2}}{v} H^+ \Big[\cot\beta \left(-\overline{u_{\text{R}}^0} m_u U_{\text{CKM}} d_{\text{L}}^0 + \overline{u_{\text{L}}^0} m_d U_{\text{CKM}} d_{\text{R}}^0 \right) \\
&\qquad + \cot\beta \overline{\nu_{\text{L}}^0} m_\ell U_{\text{PMNS}}^\dagger \ell_{\text{R}}^0 + \tan\beta \overline{\nu_{\text{R}}^0} m_\nu U_{\text{PMNS}}^\dagger \ell_{\text{L}}^0 \Big] \\
&+ \text{h.c.},
\end{aligned} \tag{3.46}$$

where we have defined $v^2 = v_1^2 + v_2^2$. Note that we have also introduced the notation $m_\nu \equiv M^\nu_{\text{diag.}}$ etc. for the diagonal mass matrices and suppressed the summation over generation indices to keep the notation as simple as possible. In the following we will use $m_\nu, m_\ell, \ldots$ to denote both the mass matrices in diagonal form as well as sometimes individual masses, i.e. individual entries of these diagonal mass matrices. We trust that it will always be clear from the context which object we mean.

Let us emphasise again at this point that there holds $m_{u,d,\ell} \propto v_2$ and $m_\nu \propto v_1$, which was the main motivation behind studying the ν2HDM defined by the $U(1)$ charges of table 3.2. As we have shown the parameters of the scalar potential can be chosen such as to quite naturally lead to vevs of the order $v_2 \sim \mathcal{O}(250\text{ GeV})$ and $v_1 \sim \mathcal{O}(1\text{ eV})$. Thus the value of v_2, which enters into the masses of quarks and charged leptons, is similar to the SM Higgs vev. On the other hand the value of v_1 is small enough to generate neutrino masses smaller than 1 eV, as required by e.g. the WMAP bound, without requiring exorbitantly small Yukawa couplings.

3.5 Phenomenology of the ν2HDM

The new couplings that arise after the introduction of the second Higgs doublet impact on a wide variety of experimental observables. We therefore now turn to an analysis of the phenomenology of the ν2HDM. In subsection 3.5.1 we focus on effects that are important mainly in the context of collider experiments. In particular, we analyse effects of the additional Higgs particles on electroweak observables and gauge boson decays that have been measured precisely in the past, from which bounds on the Higgs masses can be obtained. Furthermore we consider various decay channels and branching ratios of the new Higgs particles that may be observed in future experiments. Contributions of the charged Higgs scalars to charged lepton flavour violation (cLFV) and to tree-level decay rates of the muon and tauon are analysed separately in subsections 3.5.3 and 3.5.5, respectively. In between, we discuss constraints from the requirement of unitarity in subsection 3.5.2, as well as Higgs-induced corrections to the anomalous magnetic moment of the muon in subsection 3.5.4.

3.5.1 Higgs decay rates and collider phenomenology

The key inputs for the analysis of this subsection are the Higgs-fermion interactions, the self-interaction terms of the Higgs fields and the interaction terms between Higgs particles and gauge bosons. The expansions of the corresponding terms of the Lagrangian are given in equations (3.46), (D.6)−(D.8) and (D.9), respectively. In the analysis of the ν2HDM considered here we clearly need to take into account only the leading terms in an expansion in $v_1/v_2 \sim 10^{-11}$, as all corrections from higher orders will be miniscule.

In table 3.3 we list the tree-level decay widths of the dominant decay channels for each of the five Higgs scalars. For the convenience of the reader we have also listed the relevant vertex factors that can be extracted from the Lagrangian. In appendix E we have summarised a number of identities that are used in calculating these partial decay widths as well as reviewing the decay widths of the Higgs in the Standard Model. In comparison to the listed tree-level decays, the corresponding loop-induced processes are suppressed in the limit $v_1 \ll v_2$. The important process $h^0 \to \gamma\gamma$, which of course is not possible at tree-level as h^0 is uncharged, will be discussed separately further below.

Note that, for kinematical reasons, at least one of the decays $\Gamma(H^0,\ A^0 \to W^\pm H^\mp)$ and $\Gamma(H^\pm \to W^\pm A^0,\ W^\pm H^0)$ will be forbidden on-shell. This depends on the relative size of the masses $m^2_{A^0,H^0}$ and $m^2_{H^\pm}$, which according to equation (3.32) is governed by the parameter λ_4 of the scalar potential.

The Z boson can in principle decay to A^0 and H^0 via the interaction term

$$\mathcal{L}_{\Phi,\text{kin.}} \supset \frac{\sqrt{g_1^2+g_2^2}}{2} Z^\mu \left[\sin(\alpha-\beta) H^0 \partial_\mu A^0 - \sin(\alpha-\beta) A^0 \partial_\mu H^0\right], \tag{3.47}$$

Decay mode	Vertex factor	Partial decay width Γ
$H^0 \to \bar{\nu}\nu$	$-\frac{i}{v}\frac{\cos\alpha}{\cos\beta}m_\nu$	$\frac{G_F m_{H^0} m_\nu^2}{4\sqrt{2}\pi}\frac{\cos^2\alpha}{\cos^2\beta}\left(1-\frac{4m_\nu^2}{m_{H^0}^2}\right)^{\frac{3}{2}}$
$H^0 \to W^\pm H^\mp$	$\frac{ig_2}{2}\sin(\alpha-\beta)\,(p^\mu_{H^\pm}+p^\mu_{H^0})$	$\frac{2\sqrt{2}}{\pi}m_W^3 G_F \sin^2(\alpha-\beta)\frac{m_{H^0}}{m_{H^\pm}}\times\left(-\frac{m_W^2}{4m_{H^0}^2}f+f^3\right)$
$A^0 \to \bar{\nu}\nu$	$-\frac{1}{v}\tan\beta m_\nu$	$\frac{G_F m_{A^0} m_\nu^2}{4\sqrt{2}\pi}\tan^2\beta\left(1-\frac{4m_\nu^2}{m_{A^0}^2}\right)^{\frac{3}{2}}$
$A^0 \to W^\pm H^\mp$	$\frac{g_2}{2}\,(p^\mu_{H^\pm}+p^\mu_{A^0})$	$\frac{1}{\sin^2(\alpha-\beta)}\Gamma(H^0\to W^\pm H^\mp)$
$H^\pm \to \bar{\nu}\ell,\ \bar{\ell}\nu$	$-\frac{i\sqrt{2}}{v}\tan\beta m_\nu U^{(\dagger)}_{\text{PMNS}}$	$\frac{\sqrt{2}G_F m_{H^\pm}\sum_j m_{\nu_j}^2\lvert U_{\ell j}\rvert^2}{8\pi}$
$H^\pm \to H^0 W^\pm$	$-\frac{ig_2}{2}\sin(\alpha-\beta)\,(p^\mu_{H^\pm}+p^\mu_{H^0})$	$\frac{2\sqrt{2}}{\pi}m_W^3 G_F \sin^2(\alpha-\beta)\frac{m_{H^\pm}}{m_{H^0}}\times\left(-\frac{m_W^2}{4m_{H^\pm}^2}f+f^3\right)$
$H^\pm \to A^0 W^\pm$	$-\frac{g_2}{2}\,(p^\mu_{H^\pm}+p^\mu_{A^0})$	$\frac{1}{\sin^2(\alpha-\beta)}\Gamma(H^\pm\to A^0+W^\pm)$
$h^0 \to \bar{q}q,\ \bar{\ell}\ell$	$-\frac{i}{v}\frac{\cos\alpha}{\sin\beta}m_{q,\ell}$	$\Gamma_{\text{SM-Higgs}}\,(1+\mathcal{O}(v_1/v_2))$
$h^0 \to W^-W^+$	$\frac{i}{2}g_2^2 v\sin(\alpha-\beta)g^{\mu\nu}$	$\Gamma_{\text{SM-Higgs}}\,(1+\mathcal{O}(v_1/v_2))$
$h^0 \to ZZ$	$\frac{i}{4}(g_1^2+g_2^2)v\sin(\alpha-\beta)g^{\mu\nu}$	$\Gamma_{\text{SM-Higgs}}\,(1+\mathcal{O}(v_1/v_2))$
$h^0 \to H^0H^0$	$i\lambda_{34}v_2\cos^3\alpha$	$\frac{\lambda_{34}^2\cos^6\alpha}{32\pi m_{h^0}\sqrt{2}G_F}\sqrt{1-\frac{4m_{H^0}^2}{m_{h^0}^2}}$
$h^0 \to A^0A^0$	$i\lambda_{34}v_2\cos\alpha\sin^2\beta$	$\frac{\lambda_{34}^2\cos^2\alpha\sin^4\beta}{32\pi m_{h^0}\sqrt{2}G_F}\sqrt{1-\frac{4m_{A^0}}{m_h^0}}$
$h^0 \to H^\pm H^\mp$	$i\lambda_3 v_2\sin^2\beta\cos\alpha$	on-shell process kinematically forbidden by LEP-results

Table 3.3: Dominant tree-level decay modes of the physical Higgs states in the limit $v_1 \ll v_2$. Note that some processes can be kinematically forbidden, depending on the magnitude of the Higgs masses. $\Gamma_{\text{SM-Higgs}}$ is given in appendix E and $v^2 = v_1^2 + v_2^2$. In the above expressions we have abbreviated $f := \sqrt{(m_{H^\pm} - m_{A^0,H^0})^2/m_W^2 - 1}$.

arising from equation (3.38). This would yield a contribution to the invisible partial width of the Z boson, which is experimentally constrained to $\Gamma_{\text{inv}} = 3.1$ MeV at 95% confidence level [83]. We can therefore derive a lower bound on the mass m_{A^0,H^0} from the partial decay width $\Gamma(Z \to A^0 H^0)$, which can be calculated using the formulas given in appendix (E). In the limit $v_1 \ll v_2$ we find

$$\Gamma(Z \to A^0 H^0) = \frac{1}{24\pi} m_Z^3 \sqrt{2} G_F \left(1 - \frac{4m_{A^0,H^0}^2}{m_Z^2}\right)^{\frac{3}{2}}. \tag{3.48}$$

Plugging in the values $m_Z = 91.1876$ GeV and $G_F = 1.16637 \times 10^{-5}$ GeV^{-2} [35] one then obtains a restriction on the Higgs masses, namely

$$m_{A^0,H^0} \gtrsim 43.96 \text{ GeV}. \tag{3.49}$$

A bound on the charged Higgs mass can be estimated from data obtained at LEP. One LEP search focused on charged Higgs decays, where it was assumed that the dominant contributions would come from the processes $H^+ \to \tau^+\nu$, $q\bar{q}$. However, while the second channel would be important e.g. in type I or II 2HDMs, it is strongly suppressed in our model due to $v_1 \ll v_2$. To see how strongly the decay into a tauon contributes in our model let us therefore have a look at the branching ratios for decays to the different charged lepton generations. For a charged lepton of generation ℓ we use table 3.3 and sum over all neutrino generations in the final state to find

$$BR(H^+ \to \ell^+\nu) = \frac{\Gamma(H^+ \to \ell^+\nu)}{\sum_{\ell=e,\mu,\tau} \Gamma(H^+ \to \ell^+\nu)} = \frac{\sum_j m_{\nu_j}^2 |U_{\ell j}|^2}{\sum_{\ell=e,\mu,\tau} \sum_j m_{\nu_j}^2 |U_{\ell j}|^2}. \tag{3.50}$$

Making use of the unitarity of the mixing matrix, the relevant factor appearing in this branching ratio can be rewritten as

$$\sum_{i=1}^{3} |U_{\mu i}|^2 m_{\nu,i}^2 = \begin{cases} m_{\nu,1}^2 + |U_{\mu 2}|^2 \Delta m_{21}^2 + |U_{\mu 3}|^2 \Delta m_{31}^2, & \Delta m_{31}^2 > 0 \\ m_{\nu,3}^2 - |U_{\mu 1}|^2 \Delta m_{31}^2 + |U_{\mu 2}|^2 (\Delta m_{21}^2 - \Delta m_{31}^2), & \Delta m_{31}^2 < 0\,. \end{cases} \tag{3.51}$$

Figure 3.1 shows the behaviour of $BR(H^+ \to \ell^+\nu)$ as a function of the lightest neutrino mass for normal and inverted neutrino mass ordering. We have allowed the Dirac phase, neutrino mass differences and mixing angles appearing in (3.50) to vary freely within the 3σ ranges listed in table 2.3. Recall that the newest measurements suggest the narrower region given in (2.27) for the values of $\sin^2\theta_{13}$. However, the impact on $BR(H^+ \to \ell^+\nu)$ of restricting $\sin^2\theta_{13}$ to this narrower region is negligible. The only effect worth mentioning shows up in $BR(H^+ \to e^+\nu)$ in the case of normal mass ordering, where the band of possible branching ratios becomes narrower in the limit of small neutrino masses. We therefore refrain from explicitly highlighting points compatible with the new measurements.

An interesting feature of these leptonic decays is that their observation would make it possible to distinguish between the two possible mass orderings of the

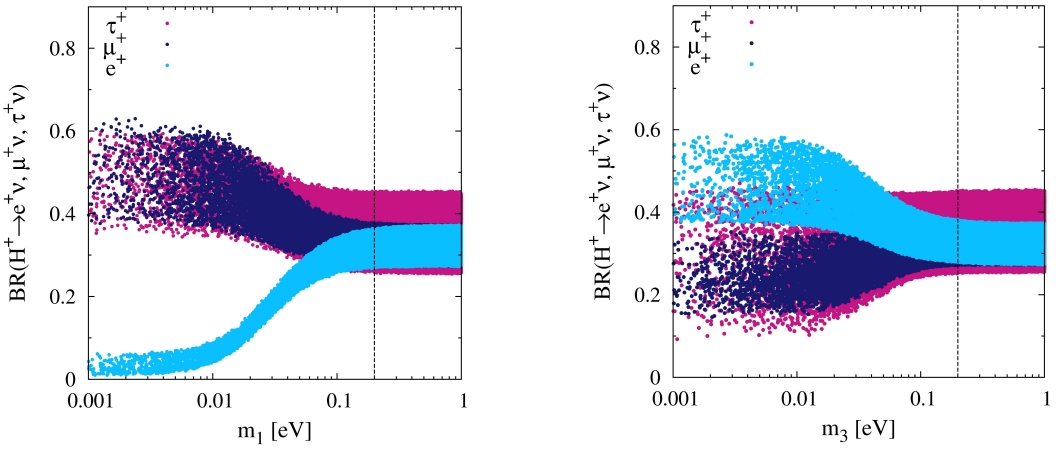

(a) Normal hierarchy

(b) Inverted hierarchy

Figure 3.1: $BR(H^+ \to \ell^+\nu)$ as a function of the lightest neutrino mass for neutrino oscillation parameters within the 3σ ranges of table 2.3. The dashed line shows the upper bound on the lightest neutrino mass given by the WMAP data, see eq. (2.47).

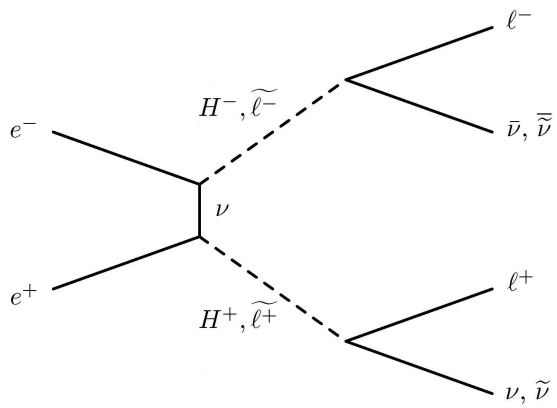

Figure 3.2: Feynman diagram of the process $e^+e^- \to \ell^-\ell^+ + E_{\text{miss}}$ at LEP.

neutrinos for a rather large region of the lightest neutrino mass. As figure 3.1 shows, it would be preferable to take more than just the τ decay channel into account in future searches for H^+ decays. This is in particular important for the case of inverted mass ordering, where the branching ratio to the τ is only about thirty percent.

In addition to the direct charged Higgs search mentioned above, LEP also looked for events of the form

$$e^+e^- \to e^+e^-,\ \mu^+\mu^- + \text{missing energy}. \tag{3.52}$$

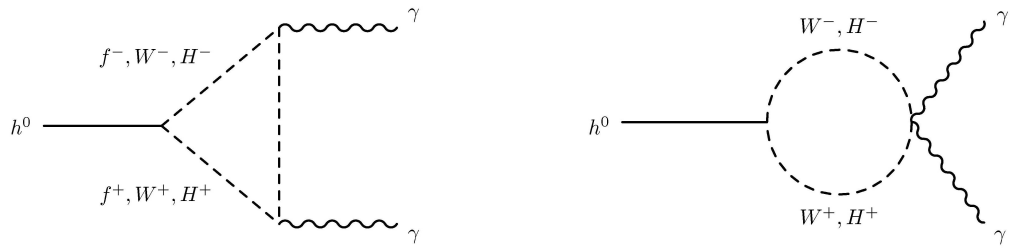

Figure 3.3: Feynman diagrams of the process $h^0 \to \gamma\gamma$, $(f = \ell, q)$.

This signature was actually investigated as part of the search for SUSY particles, with sleptons assumed to be mediating the process. However, in our 2HDM the same signature can be induced with the charged Higgs taking the place of the sleptons, see figure 3.2. The authors of [14] used the corresponding LEP results in conjunction with the branching ratios determined above to obtain a lower bound on the charged Higgs mass of

$$m_{H^\pm} \gtrsim 65 - 83 \text{ GeV}, \tag{3.53}$$

depending on the value of the lightest neutrino mass and the hierarchy. Note however that we must still take the couplings $H^\pm \to A^0 W^\pm,\ H^0 W^\pm$ into account. Their presence could in principle spoil the above mass bound, which was obtained by assuming that the couplings of $H^\pm$ were dominated by the couplings appearing in the leptonic branching ratios determined above. Note that, as listed in table 3.3, the processes $H^\pm \to A^0 W^\pm,\ H^0 W^\pm$ do not contribute for on-shell final particles. Of course, they could still give a non-vanishing contribution in processes where A^0 or H^0 and $W^\pm$ appear as off-shell intermediate particles, with magnitude depending on the size of m_{A^0,H^0}. However, the authors of [14] point out that the contribution from these off-shell processes are negligibly small if one takes the lower bound on m_{A^0,H^0} (3.49) into account and assumes that neutrino Yukawa couplings are of order one. Therefore the limit (3.53) given above remains valid.

Let us now turn to the decay channels of h^0, which as we have noted before is dominated by the contribution from Φ_2 and has couplings that are very similar to those of the Standard Model Higgs particle. Table 3.3 confirms that in the ν2HDM the tree-level decays to leptons, quarks or gauge bosons of this SM-like Higgs are indeed nearly unchanged from the SM case, with deviations suppressed by $v_1/v_2 \sim \mathcal{O}(10^{-11})$.

However, apart from tree-level processes there is also one important loop-level decay that is considered in many Higgs boson searches, including for example at the LHC. Namely, this is the decay of h^0 into two photons. In the SM this process is induced by fermion or W boson loops, as shown in figure 3.3. As stated above, the tree-level couplings of h^0 to charged leptons, quarks and W bosons is changed only at order v_1/v_2. This implies that also the contributions to $h^0 \to \gamma\gamma$ of

the loop diagrams with these particles running in the loop receive only negligible corrections to their SM values[9].

The major change in the ν2HDM thus comes from the existence of a new channel, with a charged Higgs running in the loop. Since the couplings of h^0 and γ to the charged Higgs are not suppressed by v_1/v_2 (see table 3.3 and equation (D.9)), this additional contribution can significantly alter the prediction for $\Gamma(h^0 \to \gamma\gamma)$. In [84] it was shown that the partial decay width $\Gamma(h^0 \to \gamma\gamma)$ for a general 2HDM is given by[10]

$$\Gamma(h^0 \to \gamma\gamma) = \frac{G_F \alpha^2 m_{h^0}^3}{128\sqrt{2}\pi^3} \left| \sum_{f=b,t} g_f Q_f^2 N_c A_{1/2}(\tau_f) + g_W A_1(\tau_W) + g_{H^\pm} A_0(\tau_{H^\pm}) \right|^2, \tag{3.54}$$

where $N_c = 3$ is the number of colors and $Q_t = 2/3,\ Q_b = -1/3$ are the charges of the top and bottom quarks. The parameters τ_i are defined by

$$\tau_i = \frac{m_{h^0}}{4m_i} \tag{3.55}$$

where for each channel m_i is the mass of the particle running in the loop. The factors g_f, g_W and $g_{H^\pm}$ describe the coupling strength of h^0 to the fermions, the W boson and the charged Higgs scalars. In the ν2HDM we find using $v_1 \ll v_2$

$$g_f^{\nu\text{2HDM}} = \frac{\cos\alpha}{\sin\beta} \simeq 1 = g_f^{\text{SM}}, \tag{3.56}$$

$$g_W^{\nu\text{2HDM}} = \sin(\beta - \alpha) \simeq 1 = g_W^{\text{SM}} \tag{3.57}$$

and

$$g_h^{\nu\text{2HDM}} = -\frac{\lambda_3 v_2 v \sin^2\beta \cos\alpha}{2m_{H^\pm}^2} \simeq -\frac{\lambda_3 v^2}{2m_{H^\pm}^2}. \tag{3.58}$$

Note that the partial decay width in the Standard Model can also be found from equation (3.54) by setting $g_f = g_W = 1$ and $g_{H^\pm} = 0$. It is left to specify the amplitudes $A_i(\tau_i)$ which arise from the loop integrals in the various channels. They are given by

$$A_0(\tau_{H^\pm}) = -\frac{\tau_{H^\pm}\left(\tau_{H^\pm} - \arcsin^2\sqrt{\tau_{H^\pm}}\right)}{\tau_{H^\pm}^2}, \tag{3.59}$$

$$A_{1/2}(\tau_t) = \frac{2(\tau_t + (\tau_t - 1)\arcsin^2\sqrt{\tau_t})}{\tau_t^2}, \tag{3.60}$$

$$A_{1/2}(\tau_b) = \frac{2}{\tau_b} - \frac{\tau_b - 1}{2\tau_b^2}\left(\log\frac{1+\sqrt{1-1/\tau_b}}{1-\sqrt{1-1/\tau_b}} - i\pi\right)^2 \tag{3.61}$$

[9] Note that the couplings of charged leptons, quarks and W bosons to photons are identical to the SM case in any 2HDM.

[10] As in the SM, the coupling of h^0 to the heavy quarks b and t is significantly larger than the coupling to the other fermions, so that these particles will dominate the fermionic contribution.

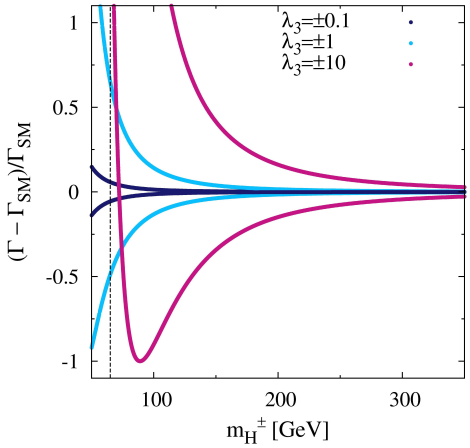

Figure 3.4: $\left(\Gamma^{\nu 2\mathrm{HDM}}(h^0 \to \gamma\gamma) - \Gamma^{\mathrm{SM}}(h^0 \to \gamma\gamma)\right)/\Gamma^{\mathrm{SM}}(h^0 \to \gamma\gamma)$ as a function of the charged Higgs boson mass. Negative values are only possible for $\lambda_3 < 0$. The dashed line marks the LEP bound $m_{H^\pm} \gtrsim 65$ GeV.

and

$$A_1(\tau_W) = -\frac{2\tau_W^2 + 3\tau_W + 3(2\tau_W - 1)\arcsin^2\sqrt{\tau_W}}{\tau_W^2}. \tag{3.62}$$

In figure 3.4 we have plotted the relative deviation of the predicted partial decay width in the ν2HDM from the corresponding SM prediction for different values of the parameter λ_3. We have assumed that $|\lambda_3|$ is of order one as it is a dimensionless parameter of the scalar potential. From figure 3.4 we see that depending on the sign of λ_3 the partial width $\Gamma^{\nu 2\mathrm{HDM}}(h^0 \to \gamma\gamma)$ can be significantly enhanced or reduced compared to the SM value, in particular for $m_{H^\pm}$ not too large. A precise measurement of this decay channel, for example at the LHC, could therefore be used to test for the presence of a second Higgs doublet coupling mainly to the neutrinos.

In addition to the various decay signatures discussed above, the presence of the second Higgs doublet will also alter the predictions for other electroweak observables, for example for the relationship between the gauge boson masses. The effects of new physics on the electroweak observables are conveniently studied by considering predicted changes of the so-called oblique parameters, in particular the parameters S, T and U [11]. These oblique parameters are defined as [85]

$$\begin{aligned}\frac{\alpha_{\mathrm{em}}}{4 s_W^2 c_W^2} S \;=\; & \frac{A_{ZZ}(m_Z^2) - A_{ZZ}(0)}{m_Z^2} - \left.\frac{\partial A_{\gamma\gamma}(q^2)}{\partial q^2}\right|_{q^2=0} \\ & + \left.\frac{c_W^2 - s_W^2}{c_W s_W}\frac{\partial A_{\gamma Z}(q^2)}{\partial q^2}\right|_{q^2=0},\end{aligned} \tag{3.63}$$

[11] Note, however, that this parametrisation is only useful if the changes of the electroweak observables result from changes of the vacuum polarisation amplitudes. This is the case for any 2HDM.

$$\alpha_{\rm em} T = \frac{A_{WW}(0)}{m_W^2} - \frac{A_{ZZ}(0)}{m_Z^2} \tag{3.64}$$

and

$$\begin{aligned} \frac{\alpha_{\rm em}}{4 s_W^2} U &= \frac{A_{WW}(m_W^2) - A_{WW}(0)}{m_W^2} - c_W^2 \frac{A_{ZZ}(m_Z^2) - A_{ZZ}(0)}{m_Z^2} \\ &\quad - s_W^2 \left.\frac{\partial A_{\gamma\gamma}(q^2)}{\partial q^2}\right|_{q^2=0} + 2 c_W s_W \left.\frac{\partial A_{\gamma Z}(q^2)}{\partial q^2}\right|_{q^2=0}, \end{aligned} \tag{3.65}$$

such that they vanish exactly in the SM case. In these definitions we have used $s_W := \sin\theta_W$ and $c_W := \cos\theta_W$, where θ_W is the Weinberg angle defined in appendix A. Furthermore $A_{xx'}(q^2)$ are the coefficients of $g^{\mu\nu}$ in the vacuum polarisation tensor, with q^2 denoting the four-momentum of the gauge bosons involved.

The parameters S, T and U have been calculated for general multi-Higgs models in [85]. The results in the case of a general 2HDM, which suffice for the analysis presented here, have been recently reviewed in [86]. Note that, to one-loop order, S, T and U do not depend on the specific type of 2HDM under consideration. This is because the choice of model affects only the structure of the Yukawa couplings, which do not enter into the calculations at one loop level. However, the value of $(\beta-\alpha)$ does affect the oblique parameters, as $(\beta-\alpha)$ appears in the relevant terms of the Lagrangian describing the couplings of gauge bosons and Higgs scalars (see equation (3.38)).

Let us now assume that the mass of the SM-like Higgs m_{h^0} is given by the SM reference value of roughly 120 GeV as suggested by the recent LHC measurements [87]. Then the oblique parameters can be viewed as functions of the additional Higgs masses m_{H^0,A^0} and $m_{H^\pm}$. These dependencies arise from contributions to the vacuum polarisation amplitudes with the additional scalars H^0, A^0 and $H^\pm$ running in the loop. This means that the restrictions on S, T and U obtained e.g. from electroweak precision tests at LEP can be used to constrain the possible mass regions of the additional Higgs fields. The results for the case relevant to our analysis, i.e. with $m_{h^0} \simeq 120$ GeV and $(\beta-\alpha) \simeq \pi/2$, have been calculated in [86] and are shown in figure 3.5.

Recall from equation (3.32) that in the model considered here the Higgs masses are related by $m_{H^0}^2 = m_{A^0}^2 = m_{H^\pm}^2 + \lambda_4 v_2^2/2$. Keeping in mind that we expect $v_2 \simeq 250$ GeV and $\lambda_4 \sim \mathcal{O}(1)$, we read off from figure 3.5 that compatibility with the experimental S, T and U bounds can be achieved, at least for $m_{H^\pm}$ varying between 250 and 750 GeV. In fact, figure 3.5 strongly suggests that this will continue to hold even for a larger mass region of $m_{H^\pm}$.

Another observable that is often considered is the so-called ρ-parameter, which is defined by

$$\rho = \frac{m_W^2}{m_Z^2 c_W^2}. \tag{3.66}$$

In the SM there holds $\rho_{\rm tree}^{\rm SM} = 1$ at tree-level, while at higher loop level the value is corrected vacuum polarization effects. The Standard Model predictions for

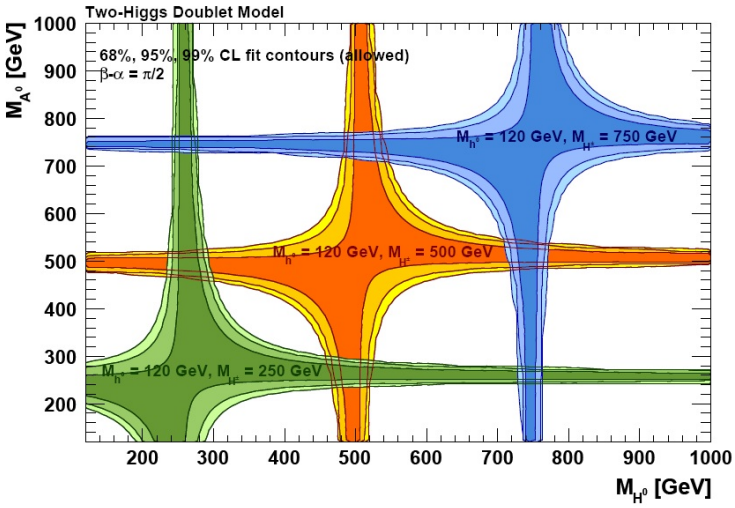

Figure 3.5: Contour plot of S, T and U restricted mass regions in a general 2HDM with $(\beta - \alpha) = \pi/2$ and $m_{h^0} = 120$ GeV, taken from [86].

these loop corrections are in very good agreement with the measured electroweak precision data. To avoid contradicting the experimental results in extensions of the SM one must therefore guarantee that the new physics do not affect ρ too strongly. However, note that the contribution of new physics to the ρ-parameter is directly related to the oblique parameter T by

$$\Delta\rho = \rho - \rho^{\mathrm{SM}} = \alpha_{\mathrm{em}} T. \tag{3.67}$$

Therefore the possible bounds that could be obtained from measurements of ρ are already contained in the restrictions on T that were expanded on above. In particular, the previous discussion implies that the contributions to $\Delta\rho$ in the model considered here will be small enough to be compatible with the electroweak precision measurements for the expected magnitudes of v_2 and λ_4.

3.5.2 Unitarity constraints

A fundamental requirement of any consistent physical theory is that probabilities must be conserved in the time evolution of the theory. In quantum mechanical systems the transition probabilities between the possible initial and final states are encoded in the so-called S-matrix. The above statement then simply translates into the requirement that the S-matrix must be unitary. Of course, the Standard Model enjoys this property, but we must still ensure that unitarity is not violated once the second Higgs doublet is included. As discussed in [67], the fact that the SM S-matrix is unitary implies that it is sufficient to study the sub-block of the S-matrix describing the scalar-scalar scattering processes. For simplicity we restrict ourselves to the tree-level scattering amplitudes, adapting the results that were recently reviewed in [67] to the scalar potential given in (3.2). Requiring

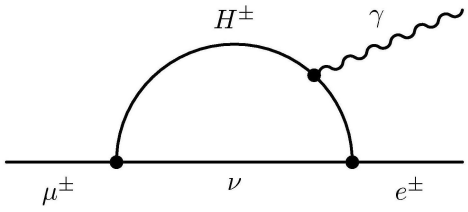

Figure 3.6: Example of a Feynman diagram contributing to the process $\mu \to e\gamma$. The photon can also be emitted by the initial or final state fermion.

unitarity of the S-matrix then translates into the constraints

$$\frac{3}{2}(\lambda_1 + \lambda_2) \pm \sqrt{\frac{9}{4}(\lambda_1 - \lambda_2)^2 + 4\lambda_{34}^2} < 8\pi, \tag{3.68}$$

$$\frac{1}{2}(\lambda_1 + \lambda_2) \pm \sqrt{(\lambda_1 - \lambda_2)^2 + 4\lambda_4^2} < 8\pi, \tag{3.69}$$

$$\lambda_{1,2,3} < 8\pi, \quad \lambda_3 + 2\lambda_4 < 8\pi, \quad \lambda_{34} < 8\pi \quad \text{and} \quad \lambda_3 - \lambda_4 < 8\pi, \tag{3.70}$$

on the parameters of the potential. These restrictions on the parameters can be translated into constraints on the Higgs vevs and therefore the masses of the various Higgs scalars. In the case where the soft breaking term m_{12}^2 in the scalar potential is absent the unitarity requirements put severe upper bounds on the magnitude of $\tan\beta$ if one wishes to keep the mass of the SM-like Higgs m_{h^0} at a realistic value. However, allowing for the soft breaking term relaxes these bounds significantly, as can be seen from equations (3.12), (3.13) and (3.31). As analysed in [67,88], $m_{h^0} \simeq 120$ GeV is compatible with $\tan\beta \sim \mathcal{O}(10^{11})$ for $m_{12} \sim \mathcal{O}(\text{MeV})$ without violating the unitarity conditions. The upper bounds on the other Higgs masses are even less restrictive (at least several hundred GeV) [88].

3.5.3 Charged lepton flavour violation via $H^\pm$ loops

A phenomenologically important feature of 2HDMs is that the appearance of the charged Higgs bosons gives rise to a new source of charged lepton flavour violation (cLFV). In particular, charged Higgs boson loops can mediate $f_1 \to f_2\gamma$ transitions, with $f_1 = \mu$ and $f_2 = e$ or $f_1 = \tau$ and $f_2 = e, \mu$. Figure 3.6 shows an exemplary one-loop Feynman diagram contributing to the process $\mu \to e\gamma$. Note that the absence of charged lepton flavour violation in the SM framework is a result of the masslessness of the neutrinos, which as discussed in chapter 2 implies that no mixing matrix appears in the leptonic sector. However, as soon as neutrino masses are introduced, cLFV can be induced via $W^\pm$ loops even in models with a single Higgs.

In the following we will discuss flavour changing processes of the form $f_1 \to f_2\gamma$ in more detail. As we will see, the contribution from $W^\pm$ loops is very highly

suppressed due to the smallness of the neutrino masses (GIM mechanism [89]). Therefore in 2HDMs the branching ration for these cLFV processes is dominated by the contribution from the charged Higgs loops.

To begin, let us recall the relevant couplings from the Yukawa Lagrangian of equation (3.46)

$$-\mathcal{L}_{\text{Yukawa}} \supset \frac{\sqrt{2}}{v}\tan(\beta)\overline{\nu_{\text{R}}^0} m_\nu U_{\text{PMNS}}^\dagger \ell_{\text{L}}^0 H^+ + \text{h.c.} \tag{3.71}$$

Note that $\tan\beta = v_2/v_1$ is of order $\mathcal{O}(10^{11})$ in the ν2HDM, so that couplings which are proportional to $\cot(\beta)$ can be safely neglected. The index 'PMNS' of the mixing matrix will be suppressed in the following chapters whenever there is no potential for confusion. As we are concerned with lepton flavour violation in this subsection, we will always normalise all branching ratios with respect to the total decay width for processes with a lepton in the final state. Adapting the results of [90] and working in the limit $m_{f_2} \ll m_{f_1} \ll m_{H^\pm}$[12], we find for an on-shell final state photon

$$BR(f_1 \xrightarrow{H^\pm} f_2\gamma) \simeq \frac{\Gamma(f_1 \xrightarrow{H^\pm} f_2\gamma)}{\Gamma(f_1 \xrightarrow{W^\pm} f_2\nu\bar{\nu})} \simeq \frac{\alpha_{\text{em}}}{192\pi G_F^2 m_{H^\pm}^4 v_1^4}\left|\sum_{j=1}^{3} U_{f_1 j}^* U_{f_2 j} m_{\nu_j}^2\right|^2 . \tag{3.72}$$

Here we have used the fact that the total rate of charged lepton decays with a given lepton f_2 in the final state is dominated by the SM decay rate

$$\Gamma(f_1 \xrightarrow{W^\pm} f_2\nu\bar{\nu}) \simeq \frac{G_F^2 m_{f_1}^5}{192\pi^3} \tag{3.73}$$

induced by tree-level W exchange, $\Gamma^{\text{tot.}}(f_1 \to f_2 + x) \simeq \Gamma(f_1 \xrightarrow{W^\pm} f_2\nu\bar{\nu})$. In particular, the tree-level W exchange channel for the decay $f_1 \longrightarrow f_2\nu\bar{\nu}$ dominates over the corresponding channel with tree-level $H^\pm$ exchange. We explicitly verify this statement in section 3.5.5.

The decay width of the corresponding W-mediated transition can be calculated in a similar manner. Requiring again that the photon is on-shell we find

$$\Gamma(f_1 \xrightarrow{W^\pm} f_2\gamma) = \frac{(m_{f_1}^2 - m_{f_2}^2)^3 g_2^4}{\pi^5 4(16)^3 m_W^4 m_{f_1}^3}\left[|f(m_{f_1}, m_{f_2})|^2 + |f(m_{f_2}, m_{f_1})|^2\right], \tag{3.74}$$

where we have defined

$$f(x,y) = \sum_{j=1}^{3} U_{f_1 j}^* U_{f_2 j} x\left(-\frac{5}{6} + \frac{1}{4}\frac{m_{\nu_j}^2}{m_{W^\pm}^2} + \frac{y^2}{m_{W^\pm}^2}\left(\frac{1}{12} - \frac{1}{6}\frac{m_{\nu_j}^2}{m_{W^\pm}^2}\right)\right). \tag{3.75}$$

[12]Note that $m_{H^\pm}$ is required to be at least of the order of 100 GeV by the LEP bound, see equation 3.19.

Taking the unitarity of the mixing matrix into account we find the leading order contribution in the limit $m_2 \ll m_1 \ll m_{W^\pm}$ to be

$$BR(f_1 \xrightarrow{W^\pm} f_2\gamma) \simeq \frac{\Gamma(f_1 \xrightarrow{W^\pm} f_2\gamma)}{\Gamma(f_1 \xrightarrow{W^\pm} f_2\nu\bar{\nu})} \simeq \frac{3\alpha_{\text{em}}}{32\pi m_W^4}\left|\sum_{j=1}^{3} U^*_{f_1 j}U_{f_2 j}m^2_{\nu_j}\right|^2 . \tag{3.76}$$

These results allow us to compare the relative frequency with which the W-mediated and Higgs-mediated decays are expected to occur. We find

$$\frac{BR(f_1 \xrightarrow{H^\pm} f_2\gamma)}{BR(f_1 \xrightarrow{W^\pm} f_2\gamma)} \simeq \frac{v_2^4}{v_1^4} \simeq \mathcal{O}(10^{45}), \tag{3.77}$$

so that as stated above the W contribution is indeed completely negligible in comparison with the $H^\pm$ contribution.

Let us therefore have a more detailed look at the branching ration of the Higgs-induced process given in equation 3.72. The sum appearing in this expression can be rewritten in terms of the neutrino mass differences

$$\left|\sum_{j=1}^{3} U^*_{f_1 j}U_{f_2 j}m^2_{\nu_j}\right|^2 = \left|U^*_{f_1 2}U_{f_2 2}\Delta m^2_{21} + U^*_{f_1 3}U_{f_2 3}\Delta m^2_{31}\right|^2 , \tag{3.78}$$

where we again made use of the unitarity of the mixing matrix. Let us now concentrate on $\mu \to e\gamma$. Using the parametrisation (2.19) of the mixing matrix one finds that the sum (3.78) (and therefore also the whole flavour violating amplitude) vanishes if

$$\sin\theta_{13} \simeq \frac{1}{2}\cot\theta_{23}\sin 2\theta_{12}\frac{\Delta m^2_{21}}{\Delta m^2_{31}} . \tag{3.79}$$

In deriving this estimate we assumed CP conservation, i.e. $\delta = 0$, for simplicity. Substituting in the best fit results for θ_{23} and θ_{12} as well as the mass differences we find that vanishing of the flavour violating amplitude requires $\sin\theta_{13} \simeq 0.014$. This value is well below the measured lower bound on $\sin\theta_{13}$, see table 2.3. Hence we see that, given the measured leptonic mixing angles and mass differences, $\mu \to e\gamma$ has to occur in the context of ν2HDMs if CP is conserved. An analogous consideration of the processes $\tau \to e\gamma$ and $\tau \to \mu\gamma$ similarly shows that they must occur as well in the CP conserving limit. In fact, our numerical analysis shows that this statement remains true even when allowing for $\delta \neq 0$ (see figure 3.7).

We are now in a position to compare the predicted branching ratios with the corresponding experimental bounds, which are collected in table 3.4. The scatter plots in figure 3.7 show the predicted branching ratios $BR(f_1 \to f_2\gamma)$ as a function of $\sin^2\theta_{13}$ for the case of normal neutrino mass ordering and for two different values of $m_{H^\pm}v_1$. The oscillation parameters and the Dirac phase were allowed to vary freely within their measured 3σ ranges, given in table 2.3. For the processes $BR(\mu \to e\gamma)$ and $BR(\tau \to \mu\gamma)$, the change in these plots when considering inverted instead of normal mass ordering is negligible. For $BR(\tau \to e\gamma)$ we observe

Process	Current bound		Future sensitivity	
$BR(\mu \to e\gamma)$	1.2×10^{-11}	[35]	10^{-13}	[91]
$BR(\tau \to e\gamma)$	3.6×10^{-8}	[92]	2×10^{-9}	[93]
$BR(\tau \to \mu\gamma)$	4.5×10^{-8}	[94]	2×10^{-9}	[93]

Table 3.4: Upper bounds on the branching ratios for the cLFV processes $f_1 \to f_2\gamma$.

a small shift upwards for inverted hierarchy, while the general behaviour remains unchanged. However, the predicted values for inverted hierarchy are still nearly one order of magnitude below the sensitivity of the planned future experiments, hence we refrain from showing the corresponding plot.

Figure 3.7 shows that, taking into account the expected magnitude of $m_{H^\pm} v_1$, only the process $\mu \to e\gamma$ is within the reach of the current experimental sensitivity. Let us therefore concentrate on this process in the following. Note that the predicted branching ratio shows a strong dependence not only on the value of $m_{H^\pm} v_1$ but also on the value of $\sin^2\theta_{13}$. For small θ_{13} compatibility with the current experimental bound on the branching ratio can be achieved even for reasonably small values of $m_{H^\pm} v_1$ (e.g. $v_1 \simeq 1$ eV and $m_{H^\pm}$ just above the LEP bound). To obtain a more stringent lower bound on $m_{H^\pm} v_1$ from these measurements we therefore first of all need stronger bounds on θ_{13}. As already mentioned in chapter 2, new results of a global analysis of the experimental data on $\sin^2\theta_{13}$ have recently been announced [44], which yield the value

$$\sin^2\theta_{13} = 0.022^{+0.0033}_{-0.0030} \tag{3.80}$$

at a significance of 6.9σ. Although these values have not yet been officially published, let us nevertheless use them in the following to illustrate the implications on $m_{H^\pm} v_1$ that result from such a precise measurement of θ_{13}. In figure 3.8 we show results of a numerical analysis of the predicted branching ratio as a function of the product $m_{H^\pm} v_1$. We again varied $\sin^2\theta_{12}$ and $\sin^2\theta_{23}$ as well as the neutrino mass differences and the Dirac phase over the full 3σ regions listed in table 2.3, but restricted $\sin^2\theta_{13}$ to the region given in (2.27). From figure 3.8 we read off that for these ranges of the mixing angles the experimental upper bound on $BR(\mu \to e\gamma)$ given in table 3.4 yields a lower bound of

$$m_{H^\pm} v_1 \gtrsim 118 \text{ GeV} \times \text{eV} \tag{3.81}$$

for the product of the charged Higgs mass and the vev of the additional Higgs. If the planned MEG experiment [91] also fails to detect the process $\mu \to e\gamma$ this will give rise to the even more stringent bound

$$m_{H^\pm} v_1 \gtrsim 395 \text{ GeV} \times \text{eV}. \tag{3.82}$$

Let us reiterate at this point that the predicted values of $BR(\tau \to \mu\gamma)$ and $BR(\tau \to e\gamma)$ are so small that neither the currently known bounds nor the bounds

which are expected from planned experiments will further constrain $m_{H^\pm} v_1$; see figure 3.7b and 3.7c. In anticipation of the upcoming publication of the more precise measurement (2.27) of $\sin^2\theta_{13}$, we will take $m_{H^\pm} v_1 \gtrsim 118$ GeV $\times$ eV in the following analysis in order to guarantee compatibility with the upper bound on $BR(\mu \to e\gamma)$.

We now briefly turn our attention to another type of lepton flavour violating process, which occurs if the emitted photon in one of the above processes decays

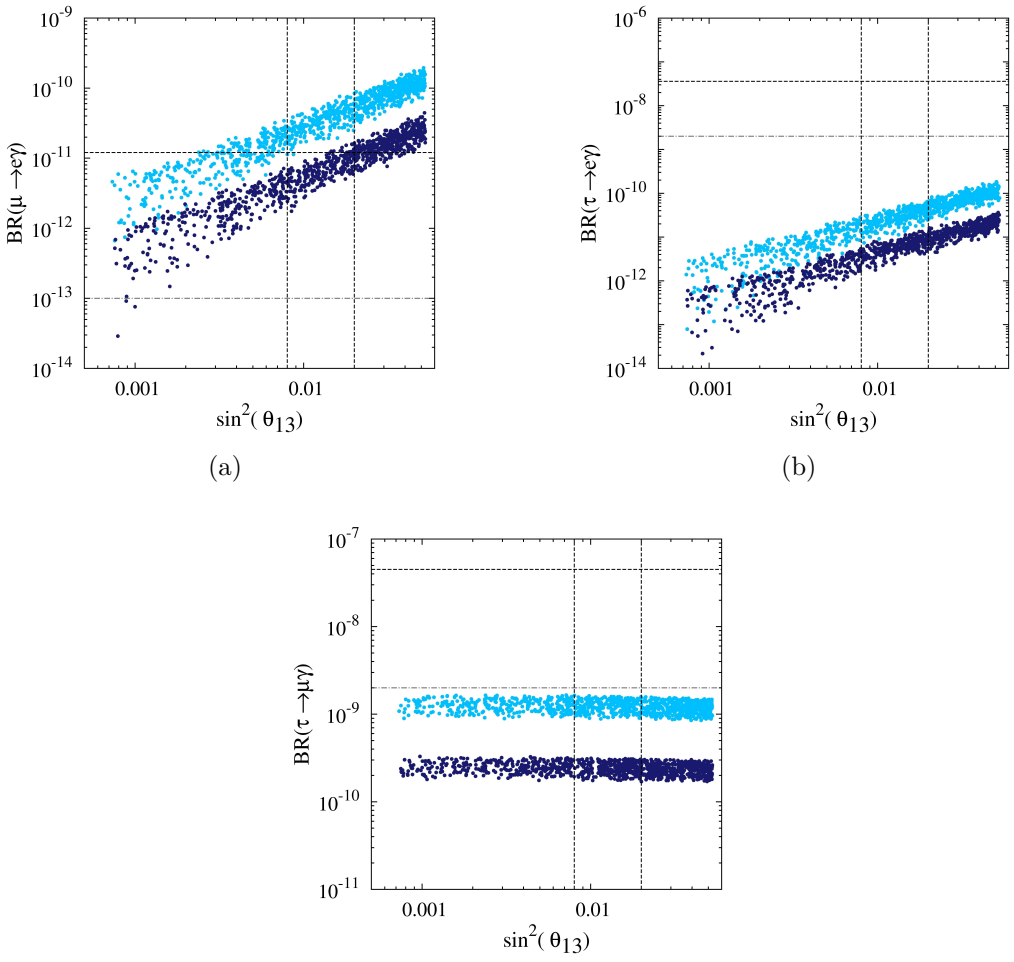

Figure 3.7: Behaviour of $BR(f_1 \to f_2\gamma)$ as a function of $\sin^2\theta_{13}$ in the 3σ region of $\sin^2\theta_{13}$ for $m_{H^\pm} v_1 = 100$ GeV$\times$eV (light blue) and for $m_{H^\pm} v_1 = 150$ GeV$\times$eV (dark blue) in the case of normal hierarchy. The other mixing angles as well as the Dirac phase and the neutrino mass differences were allowed to very freely within the 3σ ranges given in table 2.3. In addition, the current 1σ bound for $\sin\theta_{13}$ and the experimental upper bound for the branching ratios are given by the dashed lines, while the experimental sensitivities aimed at in future experiments are marked by the dash-dotted lines, see table 3.4.

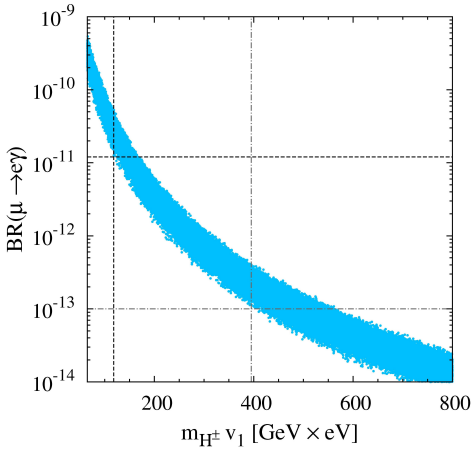

Figure 3.8: Behaviour of $BR(\mu \to e\gamma)$ as a function of $m_{H^\pm} v_1$. The horizontal dashed and dashed-dotted line mark the current upper bound on $BR(\mu \to e\gamma)$ and the expected future sensitivity, respectively. The corresponding vertical lines show the resulting lower bounds on $m_{H^\pm} v_1$.

to a lepton-antilepton pair. We therefore consider the cLFV processes $f_1 \to f_2 f_3 f_3$, where $f_1 = \mu$, $f_{2,3} = e$ or $f_1 = \tau$, $f_{2,3} = \mu, e$. We expect that such a process is suppressed by $\alpha_{\text{em}} \simeq 1/137$ compared to $f_1 \to f_2\gamma$ because of the additional vertex factor, and hence compatibility with the current upper bounds is expected (compare tables 3.4 and 3.5 and see figure 3.7). However let us prove this expectation by adapting the results of [95].

Note that only $H^\pm$-Loops contribute to $\text{BR}(f_1 \to f_2 f_3 f_3)$ at one-loop level, as can be confirmed by analysing the couplings given in equation (3.46). The associated γ-penguin Feynman diagrams of the process take the form shown in figure 3.9. Note that similar diagrams with a Z boson or one of the neutral Higgs scalars taking the place of the photon can contribute. However, we expect these contributions to be suppressed by the mass of the heavy boson and hence to be negligible compared to the γ-penguin process. A similar statement can be made regarding the contribution of box diagrams, which are expected to be suppressed by further powers of $m_{H^\pm}$. Adapting the analysis of [95] to the case at hand we find

$$\frac{BR(f_1 \xrightarrow{H^\pm} f_2 f_3 f_3)}{BR(f_1 \xrightarrow{H^\pm} f_2\gamma)} \simeq \frac{\alpha_{\text{em}}}{3\pi}\left(\ln\left(\frac{m_{f_1}^2}{m_{f_2}^2}\right) - 3\right). \tag{3.83}$$

Plugging in the measured values of the lepton masses and the fine structure constant then yields

$$\frac{BR(f_1 \xrightarrow{H^\pm} f_2 f_3 f_3)}{BR(f_1 \xrightarrow{H^\pm} f_2\gamma)} \simeq \begin{cases} 1.8 \times 10^{-3} & \mu \to 3e \\ 1.4 \times 10^{-4} & \tau \to 3\mu \\ 3.0 \times 10^{-3} & \tau \to 3e. \end{cases} \tag{3.84}$$

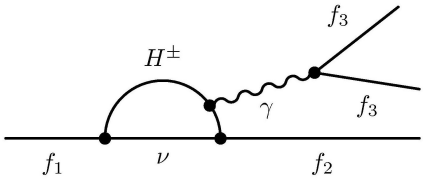

Figure 3.9: Example of a γ-penguin diagram that contributes to $\mathrm{BR}(f_1 \to f_2 f_3 f_3)$.

Process	Current bound [35]	Future sensitivity [93]
$BR(\mu \to 3e)$	1.0×10^{-12}	
$BR(\tau \to 3e)$	3.6×10^{-8}	2×10^{-10}
$BR(\tau \to 3\mu)$	3.2×10^{-8}	2×10^{-10}

Table 3.5: Bounds on the flavour violating processes $f_1 \to f_2 f_2 f_2$.

Comparing the experimental bounds of tables 3.4 and 3.5 we therefore indeed see that compatibility of the considered model with the upper limits on $BR(f_1 \to f_2\gamma)$ automatically leads to compatibility with the bounds on $BR(f_1 \to f_2 f_3 f_3)$.

To close this subsection, let us finally note that flavour changing processes in the quark sector are nearly unaffected by $H^\pm$ loops because the corresponding terms in the Lagrangian are suppressed by $\cot\beta \simeq 10^{-11}$.

3.5.4 The anomalous magnetic moment of the muon

In this subsection we consider another quantity whose predicted value is affected by the presence of a second Higgs doublet. Namely, let us have a look at the anomalous magnetic moment of the muon, a_μ, which has been measured very precisely in the past. In fact, some of the most involved calculations of SM predictions at multi-loop order have focused on a_μ, in order to obtain predictions that are precise enough to allow for meaningful comparison with the very strong experimental bound. The latest results of the measurement of a_μ performed at BNL are given by [96]

$$a_\mu^{\text{exp.}} = 11659208.0(6.3) \times 10^{-10}. \tag{3.85}$$

Note that this measurement is actually less precise than the corresponding measurement of the magnetic moment of the electron. However, the magnetic moment of the muon is a more suitable quantity to consider when looking for the effects of new physics, because such effects generally yield corrections that are proportional to the squared mass of the corresponding lepton and should therefore be much larger in the case of the muon[13].

[13] Of course, even larger corrections are expected for the magnetic moment of the τ. However, due to the extremely short lifetime the experimental precision on a_τ is very limited in comparison.

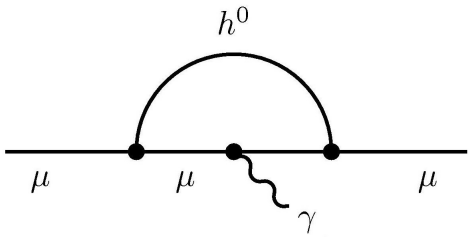

Figure 3.10: SM-like Higgs contribution to a_μ (exemplary).

To set the stage for a discussion of the contributions arising due to the presence of a second Higgs doublet, let us briefly review the SM prediction of a_μ^{SM}. The predicted SM values take into account contributions from QED loops, hadronic vacuum polarisation, hadronic light by light scattering and from EW loops, see [96] and references therein for a review on these calculations. The authors of [96] show that, taking into account QED corrections up to five-loop order and EW corrections up to two-loop order, one obtains a discrepancy from the measured value at a significance of 2.7σ

$$a_\mu^{\text{exp.}} - a_\mu^{\text{SM}} = (26.1 \pm 9.4) \times 10^{-10}. \tag{3.86}$$

In particular, this result is another strong hint for new physics beyond the Standard Model. In the following let us therefore see whether the introduction of a neutrinophilic second Higgs doublet could possibly modify the theoretical prediction in such a way as to account for the discrepancy above.

Note that the EW corrections that were part of the prediction a_μ^{SM} contain loop diagrams involving the SM Higgs particle, which will receive modifications when a second Higgs doublet is present. However, as we will discuss momentarily, the contribution involving only the SM-like Higgs h^0 (which we denote by $a_\mu^{h^0}$) will not change drastically compared to the SM case. Figure 3.10 shows an exemplary Feynman graph that contributes to $a_\mu^{h^0}$. From equation 3.46 we read off the relevant term in the Lagrangian, which is given by

$$-\mathcal{L}_{\text{Yukawa}} \supset \frac{1}{v}\frac{\cos\alpha}{\sin\beta}\overline{\ell_{\text{L}}^0} m_e e_{\text{R}}^0 h^0 + \text{h.c.} \tag{3.87}$$

Adapting the calculations of [97] to the couplings present in our model we obtain the contribution

$$\begin{aligned} a_\mu^{h^0} &= \frac{m_\mu^2}{8\pi^2}\int_0^1 \mathrm{d}x \frac{\frac{1}{v^2}\frac{\cos^2(\alpha)}{\sin^2(\beta)}\,(2x^2 - x^3)\, m_\mu^2}{m_\mu^2 x^2 + m_{h^0}^2(1-x)} \\ &\simeq \frac{G_F m_\mu^2}{4\sqrt{2}\pi^2}\frac{\cos^2(\alpha)}{\sin^2(\beta)}\frac{m_\mu^2}{m_{h^0}^2}\left(-\frac{7}{6} - \ln\left(\frac{m_\mu^2}{m_{h^0}^2}\right) + \mathcal{O}\left(\frac{m_\mu^2}{m_{h^0}^2}\ln\left(\frac{m_\mu^2}{m_{h^0}^2}\right)\right)\right), \end{aligned} \tag{3.88}$$

where we made use of $1/v^2 = \sqrt{2}G_F$. The only difference between this result and the corresponding SM prediction is an additional factor of $\cos^2(\alpha)/\sin^2(\beta)$.

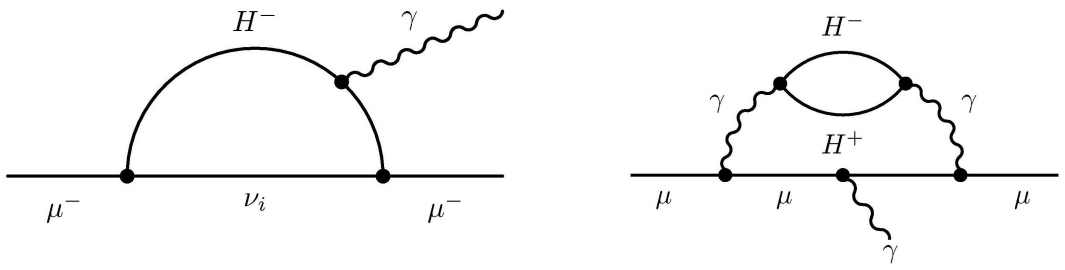

(a) (b)

Figure 3.11: One- and two-loop diagrams contributing to the magnetic moment of the muon (exemplary).

Taking equation (3.31) and $\tan\beta = v_2/v_1 \simeq \mathcal{O}(10^{11})$ into account we see that $\cos^2(\alpha)/\sin^2(\beta) \simeq 1 + \mathcal{O}(10^{-22})$. It follows that the difference from the SM result (which corresponds to the factor being exactly equal to unity) is suppressed by a relative factor of at least 10^{-22}, and is therefore clearly negligible compared to the experimental precision.

Let us therefore see whether any of the 'new' Higgs fields H^0, A^0 and $H^\pm$ can have a sizeable impact on the predictions. We immediately notice that the contribution of A^0 is clearly negligible, as its mass is of the order of the mass of the SM-like Higgs h^0 and the coupling of the muon to A^0 is suppressed by $\cot^2\beta \lesssim \mathcal{O}(10^{-22})$ compared to the coupling to h^0. Therefore $a_\mu^{A^0}$ is negligible compared to the contribution of h^0. Similarly, the coupling of H^0 to μ is suppressed by a factor of $\tan^2\alpha$. Using (3.31) and the fact that $m_{A^0} = m_{H^0}$ it again follows that the contribution $a_\mu^{H^0}$ can be neglected in comparison with the contribution of h^0.

It is therefore left to consider the contribution of the charged Higgs scalars. The relevant term in the Lagrangian giving the coupling to the muon is obtained from (3.46) and reads

$$-\mathcal{L}_{\text{Yukawa}} \supset \frac{\sqrt{2}}{v}\tan\beta\overline{\ell_{\text{L}}^0}U_{\text{PMNS}}m_\nu\nu_{\text{R}}^0H^- + \text{h.c.} \tag{3.89}$$

Figure 3.11 shows some of the Feynman diagrams that contribute to $a_\mu^{H^\pm}$. Let us first have a look at the one-loop contribution. Again making use of the expressions derived in [97] and adapting them to our case then yields the one-loop contribution

$$\begin{aligned} a_\mu^{H^\pm} &= \sum_{i=1}^{3}\frac{m_\mu^2}{8\pi^2v^2}\tan^2\beta\,|U_{\mu i}|^2\,m_{\nu,i}^2\int_0^1\mathrm{d}x\frac{x^3-x^2}{m_\mu^2x^2+(m_{H^\pm}^2-m_\mu^2)x+m_{\nu,i}^2(1-x)} \\ &= -\frac{m_\mu^2}{48\pi^2v_1^2m_{H^\pm}^2}\sum_{i=1}^{3}|U_{\mu i}|^2\,m_{\nu,i}^2\left(1-\mathcal{O}\left(\frac{m_\mu^2}{m_{H^\pm}^2}\right)\right). \end{aligned} \tag{3.90}$$

We immediately notice that $a_\mu^{H^\pm}$ is negative and is therefore of the wrong sign to alleviate the discrepancy (3.86) with the measured value. Therefore the introduction of an additional Higgs doublet cannot be used to explain the difference

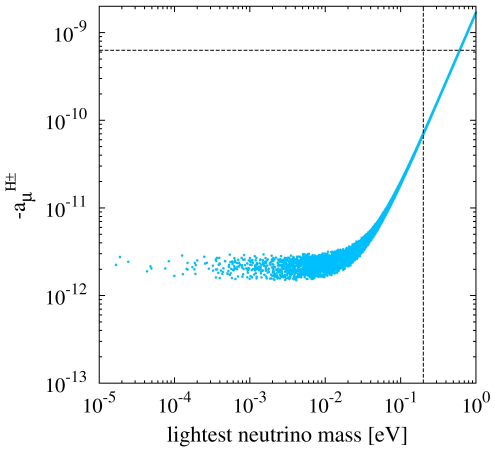

Figure 3.12: One-loop contribution of the charged Higgs boson to the muon magnetic moment as a function of the lightest neutrino mass, in the case of normal mass ordering. The neutrino oscillation parameters were once again allowed to vary freely within the 3σ ranges of table (2.3) and we assumed $m_{H^\pm} v_1 = 118$ GeV $\times$ eV (see section 3.5.3; the curve shifts downwards for larger values of $m_{H^\pm} v_1$). The dashed lines show the upper bound on the lightest neutrino mass given by the WMAP data and the experimental sensitivity of the BNL measurement.

between the experimentally measured magnetic moment of the muon and the corresponding SM prediction (at least in the neutrinophilic case considered here, where the neutral Higgs scalars do not contribute appreciably). Nevertheless, we should estimate the magnitude of this negative contribution, because if the charged Higgs contribution would significantly worsen the deviation between experimental and theoretically predicted values then this would seriously disfavour ν2HDM models.

To evaluate the contribution to $a_\mu^{H^\pm}$, we can again make use of the unitarity of the mixing matrix to rewrite the relevant factor using equation (3.51). Figure 3.12 shows the result of a numerical analysis in the case of normal mass ordering. We show the absolute value of the contribution $a_\mu^{H^\pm}$ as a function of the lightest neutrino mass, i.e. $m_{\nu,1}$ for normal mass ordering, restricting as usual the neutrino oscillation parameters to the 3σ ranges given in table 2.3. For the case of inverted mass ordering, the behaviour as a function of the smallest neutrino mass $m_{\nu,3}$ is nearly identical, and we therefore refrain from showing the corresponding plot. in the numerical analysis we have assumed $m_{H^\pm} v_1 = 118$ GeV $\times$ eV, such that as discussed in subsection 3.5.3 compatibility with the upper bound on the branching ratio of the process $\mu \to e\gamma$ is automatically guaranteed even for values of $\sin^2\theta_{13}$ in the region given in (2.27). Furthermore let us point out that restricting ourselves to this more constrained region for $\sin^2\theta_{13}$ does not change the above results, because the dominant contributions arise from terms which are proportional to

$\sin^2\theta_{23}$ or $\cos^2\theta_{12}$ (see (3.51), (2.19) and table 2.3).

As figure 3.12 shows, after taking into account the bound $m_{H^\pm} v_1 = 118\ \text{GeV} \times \text{eV}$ obtained from cLFV the absolute value of the one loop contribution of the charged Higgs to a_μ is at least one order of magnitude below the current experimental sensitivity, even if the lightest neutrino mass is assumed to be close to its upper limit. In fact, even the experimental sensitivity aimed at in next generation experiments [98] will not be sufficient to detect the small one-loop contribution of the charged Higgs.

At this point we should ensure that the smallness of the charged Higgs contribution is not spoiled by two-loop effects. Of course, two-loop diagrams where the charged Higgs couples directly to the fermions in a similar manner as in the one-loop diagram considered above are expected to be suppressed compared to the corresponding one-loop contribution. However, at two-loop level one can also consider diagrams of the form 3.11b. Note that in this case the suppression compared to the one-loop diagram is less clear because the charged Higgs particles couple to photons rather than to fermions as in the one-loop case. Let us therefore focus on the diagrams of the form shown in figure 3.11b. Their contribution was calculated by Grifols and Pascual in [99], with the result

$$a_\mu^{H^\pm}(2-\text{loop}) = \frac{1}{180}\left(\frac{\alpha_{\text{em}}}{\pi}\right)^2 \frac{m_\mu^2}{m_{H^\pm}^2} + \mathcal{O}\left(\frac{m_\mu^4}{m_{H^\pm}^4}\ln\left(\frac{m_\mu}{m_{H^\pm}}\right)\right). \tag{3.91}$$

Plugging in $m_{H^\pm} v_1 \simeq 118\ \text{GeV} \times \text{eV}$ confirms that the two-loop correction due to the charged Higgs boson is more than three orders of magnitude smaller than the one-loop contribution and can therefore be safely neglected.

Let us summarise the results of the discussion presented above. We have found that the dominant correction to the SM prediction of the muon magnetic moment in a ν2HDM is induced by charged Higgs bosons at one-loop level. This correction has the wrong sign to be able to explain the difference between a_μ^{SM} and the experimentally observed value. However, for charged Higgs masses large enough to avoid the bound $m_{H^\pm} v_1 \gtrsim 118\ \text{GeV} \times \text{eV}$ from cLFV processes, the scale of the predicted corrections $a_\mu^{H^\pm}$ lies at least one order of magnitude below the current experimental sensitivity. Therefore the discrepancy (3.86) of the experimental results and the theoretical predictions is not worsened by the introduction of a neutrinophilic second Higgs doublet.

3.5.5 Tree-level muon and tauon decay - lepton universality

In the framework of the Standard Model the muon and tauon admit tree-level decay through weak charged currents. The resulting decay width has been calculated to high precision [100]

$$\Gamma^{W^\pm}(L \to \ell\nu\bar{\nu}) = \frac{G_F^2 m_L^2}{192\pi^3} f(m_\ell^2/m_L^2)(1 + R(m_L/m_\ell))\left(1 + \frac{3m_L^2}{5m_W^2}\right), \tag{3.92}$$

where phase space and radiative corrections are taken into account in the form of the functions

$$f(x) = 1 - 8x + 8x^3 - x^4 - 12x^2 \ln x\,, \tag{3.93}$$

$$R(x) = \frac{\alpha}{2\pi}\left(\frac{25}{4} - \pi^2\right)\left[1 + \frac{\alpha}{\pi}\left(\frac{2}{3}\ln(x) - 3.7\right) + \mathcal{O}\left(\frac{\alpha^2}{\pi^2}\right)\right]. \tag{3.94}$$

We should point out that by not specifying generation indices for the neutrinos in $\Gamma^{W^\pm}(L \to \ell\nu\bar{\nu})$ we imply that we sum over all possible neutrino generations that can appear in the final state. Of course, in the pure SM case no leptonic mixing occurs, so that the only neutrinos that contribute to this sum are the ones corresponding to the considered lepton generations L and ℓ. However, the result (3.92) is applicable for the W-induced decay even if a non-trivial mixing matrix appears and decays to all neutrino species are possible. This fact is a consequence of the unitarity of the mixing matrix and the sum over final states. In particular, (3.92) gives the W-induced decay rate also in the ν2HDM case.

In the presence of a second Higgs doublet, the charged Higgs bosons give rise to a new channel that mediates tree-level lepton decay. The relevant term in the Lagrangian is given by 3.46

$$-\mathcal{L}_{\text{Yukawa}} \supset \frac{\sqrt{2}}{v}\tan\beta\overline{\ell_{\text{L}}^0}U_{\text{PMNS}}m_\nu\nu_R^0 H^- + \text{h.c.} \tag{3.95}$$

Notice that when calculating the decay rate from this channel and summing over final state neutrinos the mixing matrices do not drop out due to the presence of the mass matrices in the coupling above. Instead, neglecting radiative corrections similar to those appearing in (3.92), one finds the result [100]

$$\Gamma^{H^\pm}(L \to \ell\nu\bar{\nu}) = \frac{G_F^2 m_L^5}{192\pi^3} f(m_\ell^2/m_L^2)\tan^4\beta \frac{\sum_i m_{\nu,i}^2 |U_{Li}|^2 \sum_i m_{\nu,i}^2 |U_{\ell i}|^2}{4m_{H^\pm}^4}. \tag{3.96}$$

At leading order in $m_L^2/m_{W^\pm,H^\pm}^2$ we therefore obtain

$$\frac{\Gamma^{H^\pm}(L \to \ell\nu\bar{\nu})}{\Gamma^{\text{SM}}(L \to \ell\nu\bar{\nu})} = \frac{\sum_i m_{\nu,i}^2 |U_{Li}|^2 \sum_i m_{\nu,i}^2 |U_{\ell i}|^2}{8m_{H^\pm}^4 G_F^2 v_1^4}. \tag{3.97}$$

It seems tempting to try and obtain a bound on $m_{H^\pm}$ from the observed muon and tauon lifetimes, which have been measured with extremely high precision. However, note that a comparison of the predicted and measured lifetimes is problematic, because the best value of G_F is usually calculated from muon lifetime measurements under the assumption that the SM is the exact theory. Therefore we would need an independent measurement of G_F of sufficiently high precision in order to derive a meaningful bound. This implies that it is more advisable to consider instead observables that are less sensitive to the precise value of G_F. In the following we therefore analyse the effective charged current couplings

$g_i,\ i = e,\ \mu,\ \tau$, which are defined in terms of the muon and tauon lifetimes by [101]

$$\tau_\tau = \tau_\mu \frac{g_\mu^2}{g_\tau^2}\frac{m_\mu^5}{m_\tau^5} BR(\tau \to e\nu\bar{\nu}) \frac{f(m_e^2/m_\mu^2)}{f(m_e^2/m_\tau^2)} RC(m_e, m_\mu, m_\tau) \tag{3.98}$$

and

$$\tau_\tau = \tau_\mu \frac{g_e^2}{g_\tau^2}\frac{m_\mu^5}{m_\tau^5} BR(\tau \to \mu\nu\bar{\nu}) \frac{f(m_e^2/m_\tau^2)}{f(m_\mu^2/m_\tau^2)} RC(m_e, m_\mu, m_\tau)\,. \tag{3.99}$$

Here $RC(m_e, m_\mu, m_\tau)$ is again a correction factor that arises from radiative corrections. Note that in the SM there holds $g_\mu^{\rm SM}/g_\tau^{\rm SM} = g_e^{\rm SM}/g_\tau^{\rm SM} = 1$. This is a result of the fact that in the SM the lepton-gauge boson couplings are independent of the lepton generation, which is known as lepton universality.

From equation (3.95) we immediately see that the coupling between leptons and $H^\pm$ depends on the lepton generation, violating lepton universality. To quantify the magnitude of this violation let us first derive a simpler expression for g_μ^2/g_τ^2 from (3.98). We will use the identities

$$\begin{aligned} \frac{\tau_\tau}{\tau_\tau^{\rm SM}}\frac{BR^{\rm SM}(\tau \to e\nu\bar{\nu})}{BR(\tau \to e\nu\bar{\nu})} &= \frac{\Gamma^{W^\pm}(\tau \to e\nu\bar{\nu})}{\Gamma(\tau \to e\nu\bar{\nu})} \\ &= \frac{1}{1 + \Gamma^{H^\pm}(\tau \to e\nu\bar{\nu})/\Gamma^{W^\pm}(\tau \to e\nu\bar{\nu})}\,, \end{aligned} \tag{3.100}$$

$$\frac{\tau_\mu^{\rm SM}}{\tau_\mu} = \frac{\Gamma(\mu \to e\nu\bar{\nu})}{\Gamma^{W^\pm}(\mu \to e\nu\bar{\nu})} = 1 + \Gamma^{H^\pm}(\mu \to e\nu\bar{\nu})/\Gamma^{W^\pm}(\mu \to e\nu\bar{\nu})\,. \tag{3.101}$$

Now we note that multiplying g_μ^2/g_τ^2 by $1 = (g_\tau^{\rm SM})^2/(g_\mu^{\rm SM})^2$ cancels all the factors in (3.98) apart from the lifetimes and branching ratios, as the other factors are independent of the model. In other words

$$\frac{g_\mu^2}{g_\tau^2} = \frac{g_\mu^2}{g_\tau^2}\frac{(g_\tau^{\rm SM})^2}{(g_\mu^{\rm SM})^2} = \frac{\tau_\mu^{\rm SM}}{\tau_\mu}\frac{\tau_\tau}{\tau_\tau^{\rm SM}}\frac{BR^{\rm SM}(\tau \to e\nu\bar{\nu})}{BR(\tau \to e\nu\bar{\nu})}. \tag{3.102}$$

Putting these results together and substituting in equation (3.97) finally yields

$$\begin{aligned} \frac{g_\mu}{g_\tau} &= \sqrt{\frac{1 + \Gamma^{H^\pm}(\mu \to e\nu\bar{\nu})/\Gamma^{\rm SM}(\mu \to e\nu\bar{\nu})}{1 + \Gamma^{H^\pm}(\tau \to e\nu\bar{\nu})/\Gamma^{\rm SM}(\tau \to e\nu\bar{\nu})}} \\ &\simeq 1 + \frac{1}{16 m_{H^\pm}^4 G_F^2 v_1^4}\sum_i m_{\nu,i}^2 |U_{ei}|^2 \left(\sum_i m_{\nu,i}^2 |U_{\mu i}|^2 - \sum_i m_{\nu,i}^2 |U_{\tau i}|^2\right). \end{aligned} \tag{3.103}$$

The second independent combination of charged couplings can be more easily obtained by taking the ratio of equations (3.98) and (3.99), which immediately leads to

$$\begin{aligned} \frac{g_\mu}{g_e} &= \sqrt{\frac{1 + \Gamma^{H^\pm}(\tau \to \mu\nu_\mu\nu_\tau)/\Gamma^{\rm SM}(\tau \to \mu\nu_\mu\nu_\tau)}{1 + \Gamma^{H^\pm}(\tau \to e\nu_e\nu_\tau)/\Gamma^{\rm SM}(\tau \to e\nu_e\nu_\tau)}} \\ &\simeq 1 + \frac{1}{16 m_{H^\pm}^4 G_F^2 v_1^4}\sum_i m_{\nu,i}^2 |U_{\tau i}|^2 \left(\sum_i m_{\nu,i}^2 |U_{\mu i}|^2 - \sum_i m_{\nu,i}^2 |U_{ei}|^2\right). \end{aligned} \tag{3.104}$$

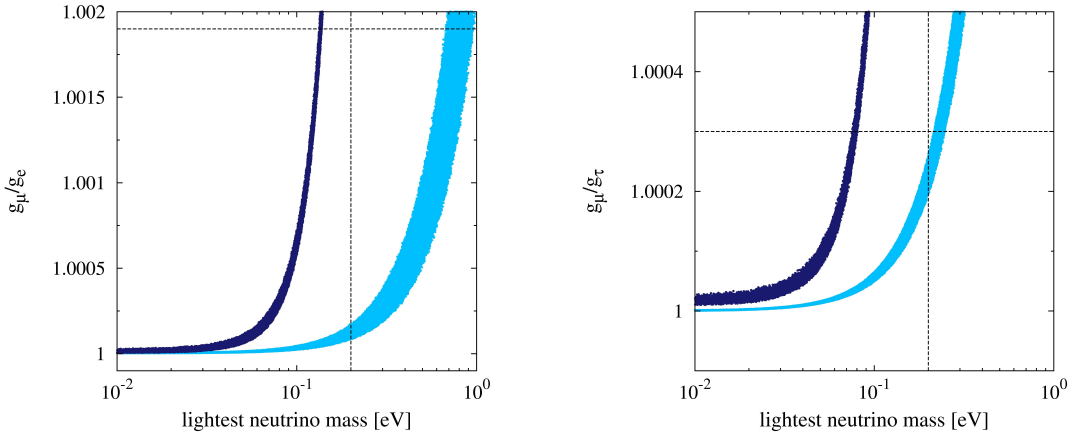

(a) (b)

Figure 3.13: Violation of lepton universality in the ν2HDM for normal (light blue) and inverted (dark blue) mass ordering of the neutrinos. We used $m_{H^\pm} v_1 = 118$ GeV $\times$ eV and restricted the neutrino mixing angles and mass differences to the 3σ ranges of table (2.3). The dashed lines show the experimental upper bounds on the lightest neutrino mass as well as the upper bounds given in (3.105). The curves are shifted to the right if one considers larger values of $m_{H^\pm} v_1$.

The current experimental bounds on these ratios of the charged current couplings are [101]

$$\frac{g_\mu}{g_\tau} = 0.9982 \pm 0.0021 \qquad \text{and} \qquad \frac{g_\mu}{g_e} = 0.9999 \pm 0.0020\,. \tag{3.105}$$

The behaviour of the predicted ratios of the effective charged coupling constants is shown in figure 3.13 as a function of the lightest neutrino mass. In this plot $m_{H^\pm} v_1$ was set to 118 GeV $\times$ eV to guarantee compatibility with the limits on the branching ratio $\mu \to e\gamma$ even for the new values of $\sin^2\theta_{13}$ given in (2.27). We have explicitly checked, that behaviour shown in figure 3.13 does not change when restricting to the more stringent bound (2.27).

Note that in the case of inverted neutrino mass ordering one finds a violation of the charged coupling upper limits for values of the lightest neutrino mass just below the WMAP bound (compare figure 3.13). However, the predicted magnitude of g_μ/g_e and g_μ/g_τ depends strongly on the value of $m_{H^\pm} v_1$, in particular the curves in figure 3.13 are shifted to the right for larger values of $m_{H^\pm} v_1$. This means that we can use the bounds (3.105) to derive a restriction on the possible parameter combinations of $m_{H^\pm} v_1$ and the lightest neutrino mass m_3 in the case of inverted mass ordering. The parameter regions that are compatible with the charged coupling bounds are shown in figure 3.14, where we have additionally highlighted

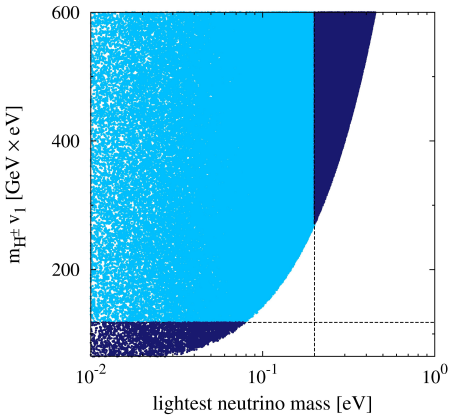

Figure 3.14: Parameter regions which are consistent with the upper bounds on g_μ/g_e and g_μ/g_τ for inverted neutrino mass ordering. The light blue region is in addition consistent with the upper bound on the lightest neutrino by WMAP and with the lower bound on $m_{H^\pm} v_1$ which was derived in the analysis of $BR(\mu \to e\gamma)$ (3.81).

regions that are ruled out either by the WMAP bound on the neutrino masses or by the bounds on charged lepton flavour violation which we had discussed previously. Note that there is a certain region of parameter space, corresponding to small values of $m_{H^\pm} v_1$ and larger neutrino masses, that would have been allowed by the previously discussed bounds from WMAP and cLFV but is ruled out by the bounds on the charged coupling ratios (3.105). In the following chapters we will analyse a model using an A_4 flavour symmetry in which the neutrino masses are naturally small enough to be compatible with these bounds, even for the lowest value of $m_{H^\pm} v_1$ that is compatible with the cLFV bound. We reiterate that this discussion applies to the case of inverted mass ordering only, in the case of normal neutrino hierarchy all parameter values that are compatible with WMAP and cLFV automatically lead to effective charged coupling ratios that lie within the experimental bounds (see figure 3.13).

Chapter 4

Leptonic mixing from an A_4 flavour symmetry

As we have discussed in detail in the previous chapter, the neutrinophilic two Higgs doublet model is very successful in explaining the smallness of the neutrino masses in comparison with the masses of charged leptons of the same generation. However, the ν2HDM predicts only the overall scale of the neutrino mass matrix, while its shape and therefore also the form of the resulting mixing matrix is determined by the Yukawa coupling matrices. In the ν2HDM the form of these Yukawa matrices is arbitrary and constitutes external input into the theory, just as in the case of the Standard Model. We had already pointed out in section 2.6 that being able to explain the observed structure of the parameters determining the mixing matrix would anyway be desirable from a theoretical point of view. This motivation is strengthened even further by our analysis of the ν2HDM phenomenology performed in section 3.5. There we found that many possible experimental signatures of the additional Higgs particles depend on the leptonic mixing matrix and the precise neutrino masses, so that being able to predict these parameters is important also in the context of Higgs searches.

Picking up on the general discussion of section 2.6, let us therefore implement an A_4 flavour symmetry in our model. As was already mentioned above, the A_4 group is a promising candidate for a flavour symmetry because it can lead to a mixing matrix of the tribimaximal form, which is close the the observed form. Models based on the A_4 group have been extensively studied in the existing literature; a very detailed list of different types of such models with corresponding references can be found in [102].

We should point out that all these previously considered A_4 models are based on the assumption that neutrinos are Majorana particles. The prevalence of this choice of Majorana neutrinos in A_4 models can be roughly understood as follows. As we will see, there is a certain A_4-invariant coupling that leads to an antisymmetric contribution to the mass matrix. This contribution takes a form that leads to deviations from the TBM form for the resulting mixing matrix. In models

aiming to achieve exact TBM mixing, this coupling must therefore be forbidden. As neutrinos with Majorana nature enforce a symmetric form of the mass matrix, the offending coupling is automatically absent in A_4 models based on Majorana neutrinos. However, the situation is changed in light of the new experimental results confirming that $\sin\theta_{13}$ is significantly different from zero, which *requires* a departure from the exact TBM form. It is therefore advantageous to consider a model based on Dirac neutrinos, which allows for the antisymmetric A_4 coupling and therefore provides a very natural source of deviations from TBM mixing. For this reason we will analyse an A_4 model based on Dirac neutrinos in this section, complementing the existing studies of Majorana neutrinos.

We will begin by summarising the most important properties of the A_4 group and reviewing why this group is a suitable starting point when looking to generate tribimaximal mixing. In section 4.3 we then proceed to apply the A_4 symmetry to our model, which involves in particular introducing flavon fields and assigning the different fields to irreducible representations of the group in an appropriate manner. As we will see, being able to achieve TBM mixing depends on breaking the A_4 symmetry in a specific way. The required vev structure cannot be easily achieved with the most general ansatz for the potential. We discuss this so-called vev alignment problem as well as several possible solutions in section 4.4. In section 4.5 we consider in detail an extra-dimensional model in which the vev alignment problem is solved by localising groups of fields on separate branes separated along the extra dimension. In this context we also discuss higher order corrections to the mass matrices. We then discuss possible scenarios which could explain the appearance of the A_4 symmetry dynamically, before closing the chapter with a very brief look at the implications for the quark sector.

4.1 The A_4 group

In this section we will recall a number of basic results from the theory of finite groups and apply them to the A_4 group. While we will give only the most important statements in the following, the interested reader may refer to mathematical textbooks on this topic, for example [103], for proofs and additional details on the quoted results.

The A_4 group contains all even permutations of 4 objects and is also known as the alternating group of degree 4. Geometrically, A_4 may be viewed as the rotation group of a tetrahedron. The order, or number of elements, of A_4 is $n_g = 4!/2 = 12$. In general a permutation σ of the set $\{1,2,3,4\}$ can be specified by

$$\sigma: \quad (1,2,3,4) \to (n_1,n_2,n_3,n_4), \tag{4.1}$$

with pairwise distinct $n_1,n_2,n_3,n_4 \in \{1,2,3,4\}$. Such a permutation will be denoted in following simply as $(n_1n_2n_3n_4)$.

One can immediately check that every permutation $\sigma \in A_4$ can be generated by a

Class	Presentation			
C1	$\mathbb{1} = (1234)$			
C2	$T = (2314)$	$ST = (4132)$	$TS = (3241)$	$STS = (1423)$
C3	$T^2 = (3124)$	$ST^2 = (4213)$	$T^2S = (2431)$	$TST = (1342)$
C4	$S = (4321)$	$T^2ST = (3412)$	$TST^2 = (2143)$	

Table 4.1: The conjugacy classes of the A_4 group.

composition of the two basic permutations $S := (4321)$ and $T := (2314)$. S and T thus define a so-called presentation of A_4. Note that they obey $S^2{=}T^3{=}(ST)^3 = \mathbb{1}$, so that S generates the subgroup $\mathbb{Z}_2$ while T generates $\mathbb{Z}_3$. The permutations making up A_4 may be assigned to four different equivalence or conjugacy classes Ci, i=1,2,3,4[1], which are given in table 4.1.

Note that the number of different conjugacy classes is identical to the number of different irreducible representations of A_4. The dimensions n_R of the distinct irreducible representations R can be related to the order of the group by

$$\sum_R n_R^2 = n_g \,. \tag{4.2}$$

As the number of representations is four and there is always the trivial one-dimensional representation this relation can be solved uniquely and one finds that there are three one-dimensional and one three-dimensional representations. These representations will be denoted by 1, $1'$, $1''$ and 3, respectively.

Let $D^R(g)$ denote the matrix corresponding to the group element g in the representation R. The traces of these matrices define the so-called characters χ

$$\chi_g^R = \mathrm{tr} D^R(g) \,. \tag{4.3}$$

Note that because equivalent group elements are represented by similar matrices, and the trace is invariant under similarity transformations, it is sufficient to give the characters for each of the four different conjugacy classes defined above. The completeness and orthonormality relations[2] obeyed by these traces can be used to calculate the character table of the A_4 group, which is given in table 4.2. The character table of course uniquely determines the representation of the generators

[1] Two group elements a and b of the group belong to same conjugacy class when there exists an element $p \in A_4$ such that $a = pbp^{-1}$.

[2] Let n_i denote the number of elements in the conjugacy class Ci. The orthonormality relation then reads $\sum_i \frac{n_i}{n_g} (\chi_i^R)^\dagger \chi_i^{R'} = \delta_{RR'}$, where we sum over the distinct equivalence classes. χ_i^R denotes the character of an arbitrary group element $g \in$ Ci in the representation R. The completeness relation states that $\frac{n_i}{n_g} \sum_R \chi_i^R (\chi_j^R)^\dagger = \delta_{ij}$, where the sum runs over all distinct irreducible representations.

Class	χ^1	$\chi^{1'}$	$\chi^{1''}$	χ^3
C1	1	1	1	3
C2	1	ω	ω^2	0
C3	1	ω^2	ω	0
C4	1	1	1	-1

Table 4.2: Character table of the A_4 group, $\omega = e^{2\pi i/3}$.

S and T in the one-dimensional representations 1, $1'$ and $1''$, yielding

$$\begin{aligned} 1 &: \quad S' = 1, \qquad T' = 1, \\ 1' &: \quad S' = 1, \qquad T' = e^{2\pi i/3} = \omega, \\ 1'' &: \quad S' = 1, \qquad T' = e^{4\pi i/3} = \omega^2. \end{aligned} \tag{4.4}$$

To find matrices furnishing a three-dimensional representation of S and T we note that we can restrict ourselves to unitary representations due to the fact that for finite groups every representation is equivalent to a unitary representation. As $S^2 = \mathbb{1}$, this implies that S is also Hermitian, so that we may in particular look for a representation in which S is real and diagonal. Finally using the trace restrictions required by table 4.2 and applying similar considerations to T, we find

$$3: \qquad S' = \begin{pmatrix} 1 & 0 & 0 \\ 0 & -1 & 0 \\ 0 & 0 & -1 \end{pmatrix}, \qquad T' = \begin{pmatrix} 0 & 1 & 0 \\ 0 & 0 & 1 \\ 1 & 0 & 0 \end{pmatrix}. \tag{4.5}$$

We reiterate that the matrices S' and T' for the three-dimensional representation are unique only up to similarity transformations. The basis we have chosen here, where S' is diagonal, is known as the Ma-Rajasekaran (MR) basis. As we will see it is sometimes useful to work in a basis where T is diagonal (known as the Altarelli-Feruglio basis), and we will give the expressions for S and T in this alternative basis at the end of this section. However, let us first proceed with our considerations in the Ma-Rajasekaran basis.

Let us now consider how to multiply objects in the different representations of A_4. In general, the multiplication of two representations is given by their tensor product, but this will generally lead to a reducible representation. However, to be able to easily evaluate the transformation behaviour of a given product it is helpful to decompose the tensor product into irreducible representations. The multiplicity with which a given irreducible representations R of the group occurs in such a product is given by

$$m_R = \frac{1}{n_g} \sum_i n_i \left(\chi_i^R\right)^* \chi_i \,. \tag{4.6}$$

Here n_i is the number of elements in the conjugacy class Ci and χ_i denotes the

character of the tensor product[3]. This allows us to find

$$\begin{aligned} &1 \otimes \alpha = \alpha\,, \qquad 1' \otimes 1'' = 1\,, \qquad 1' \otimes 1' = 1'', \qquad 1'' \otimes 1'' = 1', \\ &1' \otimes 3 = 3\,, \qquad 1'' \otimes 3 = 3\,, \qquad 3 \otimes 3 = 1 \oplus 1' \oplus 1'' \oplus 3 \oplus 3\,, \end{aligned} \tag{4.7}$$

where $\alpha = 1,\, 1',\, 1'',\, 3$ is any representation. In particular we find that using two triplets (a_1, a_2, a_3) and (b_1, b_2, b_3) we can construct the following bilinears transforming in the different irreducible representations

$$\begin{aligned} (ab)_1 &= (a_1b_1 + a_2b_2 + a_3b_3), \\ (ab)_{1'} &= (a_1b_1 + \omega^2 a_2b_2 + \omega a_3b_3), \\ (ab)_{1''} &= (a_1b_1 + \omega a_2b_2 + \omega^2 a_3b_3), \\ (ab)_{3_1} &= (a_2b_3, a_3b_1, a_1b_2), \\ (ab)_{3_2} &= (a_3b_2, a_1b_3, a_2b_1). \end{aligned} \tag{4.8}$$

As already mentioned above it is sometimes more convenient to work in the Altarelli-Feruglio (AF) basis, where the presentation T rather than S is represented by a diagonal matrix. The basis change matrix diagonalising T' is the so-called 'magic matrix', which is given by

$$V = \frac{1}{\sqrt{3}} \begin{pmatrix} 1 & 1 & 1 \\ 1 & \omega^2 & \omega \\ 1 & \omega & \omega^2 \end{pmatrix}. \tag{4.9}$$

One then straightforwardly obtains the following expressions for the generators in the AF basis

$$T = VT'V^\dagger = \begin{pmatrix} 1 & 0 & 0 \\ 0 & \omega & 0 \\ 0 & 0 & \omega^2 \end{pmatrix}, \qquad S = VS'V^\dagger = \frac{1}{3} \begin{pmatrix} -1 & 2 & 2 \\ 2 & -1 & 2 \\ 2 & 2 & 1 \end{pmatrix}. \tag{4.10}$$

The representations of the other group elements can now be calculated easily using the relations given in table 4.1. Furthermore we must take into account that the explicit expressions for the bilinears constructed from two triplets change under this basis transformation, because (a_1, a_2, a_3) and (b_1, b_2, b_3) have to be transformed. In the AF basis where T is diagonal we find that the multiplication rules given in (4.8) must be replaced by

$$\begin{aligned} (ab)_1 &= (a_1b_1 + a_2b_3 + a_3b_2), \\ (ab)_{1'} &= (a_3b_3 + a_1b_2 + a_2b_1), \\ (ab)_{1''} &= (a_2b_2 + a_1b_3 + a_3b_1), \\ (ab)_{3_s} &= \frac{1}{3}(2a_1b_1 - a_2b_3 - a_3b_2, 2a_3b_3 - a_1b_2 - a_2b_1, 2a_2b_2 - a_1b_3 - a_3b_1), \\ (ab)_{3_a} &= \frac{1}{3}(a_2b_3 - a_3b_2, a_1b_2 - a_2b_1, a_3b_1 - a_1b_3). \end{aligned} \tag{4.11}$$

[3]The character χ_i of the tensor product of two representation R_1 and R_2 is given by $\chi_i = \chi_i^{R_1}\chi_i^{R_2}$.

Note that that the two bilinears that transform again in the triplet representation are either symmetric or a antisymmetric. This distinction will turn out to be useful in the following and is not as obvious in the MR basis, as (4.8) shows.

4.2 TBM mixing as a consequence of the A_4 symmetry

Let us now discuss the relationship between the A_4 symmetry and tribimaximal mixing. First of all we note that the matrices S and T derived in the previous section in the AF basis are the same matrices that we have already considered in section 2.6. There we had searched for a set of symmetries, such that requiring invariance of a mass matrix under these symmetries leads to a matrix of the specific TBM form given in equation (2.54). Recall that in addition to invariance under S and T we had to additionally require $\mu\tau$-symmetry of the mass matrix in order to obtain a tribimaximal mixing matrix. This $\mu\tau$-symmetry could be guaranteed by requiring invariance under the transformation A_{23} (see (2.58)). Note that the discussion in the previous section shows that A_{23} is not contained in A_4. Therefore this symmetry has to be implemented additionally.

In section 2.6 we already pointed out that finite groups including the matrices S and T among their generators can be used to give rise to TBM mixing in a natural way. Note that A_4 is one of the simplest possible examples of this class of groups, which is the main motivation behind using it as the flavour symmetry. We will first discuss the general mechanism before proceeding to consider a specific model for the lepton sector. Let us start with the Standard Model Lagrangian $\mathcal{L}$, which is of course invariant under the SM gauge group $G_{SM} = SU(3)\times SU(2)\times U(1)$. We now demand $\mathcal{L}$ to be invariant under the extended group $G_{SM} \times A_4$. Assuming that the lepton mass matrix is already diagonal, we want to ensure that the neutrino mass matrix is of the specific TBM form, which will lead to U_{TBM} as the leptonic mixing matrix. The full flavour group should thus be broken down to $G_{SM} \times G_T$ in the charged lepton mass sector and to $G_{SM} \times G_S$ in the neutrino mass sector[4]. G_S and G_T denote the symmetries generated by S and T, respectively. In addition we have to require an A_{23} symmetry in the neutrino sector if we want to reproduce exact TBM mixing. We will postpone the discussion of this point for now and will first consider the breaking mechanism. The required breaking pattern can be achieved via the introduction of fields which obtain a vev in just the right way to keep the G_S and G_T symmetry unbroken in the neutrino and lepton sectors, respectively. Since we want to break A_4 down to G_S in one part of $\mathcal{L}$ and to G_T in another part, we need at least two distinct fields which acquire different vevs. In fact, as we will see in the next section, fields transforming in the triplet representation of A_4 are needed to obtain suitable mass matrices.

[4] The quark sector will be briefly discussed in 4.7. For now we will stick to the lepton sector and assume that the A_4 symmetry does not affect the quark sector.

There are two possible ways to go. One possibility is to introduce new fields which are uncharged under G_{SM}, the so-called flavons, which transform under A_4 and can break this symmetry by acquiring a suitable vev. The other possibility is to consider Higgs-like fields that are charged under the G_{SM} gauge group as well as A_4. In particular, we could assign A_4 charges to the SM Higgs and the additional Higgs of chapter 3. However, note that in this case one must always introduce further $SU(2)$ doublets, because as mentioned above an A_4 triplet is required. Furthermore, assigning an A_4 charge to the SM Higgs enforces the breaking of the A_4 symmetry at the electroweak scale. On the other hand, breaking A_4 via new flavon fields gives rise to a new breaking scale. In the process of A_4 breaking, the flavons then naturally acquire a mass of the order of the breaking scale. Now if the breaking scale is chosen to be large, e.g. close to the GUT or Planck scale, the flavons will be so heavy that they will not have an impact on any observed low-energy processes. Therefore our previous discussion of the Higgs phenomenology given in chapter 3 is unaffected by the introduction of the flavons, and the only change is that the form of the effective Yukawa coupling matrices is now determined by the flavon vevs. This will clearly not be the case if one takes the second option and introduces additional Higgs doublets. In order to avoid having to worry about changes to the ν2HDM phenomenology, we will therefore keep our Higgs doublets uncharged under A_4 and will introduce the required flavons in the next section.

Let us now consider in more detail the effect of the flavons on the Yukawa couplings of the charged leptons and neutrinos. As motivated above, we are interested in the case of Dirac neutrinos, which requires the addition of three right-handed sterile neutrinos to the SM particle content. A generic Yukawa coupling in the presence of a flavon field χ will take the form

$$-\mathcal{L}_{\text{Yukawa}} = Y\overline{\psi^a_{\text{L}}}\Phi\psi^b_{\text{R}}\chi + \text{h.c.}, \tag{4.12}$$

where Φ denotes one of the Higgs fields (or its conjugate) and $\psi^{a,b}$ denote Dirac spinors describing the charged leptons or neutrinos. Note that if χ is not in the trivial representation of A_4 we have to assign A_4 charges to the leptons and couple the various field appropriately according to the multiplication rules given above, to ensure that $\mathcal{L}_{\text{Yukawa}}$ is invariant under A_4 (see equations (4.8) or (4.11)).

As was repeatedly mentioned above, we want this Yukawa interaction to remain invariant under either G_S or G_T after symmetry breaking, depending on whether it describes a mass term for the neutrinos or for the charged leptons. We can guarantee that this is the case by requiring that the vev of the flavon field appearing in this interaction is invariant under either G_S or G_T, as appropriate. Let us first consider invariance under G_S. From equation (4.4) we immediately see that G_S invariance is trivially fulfilled if χ is a flavon in any of the singlet representations of A_4. However, if χ is in the triplet representation of A_4 we have to choose the specific vev structure $\langle\chi\rangle = (v_S, v_S, v_S)$ to ensure that $S\langle\chi\rangle = \langle\chi\rangle$. Here and in the following we use the subscript S for A_4 triplet fields and vevs appearing in the S invariant neutrino mass sector, and a subscript T for triplet flavons or vevs

Field	Φ_1	Φ_2	φ_T	φ_S	ξ	ξ'	ξ''
A_4	1	1	3	3	1	$1'$	$1''$
$U(1)$	1	0	0	0	0	0	0
$\mathbb{Z}_2^\ell \times \mathbb{Z}_2^\nu$	$(1,1)$	$(1,1)$	$(-1,1)$	$(1,-1)$	$(1,-1)$	$(1,-1)$	$(1,-1)$

Field	$\mathrm{L_L}$	e_R	μ_R	τ_R	ν_R
A_4	3	1	$1''$	$1'$	3
$U(1)$	0	0	0	0	1
$\mathbb{Z}_2^\ell \times \mathbb{Z}_2^\nu$	$(1,1)$	$(-1,1)$	$(-1,1)$	$(-1,1)$	$(1,-1)$

Table 4.3: Charges of leptons and scalars under global symmetries. The quarks and gauge bosons do not transform under these groups.

appearing in the T invariant charged lepton mass sector. Note that this expression for the vev is only valid in the Altarelli-Feruglio basis where T is diagonal. Before giving the corresponding form in the MF basis let us first consider G_T invariance. Equation (4.4) shows that G_T invariance cannot be maintained after symmetry breaking if the flavon is in the representation $1'$ or $1''$. One finds that G_T invariance can be achieved either by taking χ in the trivial representation or by taking χ in the triplet representation of A_4 and requiring $\langle\chi\rangle = (v_T, 0, 0)$, so that $T\langle\chi\rangle = \langle\chi\rangle$ (again in the AF basis).

Let us now give the corresponding forms of the triplet vevs necessary to maintain either G_S or G_T invariance in the Ma-Rajasekaran basis. Using the matrices given in (4.5) one finds that the necessary forms are $(v_S, 0, 0)$ for G_S invariance and (v_T, v_T, v_T) for G_T invariance. These forms could of course have also been obtained from the expressions in the AF basis by simply performing the basis change using the magic matrix V. The consequences for the physical observables are of course independent of the choice of the basis.

4.3 Applying A_4 to the lepton sector

Following these general remarks let us now consider a specific A_4 model for Dirac neutrinos, thus introducing three right-handed sterile neutrinos. In order to explain the smallness of the neutrino masses we keep the second Higgs doublet with a vev of order 1 eV, which was introduced in chapter 3. In other words, we will combine the desirable properties of the ν2HDM with an A_4 flavour symmetry. Let us therefore keep the $U(1)$ symmetry which was initially introduced in 3 and the corresponding charge assignments (see table 4.3). The implications of the predicted form of the mixing matrix on the phenomenology of the ν2HDM will be discussed in chapter 5.

In order to implement the A_4 symmetry we introduce the real scalar flavon fields

φ_T, φ_S, ξ, ξ' and ξ'', which are singlets of the SM gauge group and the $U(1)$ symmetry. We assign the flavons to representations of A_4 according to table 4.3. We will refer to φ_T and φ_S as flavon triplets and to ξ, ξ' and ξ'' as flavon singlets, even though ξ' and ξ'' have a non-trivial transformation behaviour under A_4. We will assume for now that a flavon potential with the right properties to produce the abovementioned vev patterns exists, postponing the discussion of how the required vev alignment can be obtained to the subsequent sections. The assignment of the A_4 representations to the charged leptons and neutrinos can also be found in table 4.3. The reason for this choice of charge assignments for the leptons is that, taken together with the requirement of vev alignment, it will lead to a diagonal mass matrix in the charged lepton sector in the AF basis. As T is also diagonal in this basis G_T invariance is thus manifestly preserved. Let us also mention that the sterile neutrinos cannot be assigned to the same A_4 representation as the corresponding charged leptons, because this would give rise to a phenomenologically unacceptable vanishing of Δm^2_{31} at leading order. While this might in principle be remedied by allowing for next-to-leading order corrections or by allowing for deviations from the vev alignment discussed above, we will stick to the charge assignments given in table 4.3, in which case no such problem appears.

We should comment on the additional $\mathbb{Z}_2^\ell \times \mathbb{Z}_2^\nu$ symmetry that we have introduced in table 4.3. This symmetry was introduced in order to forbid unwanted terms in the Yukawa interaction[5]. In particular, this additional symmetry distinguishes between φ_T and φ_S and ensures that φ_T can couple only to the charged leptons whereas φ_S can only couple to the neutrinos.

With the above assignments we are now in a position to write down the resulting Yukawa couplings. The first thing to note is that this will be an effective Lagrangian, because the given charge assignments imply that any gauge invariant operators that we can build with the fields at hand will have a mass dimension of at least 5. The operators will therefore involve suitable factors of $1/\Lambda$, where Λ is the cut-off scale of the effective theory given by the mass scale of the underlying UV-complete theory. While the precise value of this cut-off scale is not important in the following, we will take Λ to lie at the GUT scale $\Lambda \sim 10^{16}$ GeV for definiteness. The most general Yukawa Lagrangian at order $1/\Lambda$ is then given by

$$\begin{aligned} -\mathcal{L}_{\text{Yukawa}} \;=\; & \frac{Y^e}{\Lambda}(\varphi_T \overline{\text{L}_\text{L}})_1 \Phi_2 e_\text{R} + \frac{Y^\mu}{\Lambda}(\varphi_T \overline{\text{L}_\text{L}})_{1'} \Phi_2 \mu_\text{R} + \frac{Y^\tau}{\Lambda}(\varphi_T \overline{\text{L}_\text{L}})_{1''} \Phi_2 \tau_\text{R} \\ & + \frac{Y^s}{\Lambda}(\overline{\text{L}_\text{L}} \widetilde{\Phi}_1 \nu_\text{R})_{3s} \varphi_S + \frac{Y^a}{\Lambda}(\overline{\text{L}_\text{L}} \widetilde{\Phi}_1 \nu_\text{R})_{3a} \varphi_S \\ & + \frac{Y}{\Lambda}(\overline{\text{L}_\text{L}} \widetilde{\Phi}_1 \nu_\text{R})_1 \xi + \frac{Y'}{\Lambda}(\overline{\text{L}_\text{L}} \widetilde{\Phi}_1 \nu_\text{R})_{1'} \xi'' + \frac{Y''}{\Lambda}(\overline{\text{L}_\text{L}} \widetilde{\Phi}_1 \nu_\text{R})_{1''} \xi' \\ & + \text{h.c.} \end{aligned} \tag{4.13}$$

[5] We could also have achieved this aim using a $\mathbb{Z}_2$ symmetry instead of the $\mathbb{Z}_2^\ell \times \mathbb{Z}_2^\nu$. Choosing an adequate charge assignment would then lead to the same Yukawa term. However, the larger symmetry group guarantees that we can treat the two triplet flavons in the same way in the flavon potential, which will simplify our considerations in section 4.4.

Here we have worked in the Altarelli-Feruglio basis and have therefore used the symmetric and antisymmetric triplet couplings.

Naively, one might think that there occur additional terms arising from different ways of coupling the A_4 triplets. For example, one might consider terms like $\overline{\mathrm{L_L}}\widetilde{\Phi_1}(\nu_\mathrm{R}\varphi_S)_{3s}$. However, one can explicitly check that all these extra terms are either equivalent to terms that are already included above (and can therefore be absorbed into a redefinition of the corresponding Yukawa coupling) or vanish by antisymmetry. We would like to emphasise that the appearance of the antisymmetric triplet coupling is special to the case of Dirac neutrinos considered here. This coupling would have been forbidden if we had used Majorana neutrinos obeying the Majorana relation $\nu_\mathrm{R} = \nu_\mathrm{L}^c$ (see appendix C), as can be seen by applying the identities $\overline{\Psi_1}\Psi_2^c = \overline{\Psi_2^c}\Psi_1$ and $\overline{\Psi_1}\Psi_2 = \overline{\Psi_2^c}\Psi_1^c$ that hold for arbitrary four component spinors. In the following we will show that this antisymmetric coupling provides a new source of deviations from the TBM mixing form compared to A_4 models studied in the existing literature, as the existing models have focused on Majorana neutrinos.

From the Lagrangian (4.13) we immediately see that after flavour symmetry breaking the effective Yukawa couplings will take the form $Y^{\text{eff.}} = Yv/\Lambda$, where v is a generic flavon vev. This means that the A_4 breaking scale should not lie too far below the cut-off scale Λ, to avoid having to make the Yukawa coupling constants in (4.13) unnaturally large. Note that this also ensures that the flavons are very heavy, as after symmetry breaking they naturally acquire masses of the order of the breaking scale[6]. In particular, we may indeed safely assume that the flavons are heavy enough and therefore also decay fast enough that their presence does not impact on any processes at the low observable energy scale, apart from predicting the form of the effective Yukawa couplings through their vev structure.

Before proceeding with the evaluation of the mass matrices, let us finally point out that apart from ensuring that each triplet flavon couples either only in the neutrino sector or only in the charged lepton sector, the $\mathbb{Z}_2^\nu$ symmetry with charges chosen as above has the added advantage of forbidding a term $Y(\overline{\mathrm{L_L}}\widetilde{\Phi_1}\nu_\mathrm{R})$. Such a term would yield a relatively large diagonal contribution to the neutrino mass matrix as it has no suppression by v/Λ, which would lead to a large deviation from the TBM form for the resulting mixing matrix. Note that the presence of such a term and a corresponding large diagonal contribution (in the Altarelli-Feruglio basis) in the charged lepton sector would not be problematic. However, in the charged lepton sector such a term is anyway automatically forbidden by A_4 invariance. As already mentioned above, the introduction of the additional $\mathbb{Z}_2^\ell$ symmetry has the advantage of being able to treat both flavon triplets in a similar manner in the flavon potential.

To derive the leptonic mass matrices from the Yukawa interaction (4.13) after

[6] We will briefly return to this point in subsection 4.5.1, where we will confirm that all flavons will indeed acquire very large masses after higher order effects in the flavon potential are taken into account. There we will also give more precise estimates of v/Λ for the different flavon vevs.

electroweak and A_4 symmetry breaking, we plug in the Higgs vevs as obtained in section 3

$$\langle \Phi_i \rangle = \frac{1}{\sqrt{2}} \begin{pmatrix} 0 \\ v_i \end{pmatrix}, \qquad i = 1, 2\,, \tag{4.14}$$

with $v_1 \ll v_2$. For the vevs of triplet flavons we use the natural component notation

$$\langle \varphi_T \rangle = (\langle \varphi_T \rangle_1, \langle \varphi_T \rangle_2, \langle \varphi_T \rangle_3), \qquad \langle \varphi_S \rangle = (\langle \varphi_S \rangle_1, \langle \varphi_S \rangle_2, \langle \varphi_S \rangle_3), \tag{4.15}$$

where in addition we will soon impose the restricted form

$$\langle \varphi_T \rangle = (v_T, 0, 0), \qquad \langle \varphi_S \rangle = v_S(1, 1, 1), \tag{4.16}$$

as required by T and S invariance, according to the discussion in section 4.2. Recall that this particular expression for the flavon vev patterns is appropriate for the AF basis where T is diagonal. Finally, the vevs of the singlet flavons will be denoted as

$$\langle \xi \rangle = u\,, \qquad \langle \xi' \rangle = u'\,, \qquad \langle \xi'' \rangle = u''\,. \tag{4.17}$$

Now using equation (4.13) and the multiplication rules in the AF basis given in (4.11) we find the charged lepton mass matrix to be

$$m_\ell = \frac{v_2}{\Lambda} \begin{pmatrix} Y^e \langle \varphi_T \rangle_1 & Y^\mu \langle \varphi_T \rangle_2 & Y^\tau \langle \varphi_T \rangle_3 \\ Y^e \langle \varphi_T \rangle_3 & Y^\mu \langle \varphi_T \rangle_1 & Y^\tau \langle \varphi_T \rangle_2 \\ Y^e \langle \varphi_T \rangle_2 & Y^\mu \langle \varphi_T \rangle_3 & Y^\tau \langle \varphi_T \rangle_1 \end{pmatrix} = \frac{v_2 v_T}{\Lambda} \begin{pmatrix} Y^e & 0 & 0 \\ 0 & Y^\mu & 0 \\ 0 & 0 & Y^\tau \end{pmatrix}. \tag{4.18}$$

In the second step we have used the claimed vev alignment (4.16). The predicted lepton masses are therefore simply given by

$$m_e = \frac{|Y^e| v_2 v_T}{\Lambda}, \qquad m_\mu = \frac{|Y^\mu| v_2 v_T}{\Lambda}, \qquad m_\tau = \frac{|Y^\tau| v_2 v_T}{\Lambda}. \tag{4.19}$$

Of course, the Yukawa coupling constants are in general complex, but as the mass matrix is diagonal we may absorb their phases into a redefinition of the charged lepton fields. Note also that the diagonal form of m_ℓ implies that the PMNS mixing matrix is determined fully by the matrices diagonalising the neutrino mass matrix, and the charged lepton sector plays no further role with regard to leptonic mixing. The fact that the charged lepton mass matrix is automatically diagonal is one of the advantages of working in the Altarelli-Feruglio basis. However, we should emphasise that even in this basis one obtains deviations from the diagonal form once one considers higher order corrections or deviations from the vev alignment of $\langle \varphi_T \rangle$.

The mass matrix of the neutrinos can be derived in an analogous manner and is given by

$$M^\nu = \begin{pmatrix} 2a_1 + b & -a_3 + a_3' + d & -a_2 - a_2' + c \\ -a_3 - a_3' + d & 2a_2 + c & -a_1 + a_1' + b \\ -a_2 + a_2' + c & -a_1 - a_1' + b & 2a_3 + d \end{pmatrix}, \tag{4.20}$$

where we have defined

$$\begin{aligned} b &= \frac{1}{\Lambda} Y v_1 u\,, & c &= \frac{1}{\Lambda} Y' v_1 u'\,, & d &= \frac{1}{\Lambda} Y'' v_1 u''\,, \\ a_i &= \frac{1}{3\Lambda} Y^s v_1 \langle \varphi_S \rangle_i\,, & a'_i &= \frac{1}{3\Lambda} Y^a v_1 \langle \varphi_S \rangle_i\,. \end{aligned} \tag{4.21}$$

Note that these parameters are in general complex despite the fact that all the various vevs are real, because the Yukawa couplings can be complex. However, one of the phases can be absorbed by a redefinition of the neutrino fields, which allows us to assume $a_3 \in \mathbb{R}$ in the following. Let us now demand that the triplet vev $\langle \varphi_S \rangle = v_S(1,1,1)$ has the aligned form, so that we can simplify the mass matrix to

$$M^\nu = \begin{pmatrix} 2a+b & -a+a'+d & -a-a'+c \\ -a-a'+d & 2a+c & -a+a'+b \\ -a+a'+c & -a-a'+b & 2a+d \end{pmatrix}, \tag{4.22}$$

where now

$$a = \frac{1}{3\Lambda} Y^s v_1 v_S \qquad \text{and} \qquad a' = \frac{1}{3\Lambda} Y^a v_1 v_S\,, \tag{4.23}$$

and a is taken to be real.

Let us now discuss how TBM mixing can be achieved when starting from this general form of the mass matrix. We will focus on exact TBM mixing in this section and postpone a discussion of deviations from TBM mixing to the subsequent sections. Note that although M^ν is invariant under S due to the chosen vev alignment, one can explicitly check that $M^\nu (M^\nu)^\dagger$ does not yet have the right form to be diagonalised by the TBM mixing matrix U_{TBM}. This is of course consistent with the findings of section 2.6, where we recognised that we must in addition ensure invariance of $M^\nu (M^\nu)^\dagger$ under the A_{23} symmetry. The requirement of generating exact TBM mixing can be translated into the following two conditions on the parameters

$$0 \stackrel{!}{=} -6a(a'-\bar{a}') + \bar{b}(d-c) + \bar{c}(d-b) + \bar{d}(b-c)\,, \tag{4.24}$$

$$0 \stackrel{!}{=} 3a(d-c) + \bar{a}'(c+d-2b) - 2a'\bar{b} + \bar{c}(a'-3a) + \bar{d}(a'+3a)\,. \tag{4.25}$$

As the most general solution of these equations cannot be simply given in a closed form, we will impose instead the simpler sufficient condition that M^ν itself (rather than $M^\nu (M^\nu)^\dagger$) should be invariant under $G_S \times A_{23}$. This amounts to requiring that $c = d$ and $a' = 0$, which of course suffices to ensure that the above equations are fulfilled. Let us comment in particular on the requirement $a' = 0$. As we have mentioned before, this is automatically fulfilled in models based on Majorana neutrinos as the appearance of the antisymmetric coupling is a new feature of the considered model due to the Dirac nature of the neutrinos. While it may seem unnatural to impose the vanishing of a coupling that is not forbidden by any symmetry, we would like to point out that this is actually an artifact of the

choice of basis. If we had used the MF basis instead, absence of the antisymmetric contribution would have amounted to choosing equal strengths for the 3_1 and 3_2 triplet couplings, which seems much more natural. However, let us not go into further detail here as we will anyway relax the conditions $c = d$ and $a' = 0$ as well as the vev alignment later on, when looking for deviations from the TBM form that are needed to obtain compatibility with the measurements of the neutrino mixing angles.

Imposing the discussed restrictions the neutrino mass matrix thus reads

$$m_\nu = \begin{pmatrix} 2a+b & -a+c & -a+c \\ -a+c & 2a+c & -a+b \\ -a+c & -a+b & 2a+c \end{pmatrix}. \tag{4.26}$$

Recall that we can assume $a \in \mathbb{R}$ but in general we have $b,\, c \in \mathbb{C}$.

So far we have kept the discussion quite general in the sense that we have included flavons transforming in all irreducible representations of A_4[7]. Of course, there is no need for a given model to include all possible representations, for example in the SM Higgs sector one also uses only an $SU(2)$ doublet field instead of introducing a field for each irreducible representation of $SU(2)$. Let us therefore consider models with different flavon contents and the resulting mass matrices. While up to now we have only asked for tribimaximal mixing, let us now also consider the predicted mass eigenvalues and see which models have a chance of being compatible with the measured neutrino mass differences.

Table 4.4 shows the different possible flavon contents leading to models in which M^ν is $G_S \times A_{23}$ invariant, so that $M^\nu (M^\nu)^\dagger$ will be diagonalised by U_{TBM}. A glance at the resulting mass eigenvalues shows that only the last three cases have a chance of being compatible with the measured mass differences, given in table 2.3. However, the case where in addition to the triplets φ_S and φ_T only one singlet ξ is present yields $\Delta m^2_{21} = -9a^2 - 6a\Re(b)$ and $\Delta m^2_{31} = -12a\Re(b)$. As the experimental data requires $\Delta m^2_{21} > 0$ compatibility requires $\mathrm{sgn}(a) \neq \mathrm{sgn}(\Re(b))$, which then automatically implies $\Delta m^2_{31} > 0$. Thus only normal hierarchy is possible in models with this flavon content. When allowing for more than one singlet in addition to the two triplets this is no longer true, and both normal and inverted neutrino mass ordering can be generated depending on the specific choice of parameters.

In the following we want to analyse one of these A_4 models in more detail. We will later study deviations from the TBM form in order to obtain mixing angles and mass differences in agreement with the experimental results of table 2.3, in particular allowing for $\sin^2\theta_{13} \neq 0$. However, we do not want to deviate too much from the TBM form, as this already predicts the other mixing angles quite well. As a starting point for our studies of the deviations we would therefore like to choose a model in which the correct mass differences can already be obtained in

[7] Note in particular that including additional flavon singlets coupling in the charged lepton sector, i.e. having the same $\mathbb{Z}_2^\ell \times \mathbb{Z}_2^\nu$ charges as φ_T, cannot change the Yukawa interactions at leading order for the given A_4 representations of ℓ_R and $\overline{\mathrm{L_L}}$.

the exact TBM case, i.e. one of the last three cases in table 4.4. As we also want to allow for both normal and inverted hierarchies we need to take more than one singlet flavon, while to increase the predictive power of the model we favour a model with as few parameters as possible. We will therefore settle on the model with the flavon content φ_T, φ_S, ξ', ξ'', which we will dub the 2S2T model, as the starting point for the upcoming analysis.

To confirm that the 2S2T model will be a good basis for our further studies, let us

Flavon content	Neutrino mass matrix M^ν (before diagonalisation)	Eigenvalues m_ν^2
φ_T, ξ	$\begin{pmatrix} b & 0 & 0 \\ 0 & 0 & b \\ 0 & b & 0 \end{pmatrix}$	$\begin{pmatrix} \lvert b\rvert^2 \\ \lvert b\rvert^2 \\ \lvert b\rvert^2 \end{pmatrix}$
φ_T, ξ', ξ''	$\begin{pmatrix} 0 & c & c \\ c & c & 0 \\ c & 0 & c \end{pmatrix}$	$\begin{pmatrix} \lvert c\rvert^2 \\ 4\lvert c\rvert^2 \\ \lvert c\rvert^2 \end{pmatrix}$
φ_T, ξ, ξ', ξ''	$\begin{pmatrix} b & c & c \\ c & c & b \\ c & b & c \end{pmatrix}$	$\begin{pmatrix} \lvert b-c\rvert^2 \\ \lvert b+2c\rvert^2 \\ \lvert b-c\rvert^2 \end{pmatrix}$
φ_T, φ_S	$\begin{pmatrix} 2a & -a & -a \\ -a & 2a & -a \\ -a & -a & 2a \end{pmatrix}$	$\begin{pmatrix} 9a^2 \\ 0 \\ 9a^2 \end{pmatrix}$
φ_T, φ_S, ξ	$\begin{pmatrix} 2a+b & -a & -a \\ -a & 2a & -a+b \\ -a & -a+b & 2a \end{pmatrix}$	$\begin{pmatrix} \lvert 3a+b\rvert^2 \\ \lvert b\rvert^2 \\ \lvert 3a-b\rvert^2 \end{pmatrix}$
φ_T, φ_S, ξ', ξ''	$\begin{pmatrix} 2a & -a+c & -a+c \\ -a+c & 2a+c & -a \\ -a+c & -a & 2a+c \end{pmatrix}$	$\begin{pmatrix} \lvert 3a-c\rvert^2 \\ \lvert 2c\rvert^2 \\ \lvert 3a+c\rvert^2 \end{pmatrix}$
φ_T, φ_S, ξ, ξ', ξ''	$\begin{pmatrix} 2a+b & -a+c & -a+c \\ -a+c & 2a+c & -a+b \\ -a+c & -a+b & 2a+c \end{pmatrix}$	$\begin{pmatrix} \lvert 3a+b-c\rvert^2 \\ \lvert b+2c\rvert^2 \\ \lvert 3a-b+c\rvert^2 \end{pmatrix}$

Table 4.4: Neutrino mass matrices leading to exact TBM mixing in the context of an A_4 flavour symmetry. The transformation properties of the fields φ_T, φ_S, ξ, ξ' and ξ'' are listed in table 4.3.

take a quick look at how the neutrino masses are predicted in this model for the case of exact TBM mixing, and in particular confirm that compatibility with the measured neutrino mass differences can be obtained. Using the expressions for the neutrino masses given in table 4.4, and recalling that $a \in \mathbb{R}$, we immediately find the predicted mass differences

$$\begin{aligned} \Delta m^2_{21} &= 3|c|^2 - 9a^2 - 6a\Re(c)\,, \\ \Delta m^2_{31} &= 12a\Re(c). \end{aligned} \tag{4.27}$$

Clearly both normal and inverted neutrino mass ordering is in principle possible, depending on the signs of a and $\Re(c)$. As shown in table 2.3, these neutrino mass differences have been measured with high precision. If we restrict ourselves to real values of the parameter c for a moment, these experimental bounds restrict a and c to a very narrow region in parameter space. However, we can of course allow for complex c in general, in which case much larger parameter regions are possible. Figure 4.1 shows the contours in parameter space corresponding to the measured 3σ ranges of Δm^2_{21} and Δm^2_{31} for the cases of normal and inverted hierarchy. The parameter regions compatible with both mass differences, Δm^2_{21} and Δm^2_{31}, therefore lie at the intersections of these contours.

Note that in the case where c is restricted to real values, the bounds on the neutrino mass differences can only be fulfilled with $|c| < 3|a|$. This allows us to simplify the expressions for the masses given in table 4.4 and leads to the sum rule

$$m_1 + m_2 = m_3. \tag{4.28}$$

This sum rule shows that in the real case the magnitude of the smallest neutrino mass must be of the order of the observed mass differences, and can in particular not be much larger than about 10^{-3} eV. In particular, the resulting neutrino masses for real c when requiring compatibility with the measured mass differences

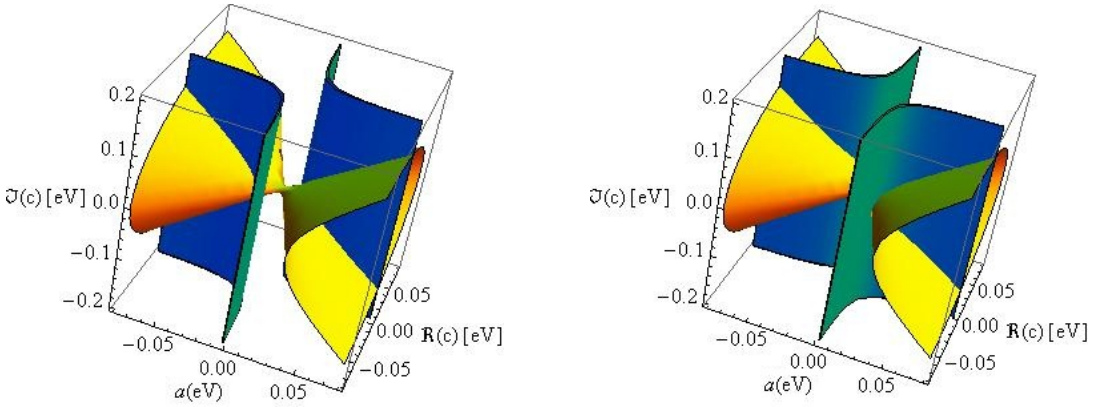

(a) Normal hierarchy.

(b) Inverted hierarchy.

Figure 4.1: Parameter regions that are compatible with the 3σ bound on Δm^2_{21} (yellow) and Δm^2_{31} (blue), respectively.

will automatically lie far below the bounds from Tritium beta decay and from WMAP data as given in equations (2.45) and (2.47), respectively. A general discussion of the significance of such sum rules in the context of neutrino physics can be found in [104]. Let us emphasise that the above statement is no longer true when allowing for complex c. A closer look at equation (4.27) shows that the mass differences can be kept sufficiently small for arbitrarily large values of $\Im(c)$, as long as a and $\Re(c)$ are adjusted accordingly. For large $\Im(c)$ also the predicted neutrino masses will become large, as shown by the expressions in table 4.4. However, let us not go into further detail on the bounds on the neutrino masses here, as the case at hand leads to exact TBM mixing and is therefore anyway in conflict with the measured neutrino oscillation angles. We will return to this point as part of the more general numerical analysis in chapter 5.

4.4 The vev alignment problem

According to the general discussion of section 4.2, two triplet flavons with special vacuum patterns are needed to obtain a mixing matrix of the TBM form after breaking the A_4 symmetry. Let us now face up to the problem of how this required vacuum structure can be obtained, which means that we must study the potential of the flavon fields. We restrict ourselves to studying the potential of the 2S2T model as this will be the model that we focus on in chapter 5. At this point it is advantageous to switch into the Ma-Rajasekaran basis in which S is diagonal, as the multiplication rules for the couplings in the potential take a simpler form in this basis. We will therefore search for a minimum of the form $\langle\varphi_S\rangle = (v_s, 0, 0)$ and $\langle\varphi_T\rangle = v_T(1, 1, 1)$, instead of $\langle\varphi_S\rangle = v_s(1, 1, 1)$ and $\langle\varphi_T\rangle = (v_T, 0, 0)$ which would be needed in the Altarelli-Feruglio basis (see section 4.2). This switch is of course not problematic since one can always perform a basis change and can therefore transform the resulting expressions to the AF basis by applying the 'magic matrix' V given in (4.9). However, we will not explicitly perform this transformation because the exact expressions will not be needed in the following. In this section we only aim to check whether the specific vacuum pattern can be obtained and which additional requirements have to be made to ensure this.

The most general renormalisable flavon potential which is invariant under A_4 and where the additional $\mathbb{Z}_2^\ell \times \mathbb{Z}_2^\nu$ symmetry is taken into account has the form

$$\begin{aligned} V_{\text{flavon}}(\varphi_S, \varphi_T, \xi', \xi'') &= V_S(\varphi_S) + V_T(\varphi_T) + V_{\text{singlet}}(\xi', \xi'') \\ &\quad + V_{\text{int,T}}(\varphi_T, \xi', \xi'') + V_{\text{int,S}}(\varphi_S, \xi', \xi'') \\ &\quad + V_{\text{int,ST}}(\varphi_T, \varphi_S, \xi', \xi''). \end{aligned} \tag{4.29}$$

Here we have split the potential into separate contributions according to which flavon fields appear, so for example $V_{S,T}(\varphi_{S,T})$ will contain all terms involving only one of the triplet flavons and no singlet flavons. We trust that the notation is self-explanatory and that it is clear which terms the other contributions to the

potential include. Making use of the multiplication rules given in (4.8) one finds, for $i = S, T$, the explicit expressions [8]

$$\begin{aligned} V_i(\varphi_i) &= -m_i^2(\varphi_i\varphi_i)_1 + \lambda_{i,1}(\varphi_i\varphi_i)_1(\varphi_i\varphi_i)_1 + \lambda_{i,2}(\varphi_i\varphi_i)_{1'}(\varphi_i\varphi_i)_{1''} \\ &\quad +\lambda_{i,3}(\varphi_i\varphi_i)_3(\varphi_i\varphi_i)_3 \\ &= -m_{\varphi_i}^2(\varphi_{i,1}^2 + \varphi_{i,2}^2 + \varphi_{i,3}^2) \\ &\quad +\lambda_{i,1}(\varphi_{i,1}^4 + \varphi_{i,2}^4 + \varphi_{i,3}^4 + 2\varphi_{i,1}^2\varphi_{i,3}^2 + 2\varphi_{i,1}^2\varphi_{i,2}^2 + 2\varphi_{i,2}^2\varphi_{i,3}^2) \\ &\quad +\lambda_{i,2}(\varphi_{i,1}^4 + \varphi_{i,2}^4 + \varphi_{i,3}^4 - \varphi_{i,1}^2\varphi_{i,3}^2 - \varphi_{i,1}^2\varphi_{i,2}^2 - \varphi_{i,2}^2\varphi_{i,3}^2) \\ &\quad +\lambda_{i,3}(\varphi_{i,1}^2\varphi_{i,2}^2 + \varphi_{i,2}^2\varphi_{i,3}^2 + \varphi_{i,3}^2\varphi_{i,1}^2), \end{aligned} \tag{4.30}$$

$$V_{\text{singlet}}(\xi', \xi'') = m_{\xi'\xi''}^2\xi'\xi'' + \lambda_5(\xi'\xi'')^2, \tag{4.31}$$

$$\begin{aligned} V_{\text{int,ST}}(\varphi_T, \varphi_S, \xi', \xi'') &= \rho_1(\varphi_S\varphi_S)_3(\varphi_T\varphi_T)_3 + \rho_2(\varphi_S\varphi_S)_1(\varphi_T\varphi_T)_1 \\ &\quad +\rho_3(\varphi_S\varphi_S)_{1'}(\varphi_T\varphi_T)_{1''} + \rho_4(\varphi_S\varphi_T)_{3_1}(\varphi_S\varphi_T)_{3_1} \\ &\quad +\rho_5(\varphi_S\varphi_T)_{3_2}(\varphi_S\varphi_T)_{3_2} + \rho_6(\varphi_S\varphi_T)_{3_1}(\varphi_S\varphi_T)_{3_2} \\ &\quad +\rho_7((\varphi_T\varphi_T)_3\varphi_S)_{1'}\xi'' + \rho_8((\varphi_T\varphi_T)_3\varphi_S)_{1''}\xi' + \text{h.c.} \\ &= \rho_1(\varphi_{S,2}\varphi_{S,3}\varphi_{T,2}\varphi_{T,3} + \varphi_{S,3}\varphi_{S,1}\varphi_{T,3}\varphi_{T,1} \\ &\quad +\varphi_{S,1}\varphi_{S,2}\varphi_{T,1}\varphi_{T,2}) \\ &\quad +\rho_2(\varphi_{S,1}^2 + \varphi_{S,2}^2 + \varphi_{S,3}^2)(\varphi_{T,1}^2 + \varphi_{T,2}^2 + \varphi_{T,3}^2) \\ &\quad +\rho_3(\varphi_{S,1}^2\varphi_{T,1}^2 + \varphi_{S,2}^2\varphi_{T,2}^2 + \varphi_{S,3}^2\varphi_{T,3}^2 \\ &\quad\quad -\varphi_{S,1}^2\varphi_{T,2}^2 - \varphi_{S,1}^2\varphi_{T,3}^2 - \varphi_{S,2}^2\varphi_{T,1}^2 \\ &\quad\quad -\varphi_{S,2}^2\varphi_{T,3}^2 - \varphi_{S,3}^2\varphi_{T,1}^2 - \varphi_{S,3}^2\varphi_{T,2}^2) \\ &\quad +\rho_4((\varphi_{S,2}\varphi_{T,3})^2 + (\varphi_{S,3}\varphi_{T,1})^2 + (\varphi_{S,1}\varphi_{T,2})^2) \\ &\quad +\rho_5((\varphi_{T,2}\varphi_{S,3})^2 + (\varphi_{T,3}\varphi_{S,1})^2 + (\varphi_{T,1}\varphi_{S,2})^2) \\ &\quad +\rho_6(\varphi_{S,2}\varphi_{T,3}\varphi_{S,3}\varphi_{T,2} + \varphi_{S,3}\varphi_{T,1}\varphi_{S,1}\varphi_{T,3} \\ &\quad\quad +\varphi_{S,1}\varphi_{T,2}\varphi_{S,2}\varphi_{T,1}) \\ &\quad +\rho_7(2\varphi_{S,1}\varphi_{T,2}\varphi_{T,3} - \varphi_{S,2}\varphi_{T,1}\varphi_{T,3} - \varphi_{S,3}\varphi_{T,1}\varphi_{T,2})\xi'' \\ &\quad +\rho_8(2\varphi_{S,1}\varphi_{T,2}\varphi_{T,3} - \varphi_{S,2}\varphi_{T,1}\varphi_{T,3} - \varphi_{S,3}\varphi_{T,1}\varphi_{T,2})\xi', \end{aligned} \tag{4.32}$$

and

$$\begin{aligned} V_{\text{int,i}}(\varphi_i, \xi', \xi'') &= \lambda_{i,6}\xi'\xi''(\varphi_i\varphi_i)_1 + \lambda_{i,7}(\varphi_i\varphi_i)_{1'}\xi'^2 + \lambda_{i,8}(\varphi_i\varphi_i)_{1''}\xi''^2 \\ &\quad +\text{h.c.} \\ &= \lambda_{i,6}\xi'\xi''(\varphi_{i,1}^2 + \varphi_{i,2}^2 + \varphi_{i,3}^2) \\ &\quad +(\lambda_{i,7}\xi'^2 + \lambda_{i,8}\xi''^2)(\varphi_{i,1}^2 - \varphi_{i,2}^2 - \varphi_{i,3}^2). \end{aligned} \tag{4.33}$$

All parameters appearing here are assumed to be real. The occurrence of the Hermitian conjugate in the last two expressions results from the fact that in some

[8] Recall that the flavon fields were assumed to be real scalar fields.

of the products terms which depend on $\omega = e^{2\pi i/3}$ arise (see (4.8)). Furthermore the subscript 3 has been used in products where the 3_1 and 3_2 couplings lead to the same term.

While the expression above gives the most general potential compatible with the symmetries we have imposed, some terms can actually be ruled out by requiring that the flavon potential has to be bounded from below. In this way one finds that

$$\lambda_{i,7} = \lambda_{i,8} = \rho_7 = \rho_8 = 0. \tag{4.34}$$

Let us demonstrate how this can be derived for the example of $\lambda_{i,7}$. If $\lambda_{i,7}$ were positive, we could consider the direction in field space where $\varphi_{i,2} = \text{const.} \neq 0$, ξ' is taken to infinity and all other component fields are zero. In this limit we would clearly have $V \to -\infty$. If on the other hand $\lambda_{i,7}$ were negative, we could consider $\varphi_{i,1} = \text{const.} \neq 0$, $\xi' \to \infty$ with all other fields set to zero, and would find the same behaviour of the potential. Therefore we must impose $\lambda_{i,7} = 0$. The necessity for the vanishing of the other parameters mentioned above can be derived by similar arguments. It is clear that there exist further conditions that can be derived from the requirement of boundedness from below. However, as we will see momentarily, the full flavon potential suffers from the so-called vev alignment problem and will not in general allow for the required vev structure. Therefore we refrain from a full analysis of the bounded from below conditions at this point, and will instead give them only for the restricted potential that will be found in section 4.5, in which the vev alignment problem is absent.

Let us now have a look at the necessary minimum conditions and check if there exists a nontrivial minimum of the given potential V_{flavon} with $\langle\varphi_S\rangle = (v_s, 0, 0)$ and $\langle\varphi_S\rangle = v_T(1,1,1)$. After plugging in the required form of the vevs the necessary minimum conditions read

$$\begin{aligned}
0 \stackrel{!}{=} \frac{\partial V_{\text{flavon}}}{\partial\varphi_{S,1}} &= 2m_S^2 v_S + 4\lambda_{S,1}v_S^3 + 4\lambda_{S,2}v_S^3 + 2\lambda_{S,6}v_S u'u'' && (4.35)\\
&\quad +6\rho_2 v_S v_T^2 - 4\rho_3 v_S v_T^2 + 2\rho_4 v_s v_T^2 + 2\rho_5 v_S v_T^2\,,\\
0 \stackrel{!}{=} \frac{\partial V_{\text{flavon}}}{\partial\varphi_{S,2}} &= \frac{\partial V_{\text{flavon}}}{\partial\varphi_{S,3}} = \rho_1 v_S v_T^2 + \rho_6 v_S v_T^2\,, && (4.36)\\
0 \stackrel{!}{=} \frac{\partial V_{\text{flavon}}}{\partial\varphi_{T,1}} &= -2m_T^2 v_T + 12\lambda_{T,1}v_T^3 + 4\lambda_{T,3}v_T^3 + 2\lambda_{T,6}v_T u'u'' && (4.37)\\
&\quad +2\rho_2 v_S^2 v_T\,,\\
0 \stackrel{!}{=} \frac{\partial V_{\text{flavon}}}{\partial\varphi_{T,2}} &= -2m_T^2 v_T + 12\lambda_{T,1}v_T^3 + 4\lambda_{T,3}v_T^3 + 2\lambda_{T,6}v_T u'u'' && (4.38)\\
&\quad +2\rho_2 v_S^2 v_T - 2\rho_3 v_S^2 v_T + 2\rho_4 v_S^2 v_T\,,\\
0 \stackrel{!}{=} \frac{\partial V_{\text{flavon}}}{\partial\varphi_{T,3}} &= -2m_T^2 v_T + 12\lambda_{T,1}v_T^3 + 4\lambda_{T,3}v_T^3 + 2\lambda_{T,6}v_T u'u'' && (4.39)\\
&\quad +2\rho_2 v_S^2 v_T - 2\rho_3 v_S^2 v_T + 2\rho_5 v_S^2 v_T\,,\\
0 \stackrel{!}{=} \frac{\partial V_{\text{flavon}}}{\partial(\xi'\xi'')} &= m_{\xi'\xi''}^2 + 2\lambda_5 u'u'' + \lambda_{S,6}v_S^2 + 3\lambda_{T,6}v_T^2\,. && (4.40)
\end{aligned}$$

Note that after taking (4.34) into account, one finds that V_{flavon} depends only on the product of ξ' and ξ'' and not on the individual fields themselves. Therefore it is sufficient to consider $\partial V_{\text{flavon}}/\partial(\xi'\xi'')$. In particular, interpreting V_{flavon} as a function of the product $\xi'\xi''$ rather than of independent variables ξ' and ξ'' is useful when verifying whether the sufficient minimum condition (positive definite Hesse matrix) is fulfilled. The fact that V_{flavon} depends on only on a combination of ξ' and ξ'' implies that there is an 'orthogonal' direction in field space (which is related to ξ' and ξ'' non-linearly) along which the potential is flat. This flat direction can be seen as the result of an accidental continuous $\mathbb{R}^*$ symmetry acting by $\xi' \to \alpha\xi',\ \xi'' \to \xi''/\alpha,\ \alpha \in \mathbb{R}^*$. Associated to this symmetry one thus obtains an unwanted massless Goldstone boson. However, higher order corrections to the potential will lift this flat direction when considering the full theory, such that the would-be Goldstone boson becomes massive. This will be discussed in more detail section 4.5.1.

Let us now return to solving the necessary minimum conditions given above. For general parameters one finds that the only solution is $v_S = 0$ and $v_T = 0$. Hence a certain fine-tuning of the parameters of the flavon potential is needed in order to admit non-trivial solutions for the triplet vevs. For example, by comparing equation (4.38) and (4.39) one immediately sees that one must impose $\rho_4 = \rho_5$. This could still be justified in some sense by noting that these parameters describe the strength of the two different coupling possibilities of two triplets to 3_1 and 3_2, which one might expect to naturally occur with the same strength. However, there are further constraints which cannot be justified in such a simple manner. For example, one has to require

$$2\rho_3 - 2\rho_4 + \rho_1 + \rho_6 = 0, \tag{4.41}$$

as can be seen by combining equations (4.36), (4.37) and (4.38). The fact that such fine-tuning is necessary is known as the 'vev alignment problem'.

Many approaches have been considered in the existing literature to solve the alignment problem. Altarelli and Feruglio showed in [105] that the vev alignment may be explained by embedding the A_4 theory into a supersymmetric (SUSY) extension. They introduced an additional $U_R(1)$ symmetry, which contains the usual R-parity. The flavons are kept uncharged under this additional symmetry, whereas all leptons carry $U_R(1)$ charge 1. In addition, Altarelli and Feruglio introduced an additional copy of each flavon with $U_R(1)$ charge 2, which implies that they can only occur in linear order in the superpotential and therefore play the role of driving fields. Furthermore, the vevs of these additional flavons are required to vanish. The minimisation of the SUSY scalar potential with respect to the driving fields then leads immediately to the required form of the flavon vevs. Further details on this proposal can be found in the original paper [105].

A different approach to solving the vev alignment problem is based on the observation that the problem is absent as long as dangerous cross-couplings between the two scalar triplets are forbidden. One way to achieve this is a group theoretical

approach, which was first considered by Babu and Gabriel in [106]. They extended the discrete symmetry group A_4 to the semidirect product group $G = S_3^4 \rtimes A_4$[9] and enforced that φ_T transforms only under the A_4 group while φ_S transforms under the full group G. This assignment suffices to forbid the dangerous cross-couplings mentioned above. The main disadvantage of this models is that fields transforming in high-dimensional representations are needed. Avoiding these large representations was one motivation for the work [107], in which Holthausen and Schmidt further developed the ideas of Babu and Gabriel. They analysed which discrete groups could be used instead of the S_3^4 group to play the same role, searching in particular for groups in which smaller representations were sufficient to avoid the problem[10]. They found that the smallest possible group which solves the vev alignment problem and which leads to a model that can be made consistent with all known bounds is the quaternion group Q_8, whose maximal representation is of dimension 4.

In the following we will not pursue either of the above approaches any further, and will instead focus on another possible solution of the alignment problem which was first considered by Altarelli and Feruglio in [108]. They introduced an extra spatial dimension and enforced a separate localisation of the scalar and matter fields in a way which guarantees the absence of the unwanted cross-couplings in the potential. As Altarelli and Feruglio did not consider the presence of right-handed neutrinos, let us adapt their model to the case at hand.

4.5 Explaining the vev alignment in the 2S2T model via extra dimensions

Following the approach of [108], we consider a five-dimensional spacetime taken to be the product of the usual four-dimensional Minkowski space and an extra spatial dimension with coordinate y. More concretely, the additional dimension is assumed to be a flat and compact interval of finite length L. The boundary of the considered spacetime is thus given by a pair of four-dimensional branes spanning the 'external' Minkowski space.

Our aim is to forbid the problematic cross-couplings of the triplets in the scalar potential that lead to the vev alignment problem. This can be achieved by enforcing that the matter and scalar fields are localised in a particular way on the two different branes. The localisation of the fields that will be required in our model is pictured schematically in figure 4.2. We introduce two additional Weyl fermions F_1 and F_2, which we combine into a Dirac spinor $F = (F_1, \overline{F_2})$. This field F is not restricted to either of the branes and instead propagates over the

[9] Note that a direct product is not suitable since not all generators of the additional group are allowed to commute with the generators of the A_4 group in order for the mechanism to work.

[10] Holthausen and Schmidt considered also flavour groups other than A_4 which suffer from the same alignment problem.

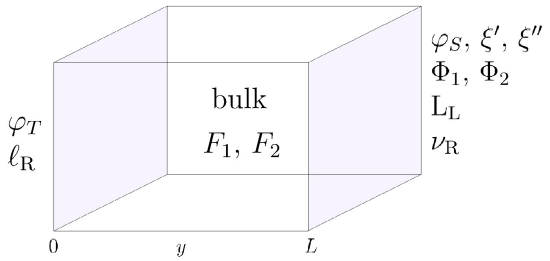

Figure 4.2: Localisation of the matter and scalar fields. All other SM fields are assumed to be localised at $y = L$.

full bulk spacetime. We take F to be a singlet under the SM gauge group except for the hypercharge $U(1)_Y$, where we assign the charge $Y_F = -2$. The mass of the bulk fermion will be denoted as M_F. Finally, F is assumed to transform in the triplet representation of A_4, whereas it is uncharged under the global $\mathbb{Z}_2^\ell \times \mathbb{Z}^\nu$ and $U(1)$ symmetries introduced above.

In this section we will initially work in the Ma-Rajasekaran basis for the triplet representation of A_4, before transferring the final results to the Altarelli-Feruglio basis at the end of the section. The action including the five-dimensional kinetic terms of F and the most general interactions of Yukawa type that are compatible with the various charge assignments and the localisation of the flavon and matter is given by

$$\begin{aligned}
S = \int d^4x dy \Big[& i F_1 \sigma^\mu \partial_\mu \overline{F_1} + i F_2 \sigma^\mu \partial_\mu \overline{F_2} + \frac{1}{2}(F_2 \partial_y F_1 - F_1 \partial_y F_2 + \text{h.c.}) \\
& - M_F (F_1 F_2 + \overline{F_1}\,\overline{F_2}) \\
& + \left[V_S(\varphi_S) + V_\text{singlet}(\xi', \xi'') + V_\text{int,S}(\varphi_S, \xi', \xi'') \right] \delta(y - L) \\
& + V_T(\varphi_T) \delta(y) \\
& + \Big(\widetilde{Y}^e (\varphi_T \overline{F_1})_1 e_\mathrm{R} + \widetilde{Y}^\mu (\varphi_T \overline{F_1})_{1'} \mu_\mathrm{R} + \widetilde{Y}^\tau (\varphi_T \overline{F_1})_{1''} \tau_\mathrm{R} + \text{h.c.} \Big) \delta(y) \\
& + \frac{1}{\Lambda} \Big(Y^{3_{1,2}} \varphi_S (\overline{\mathrm{L_L}} \widetilde{\Phi}_1 \nu_\mathrm{R})_{3_{1,2}} + Y'' (\overline{\mathrm{L_L}} \widetilde{\Phi}_1 \nu_\mathrm{R})_{1'} \xi'' + Y' (\overline{\mathrm{L_L}} \widetilde{\Phi}_1 \nu_\mathrm{R})_{1''} \xi' \\
& \qquad + \text{h.c.} \Big) \delta(y - L) \\
& + \Big(Y (\overline{\mathrm{L_L}} \Phi_2 \overline{F_2})_1 + \text{h.c.} \Big) \delta(y - L) \Big] .
\end{aligned} \tag{4.42}$$

Note that the five-dimensional bulk fermion fields have mass dimension two. This implies that the constants Y and $\widetilde{Y}^\ell$ ($\ell = e, \mu, \tau$) appearing here have mass dimension -1/2. We have restricted ourselves to operators of the lowest possible mass dimension for now, while higher order corrections that are suppressed by further powers of $1/\Lambda$ will be taken into account in the next subsection. Varying

the action with respect to $\overline{F}$ gives

$$\begin{aligned}
\delta S &= \int d^4x dy \Big[\left(-i\sigma^\mu \partial_\mu F_1 - \partial_y \overline{F_2} - M_F \overline{F_2}\right) \delta\overline{F_1} \\
&\qquad + \left(-i\sigma^\mu \partial_\mu F_2 + \partial_y \overline{F_1} - M_F \overline{F_1}\right) \delta\overline{F_2} \Big] \\
&\quad + \frac{1}{2} \int d^4x \left[\overline{F_1}(0)\delta\overline{F_2}(0) - \overline{F_2}(0)\delta\overline{F_1}(0) \right. \\
&\qquad \left. + \overline{F_2}(L)\delta\overline{F_1}(L) - \overline{F_1}(L)\delta\overline{F_2}(L) \right] \\
&\quad + \int d^4x \left(\widetilde{Y}^e e_{\mathrm{R}} \varphi_T^e + \widetilde{Y}^\mu \mu_{\mathrm{R}} \varphi_T^\mu + \widetilde{Y}^\tau \tau_{\mathrm{R}} \varphi_T^\tau \right) \delta\overline{F_1}(0) \\
&\quad + \int d^4x Y \overline{\mathrm{L_L}} \Phi_2 \delta\overline{F_2}(L).
\end{aligned} \tag{4.43}$$

Here we made use of a symbolic notation in order to properly account for the different ways of coupling the triplets, namely we have defined

$$\varphi_T^e := \varphi_T = \begin{pmatrix} \varphi_{T,1} \\ \varphi_{T,2} \\ \varphi_{T,3} \end{pmatrix}, \qquad \varphi_T^\mu := \begin{pmatrix} \varphi_{T,1} \\ \omega^2 \varphi_{T,2} \\ \omega \varphi_{T,3} \end{pmatrix}, \qquad \varphi_T^\tau := \begin{pmatrix} \varphi_{T,1} \\ \omega \varphi_{T,2} \\ \omega^2 \varphi_{T,3} \end{pmatrix}. \tag{4.44}$$

Note that φ_T^μ and φ_T^τ do not have a well-defined transformation behaviour under the action of the transformations S and T of the A_4 group. However the multiplication with the corresponding right-handed charged leptons yields a vector that transforms as a triplet of A_4. The multiplication with $\delta\overline{F_1}(0)$ in (4.43) is then just the normal Euclidean scalar product of two vectors and yields an A_4 singlet. One can explicitly check that one gets exactly the same expression from (4.42) if one writes down the corresponding term in terms of components of the triplet fields, taking into account the multiplication rules of the A_4 group (4.8).

The last three lines in the variation of the action are the boundary terms. We can ensure that these boundary terms of the variation vanish by imposing the boundary conditions

$$\begin{aligned}
\overline{F_1}(L) &= 2Y\overline{\mathrm{L_L}}\Phi_2\,, \\
\overline{F_2}(0) &= 2\left(\widetilde{Y}^{\mathrm{e}} e_{\mathrm{R}} \varphi_T^e + \widetilde{Y}^\mu \mu_{\mathrm{R}} \varphi_T^\mu + \widetilde{Y}^\tau \tau_{\mathrm{R}} \varphi_T^\tau\right)\,,
\end{aligned} \tag{4.45}$$

for the bulk fields, which imply that $\delta\overline{F_1}(L) = 0$ and $\delta\overline{F_2}(0) = 0$.

From the first two lines of the variation (4.43) we read off the equations of motion for F_1 and F_2

$$\begin{aligned}
i\sigma^\mu \partial_\mu F_1 + \partial_y \overline{F_2} + M_F \overline{F_2} &= 0, \\
-i\sigma^\mu \partial_\mu F_2 + \partial_y \overline{F_1} - M_F \overline{F_1} &= 0.
\end{aligned} \tag{4.46}$$

Let us assume that the extra dimension is sufficiently small so that $1/L$ is much larger then the electroweak scale. Then the internal momentum scale governing

$\partial_y \overline{F_i}$ is large compared to the scale of $i\sigma^\mu \partial_\mu F_i$ for $i = 1, 2$. Hence we can work in the so-called static approximation where equation (4.46) simplifies to

$$\begin{aligned} \partial_y \overline{F_1} - M_F \overline{F_1} &= 0, \\ \partial_y \overline{F_2} + M_F \overline{F_2} &= 0. \end{aligned} \tag{4.47}$$

These equations are solved by

$$\begin{aligned} \overline{F_1}(y) = \overline{F_1}(L) e^{M_F(y-L)} &= 2Y \overline{\mathrm{L_L}} \Phi_2 e^{M_F(y-L)}, \\ \overline{F_2}(y) = \overline{F_2}(0) e^{-M_F y} &= 2\left(\widetilde{Y}^e e_\mathrm{R} \varphi_T^e + \widetilde{Y}^\mu \mu_\mathrm{R} \varphi_T^\mu + \widetilde{Y}^\tau \tau_\mathrm{R} \varphi_T^\tau\right) e^{-M_F y}, \end{aligned} \tag{4.48}$$

where the second equality follows from the boundary conditions for $F_{1,2}$ chosen in (4.45).

Now integrating out the bulk fermion, i.e. substituting equation (4.46), (4.47) and (4.48) into the original action (4.42) yields

$$\begin{aligned} S = \int d^4x \Big[& V_T(\varphi_T) + V_S(\varphi_S) + V_\mathrm{singlet}(\xi', \xi'') + V_\mathrm{int,S}(\varphi_S, \xi', \xi'') \\ & + 4Y\widetilde{Y}^e (\overline{\mathrm{L_L}} \Phi_2 \varphi_T)_1 e_\mathrm{R} e^{-M_F L} + 4Y\widetilde{Y}^\mu (\overline{\mathrm{L_L}} \Phi_2 \varphi_T)_{1'} \mu_\mathrm{R} e^{-M_F L} \\ & + 4Y\widetilde{Y}^\tau (\overline{\mathrm{L_L}} \Phi_2 \varphi_T)_{1''} \tau_\mathrm{R} e^{-M_F L} + \mathrm{h.c.} \\ & + \frac{1}{\Lambda} \Big(Y^{3_{1,2}} \varphi_S (\overline{\mathrm{L_L}} \widetilde{\Phi_1} \nu_\mathrm{R})_{3_{1,2}} + Y'' (\overline{\mathrm{L_L}} \widetilde{\Phi_1} \nu_\mathrm{R})_{1'} \xi'' \\ & \quad + Y' (\overline{\mathrm{L_L}} \widetilde{\Phi_1} \nu_\mathrm{R})_{1''} \xi' + \mathrm{h.c.} \Big) \Big]. \end{aligned} \tag{4.49}$$

Defining $Y^\ell/\Lambda = 4Y\widetilde{Y}^\ell e^{-M_F L}$ for $\ell = e,\ \mu,\ \tau$, the last four lines correspond exactly to the Lagrangian $\mathcal{L}_\mathrm{Yukawa}$ which we introduced in section 4.3. Note that to confirm the precise match one of course has to perform a basis change of the expression (4.49) into the Altarelli-Feruglio basis.

We would like to emphasise that the triplet cross-couplings in the flavon potential, which were absent in the original action (4.42) due to the separation of the two triplets to different branes, are not induced at leading order by integrating out the bulk fermions[11]. Therefore the dangerous cross-couplings which caused the vev alignment problem are forbidden.

Considering the resulting reduced scalar potential, in which $V_\mathrm{int,T}(\varphi_T, \xi', \xi'')$ and $V_\mathrm{int,ST}(\varphi_T, \varphi_S, \xi', \xi'')$ are absent, we get a corresponding simplification of the minimisation conditions of equation (4.40). This simplification allows us to solve these

[11] We will briefly consider the effects of bulk fermion loops in the next subsection.

equations and find the following explicit expressions for the flavon vevs

$$u'u'' = \frac{2(\lambda_{S,1}+\lambda_{S,2})m^2_{\xi'\xi''}+m^2_S\lambda_{S,6}}{-4(\lambda_{S,1}+\lambda_{S,2})\lambda_5+\lambda^2_{S,6}}\,, \tag{4.50}$$

$$v_T = \pm\frac{m_T}{\sqrt{6\lambda_{T,1}+2\lambda_{T,3}}}\,, \tag{4.51}$$

$$v_S = \pm\frac{\sqrt{2m^2_S\lambda_5+m^2_{\xi'\xi''}\lambda_{S,6}}}{\sqrt{4(\lambda_{S,1}+\lambda_{S,2})\lambda_5-\lambda^2_{S,6}}}. \tag{4.52}$$

By considering the Hesse matrix of the potential and plugging in these solutions for the vevs one can confirm that they indeed correspond to minima of the potential (for suitable choices of the parameters). For the sake of completeness let us also give the conditions guaranteeing boundedness from below for the simplified flavon potential considered here. They are given by

$$\lambda_{S,6}>0,\quad 3\lambda_{i,1}+\lambda_{i,3}>0,\quad \lambda_{i,1}+\lambda_{i,2}>0,\quad \lambda_5>0,\quad \text{and}\quad \lambda_{S,7}=\lambda_{S,8}=0\,,$$

with $i=S,T$.

4.5.1 Next-to-leading order effects in the 2S2T model with an extra dimension

As the A_4 invariant Yukawa interactions that we have studied in this chapter arise as part of an effective theory, it is natural to consider also corrections at higher order in the $1/\Lambda$ expansion. For definiteness the discussion of next-to-leading order (NLO) effects will be performed in the framework of the extradimensional A_4 model discussed above, in which the problematic cross-couplings between the two scalar triplet flavons in the scalar potential are absent at leading order. We again follow the approach of Altarelli and Feruglio [108], adapting their calculations to the case of Dirac neutrinos. As in the previous two sections we will work in the Ma-Rajasekaran basis and then transform the results to the to the Altarelli-Feruglio basis, to allow for comparison with the mass matrices that were calculated in section 4.3.

Before proceeding with the explicit computation of the higher order corrections, let us give a rough estimate for their expected suppression. As we will see, most corrections will be suppressed by powers of v_T/Λ or v_ν/Λ. Here v_ν is a vev of one of the flavons coupling in the neutrino mass sector, i.e. either one of the singlet flavon vevs or v_S. As a guiding principle for an estimate of the magnitude of these ratios we will assume that the Yukawa coupling constants appearing in the leading order Lagrangian (4.13) should be roughly of order one. Taking into account the expected values for the vevs of the two Higgs fields given in chapter 3 as well as the values of the charged lepton masses and the expected neutrino mass scale of $\lesssim 0.1$ eV, we are led to the estimates

$$\frac{v_T}{\Lambda}\sim 5\times 10^{-3}, \qquad \frac{v_\nu}{\Lambda}\sim 5\times 10^{-2}. \tag{4.53}$$

We will also briefly consider corrections arising from bulk fermion loops, which will be suppressed by powers of $1/(\Lambda L)$ with L the length scale of the extra dimension. While this dimensionless suppression factor is not directly related to the $v_{T,\nu}/\Lambda$ ratios considered above, we will choose $1/(\Lambda L)$ to be of similar magnitude for definiteness.

Let us first consider corrections to the neutrino mass matrix. Due to the $\mathbb{Z}_2^\nu$ charges of the flavons the next-to-leading order terms will have to involve two further flavons in comparison with the terms considered in the action (4.42), i.e. three flavon fields in total. However, most possible ways of coupling the A_4 fields will lead to terms that are equivalent to the terms already considered in (4.42), so that their effects can be absorbed into a redefinition of the Yukawa coupling constants. In fact, one immediately sees that the only corrections that are not similar in form to contributions that were already considered arise from terms of the form $\left(\overline{\mathrm{L_L}}\widetilde{\Phi}_1\nu_\mathrm{R}\right)_1\Psi^3$, where Ψ^3 is an arbitrary combination of the flavon fields φ_S, ξ' and ξ'' coupled in such a way as to yield an A_4 singlet. The general form of the relevant NLO correction to the action (4.42) is therefore given by

$$\begin{aligned}\mathcal{L}^\nu_\mathrm{NLO} \;=\; \frac{1}{\Lambda^3}\left(\overline{\mathrm{L_L}}\widetilde{\Phi}_1\nu_\mathrm{R}\right)_1 \big[&Y_1^\nu(\varphi_S\varphi_S)_3\varphi_S + Y_2^\nu(\varphi_S\varphi_S)_{1'}\xi'' + Y_3^\nu(\varphi_S\varphi_S)_{1''}\xi' \\ &+Y_4^\nu\xi'^3 + Y_5^\nu\xi''^3\big]\,\delta(y-L) + \mathrm{h.c.}\end{aligned} \tag{4.54}$$

Making use of the multiplication rules given in (4.8) this can be expanded in terms of the component fields to give

$$\begin{aligned}\mathcal{L}^\nu_\mathrm{NLO} \;=\; \frac{1}{\Lambda^3}\sum \overline{\mathrm{L_L}}_i\widetilde{\Phi}_1\nu_{\mathrm{R},i}\,\big[&3Y_1^\nu\varphi_{S,1}\varphi_{S,2}\varphi_{S,3} \\ &+Y_2^\nu\xi''(\varphi_{S,1}^2+\omega^2\varphi_{S,2}^2+\omega\varphi_{S,3}^2) \\ &+Y_3^\nu\xi'(\varphi_{S,1}^2+\omega\varphi_{S,2}^2+\omega^2\varphi_{S,3}^2) + Y_4^\nu\xi'^3 \\ &+Y_5^\nu\xi''^3\big]\,\delta(y-L) + \mathrm{h.c.}\end{aligned} \tag{4.55}$$

To find the resulting contribution to the neutrino mass matrix we make use of the vev alignment, which in the MR basis reads $\langle p_s\rangle = (v_S, 0, 0)$. After A_4 and electroweak symmetry breaking we then find

$$\mathcal{L}^\nu_\mathrm{NLO} = (\overline{\nu_{\mathrm{L}1}}, \overline{\nu_{\mathrm{L}2}}, \overline{\nu_{\mathrm{L}3}})\begin{pmatrix} x & 0 & 0 \\ 0 & x & 0 \\ 0 & 0 & x \end{pmatrix}\begin{pmatrix} \nu_{\mathrm{R},1} \\ \nu_{\mathrm{R},2} \\ \nu_{\mathrm{R},1}\end{pmatrix}\delta(y-L) + \mathrm{h.c.}\,, \tag{4.56}$$

where we have defined

$$x = \frac{v_1}{\Lambda^3}\left(Y_2^\nu u'' v_S^2 + Y_3^\nu u' v_S^2 + Y_4^\nu u'^3 + Y_5^\nu u''^3\right). \tag{4.57}$$

We therefore find a correction to the diagonal elements of the mass matrix in the MR basis. The corresponding matrix in the Altarelli-Feruglio basis that was used

in section 4.3 can be derived by performing the basis change using the 'magic' matrix V given in (4.9). This results in the correction[12]

$$\delta m_\nu^T = V^\dagger \begin{pmatrix} x & 0 & 0 \\ 0 & x & 0 \\ 0 & 0 & x \end{pmatrix} V^\dagger = \begin{pmatrix} x & 0 & 0 \\ 0 & 0 & x \\ 0 & x & 0 \end{pmatrix} \tag{4.58}$$

to the leading order neutrino mass matrix given in (4.22). In comparison with the leading order entries, this NLO contribution is therefore suppressed by $v_\nu^2/\Lambda^2 \sim 2 \times 10^{-3}$, where we have used the estimate (4.53).

By comparison with (4.22), we see that this correction has the same form as the contribution that would have been induced by at leading order by an additional flavon in the representation 1 (which we denoted as ξ). As we have seen in section 4.3, a contribution of this form does not lead to any deviations from the TBM form of the mixing matrix and leads to the masses given in table 4.4[13]. In the next chapter we will consider relaxing the conditions $c = d$ and $a' = 0$ to obtain deviations from the TBM form. There is no reason to expect these deviations to be especially small, in particular they will be assumed to be much larger than the NLO corrections considered here. Hence we will neglect the small corrections to the masses calculated here in the following.

We now turn to corrections to the mass matrix of the charged leptons. We could first of all consider corrections to the couplings between $\overline{F}_1$ and ℓ_R, whose leading order form in (4.42) is $\widetilde{Y^\ell}(\varphi_T \overline{F_1})\ell_\mathrm{R}$. Such correction terms would have the generic form $\varphi_T^3 \overline{F_1}\ell_\mathrm{R}/\Lambda^2$. However, it turns out that all terms of this type that may be written down using the A_4 coupling rules either vanish or lead to contributions that can be absorbed into a redefinition of the coupling constants. This can be seen immediately from the multiplication rules (4.8) after plugging in the aligned form $\langle \varphi_T \rangle = v_T(1,1,1)$ of the triplet vev and recalling that $\omega = \exp(2\pi i/3)$, so that

$$1 + \omega + \omega^2 = 0. \tag{4.59}$$

Therefore corrections to the charged lepton mass matrix that arise from corrections to $\widetilde{Y^\ell}(\varphi_T \overline{F_1})\ell_\mathrm{R}$ must be suppressed by at least v_T^4/Λ^4.

However, another correction to the lepton mass matrix comes from corrections to the couplings between $\overline{F}_2$ and $\overline{\mathrm{L_L}}$, where the leading term in (4.42) reads $Y(\overline{\mathrm{L_L}}\Phi_2\overline{F_2})_1$. Corrections that cannot be absorbed by a redefinition of Y are

[12] Note that for the purpose of the A_4 couplings a barred A_4 triplet transforms in the same manner as an unbarred triplet, so that $\overline{\nu_\mathrm{L}}_i^\mathrm{AF} = V_{ij}\overline{\nu_\mathrm{L}}_j^\mathrm{MR}$ and $\nu_{\mathrm{R},i}^\mathrm{AF} = V_{ij}\nu_{\mathrm{R},j}^\mathrm{MR}$. This transformation behaviour was chosen in order to avoid having to define separate A_4 multiplication rules for triplets depending on whether one couples a barred and an unbarred field or only unbarred fields like the flavons. This choice results in the slightly unusual form of the transformation of the mass matrix involving only $V^\dagger$.

[13] As the corrections to the masses are small, a perturbed form of the sum rule mentioned in section 4.3 still holds.

given by

$$\begin{aligned}\mathcal{L}^{F_2}_{\text{NLO}} &= \Big[(\overline{\text{L}_\text{L}}\Phi_2\overline{F_2})_{1'}\left(Y_1(\varphi_S\varphi_S)_{1''}+Y_2\xi'^2\right)\\ &\quad+(\overline{\text{L}_\text{L}}\Phi_2\overline{F_2})_{1''}\left(Y_3(\varphi_S\varphi_S)_{1'}+Y_4\xi''^2\right)\\ &\quad+(\overline{\text{L}_\text{L}}\Phi_2\overline{F_2})_{3_1}\Big(Y_{5,1}(\varphi_S\varphi_S)_3+Y_{6,1}(\varphi_S\xi')_3+Y_{7,1}(\varphi_S\xi'')_3\Big)\\ &\quad+(\overline{\text{L}_\text{L}}\Phi_2\overline{F_2})_{3_2}\Big(Y_{5,2}(\varphi_S\varphi_S)_3+Y_{6,2}(\varphi_S\xi')_3+Y_{7,2}(\varphi_S\xi'')_3\Big)\\ &\quad+\text{h.c.}\Big]\delta(y-L).\end{aligned} \tag{4.60}$$

Again we expand this into components using the multiplication rules in the MR basis given in (4.8), which yields

$$\begin{aligned}\mathcal{L}^{F_2}_{\text{NLO}} = &\left(\overline{\text{L}_{\text{L},1}}\,\overline{F_{2,1}}+\omega^2\overline{\text{L}_{\text{L},2}}\,\overline{F_{2,2}}+\omega\overline{\text{L}_{\text{L},3}}\,\overline{F_{2,3}}\right)\Big[Y_1(\varphi^2_{S,1}+\omega\varphi^2_{S,2}+\omega^2\varphi^2_{S,3})\\ &\qquad+Y_2\xi'^2\Big]\Phi_2\delta(y-L)/\Lambda^2\\ &+\left(\overline{\text{L}_{\text{L},1}}\,\overline{F_{2,1}}+\omega\overline{\text{L}_{\text{L},2}}\,\overline{F_{2,2}}+\omega^2\overline{\text{L}_{\text{L},3}}\,\overline{F_{2,3}}\right)\Big[Y_3(\varphi^2_{S,1}+\omega^2\varphi^2_{S,2}+\omega\varphi^2_{S,3})\\ &\qquad+Y_4\xi''^2\Big]\Phi_2\delta(y-L)/\Lambda^2\\ &+\Big(\overline{\text{L}_{\text{L},2}}\,\overline{F_{2,3}}\Big[Y_{5,1}\varphi_{S,2}\varphi_{S,3}+\varphi_{S,1}(Y_{6,1}\xi'+Y_{7,1}\xi'')\Big]\\ &\quad+\overline{\text{L}_{\text{L},3}}\,\overline{F_{2,1}}\Big[Y_{5,1}\varphi_{S,3}\varphi_{S,1}+\varphi_{S,2}(Y_{6,1}\xi'+Y_{7,1}\xi'')\Big]\\ &\quad+\overline{\text{L}_{\text{L},1}}\,\overline{F_{2,2}}\Big[Y_{5,1}\varphi_{S,1}\varphi_{S,2}+\varphi_{S,2}(Y_{6,1}\xi'+Y_{7,1}\xi'')\Big]\Big)\Phi_2\delta(y-L)/\Lambda^2\\ &+\Big(\overline{\text{L}_{\text{L},3}}\,\overline{F_{2,2}}\Big[Y_{5,2}\varphi_{S,2}\varphi_{S,3}+\varphi_{S,1}(Y_{6,2}\xi'+Y_{7,2}\xi'')\Big]\\ &\quad+\overline{\text{L}_{\text{L},1}}\,\overline{F_{2,3}}\Big[Y_{5,2}\varphi_{S,3}\varphi_{S,1}+\varphi_{S,2}(Y_{6,2}\xi'+Y_{7,2}\xi'')\Big]\\ &\quad+\overline{\text{L}_{\text{L},2}}\,\overline{F_{2,1}}\Big[Y_{5,2}\varphi_{S,1}\varphi_{S,2}+\varphi_{S,3}(Y_{6,2}\xi'+Y_{7,2}\xi'')\Big]\Big)\Phi_2\delta(y-L)/\Lambda^2\\ &+\text{h.c.}\end{aligned} \tag{4.61}$$

After A_4 symmetry breaking and plugging in the vev alignment condition $\langle\varphi_S\rangle = v_S(1,1,1)$ the expression finally reads

$$\begin{aligned}\mathcal{L}^{F_2}_{\text{NLO}} &= (\overline{\text{L}_{\text{L},1}},\overline{\text{L}_{\text{L},2}},\overline{\text{L}_{\text{L},1}})\begin{pmatrix}z_1+z_2 & z_3 & z_4\\ z_4 & \omega^2 z_1+\omega z_2 & z_3\\ z_3 & z_4 & \omega z_1+\omega^2 z_2\end{pmatrix}\begin{pmatrix}\overline{F_{2,1}}\\ \overline{F_{2,2}}\\ \overline{F_{2,3}}\end{pmatrix}\\ &\quad\times Y\Phi_2\delta(y-L)+\text{h.c.}\,,\end{aligned} \tag{4.62}$$

where we have introduced the abbreviations

$$\begin{aligned}z_1=\frac{u'^2}{\Lambda^2}\frac{Y_2}{Y}\,,\quad z_2=\frac{u''^2}{\Lambda^2}\frac{Y_4}{Y}\,,\quad z_3=\frac{v_S^2}{\Lambda^2}\frac{Y_{5,1}}{Y}+\frac{v_S}{\Lambda^2}\left(\frac{Y_{6,1}}{Y}u'+\frac{Y_{7,1}}{Y}u''\right),\\ z_4=\frac{v_S^2}{\Lambda^2}\frac{Y_{5,2}}{Y}+\frac{v_S}{\Lambda^2}\left(\frac{Y_{6,2}}{Y}u'+\frac{Y_{7,2}}{Y}u''\right).\end{aligned} \tag{4.63}$$

Note that in order to obtain the correction to the actual charged lepton mass matrix we must still integrate out the bulk fermions. To simplify this procedure we define

$$\overline{\mathrm{L_L}}^{\mathrm{NLO}} := (\overline{\mathrm{L_{L,1}}}, \overline{\mathrm{L_{L,2}}}, \overline{\mathrm{L_{L,1}}}) \begin{pmatrix} 1+z_1+z_2 & z_3 & z_4 \\ z_4 & 1+\omega^2 z_1+\omega z_2 & z_3 \\ z_3 & z_4 & 1+\omega z_1+\omega^2 z_2 \end{pmatrix}, \quad (4.64)$$

so that we can take the corrections into account by simply replacing the leading term in the action (4.42) by $Y\overline{\mathrm{L_L}}^{\mathrm{NLO}}\Phi_2\overline{F_2}$. This replacement changes the boundary term of the variation of the action, so that we must accordingly adapt the boundary condition for $\overline{F}_1(L)$ in equation (4.45) to

$$\overline{F_1}(L) = 2Y\overline{\mathrm{L_L}}^{\mathrm{NLO}}\Phi_2. \quad (4.65)$$

We can now integrate out the heavy bulk fermion fields at tree level in complete analogy to the calculations of the previous section. This yields the corrected entries of the leptonic mixing matrix

$$\begin{aligned}
(m_\ell)_{11} &= \frac{v_T v_2}{\Lambda} Y^e (1 + z_1 + z_2 + z_3 + z_4), \\
(m_\ell)_{12} &= \frac{v_T v_2}{\Lambda} Y^\tau (1 + z_1 + z_2 + \omega^2 z_3 + \omega z_4), \\
(m_\ell)_{13} &= \frac{v_T v_2}{\Lambda} Y^\mu (1 + z_1 + z_2 + \omega z_3 + \omega^2 z_4), \\
(m_\ell)_{21} &= \frac{v_T v_2}{\Lambda} Y^e (1 + \omega^2 z_1 + \omega z_2 + z_3 + z_4), \\
(m_\ell)_{22} &= \frac{v_T v_2}{\Lambda} Y^\tau (\omega^2 + \omega z_1 + z_2 + \omega z_3 + z_4), \\
(m_\ell)_{23} &= \frac{v_T v_2}{\Lambda} Y^\mu (\omega + z_1 + \omega^2 z_2 + \omega^2 z_3 + z_4), \\
(m_\ell)_{31} &= \frac{v_T v_2}{\Lambda} Y^e (1 + \omega z_1 + \omega^2 z_2 + z_3 + z_4), \\
(m_\ell)_{32} &= \frac{v_T v_2}{\Lambda} Y^\tau (\omega + \omega^2 z_1 + z_2 + z_3 + \omega^2 z_4), \\
(m_\ell)_{33} &= \frac{v_T v_2}{\Lambda} Y^\mu (\omega^2 + z_1 + \omega z_2 + z_3 + \omega z_4),
\end{aligned}$$

in the Ma-Rajasekaran basis in which S is diagonal. Recall that we had defined $Y^\ell/\Lambda = 4\widetilde{Y}^\ell Y e^{-ML}$. This result can finally be transformed into the Altarelli-Feruglio basis. Note that the right-handed charged leptons transforming in the singlet representations of A_4 are unaffected by this basis change, and only the left-handed lepton fields in the triplet representation need to be transformed. The correction to the diagonal leptonic mixing matrix given in (4.18) then reads

$$\delta m_\ell^T = V^\dagger \delta m_\ell = \frac{v_T v_2}{\Lambda} \begin{pmatrix} Y^e(z_3+z_4) & Y^\mu z_2 & Y^\tau z_1 \\ Y^e z_1 & Y^\mu(\omega^2 z_3+\omega z_4) & Y^\tau z_2 \\ Y^e z_2 & Y^\mu z_1 & Y^\tau(\omega z_3+\omega^2 z_4) \end{pmatrix}, \quad (4.66)$$

so that the charged lepton mass matrix is corrections at the same relative order $v_\nu^2/\Lambda^2 \sim 2 \times 10^{-3}$ as the neutrino mass matrix. The diagonal contributions can be absorbed by a redefinition of the corresponding Yukawa coupling constants. By comparison with equation (4.18), we see that the off-diagonal corrections are of the same form as those that would be induced by a slight misalignment of the triplet vev, i.e. $\langle \varphi_T \rangle = v_T(1, \epsilon_{T,1}, \epsilon_{T,2})$. As we will take the possibility of such a vev misalignment into account in chapter 5, we will therefore automatically also account for this higher order correction. Therefore we postpone a discussion of the effects of such corrections on the masses and the mixing matrix to the next chapter.

Let us also briefly consider corrections that may arise from exchange of the bulk fermions at one-loop level. We will keep the discussion quite schematic, as we will see that these corrections will be even more highly suppressed than the local NLO corrections considered above. We denote by Ψ_S some general combination of fields localised on the brane S on which the neutrinos are localised, while Ψ_T is some combination of fields on the other brane T. We will look to generate couplings of the form $\Psi_S \Psi_T$ via one-loop bulk fermion exchange. Note that the resulting operator $\Psi_S \Psi_T$ may be a coupling that could already be generated via tree-level bulk fermion exchange, but there are also certain couplings generated at one-loop level that cannot be obtained at tree-level. We will consider each case separately below after giving the general expressions. In order to generate such a coupling via one-loop F exchange the original action must contain couplings of the form

$$\frac{1}{\Lambda^{d_T}} \Psi_T F_1 F_2 \delta(y) \quad \text{and} \quad \frac{1}{\Lambda^{d_S}} \Psi_S F_1 F_2 \delta(y - L). \tag{4.67}$$

Here d_T and d_S are the total mass dimensions of the fields Ψ_T and Ψ_S, respectively. The loop integral is convergent and contributes a factor of $1/L^4$ up to dimensionless coefficients [108] (note that $1/L$ is the momentum scale of the massive modes of the bulk fermions). The resulting coupling therefore takes the form

$$\frac{1}{\Lambda^{d_T + d_S} L^4} \Psi_S \Psi_T. \tag{4.68}$$

Let us now consider the case where $\Psi_S \Psi_T$ is a coupling that is also generated at tree-level, and estimate the importance of the one-loop contribution. For example, we could consider generating a one-loop correction to the charged lepton masses by taking the combinations $\Psi_T = \ell_{\mathrm{R}} \varphi_T$ and $\Psi_S = \overline{\mathrm{L_L}} \Phi_2 \varphi_S^2$, which are compatible with the various $\mathbb{Z}_2$ charges of the fields. Counting up the mass dimensions of the fields one sees that this leads to a correction of the schematic form

$$\frac{v_T v_S^2}{\Lambda^7 L^4} \overline{\mathrm{L_L}} \Phi_2 \ell_{\mathrm{R}}. \tag{4.69}$$

We see that as expected this correction to the charged fermion mass matrix is suppressed by $1/(\Lambda L)^4$ in comparison with the NLO corrections computed above. Using the estimate for ΛL discussed above, we see that this is a suppression by

about $1/(\Lambda L)^4 \sim 10^{-12}$. Similar considerations of course apply for the other next-to-leading order contributions discussed above, so that these loop corrections are clearly negligible in comparison with the NLO corrections.

From the discussion above, it is clear that the one-loop bulk fermion exchange can only be important for couplings that cannot be generated in any other way. For example, they would give the leading source of corrections to the flavon potential involving $\varphi_T\varphi_S$ cross-couplings, which could e.g. be generated by taking $\Psi_{S,T} = (\varphi_{S,T}\varphi_{S,T})_1$ in the above notation. As discussed in section 4.4, the appearance of such cross-couplings can lead to problems with the flavon vev alignment. However we point out that these corrections are again suppressed by $\Lambda^4 L^4$ in comparison with the other couplings appearing in the flavon potential (4.29). Therefore we would also expect any vev misalignment generated in this manner to be correspondingly small.

However, the parts of the flavon potential not involving any triplet cross-couplings can of course also receive higher order corrections directly without involving bulk fermion loops. For example, we could consider the local couplings $(\xi')^6/\Lambda^2$ or $(\xi'')^6/\Lambda^2$ on the brane where these flavons are localised. These couplings are important because they break the accidental $\mathbb{R}^*$ symmetry of the flavon potential that was discussed in section 4.4 and induce a mass $m_{\rm GB}$ for the would-be Goldstone boson. This mass is therefore expected to be suppressed by about v_ν^2/Λ^2 in relation to the masses of the other flavons of the neutrino sector, which naturally lie at the scale v_ν. In particular we expect

$$m_{\rm GB} \sim \frac{v_\nu^3}{\Lambda^3}\Lambda \sim 10^{-4}\Lambda \sim 10^{12}\ \text{GeV}, \tag{4.70}$$

as Λ was taken to lie at the GUT scale. Even this would-be Goldstone boson is therefore clearly so heavy and will decay so quickly that we may safely neglect its presence in any discussion of low-energy phenomenology, as previously claimed.

Of course, there are many other higher order operators correcting the flavon potential in addition to the two examples mentioned above. These higher order contributions will of course also alter the minimisation conditions of section 4.4, which may lead to deviations from the aligned form of the triplet vevs that was required for TBM mixing. Of course, as they are induced by higher order corrections to the potential such deviations are again expected to be suppressed by powers of v/Λ compared to the aligned vevs obtained at leading order.

4.6 Possible dynamical origin of A_4

In the previous sections we have discussed in quite some detail how an A_4 flavour symmetry could help in explaining the observed leptonic mixing patterns. However, so far we have simply imposed this flavour symmetry by hand. In this context it is of course interesting to ask whether the appearance of the A_4 flavour

symmetry could be motivated by some underlying, more fundamental symmetry principle. Two main ideas have been put forward in the existing literature to answer this question [105, 109], which we will briefly summarise in the following.

In reference [105], Altarelli and Feruglio pointed out that the A_4 group can be understood as subgroup of the modular group $\Gamma = \mathrm{PSL}(2, \mathbb{Z})$. An action of this group on $z \in \mathbb{C}$ can be defined in the form of a Möbius transformation given by

$$z \to \frac{az + b}{cz + d}, \tag{4.71}$$

where the coefficients are integers satisfying $ad - bc = 1$. Every such transformation can be generated by a suitable composition of the two basic transformations

$$s : z \ \to \ -\frac{1}{z}\,, \tag{4.72}$$

$$t : z \ \to \ z + 1\,. \tag{4.73}$$

It is straightforward to check that s and t obey the relation $s^2 = (st)^3 = 1$. This is of course reminiscent of the relations $S^2 = (ST)^3 = T^3 = 1$ obeyed by the generators of the A_4 group. In particular, this implies that the matrices S and T introduced in section 4.1 define a certain representation of the modular group. Of course, the modular group has an infinite number of inequivalent three-dimensional representations. Altarelli and Feruglio discuss the moduli space of these representations of Γ in detail and comment in particular on the restrictions that must be imposed in order to obtain representations that are also representations of the A_4 group. Further details on the relationship between the two groups can be found in [105].

The observed relationship with Γ hints at a more fundamental origin of the A_4 group, as the modular group appears at a deep level in many physical contexts. For example, modular invariance is a fundamental requirement of the worldsheet action of string theory and plays an important role e.g. in guaranteeing the famous UV finiteness of string theory scattering amplitudes. The $\mathrm{PSL}(2, \mathbb{Z})$ symmetry also appears as a symmetry of the supergravity theories describing the low-energy dynamics of Type IIB string theory, where it acts by permuting certain fields into one another in a manner reminiscent of the A_4 action on flavons in the triplet representation. In light of the abovementioned relationship between Γ and A_4 it is thus not inconceivable that the A_4 representations may arise in the context of string theory compactifications, with the roles of the flavons perhaps played by certain axionic scalars.

A different possibility is that the A_4 symmetry arises in a geometric context. This possibility was considered by the authors of [109], who showed that the A_4 symmetry can arise by compactifying a six-dimensional theory to four dimensional Minkowski space on the orbifold $T^2/\mathbb{Z}_2$. Here the A_4 group appears initially in the fundamental four-dimensional representation, where it acts by permuting the four fixed points of the orbifold action. One starts by considering six-dimensional

fermion fields which are localised at the different fixed points. The A_4 action on the fixed points clearly gives rise to an action on these fermion fields in a natural way. As each individual field is associated to only one of the fixed points, these initial fields do not have a well-defined transformation behaviour under one of the irreducible representation of A_4. However, one can construct combinations of these fields which transform under the well-known singlet and triplet representations, which can then be identified with the fermionic matter fields. Note that the matter fields then have non-vanishing contributions from all four fixed points, as is necessary to exhibit a well-defined transformation behaviour under the action of the A_4 group. The flavon fields are taken to be bulk fields transforming as singlets or triplets under the A_4 group. As shown in [109], integrating out the extra spatial dimensions in the six-dimensional action then yields the four-dimensional Lagrangian (4.13).

Finally, the discrete A_4 group can of course also appear as a remnant symmetry after the breaking of a suitable underlying continuous symmetry. This possibility was discussed for example in [110].

4.7 What about the quark sector?

In this chapter we have so far focused exclusively on the lepton mass sector, for which the A_4 symmetry was first introduced due to its close relationship with the tribimaximal mixing form. To close the chapter let us now very briefly discuss how the model might be extended in order to account also for the observed mixing in the quark sector. The problem of extending the A_4 model to the quark sector has been extensively studied in the literature, see for example [63] for a review.

There are two possible ways to go. On one hand an extension within the context of GUTs has been considered. Here one is faced with the problem that all components of a given GUT multiplet have to have the same transformation properties under the flavour group. This imposes severe constraints on the realisation of such models, because fields that are wanted to transform in different A_4 representations must also be assigned to different GUT multiplets. However, in reference [111] an $SU(5) \times A_4 \times U(1)$ GUT model which predicts the right mixing patterns and mass hierarchies in the lepton and quark sectors was constructed.

On the other hand one could ask for an extension to the quark sector without embedding the model into a GUT, so that the abovementioned problem is absent. The simplest possibility is to treat the quark sector in the same way as the charged lepton sector. This yields the quark mixing matrix $U_{\text{CKM}} = \mathbb{1}$ in leading order, which seems promising. However, it can be shown that higher order corrections cannot give the right mixing matrix in the quark and lepton sector at the same time (see for example [105, 112]). A possible way out is to extend the discrete group, giving us the possibility to treat the quark and lepton sectors differently. A promising candidate in this context is the binary tetrahedral group T', which

is the double cover of A_4. Apart from the 1, $1'$, $1''$ and 3 representations T' also has three doublet representations. Treating the lepton sector in the same way as in the usual A_4 model and making use of the three additional doublet representations in the quark sector yields a viable model (to be more precise, the first and second quarks generation are treated as a doublet under T' whereas the top quark is uncharged). Note that this assignment is indeed not compatible within a GUT context, as there are fermions and quarks of the same generation that arise from the same GUT multiplets and would therefore have to lie in the same A_4 representation. We refer to [113] and references in [63] for further details on such models.

Chapter 5

Phenomenology of the combined 2S2T and ν2HDM model

Since an exact $G_S \times A_2 3$ symmetry in the neutrino sector and an exact G_T symmetry in the charged lepton sector would lead to (now experimentally excluded) TBM mixing, it is necessary to take deviations into account. Following the discussion of the previous chapter, we will consider three different sources of deviations from the tribimaximal mixing form, namely (i) relaxing the condition $a' = 0$ (i.e. allowing for the antisymmetric coupling), (ii) relaxing the condition $c = d$ (i.e. allowing the singlet vevs to differ from each other) and (iii) allowing the vevs of the two A_4 triplets to deviate from the aligned form we required in the previous chapter. To begin with we will consider each deviation separately and show that compatibility with the measured leptonic mixing angles, in particular with the rather large value of θ_{13} indicated by recent experiments, can be ensured.

In appendix F we analyse deviations of the types (i) and (ii) for the case of real parameters analytically. An analytic derivation of the mixing matrix is only possible when restricting to the case of aligned triplet vevs and real parameters. However the Yukawa couplings are expected to be complex in general. We will therefore focus more extensively on a numerical approach, which allows us to treat also the complex case and to take deviations of type (iii) into account. The numerical analysis will be performed by varying the various parameters appearing in the mass matrices and checking for compatibility of the predicted mixing parameters and masses with the experimental data.

Furthermore there is in principle no reason to expect any one of the abovementioned deviations to vanish exactly. For example, there is no underlying symmetry which enforces the singlet vevs to be equal, and the antisymmetric coupling need not vanish in the case of Dirac neutrinos. Although we have argued that the alignment of the triplet vevs at leading order can be engineered in specific setups such as the extradimensional model considered in section 4.5, even then we expect higher order corrections to break the exact alignment. Therefore we will consider the general case and allow all three sources of deviations in section 5.2. Finally,

we will use the values of the mixing angles and neutrino masses obtained from the numerical analysis to investigate the predictions for the Higgs phenomenology discussed in chapter 3.5 that arise in a combined A_4 and ν2HDM model.

5.1 Three ways to break $G_S \times A_{23}$

We will perform a brief analysis of the predicted mixing angles in the case where only one of the three different deviations mentioned above is turned on. The numerical data is evaluated with the use of a Fortran program using the LAPACK routine in order to diagonalise $M^\nu M^{\nu\,\dagger}$ and $M^\ell M^{\ell\,\dagger}$ respectively, which allows us to extract the lepton masses as well as the leptonic mixing angles and the Dirac phase as defined by the standard parametrisation of the mixing matrix. We allowed the parameters appearing in the mass matrices to vary uniformly over appropriate regions, and selected only data points leading to neutrino oscillation parameters compatible with the 3σ ranges given in table 2.3. The parameter regions were chosen in this manner to provide the best possible compromise between computing time and the extend of the parameter regions.

The separate deviations are parametrised as follows. We write

$$a' = a\eta\,, \qquad d = c(1+\epsilon) \tag{5.1}$$

for the antisymmetric coupling and the two singlet couplings, respectively, as well as

$$\langle\phi_S\rangle = v_S(1+\epsilon_{S,1}, 1+\epsilon_{S,2}, 1)\,, \qquad \langle\phi_T\rangle = v_T(1, \epsilon_{T,1}, \epsilon_{T,2}) \tag{5.2}$$

for the vev misalignment of the two triplets. Let us emphasise that the lepton mass matrix (4.18) is no longer diagonal once $\epsilon_{T,i} \neq 0$. This must of course be taken into account when deriving the mixing matrix (see (2.11)). In the numerical analysis we allow η and ϵ to take values up to order one, which is a reasonable assumption as the strengths of the two singlet flavon couplings and the symmetric resp. antisymmetric triplet couplings are naturally expected to have comparable magnitude. We expect that some mechanism should be present that leads to exact alignment of the triplet vevs at leading order, for example one of the possibilities discussed in sections 4.4 and 4.5. As the deviations from the aligned form should thus arise from some higher order corrections, we expect the deviations to be generically suppressed by a power of v/Λ in comparison with the leading order form of the triplet vevs. The precise suppression will of course depend on the details of the model under consideration. An estimate for the size of the expected generic suppression by v/Λ was given in (4.53).

Rather than trying to find a more precise estimate for the expected magnitude of the deviations in a specific model, such as the model considered in section 4.5, we will instead be more general for the purpose of the numerical analysis and allow $\epsilon_{S,i} \lesssim 1$. Nevertheless, for $\epsilon_{T,i}$ we take the smaller regions $\epsilon_{T,i} \lesssim 0.005$, for the following reason. Allowing larger $\epsilon_{T,i}$ would lead to correspondingly large shifts

of the predicted masses of the charged leptons, if the corresponding Yukawa couplings were held fixed. To be compatible with the measured charged lepton masses we would thus have to accordingly shift these Yukawa couplings by a significant amount. However, this shift is difficult to take into account numerically, because the masses have been measured with very high accuracy. It is then extremely unlikely to hit exactly the right values for the Yukawa couplings to be within the experimental bounds when varying the parameters randomly over large regions. For this reason, we will not require compatibility with the measured charged lepton masses as part of our numerical analysis, and will instead simply argue that this could in principle be achieved by a suitable shift of the Yukawa couplings. Note that such a rescaling does not impact on the predictions for the mixing matrix, as it corresponds to rescaling entire columns of the charged lepton mass matrix. However, we do not want the necessary shifts of the Yukawa couplings to become unnaturally large, so to avoid this problem we will take the smaller regions for $\epsilon_{T,i}$ as mentioned above. Finally, we would like to point out that the chosen size of $\epsilon_{T,i}$ is large enough that the considered vev misalignment automatically takes into account the NLO corrections to the charged lepton mass matrix that we found in the extradimensional model, see discussion around equation (4.66).

For the sake of completeness, we list the regions over which the parameters were allowed to randomly vary in our numerical search in appendix G.1. The appendix also contains scatter plots of the parameter regions that were found by the numerical analysis to be compatible with the experimental results. Note that these plots show that naturalness arguments favour allowing for complex parameters rather than restricting to the real case.

In appendix G.2 we have given the predicted ranges for the lightest neutrino mass which were obtained in the different cases. For the convenience of the reader we also show the related parameters m_β and $\sum m_\nu$ which are relevant for discussions of Tritium beta decay experiments and CMB measurements, and were defined in chapter 2. Of course, all predicted neutrino masses are compatible with the 3σ ranges of the neutrino mass differences given in table 2.3, as this was imposed as a requirement in our numerical analysis. Note that the predicted values of m_β and $\sum m_\nu$ are below the current experimental bounds given 2.5. In fact, the predicted values of m_β are even below the planned sensitivity of the upcoming KATRIN experiment, and only come close to this planned upper limit for the case of $c \neq d$. Let us also point out that table G.5 shows that the lightest neutrino mass can be much smaller (around two orders of magnitude) in the case of inverted hierarchy compared to the case of normal hierarchy, which may hint at the presence of a sum rule in the inverted case.

Let us now come to the main objective of this section, i.e. to analyse how the different deviations affect the various leptonic mixing angles, and in particular if they can account for the experimentally verified non-vanishing of θ_{13}. By imposing compatibility with the 3σ ranges in table 2.3 and randomly varying the parameters of the model, we indeed find that each type of deviation can lead to experimentally

acceptable values of the mixing angles for suitable parameter choices. Figure 5.1 shows the distribution of the predicted mixing angles in the $\sin^2\theta_{12} - \sin^2\theta_{23} - \sin^2\theta_{13}$ space for each of the three cases under consideration. In particular the predictions for the case of real parameters have been explicitly highlighted in these plots. For $\eta \neq 0$ and $\epsilon \neq 0$ our numerical analysis suggests a direct relation between the different mixing angles when restricting to real parameters. This is also confirmed by the analytical computation of the mixing angles performed in appendix F, where these cases were discussed in more detail. Recall that such a computation was only possible for these two cases.

Returning now to the general complex case, we find that the effects of the antisymmetric coupling parametrised by η are broadly similar to the effects of the deviation of the singlet couplings parametrised by ϵ. However, they are not identical, for example in the case of normal hierarchy the predicted value of $\sin^2\theta_{13}$ grows much faster as a function of η than as a function of ϵ. Figure 5.1 shows that it is much harder to achieve the large values of $\sin^2\theta_{13} \sim 0.022$ suggested by the most recent measurements by using only triplet vev misalignment, compared to the other two types of deviations. Let us also point out that we cannot achieve compatibility with the experimental data if we consider switching on only $\epsilon_{S,1}$ while leaving all other triplet vev misalignment parameters at zero. This is because $\epsilon_{S,1}$ does not break the $\mu\tau$ symmetry which forces $\sin^2\theta_{13}$ to vanish.

However, while it seems less suited to generating large $\sin^2\theta_{13}$, the triplet vev misalignment can play an important role in a different context. Namely, we find that switching on only $\eta \neq 0$ or $\epsilon \neq 0$ will always lead to an upward shift of $\sin^2\theta_{12}$ compared to the TBM value. As the TBM prediction for $\sin^2\theta_{12}$ is already above the current best fit value as shown in table 2.3, this may become problematic if the bounds on θ_{12} are improved in the future. Taking the triplet vev misalignment into account can thus be important as this is the only one of the considered deviations that can shift the predicted value of $\sin^2\theta_{12}$ downwards. On the other hand, also values of $\sin^2\theta_{12}$ that are close to the current upper 3σ limit can only be achieved in the presence of triplet vev misalignment.

In appendix G.3 we have plotted the predicted values of the Jarlskog variable defined in equation (2.21), which is a measure of the predicted CP violation. The region shaded in light grey shows the values of $J_{\rm CP}$ that are in principle possible given the measured 3σ regions of the mixing angles listed in table 2.3. We see that for small values of θ_{13}, the predicted values in our model cover the full possible range for $J_{\rm CP}$ for each of the three types of deviations considered here. This is because the Dirac phase δ is hardly restricted and can vary freely. For larger values of θ_{13} we find that in the cases $a' \neq 0$ and $c \neq d$ no values of $J_{\rm CP}$ close to zero are found. In other words, for $a' \neq 0$ or $c \neq d$ a large $\sin^2\theta_{13}$ automatically implies a relatively large magnitude of CP violation. This is not the case if we switch on only the triplet vev misalignment. Here the predicted values of $|J_{\rm CP}|$ no longer reach the maximal possible values for larger θ_{13}. In particular, our figures suggest that it is possible to keep CP violation small even for large θ_{13}, particularly in

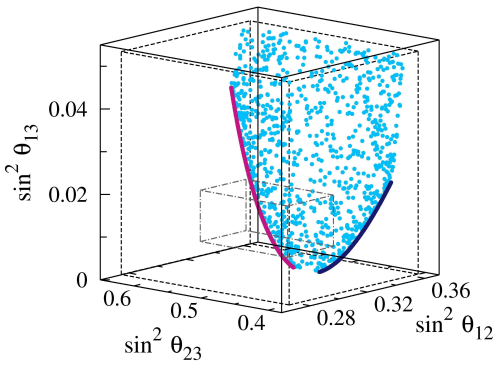

(a) $a' = a\eta$. Normal hierarchy.

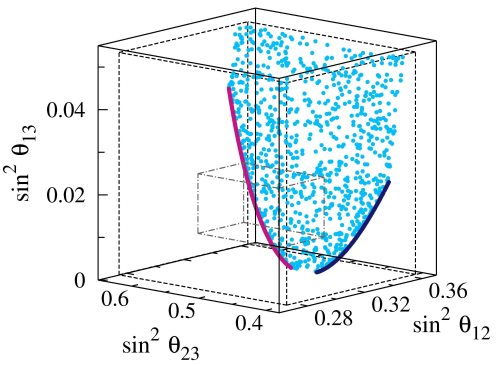

(b) $a' = a\eta$. Inverted hierarchy.

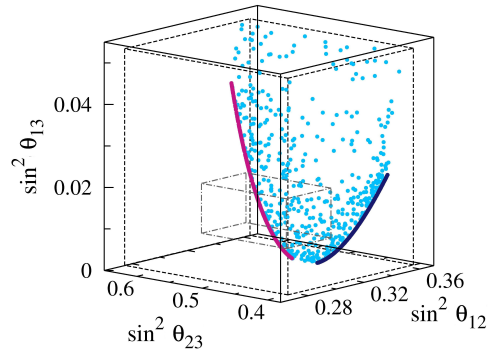

(c) $d = c(1+\epsilon)$. Normal hierarchy.

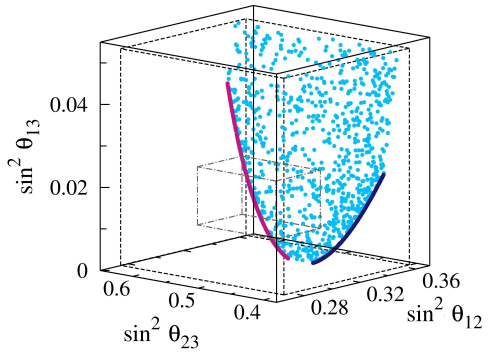

(d) $d = c(1+\epsilon)$. Inverted hierarchy.

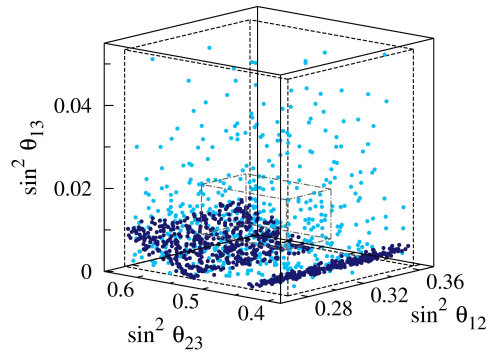

(e) $\langle\varphi_S\rangle = v_S(1+\epsilon_{S,1}, 1+\epsilon_{S,2}, 1)$ and $\langle\varphi_T\rangle = v_T(1, \epsilon_{T,1}, \epsilon_{T,2})$. Normal hierarchy.

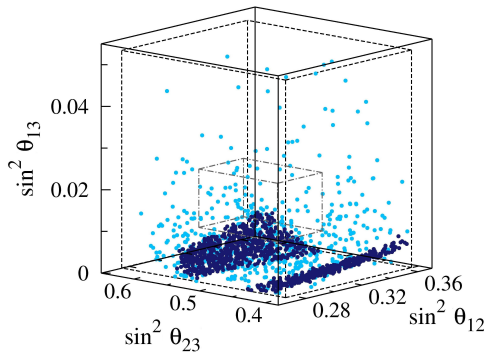

(f) $\langle\varphi_S\rangle = v_S(1+\epsilon_{S,1}, 1+\epsilon_{S,2}, 1)$ and $\langle\varphi_T\rangle = v_T(1, \epsilon_{T,1}, \epsilon_{T,2})$. Inverted hierarchy.

Figure 5.1: Behaviour of $\sin^2\theta_{ij}$ for the three different deviations. The predictions for the case where we restricted ourselves to real parameters are highlighted in dark blue, while points corresponding to ϵ, $\eta < 0$ were additionally highlighted in purple. The 3σ and 1σ regions of $\sin^2\theta_{ij}$, as given in table 2.3, are marked by dashed and dash-dotted boxes respectively.

the case of normal hierarchy. However, as the discussion above suggests that it is advantageous to allow for all three possible deviations from the TBM form, we will not go into further detail here. Instead we postpone a discussion e.g. of the impact of the new bound on $\sin^2\theta_{13}$ to the next section covering the numerical analysis of the general case.

5.2 Combining deviations: Relaxing $a' = 0$, $c = d$ and the triplet vev alignment

Having previously discussed different possibilities to break the $A_4 \times A_{23}$ symmetry, let us now investigate what happens when all the deviations from the TBM case are simultaneously switched on. We perform a numerical analysis in a similar manner as before, allowing the various parameters to vary randomly over the regions given in appendix G.1 and selecting parameter combinations leading to mixing angles and neutrino masses that are compatible with the experimental results. Scatter plots of the points in parameter space selected in this manner are shown in the appendix in figures G.3 and G.4 for both normal and inverted mass ordering. In general the parameter regions that were found to be compatible with the measured data are similar to those that were found in the cases where only one deviation was switched on (compare appendix G.1). However, the enhanced combination probabilities in the general case lead to slightly broader allowed regions.

Figure (5.2) shows the predicted values of the Jarlskog variable, while the region

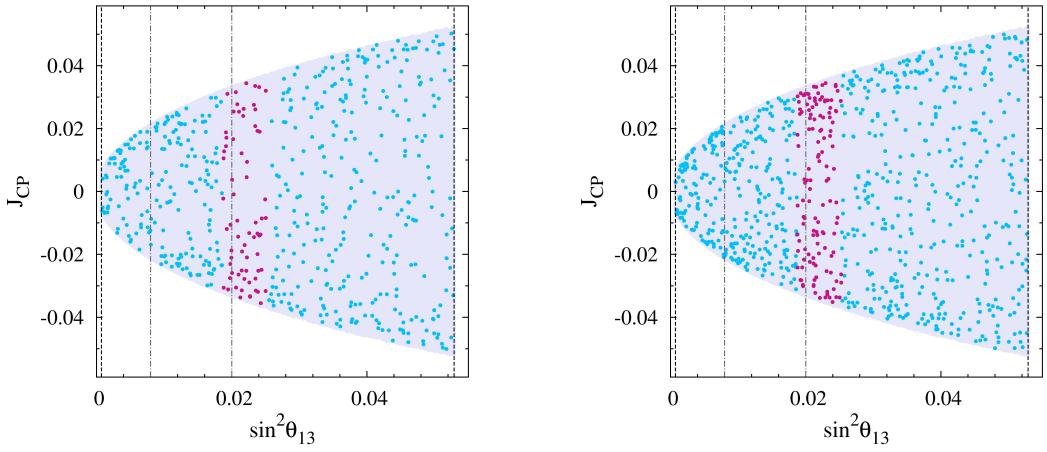

(a) Normal hierarchy.

(b) Inverse hierarchy.

Figure 5.2: Predicted magnitude of CP violation, parametrised by the Jarlskog variable J_{CP}, as a function of $\sin\theta_{13}$. The experimental 3σ and 1σ regions of $\sin^2(\theta_{13})$ are marked by dashed resp. dash-dotted lines. Purple points are compatible with the more stringent bound $\sin^2\theta_{13} = 0.022^{+0.0033}_{-0.0030}$ [44].

that is in principle possible given the bounds on $\sin\delta$, $\sin^2\theta_{12}$, $\sin^2\theta_{23}$ and the considered magnitude of $\sin^2\theta_{13}$ is shaded in light grey. We see that the full range of available values can be reached by suitable parameter combinations in the 2S2T model. This originates from two facts. Firstly, the CP-violating phase δ exhibits no correlation with $\sin^2\theta_{13}$, and can vary freely within $[0, 2\pi]$. Secondly, the magnitudes of the various mixing angles can take on nearly the full range of available values independently of each other, as suggested by figure (5.3). This is a result of the large number of possibilities of combining the effects, discussed in section (5.1), which are induced by each individual deviation. In particular this implies that the model can be made CP conserving for suitable parameter choices, even at large values of $\sin^2\theta_{13}$.

The ranges in which the lightest neutrino masses are predicted to lie are given in appendix G.2. Furthermore figure 5.4 shows the predictions for the neutrino mass observables m_β and $\sum m_\nu$, which are more directly accessible to experiments. Due to the smallness of the predicted neutrino masses the bounds on these observables as given in section 2.5 are automatically fulfilled. Note that even the sensitivity of the currently running KATRIN experiment would be insufficient to detect neutrino masses that are as small as those predicted in our model. Hence any improved upper bound that could be imposed by this experiment would also be fulfilled by our model. Conversely, if KATRIN does succeed in measuring a value of m_β then this value would automatically lie above the maximal value that we obtained in our numerical analysis. However, our analysis of the single deviations showed that larger masses close to the KATRIN reach should in principle be possible if

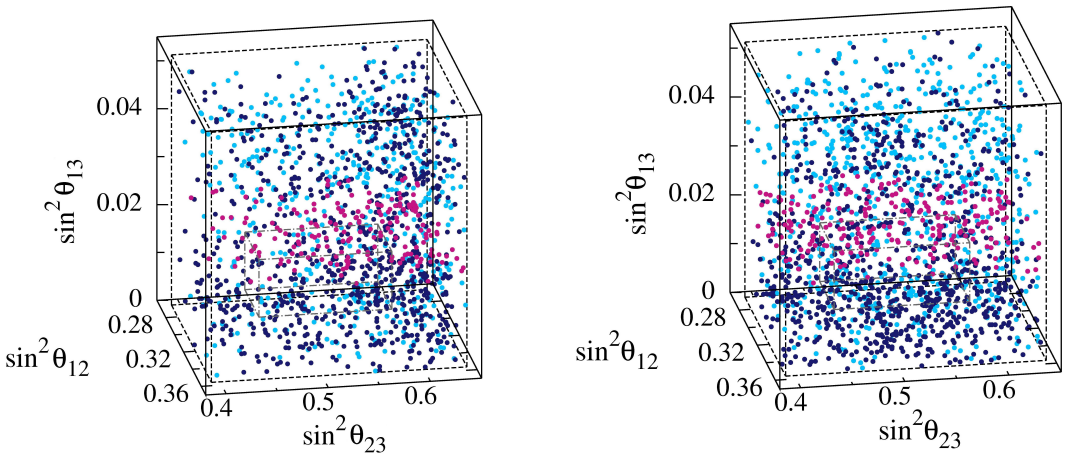

(a) Normal hierarchy.

(b) Inverse hierarchy.

Figure 5.3: Predicted behaviour of the leptonic mixing angles $\sin^2\theta_{ij}$. Dark blue points correspond to real parameter values. The experimental 3σ and 1σ regions are marked by dashed and dash-dotted lines, respectively. Once again, purple points are compatible with the more stringent new bound $\sin^2\theta_{13} = 0.022^{+0.0033}_{-0.0030}$ [44].

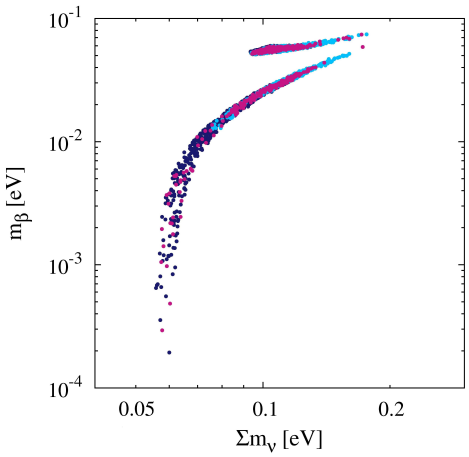

Figure 5.4: Prediction of the neutrino mass observables m_β and $\sum m_\nu$. The upper part of the plot corresponds to the case of inverted mass ordering, while the lower part belongs to normal mass ordering. The colour coding has been explained in the previous figures.

one allows for a sizeable deviation ϵ, while keeping the other deviation parameters small. A numerical analysis with higher statistics and allowing for larger ϵ would be needed to give a more precise statement on the upper limit of masses that can be obtained in our model. However, recall from the previous section that a smaller measured value of θ_{12} would require a non-negligible vev misalignment, which our numerical analysis suggests will lead to smaller masses. A more detailed discussion must therefore be postponed until more precise measurements of the mixing angles, especially θ_{12}, are available.

Note that in the various scatter plots we have highlighted in purple any points that are compatible with the recently announced new bounds on θ_{13}, given by $\sin^2\theta_{13} = 0.022^{+0.0033}_{-0.0030}$ [44]. The plots suggest that the restriction of $\sin^2\theta_{13}$ to the smaller region has no major effect on the predictions for the other observables. However, more statistics would be desirable in order to conclusively prove this statement.

5.3 Higgs phenomenology in an A_4 − symmetric ν2HDM

In this section we will analyse how the introduction of the A_4 symmetry impacts on the predictions of neutrinophilic two Higgs doublet model. In particular, we will study how the predicted values of the leptonic mixing angles and neutrino masses affect the various Higgs observables considered in section 3.5. Of course, only processes in which leptons are involved will be affected. For the predictions of the

neutrino masses and mixing angles we will use the results of the general numerical analysis discussed in the previous section, in which we allowed for different flavon singlet vevs, a non-zero antisymmetric coupling and for triplet vev misalignment. Throughout this section we will take the experimental best fit values for the charged lepton masses, as these masses were not included in our numerical analysis (see also the discussion in section (5.1)). We will also consider how our predictions are affected by the recently announced results of the newest $\sin^2\theta_{13}$ measurements. In the various plots given in this section, the regions that are accessible by varying the neutrino oscillation parameters freely within their 3σ ranges given in table 2.3 will be shaded in light grey.

A combined discussion of the significance of the various effects considered in this section will be given in the conclusions in chapter 6.

5.3.1 Leptonic decays of the charged Higgs

Let us first consider the possible decays of the charged Higgs particles to leptons. The branching ratios $BR(H^+ \to \ell^+\nu) = \Gamma(H^+ \to \ell^+\nu)/\sum_{\ell=e,\mu,\tau}\Gamma(H^+ \to \ell^+\nu)$ in the neutrinophilic two Higgs doublet model were evaluated in section 3.5.1. For the convenience of the reader we recall the resulting expression given in (3.50)

$$BR(H^+ \to \ell^+\nu) = \frac{\sum_j m_{\nu_j}^2 |U_{\ell j}|^2}{\sum_{\ell=e,\mu,\tau}\sum_j m_{\nu_j}^2 |U_{\ell j}|^2}\,. \tag{5.3}$$

Figure 5.5 shows the predicted values after the model is supplemented with an A_4 flavour symmetry, specifically the 2S2T model that we have discussed extensively. The first thing to note is that our analysis of the A_4 symmetric model only predicted values of the lightest neutrino masses that are significantly smaller than the bound obtained from CMB measurements. This for example impacts on the branching ratio $BR(H^+ \to e^+\nu)$ in the case of normal mass ordering, where a value of about 0.3 would be possible in a general ν2HDM, which at first sight seems to be excluded by our numerical analysis. However, as discussed in the previous section, we expect larger masses to be in principle attainable in our model. Before concluding that the combined $A_4 - \nu$2HDM can be distinguished from a general ν2HDM by an observation of these processes, an analysis with much higher statistics would therefore be required. In particular such an analysis would be needed to quantify possible correlations between the mixing angles for larger values of the lightest neutrino mass.

Recall that we found no correlation between the different mixing angles in the flavour symmetric model, either in the complex or in the real case (see figure 5.3). However, we observe a correlation between the lightest neutrino mass and the mixing angles for very small neutrino masses, which is particularly visible when restricting to real parameters. This explains why for small neutrino masses the branching ratios in figure 5.5 cover only a small part of the region that would be allowed in principle.

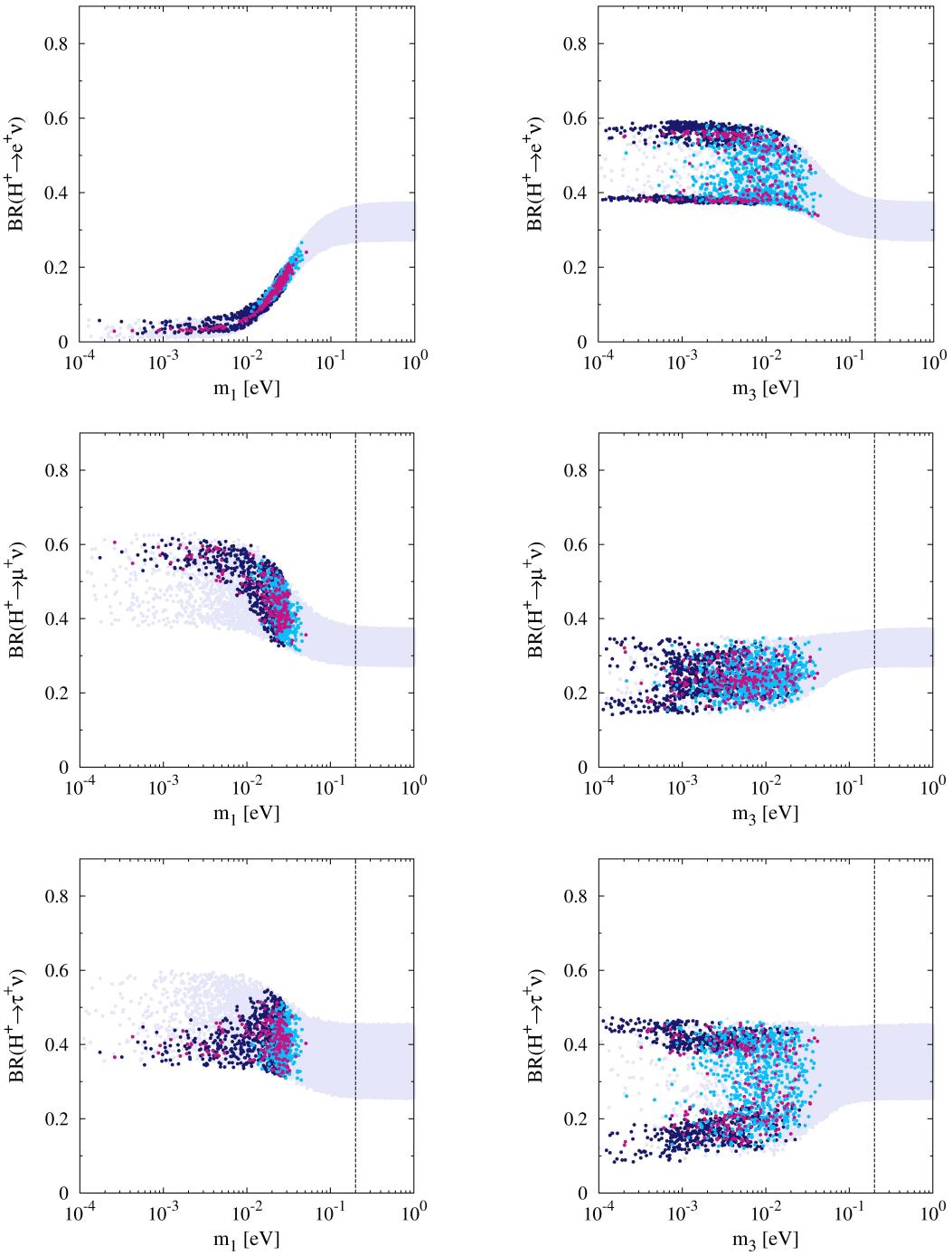

Figure 5.5: Branching ratios of leptonic decays of the charged Higgs. The predicted values in the combined model are given by light blue points for complex parameters and dark blue points for real parameters. Points compatible with the new bound on $\sin^2\theta_{13} = 0.022^{+0.0033}_{-0.0030}$ [44] are highlighted in purple. The left column shows the results for normal, the right column for inverted mass ordering. The dashed line marks the upper bound on the lightest neutrino mass given by the CMB measurement (see section 2.5).

Furthermore we note that for the case of inverted hierarchy and real mass matrix parameters, the predicted values of the branching ratios exhibit a clear split into two separate regions. This split is a result of the fact that in the real case we have only two possibilities for the Dirac phase δ, namely $e^{-i\delta} = \pm 1$. To understand why this effect does not show up for normal mass ordering, let us recall equation (3.51), where we have rewritten the sums that occur in the branching ratio in terms of the lightest neutrino mass and the neutrino mass differences. Taking into account $\Delta m^2_{21} \ll \Delta m^2_{31}$ we can approximate

$$\begin{aligned} \sum_i m^2_{\nu,i}|U_{\ell,i}|^2 &= m_1^2 + \Delta m^2_{21}|U_{\ell 2}|^2 + \Delta m^2_{31}|U_{\ell 3}|^2 \\ &\simeq m_1^2 + \Delta m^2_{31}|U_{\ell 3}|^2\,, \end{aligned} \tag{5.4}$$

$$\begin{aligned} \sum_i m^2_{\nu,i}|U_{\ell,i}|^2 &= m_3^2 - \Delta m^2_{31}|U_{\ell 1}|^2 + (\Delta m^2_{21} - \Delta m^2_{31})|U_{\ell 2}|^2 \\ &\simeq m_3^2 - \Delta m^2_{31}(|U_{\ell 1}|^2 + |U_{\ell 2}|^2)\,. \end{aligned} \tag{5.5}$$

Equations (5.4) and (5.5) apply to the cases of normal and inverted mass ordering, respectively. Now from the standard parametrisation of the mixing matrix (2.19) we immediately see that $|U_{\ell 3}|$ is independent of the Dirac phase for any ℓ, so that the dependence of the branching ratios on δ is negligible in the case of normal mass ordering. However, this is not true for $|U_{\ell 1}|$ or $|U_{\ell 2}|$ with $\ell = \mu,\ \tau$. For example we have

$$|U_{\mu 1}| = \left|\sin\theta_{12}\cos\theta_{23} + \cos\theta_{12}\sin\theta_{23}\sin\theta_{13}e^{i\delta}\right|, \tag{5.6}$$

such that the Dirac phase δ does not drop out. This leads to the observed split in the inverted case. Note that these entries of the mixing matrix enter into the denominator in (5.3) for the case of inverse hierarchy, explaining why we observe the split also for the branching ratio $BR(H^+ \to e^+\nu)$. Furthermore, equations (5.4) and (5.5) show that the exact values of the mixing angles (and the Dirac phase) are only important if the lightest neutrino masses is of the order of or smaller than Δm^2_{31}, which can also be seen in the given figures.

Finally, let us point out that restricting $\sin^2\theta_{13}$ to the narrower region suggested by the recent measurements only influences the branching ratio of $H^\pm \to e^\pm\nu$ for normal hierarchy, as here the main contribution to the nominator in the branching ratio is proportional to $\sin^2\theta_{13}\Delta m^2_{31}$ (compare equation (5.4)).

5.3.2 Charged lepton flavour violation

Let us now turn our attention to processes violating charged lepton flavour violation. As was discussed in section 3.5.3, the most promising candidates to observe cLFV experimentally are processes of the form $f_1 \to f_2\gamma$, which are mainly induced by $H^\pm$ loops in the ν2HDM. We will place particular emphasis on the process $\mu \to e\gamma$, which is the most important of these processes. In

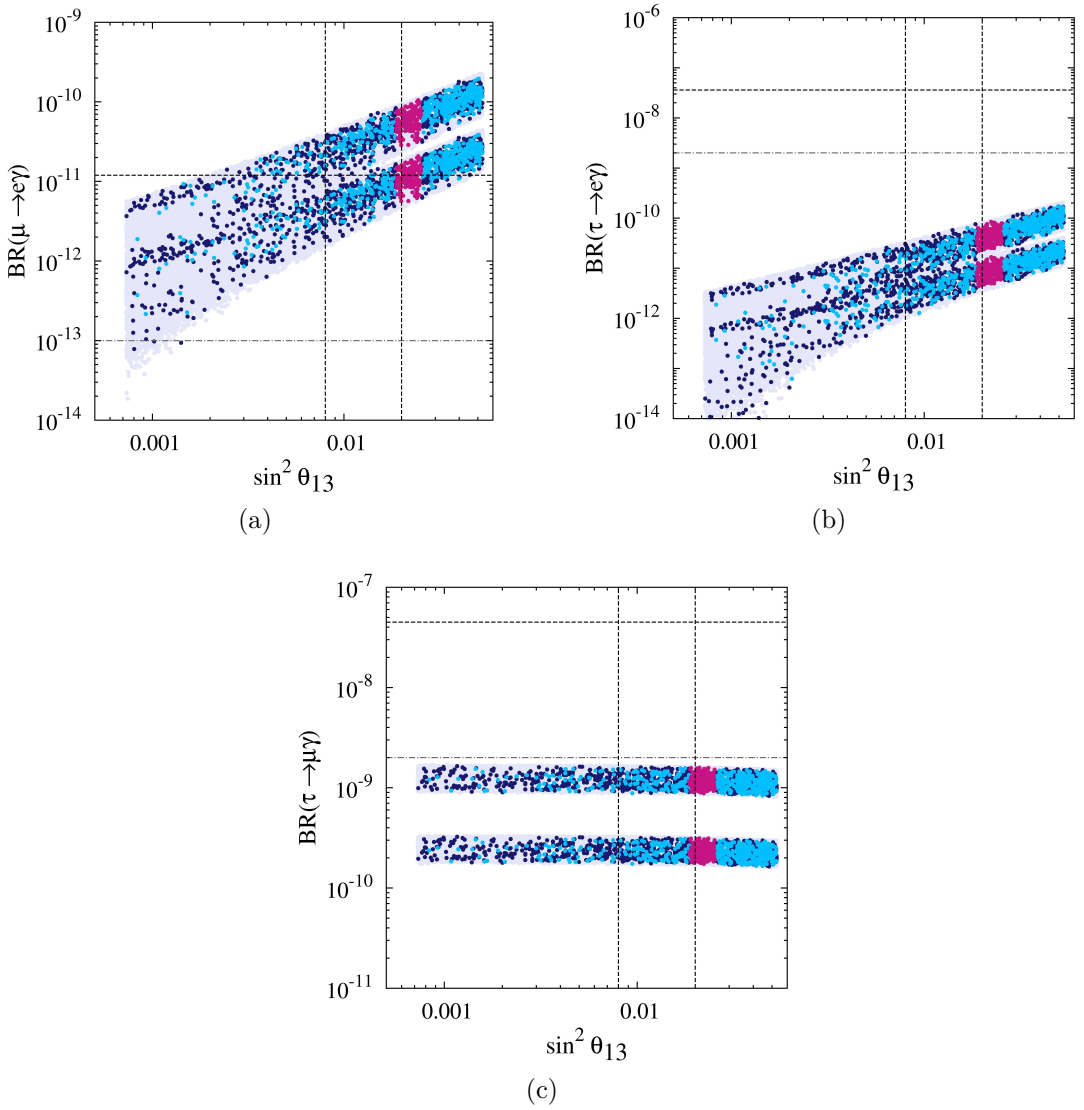

Figure 5.6: Behaviour of BR($f_1 \to f_2\gamma$) as a function of $\sin^2\theta_{13}$ in the 3σ region of $\sin^2\theta_{13}$ for $m_{H^\pm}v_1 = 100$ GeV $\times$ eV (upper part of the plot) and for $m_{H^\pm}v_1 = 150$ GeV $\times$ eV (lower part of the plot) in the case of normal hierarchy. The predictions of the combined model are marked by light blue (complex parameters) and dark blue (real parameters) points, respectively. In addition we have marked points which are compatible with the restricted $\sin^2\theta_{13}$ region of equation (2.27) in purple. The current 1σ bound for $\sin^2\theta_{13}$ and the experimental upper bounds for the processes are described by the dashed lines. The experimental sensitivity aimed at in future experiments is marked by the dash-dotted lines. The various bounds can be found in tables 2.3 and 3.4.

equations (3.72) and (3.78) we derived that the branching ratio for this process is independent of the absolute neutrino mass scale and depends only on the neutrino mass squared differences and the leptonic mixing angles. As discussed in the previous section 5.2, the predicted mass squared differences and the mixing angles are nearly uncorrelated in the A_4 symmetric model. Hence we expect that the ν2HDM predictions are nearly unchanged in the combined flavour symmetric model. This is shown in the corresponding scatter plot, figure 5.6, where normal neutrino mass ordering is assumed. As was already observed in the discussion in subsection 3.5.3, the behaviour of the branching ratio is nearly the same for inverted hierarchy. Therefore we again refrain from showing the corresponding scatter plots.

The fact that the range of possible branching ratios that can be obtained in our combined model is not smaller than in a general ν2HDM implies that we can carry over the results of subsection 3.5.3. Therefore, the observation that the bound on $BR(\mu \to e\gamma)$ together with the new measurement $\sin^2\theta_{13} = 0.022^{+0.0033}_{-0.0030}$ [44] could be used to derive an upper bound of $m_{H^\pm} v_1 \gtrsim 118$ GeV $\times$ eV is unchanged in the flavour symmetric ν2HDM model. In particular, the introduction of the A_4 symmetry does not lead to a more stringent bound on $m_{H^\pm} v_1$. As in section 3.5 we will therefore assume $m_{H^\pm} v_1 \gtrsim 118$ GeV $\times$ eV for the following analysis.

5.3.3 The anomalous magnetic moment of the muon

For the analysis of the charged Higgs contribution to the anomalous magnetic moment of the muon we can directly transfer many of the statements of subsection 5.3.1. As we have seen in section 3.5.4, the contribution of the charged Higgs to the magnetic moment of the muon is is given by

$$a_\mu^{H^\pm} \simeq -\frac{m_\mu^2}{48\pi^2 v_1^2 m_{H^\pm}^2} \sum_{i=1}^{3} |U_{\mu i}|^2 \, m_{\nu,i}^2 \tag{5.7}$$

(see equation (3.90)). From the discussion in subsection 5.3.2, we again expect that the only difference to the case of a general ν2HDM arises in our A_4 model from the restriction a smaller neutrino mass region and from the predicted correlation of the mixing angles with the lightest neutrino mass for very light masses. This expectation is indeed verified by the scatter plots of the predicted contribution to $a_\mu^{H^\pm}$ illustrated in figure (5.7). Note that a splitting of the predicted values into two distinct regions, as observed for the branching ratios of the leptonic Higgs decays in the case of inverted mass ordering (see figure 5.5), is not clearly visible here. However, we note that even in the predictions for the leptonic Higgs decays, this splitting was least pronounced for the decay to a muon, where the numerator in the branching ratio (3.50) contains the same elements of the mixing matrix that are relevant in $a_\mu^{H^\pm}$. In addition, $a_\mu^{H^\pm}$ does not involve the denominator that is present in (3.50), which also contributes to the observed splitting in the leptonic decay branching ratios. Hence the absence of a clearly visible splitting in the predictions for $a_\mu^{H^\pm}$ is not in contradiction with the discussion of section 5.3.1.

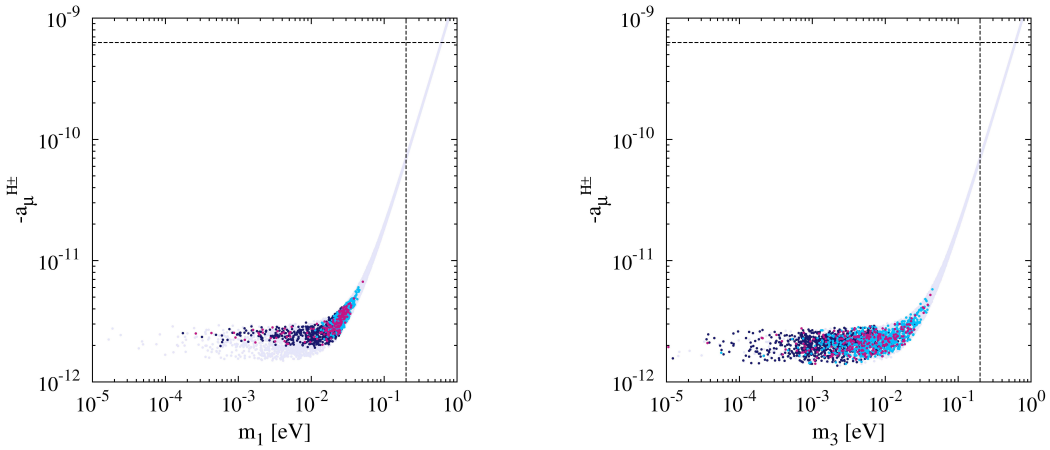

(a) Normal hierarchy.

(b) Inverted hierarchy.

Figure 5.7: Charged Higgs contribution to the muon magnetic moment for $m_{H^\pm} v_1 = 118$ GeV $\times$ eV. Predictions of the combined model are given by the light blue (complex parameters) and dark blue (real parameters) points. Points which are compatible with $\sin^2\theta_{13} = 0.022^{+0.0033}_{-0.0030}$ [44] are highlighted in purple. The WMAP bound on the lightest neutrino mass is given by the dashed line.

Furthermore let us note that restricting to the region for θ_{13} required by the new result $\sin^2\theta_{13} = 0.022^{+0.0033}_{-0.0030}$ [44] has no significant impact on the predictions for $a_\mu^{H^\pm}$.

Recall that in a generic ν2HDM we found that the contribution of the charged Higgs to the magnetic moment is negligible compared to the current and next generation experimental sensitivity, even if one assumes the smallest possible value of $m_{H^\pm} v_1$ which is compatible with the measurements of the branching ratio of $\mu \to e\gamma$ and considers neutrino masses close to the WMAP bound. As the predicted neutrino masses in our combined model lie well below the WMAP bound, leading to even smaller contributions to $a_\mu^{H^\pm}$, no new conclusions are obtained after introducing the A_4 symmetry. Recall however, that we expect larger masses to be in principle possible in the combined model for suitable parameter combination, see discussions above.

5.3.4 Lepton universality

In section 3.5.5 we have discussed that the additional decay channel of the muon and tauon that arises in the presence of the charged Higgs boson leads to a violation of the universality of the effective charged lepton couplings. Let us recall from equations (3.103) and (3.104) that the ratios of the effective charged coupling

constants in a ν2HDM are given by

$$\frac{g_\mu}{g_\tau} \simeq 1 + \frac{1}{16 m_{H^\pm}^4 G_F^2 v_1^4} \sum_i m_{\nu,i}^2 |U_{ei}|^2 \left(\sum_i m_{\nu,i}^2 |U_{\mu i}|^2 - \sum_i m_{\nu,i}^2 |U_{\tau i}|^2 \right), \tag{5.8}$$

$$\frac{g_\mu}{g_e} \simeq 1 + \frac{1}{16 m_{H^\pm}^4 G_F^2 v_1^4} \sum_i m_{\nu,i}^2 |U_{\tau i}|^2 \left(\sum_i m_{\nu,i}^2 |U_{\mu i}|^2 - \sum_i m_{\nu,i}^2 |U_{ei}|^2 \right). \tag{5.9}$$

The results of the numerical analysis for these ratios in the combined flavour symmetric model are given in figure (5.8), where we again assumed that $m_{H^\pm} v_1$

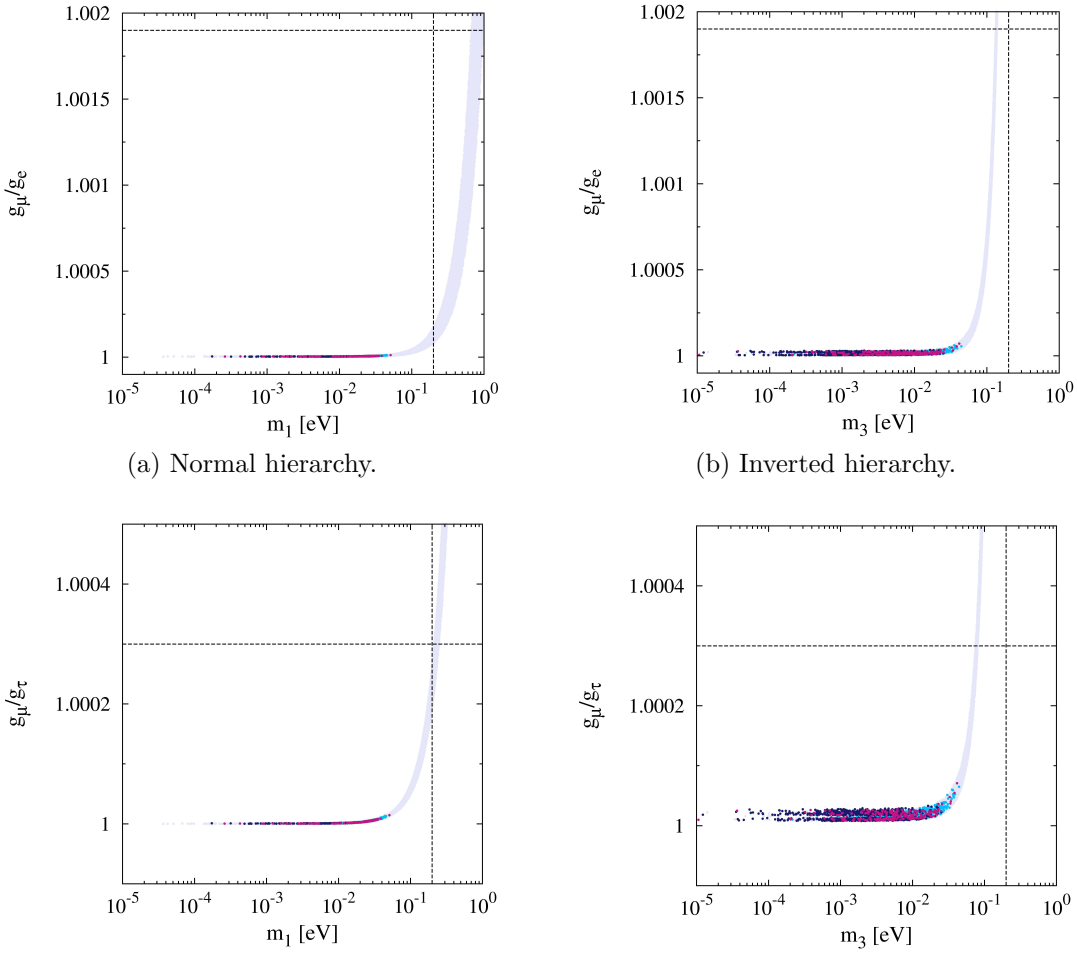

(a) Normal hierarchy.

(b) Inverted hierarchy.

(c) Normal hierarchy.

(d) Inverted hierarchy.

Figure 5.8: Violation of lepton universality: ratios of the effective charged current couplings for $m_{H^\pm} v_1 = 118$ GeV × eV. The predictions of the combined model are given by light blue (complex parameters) respectively dark blue (real parameters) points, while purple points are compatible with $\sin^2\theta_{13} = 0.022^{+0.0033}_{-0.0030}$ [44]. The current upper bounds on the coupling ratios and on the lightest neutrino mass are marked by the dashed lines.

is given by the smallest value compatible with the measurements of $\mu \to e\gamma$. Note that the possibility to obtain small lightest neutrino masses in the combined $A_4-\nu$2HDM ensures compatibility with the experimental bounds given in (3.105), even for the smallest value of $m_{H^\pm} v_1$ compatible with the bound from the process $\mu \to e\gamma$. In other words, we can always find neutrino masses that are small enough to lie in the blue shaded region in figure 3.14. Once again, this conclusion will not be affected by a restriction to the more stringent bound $\sin^2\theta_{13} = 0.022^{+0.0033}_{-0.0030}$ [44]. Finally, we expect that the splitting observed in the case of real parameters and inverted hierarchy can be explained in a similar way as in subsection 5.3.1.

Chapter 6

Summary and conclusion

In this thesis we have combined two important concepts of neutrino physics with the aim of explaining both the smallness of the neutrino masses and the observed leptonic mixing patterns. Specifically, we introduced a neutrinophilic second Higgs doublet and analysed the effects of combining this with an A_4 flavour symmetry. Our analysis was performed for the case of Dirac neutrinos, for which models with the A_4 symmetry had not been studied previously.

As we have seen, the ν2HDM discussed here provides small neutrino masses in a natural way due to the smallness of the vev of the additionally introduced second Higgs field. The separation of the two Higgs fields to the charged fermion sector and the neutrino sector, respectively, was guaranteed by the introduction of a suitable $U(1)$ symmetry. We allowed for the presence of a soft breaking term of this $U(1)$ symmetry in the Higgs potential, which ensured the absence of a light Higgs scalar so that compatibility with cosmological constraints was achieved. We have shown that in the presence of this soft breaking term the vevs of the two Higgs fields are connected by a seesaw-like relation, where the ordinary SM-Higgs vev suppresses the size of the additional vev. The smallness of the vev of the second Higgs can thus be ensured in a natural manner. The introduction of the $U(1)$ symmetry also automatically forbade Majorana mass terms for the neutrinos, even after taking into account the soft breaking in the Higgs potential. Furthermore, we have shown that a minimum of the Higgs potential with the required properties can be made to be absolutely stable. After deriving the Higgs-Higgs interactions as well as the Higgs-gauge boson and Higgs-fermion interaction terms, we have discussed the phenomenology of the ν2HDM, placing a special emphasis on effects in the lepton sector. We have analysed restrictions on the ν2HDM that can be derived from past experimental measurements. The most important constraints come from the bounds on the process $\mu \to e\gamma$ and on the violation of charged lepton universality. In the first instance we were able to derive a lower bound on the charged Higgs mass times the additional vev $m_{H^\pm} v_1$. This bound is strengthened by the experimental restrictions on violations of lepton universality, unless the neutrino masses lie significantly below the bounds obtained

from measurements of the cosmic microwave background or from Tritium beta decay experiments. However, in all of these processes not only the absolute scale of the lightest neutrino mass but also the specific form of the leptonic mixing matrix play important roles.

The second part of this work therefore deals with the question of how the texture of the leptonic mixing matrix can be explained by a fundamental principle. Our starting point was the A_4 symmetry group, whose impact in this context has been well studied in the past. The main difference compared to previously studied models is that we have considered the case of Dirac neutrinos. This gave rise to an additional possible coupling of the neutrinos, namely the antisymmetric coupling of fields transforming in the triplet representation of A_4. In order to keep the model as simple as possible and to allow for both normal and inverted neutrino mass ordering, we focused our more detailed analysis on an A_4 model including two singlet and two triplet flavons. We began by restricting ourselves to the case of exact TBM mixing. To guarantee this, we initially forbade the antisymmetric coupling, required equal couplings for the two singlets and enforced a specific vev alignment for the two triplets. In the following we discussed how the specific vev alignment could be obtained, and considered in detail a model based on the introduction of an extra spatial dimension in which the required vev alignment could be enforced in a very simple manner. In this context we also analysed the impact of next-to-leading order effects, which lead to deviations of the mixing matrix from the tribimaximal form.

Considering deviations from the tribimaximal mixing form is important in light of the new results confirming that the mixing angle θ_{13} does not vanish. Working in the specific framework of the extradimensional model mentioned above, we showed that NLO effects are suppressed by powers of v/Λ or of $1/\Lambda L$, where v is a generic flavon vev while Λ denotes the cut-off scale of the effective theory and L is the size of the extra spatial dimension. We found that the NLO corrections to the neutrino mass matrix do not lead to deviations from TBM mixing and only provide corrections suppressed by v^2/Λ^2 to the neutrino masses. The strongest NLO corrections to the charged lepton mass matrix were found to be of a form that we could take into account by allowing for a suitable misalignment of the vev of the triplet flavon coupling to the charged leptons. In addition, we also allowed for deviations of the triplet vev alignment in the neutrino sector. In particular, to be more general we allowed for larger misalignments than would have been expected in the discussed extradimensional model, in which we had argued that any deviations from the triplet vev alignment would be strongly suppressed. Furthermore, no fundamental principle is known that enforces either the equal coupling of the singlet flavons or the vanishing of the antisymmetric coupling in the case of Dirac neutrinos. There is thus no reason why a deviation from these requirements should be particularly small. We therefore expect that taking into account a weakening of these requirements is much more important than including the NLO effects on the neutrino mass matrix that only lead to small corrections to the neutrino masses.

We then proceeded to analyse how each of the abovementioned deviations impacts on the resulting mixing matrix and the neutrino masses. An analytic derivation was only possible in two special cases, therefore we focused on a numerical analysis which allowed us to treat all relevant cases. We found that a mixing matrix and neutrino masses that are compatible with all known bounds could be obtained in each case. Our analysis showed that the effects of the antisymmetric coupling, which can only be present in the case of Dirac neutrinos, are broadly similar to those that arise when allowing for different singlet couplings. In particular, we showed that the antisymmetric coupling is not restricted to be small by the experimental results, which implies that it is not unnatural to consider Dirac neutrinos in the context of an A_4 model.

For the most general case, where we allowed for all three deviations mentioned above, we then analysed how the predicted Higgs phenomenology is altered in the combined ν2HDM and A_4 model. We found that such a combined model can be easily made consistent with all relevant current bounds. In particular, we found that the restriction on $m_{H^\pm} v_1$ that was obtained for a generic ν2HDM is not strengthened by the introduction of the A_4 symmetry. Furthermore, the smallness of the neutrino masses that were predicted in our numerical analysis for the general case ensured compatibility with the bounds originating from lepton universality. However, the results of our analysis of the cases where only a single deviation was allowed suggest that larger neutrino masses should in principle be possible in the $A_4 - \nu$2HDM. The extent of our numerical analysis was limited by the available computing time. A more extensive numerical analysis with higher statistics and allowing for larger deviations would be required to investigate this further.

Our analysis suggests that the smallness of the lightest neutrino mass is a result of the presence of sizeable vev misalignments. The more extensive numerical analysis should in particular investigate the relationship between the magnitude of the triplet vev misalignments and the predicted neutrino masses more precisely. If our expectation is confirmed, that large neutrino masses are possible only if the triplet vev misalignment is kept small, this would lead to a correlation between the size of the neutrino masses and the possible values of $\sin^2\theta_{12}$ that could be achieved in the considered model. Such a possible correlation would of course impact not only on the predictions of lepton universality, but also on the predictions for the other considered processes that depended on the value of the smallest neutrino mass, namely the charged Higgs branching ratios into leptons and the contribution to the muon magnetic moment. The latter contribution is anyway predicted to be too small to be observed with current and planned experimental sensitivities both in the $A_4 - \nu$2HDM and a general ν2HDM. Given the current bounds on the mixing angles, also an observation of the charged Higgs branching ratios cannot distinguish between the two models, as we can e.g. achieve neutrino masses close to the WMAP bound by keeping the triplet vev misalignment small. However, a more precise future measurement of $\sin^2\theta_{12}$ could require larger vev misalignments which, as discussed above, could restrict the predicted neutrino masses to

smaller values. In this case, a measurement of the charged Higgs branching ratios could distinguish between the $A_4 - \nu$2HDM and a general ν2HDM. Furthermore, an absolute neutrino mass scale that could possibly be detected by the KATRIN experiment on Tritium beta decay would lead to further restrictions on the parameters of the combined $A_4 - \nu$2HDM, as is clear from the above discussion. From our analysis of the general case, it is unclear whether values of m_β within the KATRIN reach can be achieved in the A_4 model, due to limited statistics. This is of course directly connected to the question discussed above of how large the mass of the lightest neutrino can become in the A_4 model.

Apart from extending the numerical analysis, a different way to go is to consider explicit models, like e.g. the extradimensional model discussed in this thesis, and estimate more precisely the magnitude of the triplet vev misalignments that can appear. In dependence of the size of triplet vev misalignments that is allowed in such a model, future measurements of $\sin^2\theta_{12}$ could then rule out these explicit scenarios.

We expect that experimental results of the next few years will give a clearer indication of the most promising directions for further study. We took into account the recently announced preliminary new results on the reactor mixing angle $\sin^2\theta_{13} = 0.022^{+0.0033}_{-0.0030}$ [44] and showed that this restriction does not significantly alter our conclusions. We expect that measuring $\sin^2\theta_{23}$ with higher accuracy would also not have a strong impact on our predictions, in particular not as strong those that could arise from a new $\sin^2\theta_{12}$ bound. As discussed above, a more precise measurement of $\sin^2\theta_{12}$ is needed in order to decide whether models based on the A_4 symmetry, like the $A_4 - \nu$2HDM considered here, are promising candidates to explain the observed flavour structures and neutrino masses. We also expect that the restrictions on the phenomenology of an additional Higgs doublet, even in the absence of an A_4 symmetry, will be strengthened in the coming years due to the current LHC searches and other planned experiments mentioned above. For example, further investigations of the charged lepton flavour violating process $\mu \to e\gamma$ will give rise to more stringent bounds on $m_{H^\pm} v_1$. Note that if the charged Higgs is detected e.g. at the LHC, the observation of the processes $H^\pm \to \ell^\pm \nu$ may enable us to distinguish between normal and inverted hierarchy.

From a more theoretical point of view, a more detailed understanding of the fundamental origin of the A_4 symmetry would certainly be desirable. In particular, it would be interesting to see whether an underlying theory could be found that naturally gives rise to the A_4 symmetry in the lepton sector while also explaining the observed mixing patterns in the quark sector.

Appendix A

The Higgs sector in the Standard Model

The kinetic and potential terms of the Higgs field in the the Standard Model Lagrangian are given by

$$\mathcal{L}_{\text{scalar}} = (D_\mu \Phi)^\dagger D^\mu \Phi - \lambda(\Phi^\dagger \Phi)^2 + \mu^2 \Phi^\dagger \Phi \tag{A.1}$$

with

$$D_\mu \Phi = \left(\partial_\mu - \frac{ig_1}{2} B_\mu - \frac{ig_2}{2} W_\mu\right) \Phi. \tag{A.2}$$

Here g_1 and g_2 are the coupling constants of $U(1)_{\text{Y}}$ and $SU(2)_{\text{L}}$. Note that the Higgs field carries no colour charge and so no coupling to the gluon fields G_μ appears in the covariant derivative.

After the Higgs field acquires a vev v we can expand the field Φ around this value. In unitary gauge this expansion takes the form

$$\Phi = \frac{1}{\sqrt{2}} \begin{pmatrix} 0 \\ v + \varphi \end{pmatrix}, \tag{A.3}$$

where φ is a real scalar field. The vev is related to the parameters of the Higgs potential by $v^2 = \mu^2/\lambda$. Substituting (A.3) into (A.1) and expanding W_μ into the Pauli matrices generating $SU(2)_{\text{L}}$ as $W_\mu = \sum_i W_\mu^i \sigma_i$ one immediately obtains

$$\begin{aligned} \mathcal{L}_{\text{scalar}} &= \frac{1}{2}\partial_\mu \varphi \partial^\mu \varphi + \frac{g_2^2 v^2}{4} W_\mu^- W^{+\mu} + \frac{g_2^2 v}{2} \varphi W_\mu^- W^{+\mu} + \frac{g_2^2}{4} \varphi^2 W_\mu^- W^{+\mu} && \text{(A.4)} \\ &\quad + \frac{(g_1^2 + g_2^2) v^2}{8} Z_\mu Z^\mu + \frac{(g_1^2 + g_2^2) v}{4} \varphi Z_\mu Z^\mu + \frac{g_1^2 + g_2^2}{8} \varphi^2 Z_\mu Z^\mu && \text{(A.5)} \\ &\quad - \lambda v^2 \varphi^2 - \lambda v \varphi^3 - \frac{1}{4} \lambda \varphi^4. && \text{(A.6)} \end{aligned}$$

We have given the equation in terms of the physical vector boson mass eigenstates

$W^{\pm}$ and Z, which are defined by the linear combinations

$$\begin{aligned} W_\mu^+ &= \frac{1}{\sqrt{2}}(W_\mu^1 - iW_\mu^2)\,, & W_\mu^- &= \frac{1}{\sqrt{2}}(W_\mu^1 + iW_\mu^2)\,, \\ Z_\mu &= \frac{g_2 W_\mu^3 - g_1 B_\mu}{\sqrt{g_1^2 + g_2^2}}\,, & A_\mu &= \frac{g_1 W_\mu^3 + g_2 B_\mu}{\sqrt{g_1^2 + g_2^2}}\,. \end{aligned} \tag{A.7}$$

The last two terms can be rewritten in terms of the Weinberg angle θ_W, which is defined by

$$\sin\theta_W = \frac{g_1}{\sqrt{g_1^2 + g_2^2}}\,. \tag{A.8}$$

This leads to

$$Z_\mu = \cos\theta_W W_\mu^3 - \sin\theta_W B_\mu \quad \text{and} \quad A_\mu = \sin\theta_W W_\mu^3 + \cos\theta_W B_\mu. \tag{A.9}$$

One directly reads off the gauge boson masses

$$m_W = \frac{g_2}{2} v \qquad \text{and} \qquad m_Z = \sqrt{\frac{g_1^2 + g_2^2}{8}}\, v\,. \tag{A.10}$$

Further details can be found for example in [23, 114].

Appendix B

Diagonalisation of a general fermion mass matrix

In this appendix we list a number of useful identities that can be used to derive mixing matrices from a fermion mass matrix. In the following, A will denote a general complex 3×3 matrix, so that the identities derived for A can be applied to any mass matrix.

It is clear that the matrix $AA^\dagger$ is always Hermitian, which implies that we can find a unitary matrix U such that

$$U^\dagger A A^\dagger U =: D^2 \tag{B.1}$$

is diagonal. In particular the entries of D^2 defined in this manner are real and non-negative, justifying the suggestive notation as there exists a well-defined square root $D = +\sqrt{D^2}$. Defining now the Hermitian matrix $H := UDU^\dagger$, one can easily check that $H^2 = AA^\dagger$ and that the matrix $U' := A^\dagger H^{-1}$ is unitary[1]. Defining finally the unitary matrix $V := U'U$ then yields

$$U^\dagger A V = D. \tag{B.2}$$

In other words, A is brought into a diagonal form with all diagonal entries real and non-negative through a bi-unitary transformation. Note that a simple diagonalisation of A via a unitary transformation, if at all possible, would in general not lead to real and non-negative diagonal entries if A itself is not Hermitian.

Let us now consider the special case where the matrix A is symmetric, i.e. $A^{\mathrm{T}} = A$. From (B.2) we find

$$\begin{aligned} AA^* &= UDV^\dagger V D U^\dagger = UD^2U^\dagger, \\ A^*A &= VDU^\dagger U D V^\dagger = VD^2V^\dagger. \end{aligned} \tag{B.3}$$

[1] Of course, in order to be able to invert H we must assume that none of the eigenvalues of $AA^\dagger$ vanishes, but this will always be true in the cases of interest to us.

Complex conjugation of the lower equation shows that $V^* D^2 V^{\mathrm{T}} = AA^* = U D^2 U^\dagger$, i.e. AA^* is diagonalised by both U and V^*. This implies that $U = V^*$ (up to an irrelevant diagonal complex phase matrix). Equation (B.2) therefore simplifies to

$$U^\dagger A U^* = D. \tag{B.4}$$

If we take A to be the lepton or neutrino mass matrix, i.e. $A = M^{\nu,\,\ell}$, the above statements can be used to simplify the derivation of the leptonic mixing matrix, which occurs in the weak interaction Lagrangian after rewriting it in terms of the mass eigenstates. Since we want to interpret the entries of the mass matrices after diagonalisation as physical masses, these entries should be real and non-negative. As we have seen this can be guaranteed by performing a biunitary transformation

$$M^{\nu,\ell}_{\text{diag.}} = (V_{\mathrm{L}}^{\nu,\ell})^\dagger M^{\nu,\ell} V_{\mathrm{R}}^{\nu,\ell} \tag{B.5}$$

of the mass matrices. Since the leptonic mixing matrix is given by

$$U^{\mathrm{PMNS}} = V_{\mathrm{L}}^{\ell\,\dagger} V_{\mathrm{L}}^{\nu}, \tag{B.6}$$

we have to find only the matrices $V_{\mathrm{L}}^{\nu,\ell}$ (and not necessarily $V_{\mathrm{R}}^{\nu,\ell}$) in order to determine U^{PMNS}. As we have seen in (B.1), $V_{\mathrm{L}}^{\nu,\ell}$ can be easily obtained by diagonalising the Hermitian matrix $M^{\nu,\ell}(M^{\nu,\ell})^\dagger$ instead of working with $M^{\nu,\ell}$ itself.

Finally let us note that the special case $M^\nu = M^{\nu\,\mathrm{T}}$ applies if the neutrinos are Majorana particles, as can be shown using the anti-commuting property of the fermion fields. From (B.4) we therefore see that in this case we can make use of the easier relation

$$M^{\nu}_{\text{diag.}} = V_{\mathrm{L}}^{\nu\,\dagger} M^{\nu} V_{\mathrm{L}}^{\nu\,*}. \tag{B.7}$$

Appendix C

Dirac, Weyl and Majorana fermions

For the convenience of the reader we recall here a number of basic facts regarding the different possible spinor descriptions of fermionic particles. Consider first a fermion Ψ that is described by the Dirac Lagrangian [29]

$$\mathcal{L} = \bar{\Psi}\left(i\partial\!\!\!/ - m\right)\Psi, \tag{C.1}$$

where $\partial\!\!\!/ = \gamma_\mu \partial^\mu$ and Ψ is a four-component Dirac spinor. Using the projection operators defined by

$$P_{\mathrm{L}} := \frac{1-\gamma^5}{2} \qquad\qquad P_{\mathrm{R}} := \frac{1+\gamma^5}{2} \tag{C.2}$$

one can decompose the spinor as

$$\Psi = \Psi_{\mathrm{R}} + \Psi_{\mathrm{L}}\,, \qquad \text{with} \qquad \Psi_{\mathrm{L,R}} := P_{\mathrm{L,R}}\Psi\,. \tag{C.3}$$

In the chiral representation the gamma matrix appearing above is given by

$$\gamma^5 = \begin{pmatrix} -\mathbb{1} & 0 \\ 0 & \mathbb{1} \end{pmatrix}, \tag{C.4}$$

so that $\Psi_{\mathrm{L,R}}$ are the left- and right-handed components of Ψ. The Dirac Lagrangian can be expanded in terms of these components yielding

$$\mathcal{L} = \overline{\Psi_{\mathrm{R}}} i\partial\!\!\!/ \Psi_{\mathrm{R}} + \overline{\Psi_{\mathrm{L}}} i\partial\!\!\!/ \Psi_{\mathrm{L}} - m\left(\overline{\Psi_{\mathrm{R}}}\Psi_{\mathrm{L}} - \overline{\Psi_{\mathrm{L}}}\Psi_{\mathrm{R}}\right) \tag{C.5}$$

in the chiral representation. From this one immediately obtains the Euler-Lagrange equations

$$\begin{aligned} i\partial\!\!\!/\Psi_{\mathrm{R}} &= m\Psi_{\mathrm{L}}, \\ i\partial\!\!\!/\Psi_{\mathrm{L}} &= m\Psi_{\mathrm{R}}. \end{aligned} \tag{C.6}$$

Let us consider the special case of a massless fermion, i.e. $m = 0$. Equation (C.6) shows that in this case the left- and right-handed components of Ψ decouple. Therefore it is sufficient to take a two-component Weyl spinor in order to describe a massless fermion with definite chirality. This is indeed how the massless left-handed neutrinos are described in the SM, whereas the massive SM fermions have to be described by a pair of Weyl spinors, which can be combined into a four-component Dirac spinor. Note that the SM is a chiral theory, which distinguishes left- and right-handed components through the gauge kinetic couplings. This means that the chiral projections $\Psi_{\mathrm{L,R}}$ must be used when writing down the SM Lagrangian in terms of Dirac spinors.

In [115] Majorana considered defining the right-handed field[1] $\Psi_R = C\overline{\Psi_{\mathrm{L}}}^T =: (\Psi_{\mathrm{L}})^c$ with the charge conjugation operator C defined by[2] $C = i\gamma^2\gamma^0$. Majorana showed that with this definition the Majorana spinor field $\Psi = \Psi_{\mathrm{L}} + \Psi_{\mathrm{R}}$ solves the Dirac equation provided Ψ_{L} obeys the Majorana equation

$$i\partial\!\!\!/\Psi_{\mathrm{L}} = mC\overline{\Psi_{\mathrm{L}}}^T, \tag{C.7}$$

which follows from (C.6). The mass term of a Majorana particle is given by

$$\mathcal{L}_{\mathrm{mass}} = \frac{1}{2}m\overline{(\Psi_{\mathrm{L}})^c}\Psi_{\mathrm{L}} + \mathrm{h.c.} \tag{C.8}$$

Note that a particle described by a Majorana spinor $\Psi = \Psi_{\mathrm{L}} + \Psi_{\mathrm{R}}$ is its own antiparticle, since we have

$$\Psi^c = (\Psi_{\mathrm{L}} + \Psi_{\mathrm{R}})^c = (\Psi_{\mathrm{L}})^c + ((\Psi_{\mathrm{L}})^c)^c = \Psi. \tag{C.9}$$

This fact is often referred to as the Majorana condition.

Since particle and antiparticle are distinct for fermions carrying a charge-like quantum number, the only known particle that could possibly be described by a Majorana spinor is the neutrino. Note, however, that left-handed neutrinos transform under $SU(2)$ and a mass term as in (C.8) would not be gauge invariant. See section 2.3 for further discussions.

[1] An additional possible phase factor is suppressed here as it can anyway be absorbed into a redefinition of Ψ_{L}.

[2] In the chiral representation the matrices are given by $\gamma^2 = \begin{pmatrix} 0 & \sigma^2 \\ -\sigma^2 & 0 \end{pmatrix}$, $\sigma^2 = \begin{pmatrix} 0 & -i \\ i & 0 \end{pmatrix}$ and $\gamma^0 = \begin{pmatrix} 0 & \mathbb{1} \\ \mathbb{1} & 0 \end{pmatrix}$.

Appendix D

The Higgs interaction terms in the 2HDM

In this appendix we list the interaction terms of the physical Higgs particles which are obtained after inserting (3.15) into the Higgs potential (3.2) and the kinetic terms (3.34). We work in unitary gauge, in which the unphysical Goldstone bosons are set to zero. The scalar potential can be separated into terms that are respectively quadratic, cubic and quartic in the fields.

$$V = V_{\text{mass}} + V^{\text{c}}_{\text{quartic}} + V^{\text{n}}_{\text{quartic}} + V^{\text{c}}_{\text{cubic}} + V^{\text{n}}_{\text{cubic}}. \tag{D.1}$$

The quadratic term V_{mass} and the expressions for the masses of the physical Higgs fields are given in section 3.2. We have further separated the interaction terms into terms with and without involvement of the charged Higgs, labelling them by the upper index c respectively n. The quartic interactions are

$$\begin{aligned}
V^{\text{c}}_{\text{quartic}} = & \frac{1}{2}|H^+|^4\left[\lambda_1 \sin^4\beta + \lambda_2 \cos^4\beta + 2\lambda_{34}\sin^2\beta\cos^2\beta\right] \\
& + \frac{1}{2}|H^+|^2\left(H^0\right)^2\left[\lambda_1 \sin^2\beta\cos^2\alpha + \lambda_2 \sin^2\alpha\cos^2\beta\right. \\
& \qquad + \lambda_3(\sin^2\alpha\sin^2\beta + \cos^2\alpha\cos^2\beta) \\
& \qquad \left. - 2\lambda_4 \sin\alpha\cos\alpha\sin\beta\cos\beta\right] \\
& + |H^+|^2 H^0 h^0\Big[- \lambda_1 \sin\alpha\cos\alpha\sin^2\beta + \lambda_2 \sin\alpha\cos\alpha\cos^2\beta \\
& \qquad + \lambda_3 \sin\alpha\cos\alpha(\sin^2\beta - \cos^2\beta) \\
& \qquad + \lambda_4 \sin\beta\cos\beta(\sin^2\alpha - \cos^2\alpha)\Big] \\
& + \frac{1}{2}|H^+|^2\left(h^0\right)^2\left[\lambda_1 \sin^2\alpha\sin^2\beta + \lambda_2 \cos^2\alpha\cos^2\beta\right. \\
& \qquad + \lambda_3(\cos^2\alpha\sin^2\beta + \sin^2\alpha\cos^2\beta) \\
& \qquad \left. + 2\lambda_4 \sin\alpha\cos\alpha\sin\beta\cos\beta\right] \\
& + \frac{1}{2}|H^+|^2\left(A^0\right)^2\left[\lambda_1 \sin^4\beta + \lambda_2 \cos^4\beta + 2\lambda_{34}\sin^2\beta\cos^2\beta\right],
\end{aligned} \tag{D.2}$$

$$
\begin{aligned}
V^{\rm n}_{\rm quartic} \;=\;& \frac{1}{8}\left(H^0\right)^4\left[\lambda_1\cos^4\alpha+\lambda_2\sin^4\alpha+2\lambda_{34}\sin^2\alpha\cos^2\alpha\right]\\
&+\frac{1}{8}\left(h^0\right)^4\left[\lambda_1\sin^4\alpha+\lambda_2\cos^4\alpha+2\lambda_{34}\sin^2\alpha\cos^2\alpha\right]\\
&+\frac{1}{2}\left(H^0\right)^3h^0\big[-\lambda_1\sin\alpha\cos^3\alpha+\lambda_2\cos\alpha\sin^3\alpha\\
&\qquad+\lambda_{34}(\sin\alpha\cos^3\alpha-\cos\alpha\sin^3\alpha)\big]\\
&+\frac{1}{2}H^0\left(h^0\right)^3\big[-\lambda_1\cos\alpha\sin^3\alpha+\lambda_2\sin\alpha\cos^3\alpha\\
&\qquad+\lambda_{34}(\cos\alpha\sin^3\alpha-\sin\alpha\cos^3\alpha)\big]\\
&+\frac{1}{4}\left(H^0\right)^2\left(h^0\right)^2\big[3\lambda_1\sin^2\alpha\cos^2\alpha+3\lambda_2\sin^2\alpha\cos^2\alpha\\
&\qquad+\lambda_{34}(\sin^4\alpha-4\sin^2\alpha\cos^2\alpha+\cos^4\alpha)\big]\\
&+\frac{1}{4}\left(H^0\right)^2\left(A^0\right)^2\big[\lambda_1\cos^2\alpha\sin^2\beta+\lambda_2\sin^2\alpha\cos^2\beta\\
&\qquad+\lambda_{34}(\sin^2\alpha\sin^2\beta+\cos^2\alpha\cos^2\beta)\big]\\
&+\frac{1}{2}H^0h^0\left(A^0\right)^2\big[-\lambda_1\sin\alpha\cos\alpha\sin^2\beta\\
&\qquad+\lambda_2\sin\alpha\cos\alpha\cos^2\beta\\
&\qquad+\lambda_{34}\sin\alpha\cos\alpha(\sin^2\beta-\cos^2\beta)\big]\\
&+\frac{1}{4}\left(h^0\right)^2\left(A^0\right)^2\big[\sin^2\alpha\sin^2\beta+\lambda_2\cos^2\alpha\cos^2\beta\\
&\qquad+\lambda_{34}(\sin^2\alpha\cos^2\beta+\cos^2\alpha\sin^2\beta)\big]\\
&+\frac{1}{8}\left(A^0\right)^4\left[\lambda_1\sin^4\beta+\lambda_2\cos^4\beta+2\lambda_{34}\sin^2\beta\cos^2\beta\right].
\end{aligned}
\tag{D.3}
$$

Let us point out that CP parity is conserved in the Higgs interactions, as every interaction term involves an even number of CP-odd scalars A^0. This of course also holds true for the cubic interactions below.

$$
\begin{aligned}
V^{\rm c}_{\rm cubic} \;=\;& |H^+|^2h^0\big[\lambda_2v_2\cos^2\beta\cos\alpha+\lambda_3v_2\sin^2\beta\cos\alpha\\
&\qquad-\lambda_3v_1\cos^2\beta\sin\alpha-\lambda_1v_1\sin^2\beta\sin\alpha\\
&\qquad-\lambda_4v_1\sin^2\beta\cos\alpha+\lambda_4v_2\cos^2\beta\sin\alpha\big]\\
&+|H^+|^2H^0\big[\lambda_1v_1\sin^2\beta\cos\alpha+\lambda_2v_2\cos^2\beta\sin\alpha\\
&\qquad+\lambda_3v_2\sin^2\beta\sin\alpha+\lambda_3v_1\cos^2\beta\cos\alpha\\
&\qquad-\lambda_4v_1\sin^2\beta\sin\alpha-\lambda_4v_2\cos^2\beta\cos\alpha\big],
\end{aligned}
\tag{D.4}
$$

$$
\begin{aligned}
V^{\rm n}_{\rm cubic} \;=& +\frac{1}{2}\left(H^0\right)^3\Big[\lambda_1 v_1\cos^3\alpha+\lambda_2 v_2\sin^3\alpha \\
&\qquad +\lambda_{34}(v_1\cos\alpha\sin^2\alpha+v_2\sin\alpha\cos^2\alpha)\Big] \\
&+\frac{1}{2}\left(H^0\right)^2 h^0\Big[-3\lambda_1 v_1\sin\alpha\cos^2\alpha+3\lambda_2 v_2\cos\alpha\sin^2\alpha \\
&\qquad +\lambda_{34}v_1(2\sin\alpha\cos^2\alpha-\sin^3\alpha) \\
&\qquad +\lambda_{34}v_2(-2\cos\alpha\sin^2\alpha+\cos^3\alpha)\Big] \\
&+\frac{1}{2}H^0\left(h^0\right)^2\Big[3\lambda_1 v_1\cos\alpha\sin^2\alpha+3\lambda_2 v_2\sin\alpha\cos^2\alpha \\
&\qquad +\lambda_{34}v_1(\cos^3\alpha-2\cos\alpha\sin^2\alpha) \\
&\qquad +\lambda_{34}v_2(\sin^3\alpha-2\sin\alpha\cos^2\alpha)\Big] \\
&+\frac{1}{2}\left(h^0\right)^3\Big[-\lambda_1 v_1\sin^3\alpha+\lambda_2 v_2\cos^3\alpha \\
&\qquad +(\lambda_{34}v_2\cos\alpha\sin^2\alpha-v_1\sin\alpha\cos^2\alpha)\Big] \\
&+\frac{1}{2}H^0\left(A^0\right)^2\Big[\lambda_1 v_1\cos\alpha\sin^2\beta+\lambda_2 v_2\sin\alpha\cos^2\beta \\
&\qquad +\lambda_{34}(v_1\cos\alpha\cos^2\beta+v_2\sin\alpha\sin^2\beta)\Big] \\
&+\frac{1}{2}h^0\left(A^0\right)^2\Big[\lambda_1 v_1\sin\alpha\sin^2\beta+\lambda_2 v_2\cos\alpha\cos^2\beta \\
&\qquad +\lambda_{34}(v_2\cos\alpha\sin^2\beta-v_1\sin\alpha\cos^2\beta)\Big].
\end{aligned}
\tag{D.5}
$$

The expressions above contain couplings that are relatively complicated functions of the vev ratio $\tan\beta = v_2/v_1$ and the mixing angle α that arises in the sector containing h^0 and H^0. However, using the vev hierarchy $v_1 \ll v_2$ we note that the couplings can be split into a dominant contribution plus sub-leading terms that are suppressed by further relative factors of v_1/v_2. Keeping only the leading order in v_1/v_2 we obtain a significantly simplified expression. We find

$$
\begin{aligned}
V \;=\;& m^2_{H^\pm}\left|H^+\right|^2+\frac{1}{2}m^2_{A^0}\left(A^0\right)^2 \\
&+\frac{1}{2}m^2_{H^0}\left(H^0\right)^2+\frac{1}{2}m_{h^0}\left(h^0\right)^2 \\
&+V^{\rm cubic}+V^{\rm quartic},
\end{aligned}
\tag{D.6}
$$

where

$$
\begin{aligned}
V^{\text{cubic}} \simeq & + \left|H^+\right|^2 H^0 \Big[\lambda_1 v_1 \cos\alpha \sin^2\beta + \lambda_3 v_2 \sin^2\beta \sin\alpha\Big] \\
& + \left|H^+\right|^2 h^0 \lambda_3 v_2 \sin^2\beta \cos\alpha \\
& + \frac{1}{2}\left(H^0\right)^3 \Big[\lambda_1 v_1 \cos^3\alpha + \lambda_{34} v_2 \sin\alpha \cos^2\alpha\Big] \\
& + \frac{1}{2}\left(h^0\right)^3 \lambda_2 v_2 \cos^3\alpha \\
& + \frac{1}{2}\left(H^0\right)^2 h^0 \lambda_{34} v_2 \cos^3\alpha \\
& + \frac{1}{2}\left(A^0\right)^2 h^0 \lambda_{34} v_2 \cos\alpha \sin^2\beta \\
& + \frac{1}{2} H^0 \left(h^0\right)^2 \Big[3\lambda_2 v_2 \cos^2\alpha \sin\alpha + \lambda_{34} v_1 \cos^3\alpha \\
& \qquad\qquad -2\lambda_{34} v_2 \cos^2\alpha \sin\alpha\Big] \\
& + \frac{1}{2} H^0 \left(A^0\right)^2 \Big[\lambda_1 v_1 \cos\alpha \sin^2\beta + \lambda_{34} v_2 \sin\alpha \sin^2\beta\Big]
\end{aligned}
\tag{D.7}
$$

and

$$
\begin{aligned}
V^{\text{quartic}} \simeq & \frac{1}{2}\left|H^+\right|^4 \lambda_1 \sin^4\beta + \frac{1}{8}\left(H^0\right)^4 \lambda_1 \cos^4\alpha \\
& + \frac{1}{8}\left(h^0\right)^4 \lambda_2 \cos^4\alpha + \frac{1}{8}\left(A^0\right)^4 \lambda_1 \sin^4\beta \\
& + \frac{1}{2}\left|H^+\right|^2 \left(A^0\right)^2 \lambda_1 \sin^4\beta \\
& + \frac{1}{2}\left|H^+\right|^2 \left(H^0\right)^2 \lambda_1 \sin^2\beta \cos^2\alpha \\
& + \frac{1}{4}\left(H^0\right)^2 \left(A^0\right)^2 \lambda_1 \cos^2\alpha \sin^2\beta \\
& + \frac{1}{4}\left(h^0\right)^2 \left(A^0\right)^2 \lambda_{34} \cos^2\alpha \sin^2\beta \\
& + \left|H^+\right|^2 \left(h^0\right)^2 \frac{1}{2}\lambda_3 \cos^2\alpha \sin^2\beta \\
& + \frac{1}{4}\left(H^0\right)^2 \left(h^0\right)^2 \lambda_{34} \cos^4\alpha \\
& + \frac{1}{2}\left(H^0\right)^3 h^0 \Big[-\lambda_1 \sin\alpha \cos^3\alpha + \lambda_{34} \sin\alpha \cos^3\alpha\Big] \\
& + \frac{1}{2} H^0 \left(h^0\right)^3 \Big[\lambda_2 \sin\alpha \cos^3\alpha - \lambda_{34} \sin\alpha \cos^3\alpha\Big] \\
& + \frac{1}{2}\left(A^0\right)^2 H^0 h^0 \sin\alpha \cos\alpha \sin^2\beta \Big[-\lambda_1 + \lambda_{34}\Big] \\
& + \left|H^+\right|^2 H^0 h^0 \Big[-\lambda_1 \sin^2\beta \sin\alpha \cos\alpha \\
& \qquad\qquad + \lambda_3 \sin\alpha \cos\alpha \sin^2\beta \\
& \qquad\qquad - \lambda_4 \sin\beta \cos\beta \cos^2\alpha\Big] .
\end{aligned}
\tag{D.8}
$$

Finally let us also give the expansion of the kinetic term (3.34) in terms of the physical Higgs fields. This yields the interaction terms between the Higgs scalars and the gauge bosons. In unitary gauge the resulting couplings read

$$
\begin{aligned}
\mathcal{L}_{\Phi,\text{kin.}} \;=\;& \{\text{kinetic terms of the scalar fields}\} \\
&+\{\text{mass terms of the gauge bosons}\} \\
&+\frac{ig_2}{2}W_\mu^-\left[\left(\sin(\alpha-\beta)H^0+\cos(\alpha-\beta)h^0\right)\partial^\mu H^+\right. \\
&\qquad\left.-iA^0\partial^\mu H^+\right]+\text{h.c.} \\
&-\frac{ig_2}{2}W_\mu^-\left[\sin(\alpha-\beta)H^+\partial^\mu H^0+\cos(\alpha-\beta)H^+\partial^\mu h^0\right. \\
&\qquad\left.-iH^+\partial^\mu A^0\right]+\text{h.c.} \\
&+\frac{g_2\sqrt{g_1^2+g_2^2}}{4}W_\mu^-A^\mu\left[\sin(\alpha-\beta)H^0H^+\right.+\cos(\alpha-\beta)h^0H^+ \\
&\qquad\left.-iA^0H^+\right]+\text{h.c.} \\
&-\frac{g_2\sqrt{g_1^2+g_2^2}}{4}W_\mu^-Z^\mu\left[\sin(\alpha-\beta)H^0H^+\right.+\cos(\alpha-\beta)h^0H^+ \\
&\qquad\left.-iA^0H^+\right]+\text{h.c.} \\
&+\frac{g_2^2}{4}W_\mu^-W^{+\mu}\left[H^0H^0+h^0h^0+A^0A^0+2H^-H^+\right] \\
&+\frac{g_2^2}{2}\sqrt{v_1^2+v_2^2}W_\mu^-W^{+\mu}\left[\cos(\alpha-\beta)H^0+\sin(\alpha-\beta)h^0\right] \\
&+\frac{g_1^2+g_2^2}{8}Z_\mu Z^\mu\left[H^0H^0+h^0h^0+A^0A^0\right] \\
&+\frac{g_1^2+g_2^2}{8}\sqrt{v_1^2+v_2^2}Z_\mu Z^\mu\left[\cos(\alpha-\beta)H^0+\sin(\alpha-\beta)h^0\right] \\
&+\frac{g_1^2+g_2^2}{4}A_\mu A^\mu H^+H^- \\
&-\frac{i\sqrt{g_1^2+g_2^2}}{2}A^\mu(\partial_\mu H^-)H^++\text{h.c.} \\
&+\frac{\sqrt{g_1^2+g_2^2}}{2}Z^\mu\left[\sin(\alpha-\beta)H^0\partial_\mu A^0+\cos(\alpha-\beta)h^0\partial_\mu A^0\right. \\
&\qquad\left.-A^0\sin(\alpha-\beta)\partial_\mu H^0-A^0\cos(\alpha-\beta)\partial_\mu h^0\right].
\end{aligned}
\tag{D.9}
$$

The expressions for the kinetic terms of the scalars and the mass terms of the gauge bosons are given in (3.38).

Appendix E

Tree-level decay modes of the SM Higgs

In this appendix we summarise a number of spinor identities and phase space integrals that are needed when calculating decay widths. We also present the results for the tree-level decay widths of the Higgs boson in the Standard Model, which are referred to in section 3.5.

The partial decay width for an initial particle with four momentum p_i^μ which decays into n particles which four momentum p_j^μ is given by Fermi's golden rule

$$\Gamma = \int \prod_{j=1}^{n} \frac{d^3 p_j}{(2\pi)^3 2E_j} \frac{N}{2E_i} \delta^4 \left(p_i - \sum_{j=1}^{n} p_j \right) |\mathcal{A}|^2 (2\pi)^4. \tag{E.1}$$

Here N is a symmetry factor given by

$$1/N = \prod_s (\text{number of identical final-state particles of species } s), \tag{E.2}$$

while $\mathcal{A}$ is the transition amplitude which can be calculated using the Feynman rules. For a decay into fermions it is useful to take into account the spin sum rules for the fermion spinors

$$\sum_{r=1}^{2} \sum_{s=1}^{2} \bar{u}_s(p_1) v_r(p_2) \bar{v}_r(p_2) u_s(p_1) = \sum_{r=1}^{2} \sum_{s=1}^{2} Tr\left[v_r(p_2) \bar{v}_r(p_2) u_s(p_1) \bar{u}_s(p_1) \right] \tag{E.3}$$

$$\not{p} + m = \sum_s u_s(p) \bar{u}_s(p) \qquad \not{p} - m = \sum_s v_s(p) \bar{v}_s(p). \tag{E.4}$$

In the above $v_r(p_2)$ is the spinor describing an outgoing antifermion with momentum p_2 in the spin state r; $\bar{u}_s(p_1)$ describes an outgoing fermion with momentum p_1 in the spin state s. Finally we mention that

$$\text{Tr}[\text{odd number of } \gamma \text{ matrices}] = 0. \tag{E.5}$$

For the decay into gauge bosons one has to take into account the polarisation state $\epsilon_\mu^\lambda(k)$ of the external bosons. The polarisation sum for a vector boson of mass m and momentum k_μ is given by

$$\sum_\lambda \epsilon_\mu^\lambda(k) \left(\epsilon_\nu^\lambda(k)\right)^* = -g_{\mu\nu} + \frac{k_\mu k_\nu}{m^2}, \tag{E.6}$$

while for a massless gauge boson, like the photon, the second term is absent.

Taking all this into account it is straightforward to calculate the following decay widths, where f labels any quark or charged lepton [114]

$$\Gamma(h \to \bar{f}f) = \frac{\alpha_{em}\pi m_h m_f^2}{8m_W^2}\frac{g_1^2+g_2^2}{g_1^2}\left(1-\frac{4m_f^2}{m_h^2}\right)^{\frac{3}{2}}, \tag{E.7}$$

$$\Gamma(h \to W^+W^-) = \frac{m_h^3}{16\pi v^2}\left(1-4\frac{m_W^2}{m_H^2}\right)\left(12\frac{m_W^4}{m_h^4}+1-4\frac{m_W^2}{m_h^2}\right), \tag{E.8}$$

$$\Gamma(h \to ZZ) = \frac{m_H^3}{32\pi v^2}\left(1-4\frac{m_Z^2}{m_h^2}\right)\left(12\frac{m_Z^4}{m_h^4}+1-4\frac{m_Z^2}{m_h^2}\right). \tag{E.9}$$

The decay channel $h \to \gamma\gamma$, which is a loop-induced process, is discussed in section 3.5 for both the SM and the 2HDM cases. For further details on loop-induced decays see for example [114].

Appendix F

Deviations from TBM form in the real case - analytic derivation

In this appendix we consider allowing either for a difference between the couplings of the two singlets of the 2S2T model, or for a non-vanishing antisymmetric contribution to the neutrino mass matrix, while restricting all parameters appearing in the mass matrices to real values. In these cases the diagonalisation can be performed analytically, and we can extract the exact functional dependence of the mixing angles and neutrino masses on the deviation parameters. As we had already mentioned in the main text, in the case of complex parameters the diagonalisation can no longer be performed analytically as soon as any of the three considered deviations from the TBM form is turned on. Let us also emphasise that even in the real case, the analytic diagonalisation fails as soon as one allows for deviations from the triplet vev alignment. Therefore we will impose the aligned form (4.16) of the triplet vevs throughout this appendix. We work in the Altarelli-Feruglio basis, in which the neutrino mass matrix of the 2S2T model is given by

$$M^{\nu} = \begin{pmatrix} 2a & -a+a'+d & -a-a'+c \\ -a-a'+d & 2a+c & -a+a' \\ -a+a'+c & -a-a' & 2a+d \end{pmatrix}. \tag{F.1}$$

Recall that in the absence of vev misalignment, the charged lepton mass matrix is diagonal, so the mixing matrix is obtained by simply diagonalising the (squared) neutrino mass matrix (F.1).

Let us first allow for a deviation of the singlet couplings. After setting $a' = 0$ and $d = c(1+\epsilon)$ diagonalisation of the neutrino mass matrix leads to the mixing angles

$$\sin^2\theta_{13} = \frac{-2-\epsilon+2\sqrt{1+\epsilon+\epsilon^2}}{6\sqrt{1+\epsilon+\epsilon^2}} = \frac{\epsilon^2}{8} + \mathcal{O}(\epsilon^3), \tag{F.2}$$

$$\sin^2\theta_{23} = \frac{2+\epsilon(3+3\epsilon-2\sqrt{1+\epsilon+\epsilon^2})}{4+\epsilon(4+5\epsilon)} = \frac{1}{2} - \frac{\epsilon}{4} + \mathcal{O}(\epsilon^2), \tag{F.3}$$

$$\sin^2\theta_{12} = \frac{2\sqrt{1+\epsilon+\epsilon^2}}{2+\epsilon+4\sqrt{1+\epsilon+\epsilon^2}} = \frac{1}{3} + \frac{\epsilon^2}{24} + \mathcal{O}(\epsilon^3). \tag{F.4}$$

For the convenience of the reader we have given the leading terms in an expansion for $\epsilon \ll 1$, however we would like to emphasise once more that in general there is no reason for ϵ to be small. While the above expressions show that in general there is no simple relationship between the different mixing angles, one can simplify the relationship in the case $\epsilon \ll 1$ to

$$\sin^2\theta_{12} = \frac{1}{3} + \frac{1}{3}\sin^2\theta_{13} + \mathcal{O}(\epsilon^4). \tag{F.5}$$

In particular, the term cubic in ϵ matches exactly. In the case considered here, the relatively precise new measurement of $\sin^2\theta_{13}$ could of course be used to predict the values of the other angles, as all mixing angles are functions of the same parameter ϵ. This is also suggested by the scatter plots shown in figure 5.1. However, we will not pursue this direction further, because the same scatter plots show that no direct relationship between the different angles exists when complex parameters are allowed, which we expect to be the more natural case.

The neutrino masses in the case $a' = 0$ and $d = c(1+\epsilon)$ and with real parameters are found to be

$$|m_1| = \left|3a - c\sqrt{1+\epsilon+\epsilon^2}\right| = \left|3a - c - \frac{c\epsilon}{2}\right| + \mathcal{O}(\epsilon^2), \tag{F.6}$$

$$|m_2| = |c(2+\epsilon)|, \tag{F.7}$$

$$|m_3| = \left|3a + c\sqrt{1+\epsilon+\epsilon^2}\right| = \left|3a + c + \frac{c\epsilon}{2}\right| + \mathcal{O}(\epsilon^2). \tag{F.8}$$

This immediately leads to the squared mass differences

$$\begin{aligned} \Delta m^2_{21} &= -9a^2 + 3c^2(1+\epsilon) + 6|ac|\sqrt{1+\epsilon+\epsilon^2} \\ &= -9a^2 + 3c^2 + 6|ac| + 3(c^2+|ac|)\epsilon + \mathcal{O}(\epsilon^2), \end{aligned} \tag{F.9}$$

$$\Delta m^2_{31} = 12|ac|\sqrt{1+\epsilon+\epsilon^2} = 12|ac| + 6|ac|\epsilon + \mathcal{O}(\epsilon^2). \tag{F.10}$$

We would like to point out that the mass sum rule $m_1 + m_2 = m_3$ that we had found in the case of exact TBM mixing with $\epsilon = 0$ continues to hold at linear order in ϵ, so that the perturbations to the validity of this sum rule start only at quadratic order in ϵ. Nevertheless, this violation can of course become sizeable if ϵ is not small.

Let us now turn to the effects of the antisymmetric coupling, setting $c = d$ and allowing for $a' = \eta a$ in (F.1). Performing the diagonalisation, we find the mixing angles

$$\sin^2\theta_{13} = \frac{1}{3} - \frac{1}{\sqrt{9+3\eta^2}} = \frac{\eta^2}{18} + \mathcal{O}(\eta^4), \tag{F.11}$$

$$\sin^2\theta_{23} = \frac{9+\eta(3+4\eta-2\sqrt{9+3\eta^2})}{18+8\eta^2} = \frac{1}{2} - \frac{\eta}{6} + \mathcal{O}(\eta^3), \tag{F.12}$$

$$\sin^2\theta_{12} = \frac{\sqrt{9+3\eta^2}}{2\sqrt{9+3\eta^2}+3} = \frac{1}{3} + \frac{\eta^2}{54} + \mathcal{O}(\eta^4). \tag{F.13}$$

As in the case of the singlet deviations considered above, no simple general relationship between the different mixing angles is evident. However, in the limit of small η, we find a relationship between θ_{13} and θ_{12} of precisely the same form as above, namely

$$\sin^2\theta_{12} = \frac{1}{3} + \frac{1}{3}\sin^2\theta_{13} + \mathcal{O}(\eta^4). \tag{F.14}$$

This observation is in agreement with the scatter plots of figure 5.1, which shows a striking similarity in the relationships between the mixing angles in the cases with $a' = 0,\ c \neq d$ and $a' \neq 0,\ c = d$ for real parameters. Nevertheless, the relationships are exactly the same only in the limit of small deviations and not in general. However, in the case of complex parameters again no relationship between the mixing angles is evident from figure 5.1.

The neutrino masses in the presence of the antisymmetric coupling are found to be

$$|m_1| = \left|c - a\sqrt{9+3\eta^2}\right| \simeq \left|c - 3a - \frac{1}{2}a\eta^2\right| + \mathcal{O}(\eta^4), \tag{F.15}$$

$$|m_2| = 2|c|, \tag{F.16}$$

$$|m_3| = \left|c + a\sqrt{9+3\eta^2}\right| \simeq \left|c + 3a + \frac{1}{2}a\eta^2\right| + \mathcal{O}(\eta^4), \tag{F.17}$$

while the associated squared mass differences read

$$\begin{aligned} \Delta m^2_{21} &= 3c^2 - a^2(9+3\eta^2) + 2|ac|\sqrt{9+3\eta^2} \\ &= -9a^2 + 3c^2 + 6|ac| + (|ac| - 3a^2)\eta^2 + \mathcal{O}(\eta^4), \end{aligned} \tag{F.18}$$

$$\Delta m^2_{31} = 4|ac|\sqrt{9+3\eta^2} = 12|ac| + 2|ac|\eta^2 + \mathcal{O}(\eta^4). \tag{F.19}$$

Note that in the real case the sum rule $m_1 + m_2 = m_3$ therefore continues to hold exactly to all orders in the presence of the antisymmetric perturbation η. This of course implies that also the absolute scale of the neutrino masses in this case will be quite small, of order of the measured mass differences. However, we will not go into further detail here as our main focus lies on the more general case, in which all three deviations as well as complex parameters are allowed and in which case no analytic expression for the mixing matrix as a function of the deviations can be found.

Appendix G

Details of the numerical analysis of the 2S2T model

In this appendix we present the detailed results of the numerical analysis of the 2S2T models for the cases where deviations from the tribimaximal form of the mass matrices are switched on, see chapter 5. Throughout this appendix $\langle \Phi_S^0 \rangle$ and $\langle \Phi_T^0 \rangle$ denote the flavon triplet vevs in the aligned form leading to TBM mixing. In section G.1 we give the regions over which the various parameters were allowed to vary in our numerical analysis, before proceeding to the predicted neutrino mass observables and the Jarlskog variable in sections G.2 and G.3.

G.1 Parameter regions

In tables G.1−G.4 we list the input parameter regions for our the numerical analysis. The parameters were allowed to vary uniformly over the given regions. Figure G.1 and G.2 show scatter plots of the points in parameter space that were found to lead to a mixing and mass matrix compatible with the 3σ neutrino oscillation parameters, for the various cases in which only one source of deviations from TBM was taken into account. We use the abbreviation $\epsilon_{S,i}$ if the same parameters were chosen for both $\epsilon_{S,1}$ and $\epsilon_{S,2}$, and similarly for $\epsilon_{T,i}$. The various parameters are defined in equations (4.21), (4.23), (5.1) and (5.2).

Parameter	Normal hierarchy	Inverted hierarchy
a [eV]	$\pm[0.01, 0.03]$	$\pm[0.005, 0.04]$
$\Re(c)$ [eV]	$\pm[0.005, 0.025]$	$\mp[0.004, 0.034]$
$\Im(c)$ [eV]	$[-0.6, 0.6]$	$[-0.1, 0.1]$
$\Re(\eta)$	$[-2, 2]$	$[-1.5, 1.5]$
$\Im(\eta)$	$[-0.5, 0.5]$	$[-1.5, 1.5]$

Table G.1: Parameter regions for $a' = a\eta$.

Parameter	Normal hierarchy	Inverted hierarchy
a [eV]	$\pm[0.005, 0.065]$	$\pm[0.005, 0.06]$
$\Re(c)$ [eV]	$\pm[0.002, 0.03]$	$\mp[0.002, 0.05]$
$\Im(c)$ [eV]	$[-0.15, 0.15]$	$[-0.1, 0.1]$
$\Re(\epsilon)$	$[-1.2, 1.7]$	$[-1.2, 2.5]$
$\Im(\epsilon)$	$[-1, 1]$	$[-1, 1]$

Table G.2: Parameter regions for $d = c(1 + \epsilon)$.

Parameter	Normal hierarchy	Inverted hierarchy
a [eV]	$\pm[0.004, 0.026]$	$\pm[0, 0.025]$
$\Re(c)$ [eV]	$\pm[0, 0.025]$	$\mp[0, 0.03]$
$\Im(c)$ [eV]	$[-0.04, 0.04]$	$[-0.045, 0.045]$
$\Re(\epsilon_{S,1})$	$[-0.9, 0.5]$	$[-1, 1]$
$\Re(\epsilon_{S,2})$	$[-1, 0.8]$	$[-1, 1]$
$\Im(\epsilon_{S,i})$	$[-1, 1]$	$[-1, 1]$
$\Re(\epsilon_{T,i})$, $\Im(\epsilon_{T,i})$	$[-0.005, 0.005]$	$[-0.005, 0.005]$

Table G.3: Parameter regions for $\langle\varphi_S\rangle = v_S(1 + \epsilon_{S,1}, 1 + \epsilon_{S,2}, 1)$ and $\langle\varphi_T\rangle = v_T(1, \epsilon_{T,1}, \epsilon_{T,2})$.

Parameter	Normal hierarchy	Inverted hierarchy
a [eV]	$\pm[0, 0.018]$	$\pm[0.004, 0.016]$
$\Re(c)$ [eV]	$\pm[0.002, 0.023]$	$\mp[0.0065, 0.0375]$
$\Im(c)$ [eV]	$[-0.03, 0.03]$	$[-0.03, 0.03]$
$\Re(\eta)$	$[-2, 2]$	$[-1.5, 1.5]$
$\Im(\eta)$	$[-0.5, 0.5]$	$[-0.5, 0.5]$
$\Re(\epsilon)$	$[-1.8, 1.8]$	$[-0.75, 0.75]$
$\Im(\epsilon)$	$[-2, 2]$	$[-0.75, 0.75]$
$\Re(\epsilon_{S,1})$	$[-0.5, 0.5]$	$[-1, 1]$
$\Re(\epsilon_{S,2})$	$[-0.7, 1]$	$[-1, 1]$
$\Im(\epsilon_{S,i})$	$[-1, 1]$	$[-1, 1]$
$\Re(\epsilon_{T,i})$, $\Im(\epsilon_{T,i})$	$[-0.005, 0.005]$	$[-0.005, 0.005]$

Table G.4: Parameter regions, all deviations combined.

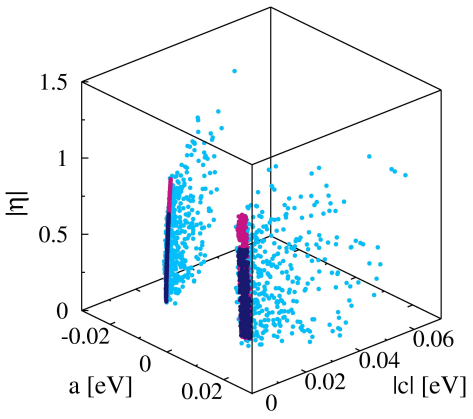

(a) $a' = a\eta$. Normal hierarchy.

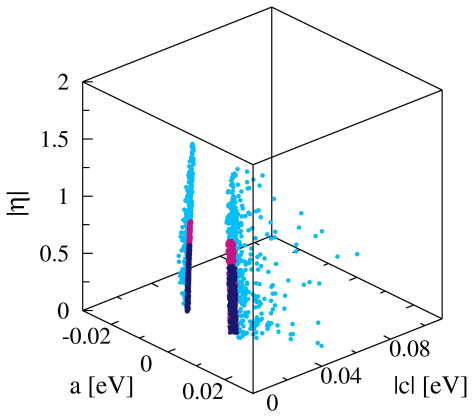

(b) $a' = a\eta$. Inverted hierarchy.

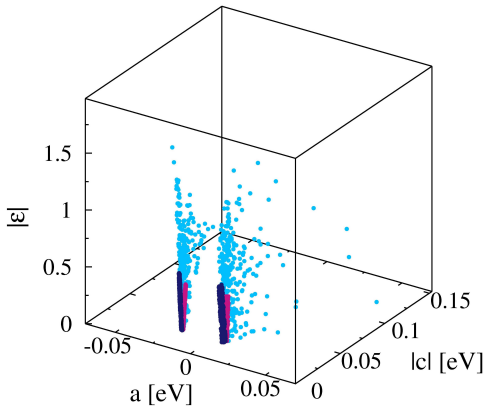

(c) $d = c(1 + \epsilon)$. Normal hierarchy.

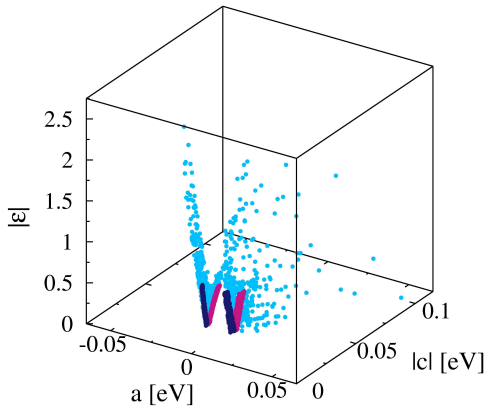

(d) $d = c(1 + \epsilon)$. Inverted hierarchy.

Figure G.1: Points in parameter space compatible with 3σ oscillation data for $a' = a\eta$ and $d = c(1 + \epsilon)$. Points that are obtained when restricting to real parameters are highlighted in dark blue for η, $e > 0$ and in purple for η, $e < 0$.

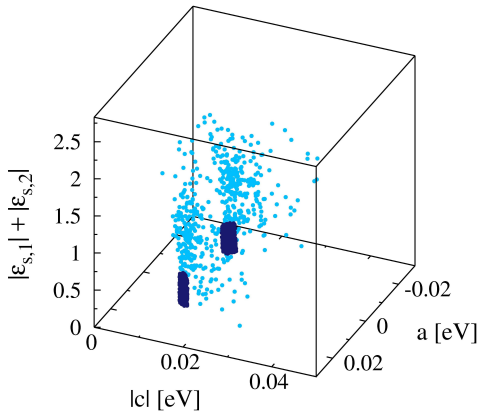

(a) Normal hierarchy.

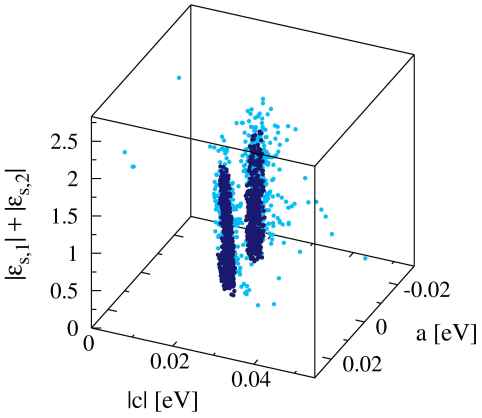

(b) Inverted hierarchy.

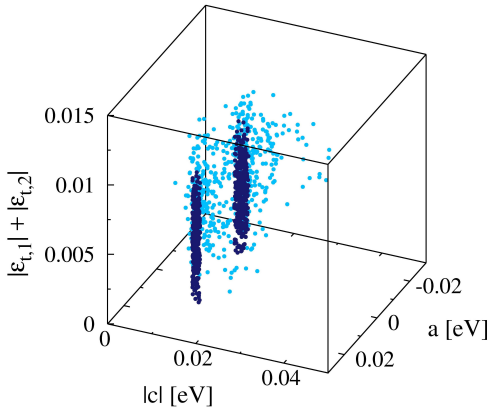

(c) Normal hierarchy.

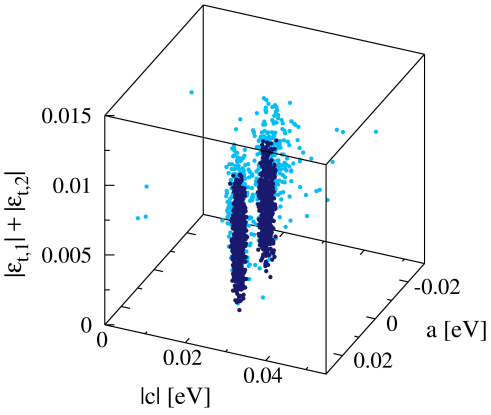

(d) Inverted hierarchy.

Figure G.2: Points in parameter space compatible with 3σ oscillation data for $\langle\varphi_S\rangle = v_S(1+\epsilon_{S,1}, 1+\epsilon_{S,2}, 1)$ and $\langle\varphi_T\rangle = v_T(1, \epsilon_{T,1}, \epsilon_{T,2})$. Points that are obtained when restricting to real parameters are highlighted in dark blue.

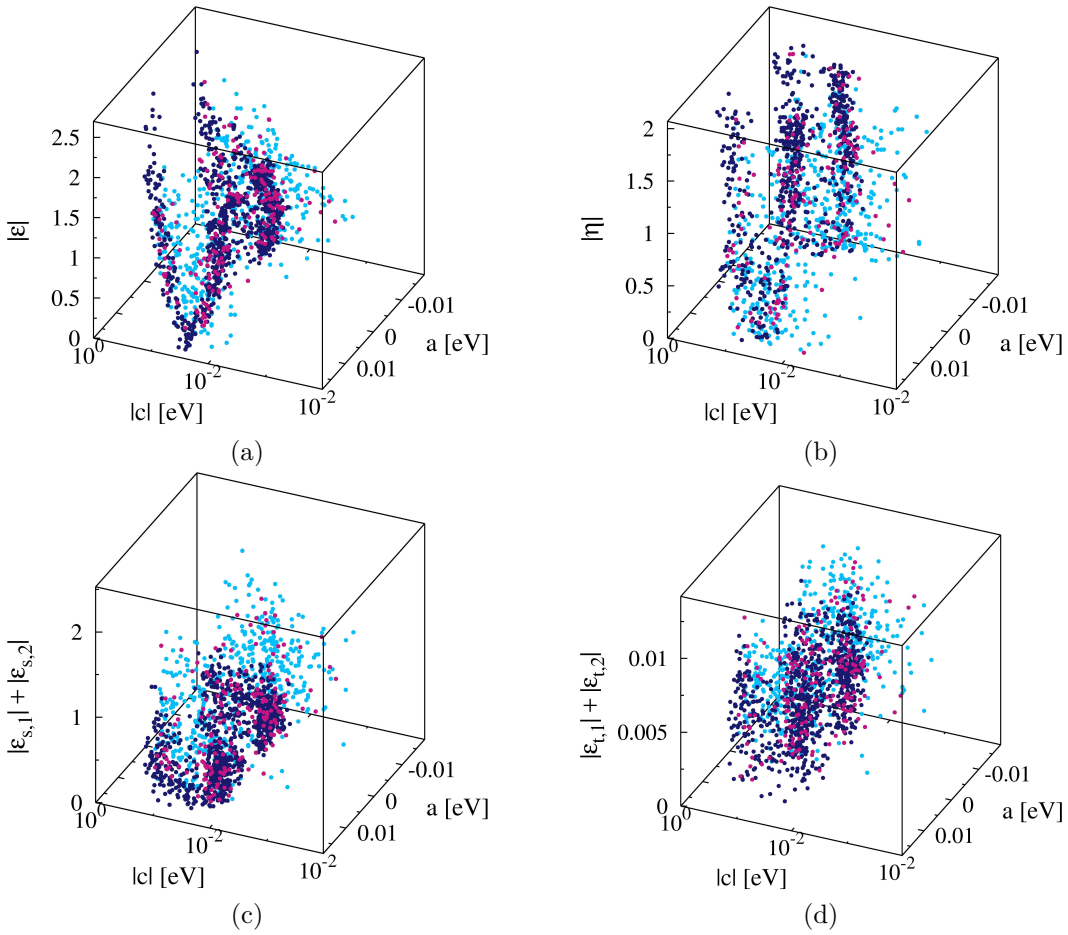

Figure G.3: Scatter plot of parameter combinations allowed by oscillation measurements for normal mass ordering. Real parameter values are highlighted in dark blue. Points which are compatible with the recently announced new bound $\sin^2\theta_{13} = 0.022^{+0.0033}_{-0.0030}$ [44] are highlighted in purple.

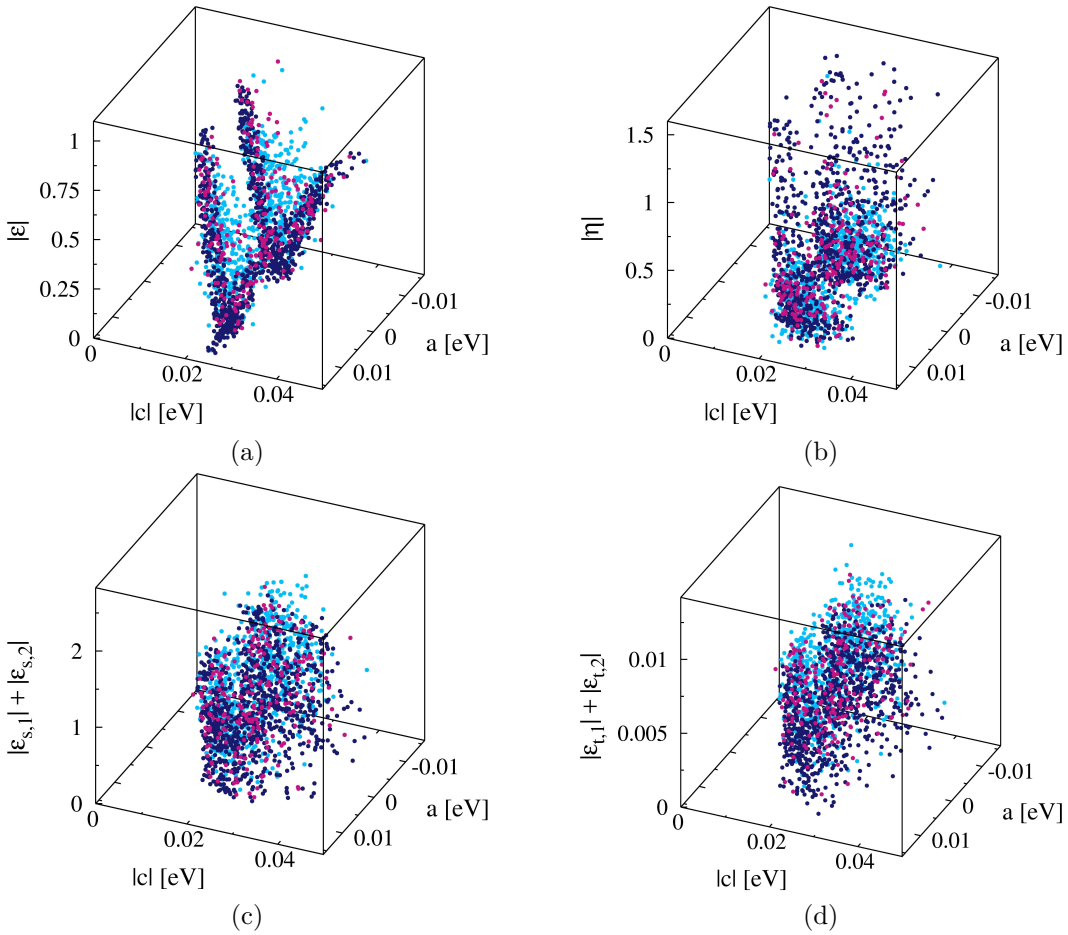

Figure G.4: Parameter combinations allowed by oscillation measurements for inverse mass ordering. Real parameter values are highlighted in dark blue. Points which are compatible with the bound $\sin^2\theta_{13} = 0.022^{+0.0033}_{-0.0030}$ [44] are highlighted in purple.

G.2 Predicted neutrino mass observables

In table G.5−G.7 we list the results for the lightest neutrino mass, for the parameter m_β relevant in β decay experiments and for the sum of the absolute neutrino masses $\sum m_\nu$, which is probed in cosmology. Compatibility with the known experimental bounds has been obtained in all cases, compare section 2.

The results presented were obtained when allowing for complex parameters in the numerical analysis. As the tables suggests, our numerical analysis returned smaller values of the listed observables for the case of combined deviations than when allowing for only one deviation. Of course this is only an artifact of the compromise between allowed parameter regions and computability as well as the finite statistics, because the combined analysis includes of course all the single deviations as special cases.

Our results show, that the largest values of the lightest neutrino mass, can be obtained for the case where only $\epsilon \neq 0$. This of course also translates to $\sum m_\nu$ and m_β. On the other hand the triplet vev misalignment leads to the smallest values of the lightest neutrino mass. The fact that the masses in the analysis where all deviations where included are predicted to be small, suggests that the effect of the vev misalignment on the masses is stronger than the effect of the other deviations.

Deviation	Lightest neutrino mass [eV]	
	Normal hierarchy	Inverted hierarchy
$a' \neq 0$	$[0.022, 0.114]$	$[7 \times 10^{-4}, 0.14]$
$c \neq d$	$[0.024, 0.205]$	$[7 \times 10^{-4}, 0.205]$
$\langle \varphi_{S,T} \rangle \neq \langle \varphi^0_{S,T} \rangle$	$[0.025, 0.070]$	$[10^{-4}, 0.077]$
Combined	$[0.011, 0.051]$	$[5 \times 10^{-6}, 0.045]$

Table G.5: Range of the predicted lightest neutrino masses m_1 and m_3 respectively.

Deviation	$\sum m_\nu$ [eV]	
	Normal hierarchy	Inverted hierarchy
$a' \neq 0$	$[0.10, 0.36]$	$[0.09, 0.44]$
$c \neq d$	$[0.10, 0.62]$	$[0.09, 0.62]$
$\langle \varphi_{S,T} \rangle \neq \langle \varphi^0_{S,T} \rangle$	$[0.11, 0.23]$	$[0.09, 0.27]$
Combined	$[0.074, 0.174]$	$[0.092, 0.176]$

Table G.6: Range of the predicted neutrino mass sum $\sum m_\nu$.

Deviation	m_β [eV]	
	Normal hierarchy	Inverted hierarchy
$a' \neq 0$	$[0.025, 0.130]$	$[0.052, 0.168]$
$c \neq d$	$[0.025, 0.235]$	$[0.05, 0.24]$
$\langle \varphi_{S,T} \rangle \neq \langle \varphi^0_{S,T} \rangle$	$[0.029, 0.081]$	$[0.052, 0.150]$
Combined	$[0.012, 0.059]$	$[0.050, 0.075]$

Table G.7: Range of the predicted beta decay parameter m_β.

G.3 Predicted magnitude of CP violation

Figure G.5 shows the behaviour of the Jarlskog variable J_{CP} as a function of $\sin^2 \theta_{13}$, obtained from the numerical analysis for the various cases in which only one of the abovementioned deviations was switched on. The observed behaviour is discussed in section 5.1.

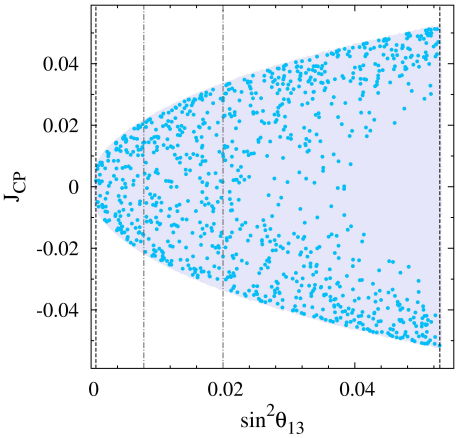

(a) $a' = a\eta$. Normal hierarchy.

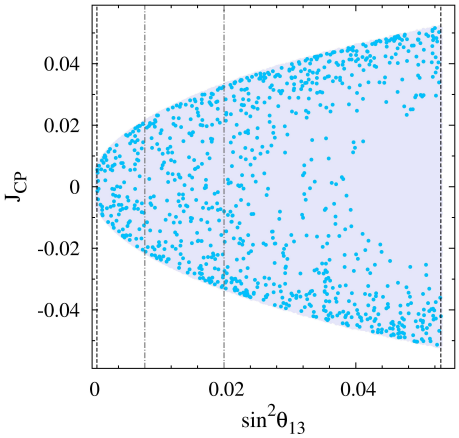

(b) $a' = a\eta$. Inverted hierarchy.

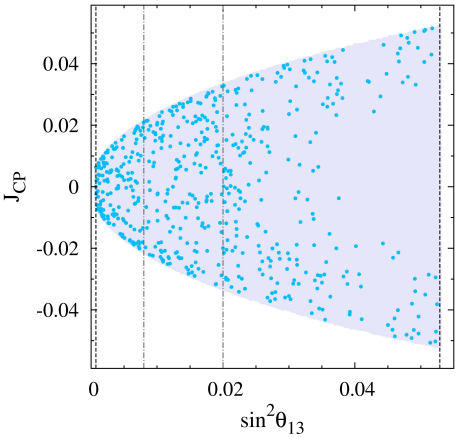

(c) $d = c(1+\epsilon)$. Normal hierarchy.

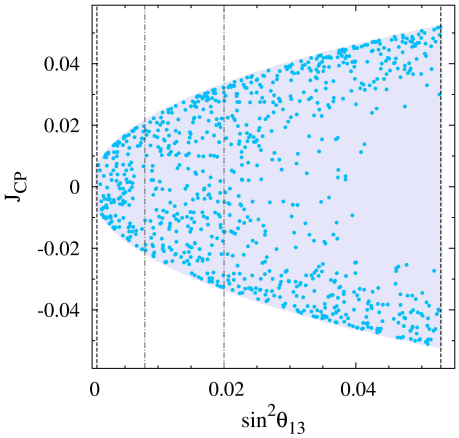

(d) $d = c(1+\epsilon)$. Inverted hierarchy.

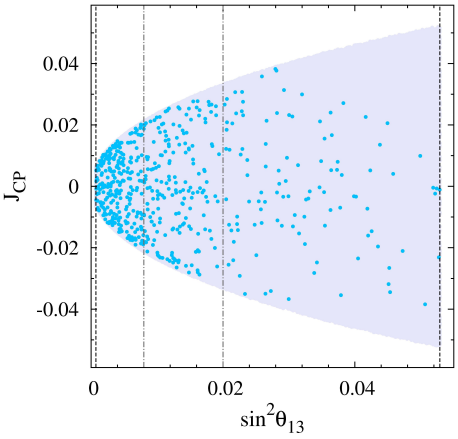

(e) $\langle\varphi_S\rangle = v_S(1+\epsilon_{S,1}, 1+\epsilon_{S,2}, 1)$ and $\langle\varphi_T\rangle = v_T(1, \epsilon_{T,1}, \epsilon_{T,2})$. Normal hierarchy.

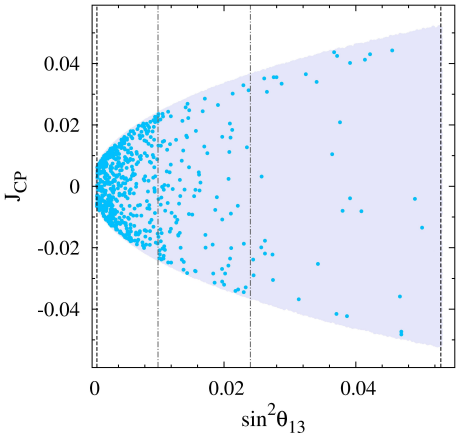

(f) $\langle\varphi_S\rangle = v_S(1+\epsilon_{S,1}, 1+\epsilon_{S,2}, 1)$ and $\langle\varphi_T\rangle = v_T(1, \epsilon_{T,1}, \epsilon_{T,2})$. Inverted hierarchy.

Figure G.5: Magnitude of CP violation: scatter plots showing predicted values of J_{CP} as a function of $\sin^2\theta_{13}$. The 3σ and 1σ regions of $\sin^2\theta_{13}$ are marked by dashed resp. dash-dotted lines. The light grey region shows possible values of $J_{\rm CP}$ that are allowed by the 3σ oscillation parameters.

Bibliography

[1] S. Glashow, "Partial Symmetries of Weak Interactions," *Nucl.Phys.* **22** (1961) 579–588.

[2] S. Weinberg, "A Model of Leptons," *Phys.Rev.Lett.* **19** (1967) 1264–1266.

[3] A. Salam, "Weak and Electromagnetic Interactions," *Conf.Proc.* **C680519** (1968) 367–377.

[4] M. Gell-Mann, "A Schematic Model of Baryons and Mesons," *Phys.Lett.* **8** (1964) 214–215.

[5] G. Zweig, "An SU(3) model for strong interaction symmetry and its breaking," *CERN-TH-401* (1964) .

[6] H. Fritzsch, M. Gell-Mann, and H. Leutwyler, "Advantages of the Color Octet Gluon Picture," *Phys.Lett.* **B47** (1973) 365–368. Introduces the term 'color'.

[7] D. Gross and F. Wilczek, "Ultraviolet Behavior of Nonabelian Gauge Theories," *Phys.Rev.Lett.* **30** (1973) 1343–1346.

[8] H. D. Politzer, "Reliable Perturbative Results for Strong Interactions?," *Phys.Rev.Lett.* **30** (1973) 1346–1349.

[9] G. 't Hooft and M. Veltman, "Proceedings of the Colloquium on Renormalization of Yang-Mills Fields, Marseille, June 19-23, 1972,".

[10] **SNO Collaboration** Collaboration, Q. Ahmad *et al.*, "Measurement of the rate of $\nu_e + d \to p + p + e^-$ interactions produced by B-8 solar neutrinos at the Sudbury Neutrino Observatory," *Phys.Rev.Lett.* **87** (2001) 071301, `arXiv:nucl-ex/0106015 [nucl-ex]`.

[11] C. Kraus, B. Bornschein, L. Bornschein, J. Bonn, B. Flatt, *et al.*, "Final results from phase II of the Mainz neutrino mass search in tritium beta decay," *Eur.Phys.J.* **C40** (2005) 447–468, `arXiv:hep-ex/0412056 [hep-ex]`.

[12] **WMAP Collaboration** Collaboration, J. Dunkley *et al.*, "Five-Year Wilkinson Microwave Anisotropy Probe (WMAP) Observations: Likelihoods and Parameters from the WMAP data," *Astrophys.J.Suppl.* **180** (2009) 306–329, arXiv:0803.0586 [astro-ph].

[13] **WMAP Collaboration** Collaboration, E. Komatsu *et al.*, "Five-Year Wilkinson Microwave Anisotropy Probe (WMAP) Observations: Cosmological Interpretation," *Astrophys.J.Suppl.* **180** (2009) 330–376, arXiv:0803.0547 [astro-ph].

[14] S. M. Davidson and H. E. Logan, "Dirac neutrinos from a second Higgs doublet," *Phys. Rev.* **D80** (2009) 095008, arXiv:0906.3335 [hep-ph].

[15] **DOUBLE-CHOOZ Collaboration** Collaboration, Y. Abe *et al.*, "Indication for the disappearance of reactor electron antineutrinos in the Double Chooz experiment," *Phys.Rev.Lett.* **108** (2012) 131801, arXiv:1112.6353 [hep-ex].

[16] **DAYA-BAY Collaboration** Collaboration, F. An *et al.*, "Observation of electron-antineutrino disappearance at Daya Bay," *Phys.Rev.Lett.* **108** (2012) 171803, arXiv:1203.1669 [hep-ex].

[17] **RENO collaboration** Collaboration, J. Ahn *et al.*, "Observation of Reactor Electron Antineutrino Disappearance in the RENO Experiment," *Phys.Rev.Lett.* **108** (2012) 191802, arXiv:1204.0626 [hep-ex].

[18] P. W. Higgs, "Broken Symmetries and the Masses of Gauge Bosons," *Phys.Rev.Lett.* **13** (1964) 508–509.

[19] F. Englert and R. Brout, "Broken Symmetry and the Mass of Gauge Vector Mesons," *Phys.Rev.Lett.* **13** (1964) 321–323.

[20] G. Guralnik, C. Hagen, and T. Kibble, "Global Conservation Laws and Massless Particles," *Phys.Rev.Lett.* **13** (1964) 585–587.

[21] T. Kibble, "Symmetry breaking in nonAbelian gauge theories," *Phys.Rev.* **155** (1967) 1554–1561.

[22] M. E. Peskin and D. V. Schroeder, "An Introduction to quantum field theory," *ISBN-9780201503975* (1995) .

[23] W. Cottingham and D. Greenwood, "An introduction to the standard model of particle physics," *ISBN-9780521852494* (2007) .

[24] N. Cabibbo, "Unitary Symmetry and Leptonic Decays," *Phys.Rev.Lett.* **10** (1963) 531–533.

[25] M. Kobayashi and T. Maskawa, "CP Violation in the Renormalizable Theory of Weak Interaction," *Prog.Theor.Phys.* **49** (1973) 652–657.

[26] B. Pontecorvo, "Inverse beta processes and nonconservation of lepton charge," *Sov.Phys.JETP* **7** (1958) 172–173.

[27] B. Pontecorvo, "Neutrino Experiments and the Problem of Conservation of Leptonic Charge," *Sov.Phys.JETP* **26** (1968) 984–988.

[28] Z. Maki, M. Nakagawa, and S. Sakata, "Remarks on the unified model of elementary particles," *Prog.Theor.Phys.* **28** (1962) 870–880.

[29] C. Giunti and C. W. Kim, "Fundamentals of Neutrino Physics and Astrophysics," *ISBN-9780198508717* (2007) .

[30] M. Fukugita and T. Yanagida, "Physics of neutrinos and applications to astrophysics," *ISBN-9783642078514* (2003) .

[31] W. Grimus and P. Stockinger, "Real oscillations of virtual neutrinos," *Phys.Rev.* **D54** (1996) 3414–3419, `arXiv:hep-ph/9603430 [hep-ph]`.

[32] M. Beuthe, "Towards a unique formula for neutrino oscillations in vacuum," *Phys.Rev.* **D66** (2002) 013003, `arXiv:hep-ph/0202068 [hep-ph]`.

[33] M. Beuthe, "Oscillations of neutrinos and mesons in quantum field theory," *Phys.Rept.* **375** (2003) 105–218, `arXiv:hep-ph/0109119 [hep-ph]`.

[34] C. Giunti, "Neutrino wave packets in quantum field theory," *JHEP* **0211** (2002) 017, `arXiv:hep-ph/0205014 [hep-ph]`.

[35] **Particle Data Group** Collaboration, K. Nakamura *et al.*, "Review of particle physics," *J.Phys.G* **G37** (2010) 075021.

[36] C. Jarlskog, "A Basis Independent Formulation of the Connection Between Quark Mass Matrices, CP Violation and Experiment," *Z.Phys.* **C29** (1985) 491–497.

[37] C. Jarlskog, "Commutator of the Quark Mass Matrices in the Standard Electroweak Model and a Measure of Maximal CP Violation," *Phys.Rev.Lett.* **55** (1985) 1039.

[38] I. Dunietz, O. Greenberg, and D.-d. Wu, "A Priori Definition of Maximal CP Violation," *Phys.Rev.Lett.* **55** (1985) 2935.

[39] O. Greenberg, "Rephase Invariant Formulation of CP Violation in the Kobayashi-Maskawa Framework," *Phys.Rev.* **D32** (1985) 1841.

[40] D.-d. Wu, "The Rephasing Invariants and CP," *Phys.Rev.* **D33** (1986) 860.

[41] K. Zuber, "Neutrino physics," *ISBN-9780750307505* (2004) .

[42] E. K. Akhmedov, "Neutrino physics," `arXiv:hep-ph/0001264 [hep-ph]`.

[43] A. de Gouvea, "TASI lectures on neutrino physics," arXiv:hep-ph/0411274 [hep-ph].

[44] M. Gonzalez-Garcia, M. Maltoni, J. Salvado, and T. Schwetz. *In preparation.*

[45] T. Schwetz, M. Tortola, and J. W. F. Valle, "Where we are on θ_{13}: addendum to 'Global neutrino data and recent reactor fluxes: status of three- flavour oscillation parameters'," *New J. Phys.* **13** (2011) 109401, arXiv:1108.1376 [hep-ph].

[46] T. Yanagida, "HORIZONTAL SYMMETRY AND MASSES OF NEUTRINOS," *Conf.Proc.* **C7902131** (1979) 95.

[47] M. Gell-Mann, P. Ramond, and R. Slansky, "COMPLEX SPINORS AND UNIFIED THEORIES," *Conf.Proc.* **C790927** (1979) 315–321. To be published in Supergravity, P. van Nieuwenhuizen & D.Z. Freedman (eds.), North Holland Publ. Co., 1979.

[48] R. N. Mohapatra and G. Senjanovic, "Neutrino Mass and Spontaneous Parity Violation," *Phys.Rev.Lett.* **44** (1980) 912.

[49] P. Minkowski, "$\mu \to e\gamma$ at a Rate of One Out of 1-Billion Muon Decays?," *Phys.Lett.* **B67** (1977) 421.

[50] S. Glashow, "THE FUTURE OF ELEMENTARY PARTICLE PHYSICS," *NATO Adv.Study Inst.Ser.B Phys.* **59** (1980) 687. Preliminary version given at Colloquium in Honor of A. Visconti, Marseille-Luminy Univ., Jul 1979.

[51] Z.-z. Xing and S. Zhou, "Neutrinos in particle physics, astronomy and cosmology," *ISBN-978-7-308-08024-8, ISBN-978-3-642-17559-6* (2011) .

[52] J. Schechter and J. Valle, "Neutrinoless Double beta Decay in SU(2) x U(1) Theories," *Phys.Rev.* **D25** (1982) 2951.

[53] L. Baudis, A. Dietz, G. Heusser, H. Klapdor-Kleingrothaus, I. Krivosheina, *et al.*, "Limits on the Majorana neutrino mass in the 0.1-eV range," *Phys.Rev.Lett.* **83** (1999) 41–44, arXiv:hep-ex/9902014 [hep-ex].

[54] H. Klapdor-Kleingrothaus, "Status and perspectives of double beta decay: Window to new physics beyond the standard model of particle physics," *Int.J.Mod.Phys.* **A13** (1998) 3953–3992.

[55] W. Rodejohann, "Neutrino-less Double Beta Decay and Particle Physics," *Int.J.Mod.Phys.* **E20** (2011) 1833–1930, arXiv:1106.1334 [hep-ph].

[56] V. Lobashev, V. Aseev, A. Belesev, A. Berlev, E. Geraskin, *et al.*, "Direct search for mass of neutrino and anomaly in the tritium beta spectrum," *Phys.Lett.* **B460** (1999) 227–235.

[57] **KATRIN Collaboration** Collaboration, L. Bornschein, "KATRIN: Direct measurement of neutrino masses in the sub-Ev region," *eConf* **C030626** (2003) FRAP14, arXiv:hep-ex/0309007 [hep-ex].

[58] **The 2DFGRS Collaboration** Collaboration, M. Colless *et al.*, "The 2dF Galaxy Redshift Survey: Spectra and redshifts," *Mon.Not.Roy.Astron.Soc.* **328** (2001) 1039, arXiv:astro-ph/0106498 [astro-ph].

[59] Y. Li and Z.-z. Xing, "Possible Capture of keV Sterile Neutrino Dark Matter on Radioactive β-decaying Nuclei," *Phys.Lett.* **B695** (2011) 205–210, arXiv:1009.5870 [hep-ph].

[60] C. Froggatt and H. B. Nielsen, "Hierarchy of Quark Masses, Cabibbo Angles and CP Violation," *Nucl.Phys.* **B147** (1979) 277.

[61] K. Babu, "TASI Lectures on Flavor Physics," arXiv:0910.2948 [hep-ph].

[62] P. Harrison, D. Perkins, and W. Scott, "Tri-bimaximal mixing and the neutrino oscillation data," *Phys.Lett.* **B530** (2002) 167, arXiv:hep-ph/0202074 [hep-ph].

[63] G. Altarelli and F. Feruglio, "Discrete Flavor Symmetries and Models of Neutrino Mixing," *Rev.Mod.Phys.* **82** (2010) 2701–2729, arXiv:1002.0211 [hep-ph].

[64] H. Ishimori, T. Kobayashi, H. Ohki, Y. Shimizu, H. Okada, *et al.*, "Non-Abelian Discrete Symmetries in Particle Physics," *Prog.Theor.Phys.Suppl.* **183** (2010) 1–163, arXiv:1003.3552 [hep-th].

[65] T. D. Lee, "A Theory of Spontaneous T Violation," *Phys. Rev.* **D8** (1973) 1226–1239.

[66] J. F. Gunion, H. E. Haber, G. L. Kane, and S. Dawson, "THE HIGGS HUNTER'S GUIDE," *Front.Phys.* **80** (2000) 1–448.

[67] G. C. Branco *et al.*, "Theory and phenomenology of two-Higgs-doublet models," arXiv:1106.0034 [hep-ph].

[68] E. A. Paschos, "Diagonal Neutral Currents," *Phys. Rev.* **D15** (1977) 1966.

[69] S. L. Glashow and S. Weinberg, "Natural Conservation Laws for Neutral Currents," *Phys. Rev.* **D15** (1977) 1958.

[70] E. Ma, "Naturally small seesaw neutrino mass with no new physics beyond the TeV scale," *Phys. Rev. Lett.* **86** (2001) 2502–2504, arXiv:hep-ph/0011121.

[71] E. Ma and M. Raidal, "Neutrino mass, muon anomalous magnetic moment, and lepton flavor nonconservation," *Phys. Rev. Lett.* **87** (2001) 011802, arXiv:hep-ph/0102255.

[72] E. Ma, "Verifiable radiative seesaw mechanism of neutrino mass and dark matter," *Phys. Rev.* **D73** (2006) 077301, arXiv:hep-ph/0601225.

[73] N. Haba and M. Hirotsu, "TeV-scale seesaw from a multi-Higgs model," *Eur. Phys. J.* **C69** (2010) 481–492, arXiv:1005.1372 [hep-ph].

[74] N. Haba and K. Tsumura, "ν-Two Higgs Doublet Model and its Collider Phenomenology," *JHEP* **06** (2011) 068, arXiv:1105.1409 [hep-ph].

[75] N. Haba and O. Seto, "Thermal leptogenesis in a supersymmetric neutrinophilic Higgs model," *Phys. Rev.* **D84** (2011) 103524, arXiv:1106.5354 [hep-ph].

[76] N. Haba, O. Seto, and O. Seto, "Low scale thermal leptogenesis in neutrinophilic Higgs doublet models," *Prog. Theor. Phys.* **125** (2011) 1155–1169, arXiv:1102.2889 [hep-ph].

[77] N. Haba and T. Horita, "Vacuum stability in neutrinophilic Higgs doublet model," *Phys. Lett.* **B705** (2011) 98–105, arXiv:1107.3203 [hep-ph].

[78] S. Gabriel and S. Nandi, "A new two Higgs doublet model," *Phys. Lett.* **B655** (2007) 141–147, arXiv:hep-ph/0610253.

[79] F. Wang, W. Wang, and J. M. Yang, "Split two-Higgs-doublet model and neutrino condensation," *Europhys. Lett.* **76** (2006) 388–394, arXiv:hep-ph/0601018.

[80] S. M. Davidson and H. E. Logan, "LHC phenomenology of a two-Higgs-doublet neutrino mass model," *Phys. Rev.* **D82** (2010) 115031, arXiv:1009.4413 [hep-ph].

[81] S. Zhou, "Comment on astrophysical consequences of a neutrinophilic 2HDM," *Phys.Rev.* **D84** (2011) 038701, arXiv:1106.3880 [hep-ph].

[82] R. H. Cyburt, B. D. Fields, K. A. Olive, and E. Skillman, "New BBN limits on physics beyond the standard model from He-4," *Astropart.Phys.* **23** (2005) 313–323, arXiv:astro-ph/0408033 [astro-ph].

[83] **ALEPH Collaboration, DELPHI Collaboration, L3 Collaboration, OPAL Collaboration, SLD Collaboration, LEP Electroweak Working Group, SLD Electroweak Group, SLD**

Heavy Flavour Group Collaboration, "Precision electroweak measurements on the Z resonance," *Phys.Rept.* **427** (2006) 257–454, arXiv:hep-ex/0509008 [hep-ex]. 302 pages, v2: minor corrections and updates of references. Accepted for publication by Physics Reports, v3: further small corrections and journal version Report-no: CERN-PH-EP/2005-041, SLAC-R-774.

[84] P. Posch, "Precision constraints and photonic Higgs decays in the Two Higgs Doublet Model,". presented 11 Aug 2009.

[85] W. Grimus, L. Lavoura, O. Ogreid, and P. Osland, "The Oblique parameters in multi-Higgs-doublet models," *Nucl.Phys.* **B801** (2008) 81–96, arXiv:0802.4353 [hep-ph].

[86] M. Baak, M. Goebel, J. Haller, A. Hoecker, D. Ludwig, *et al.*, "Updated Status of the Global Electroweak Fit and Constraints on New Physics," arXiv:1107.0975 [hep-ph].

[87] **ATLAS Collaboration** Collaboration, G. Aad *et al.*, "Search for the Standard Model Higgs boson in the diphoton decay channel with 4.9 fb^{-1} of pp collisions at $\sqrt{s} = 7$ TeV with ATLAS," *Phys.Rev.Lett.* **108** (2012) 111803, arXiv:1202.1414 [hep-ex].

[88] A. G. Akeroyd, A. Arhrib, and E.-M. Naimi, "Note on tree level unitarity in the general two Higgs doublet model," *Phys.Lett.* **B490** (2000) 119–124, arXiv:hep-ph/0006035 [hep-ph].

[89] S. Glashow, J. Iliopoulos, and L. Maiani, "Weak Interactions with Lepton-Hadron Symmetry," *Phys.Rev.* **D2** (1970) 1285–1292.

[90] L. Lavoura, "General formulae for $f_1 \to f_2\gamma$," *Eur.Phys.J.* **C29** (2003) 191–195, arXiv:hep-ph/0302221 [hep-ph]. 11 pages LATEX.

[91] **MEG Collaboration** Collaboration, O. Kiselev, "Positron spectrometer of MEG experiment at PSI," *Nucl.Instrum.Meth.* **A604** (2009) 304–306.

[92] **BABAR Collaboration** Collaboration, B. Aubert *et al.*, "Search for lepton flavor violation in the decay $\tau^{\pm} \to e^{\pm}\gamma$," *Phys.Rev.Lett.* **96** (2006) 041801, arXiv:hep-ex/0508012 [hep-ex].

[93] **SuperB Collaboration** Collaboration, M. Bona *et al.*, "SuperB: A High-Luminosity Asymmetric e+ e- Super Flavor Factory. Conceptual Design Report," arXiv:0709.0451 [hep-ex].

[94] **Belle Collaboration** Collaboration, K. Hayasaka *et al.*, "New search for $\tau \to \mu\gamma$ and $\tau \to e\gamma$ decays at Belle," *Phys.Lett.* **B666** (2008) 16–22, arXiv:0705.0650 [hep-ex].

[95] P. Paradisi, "Higgs-mediated $\tau \to \mu$ and $\tau \to e$ transitions in II Higgs doublet model and supersymmetry," *JHEP* **0602** (2006) 050, arXiv:hep-ph/0508054 [hep-ph].

[96] **Muon G-2 Collaboration** Collaboration, G. Bennett *et al.*, "Final Report of the Muon E821 Anomalous Magnetic Moment Measurement at BNL," *Phys.Rev.* **D73** (2006) 072003, arXiv:hep-ex/0602035 [hep-ex]. Summary of E821 Collaboration measurements of the muon anomalous magnetic moment, each reported earlier in Letters or Brief Reports. Revised version submitted to Phys.Rev.D.

[97] J. P. Leveille, "The Second Order Weak Correction to (G-2) of the Muon in Arbitrary Gauge Models," *Nucl.Phys.* **B137** (1978) 63.

[98] **New (g-2) Collaboration** Collaboration, F. Gray, "Measuring the muon's anomalous magnetic moment to 0.14 ppm," *J.Phys.Conf.Ser.* **312** (2011) 102006, arXiv:1009.0799 [nucl-ex].

[99] J. Grifols and R. Pascual, "CONTRIBUTION OF CHARGED HIGGS BOSONS TO THE ANOMALOUS MAGNETIC MOMENT OF THE MUON," *Phys.Rev.* **D21** (1980) 2672.

[100] T. Fukuyama and K. Tsumura, "Detecting Majorana nature of neutrinos in muon decay," arXiv:0809.5221 [hep-ph].

[101] J. M. Roney, "Tau physics prospects at SuperB," *Nucl.Phys.Proc.Suppl.* **169** (2007) 379–386.

[102] J. Barry and W. Rodejohann, "Deviations from tribimaximal mixing due to the vacuum expectation value misalignment in A_4 models," *Phys.Rev.* **D81** (2010) 093002, arXiv:1003.2385 [hep-ph].

[103] W. Tung, "GROUP THEORY IN PHYSICS," *ISBN-9789971966577* (1985) .

[104] J. Barry and W. Rodejohann, "Neutrino Mass Sum-rules in Flavor Symmetry Models," *Nucl.Phys.* **B842** (2011) 33–50, arXiv:1007.5217 [hep-ph].

[105] G. Altarelli and F. Feruglio, "Tri-Bimaximal Neutrino Mixing, A4 and the Modular Symmetry," *Nucl. Phys.* **B741** (2006) 215–235, arXiv:hep-ph/0512103.

[106] K. S. Babu and S. Gabriel, "Semidirect Product Groups, Vacuum Alignment and Tribimaximal Neutrino Mixing," *Phys. Rev.* **D82** (2010) 073014, arXiv:1006.0203 [hep-ph].

[107] M. Holthausen and M. A. Schmidt, "Natural Vacuum Alignment from Group Theory: The Minimal Case," *JHEP* **01** (2012) 126, arXiv:1111.1730 [hep-ph].

[108] G. Altarelli and F. Feruglio, "Tri-bimaximal neutrino mixing from discrete symmetry in extra dimensions," *Nucl. Phys.* **B720** (2005) 64–88, arXiv:hep-ph/0504165.

[109] G. Altarelli, F. Feruglio, and Y. Lin, "Tri-bimaximal neutrino mixing from orbifolding," *Nucl.Phys.* **B775** (2007) 31–44, arXiv:hep-ph/0610165 [hep-ph].

[110] J. Berger and Y. Grossman, "Model of leptons from SO(3) $\to$ A(4)," *JHEP* **1002** (2010) 071, arXiv:0910.4392 [hep-ph].

[111] G. Altarelli, F. Feruglio, and C. Hagedorn, "A SUSY SU(5) Grand Unified Model of Tri-Bimaximal Mixing from A(4)," *JHEP* **0803** (2008) 052–052, arXiv:0802.0090 [hep-ph].

[112] E. Ma and G. Rajasekaran, "Softly broken A(4) symmetry for nearly degenerate neutrino masses," *Phys.Rev.* **D64** (2001) 113012, arXiv:hep-ph/0106291 [hep-ph].

[113] F. Feruglio, C. Hagedorn, Y. Lin, and L. Merlo, "Tri-bimaximal Neutrino Mixing and Quark Masses from a Discrete Flavour Symmetry," *Nucl.Phys.* **B775** (2007) 120–142, arXiv:hep-ph/0702194 [hep-ph].

[114] A. Djouadi, "The Anatomy of electro-weak symmetry breaking. I: The Higgs boson in the standard model," *Phys.Rept.* **457** (2008) 1–216, arXiv:hep-ph/0503172 [hep-ph].

[115] E. Majorana, "Theory of the Symmetry of Electrons and Positrons," *Nuovo Cim.* **14** (1937) 171–184.

Acknowledgements

I would like to thank Dr. Werner Rodejohann for the support he gave me during the preparation of this thesis, and for always taking the time to thoroughly discuss any appearing problems with me. I am also grateful to Prof. Dr. Manfred Lindner for agreeing to examine my thesis. Finally, I would like to thank Julian Heeck and Max Kerstan for useful discussion and my family for their support not only while completing this thesis but over the whole course of my studies.

Erklärung

Ich versichere, dass ich diese Arbeit selbstständig verfasst habe und keine anderen als die angegebenen Quellen und Hilfsmittel benutzt habe.

Heidelberg, den 15.06.2012

.....
(Unterschrift)